Microbiological, genomic and cell-biological analyses of *Enterococcus faecalis* isolates of MLST type ST40

Von der Fakultät für Lebenswissenschaften

der Technischen Universität Carolo-Wilhelmina

zu Braunschweig

zur Erlangung des Grades

einer Doktorin der Naturwissenschaften

(Dr. rer. nat.)

genehmigte

D i s s e r t a t i o n

von Melanie Zischka

aus Wernigerode

1. Referent: Professor Dr. Dieter Jahn
2. Referent: Privatdozent Dr. Guido Werner
eingereicht am: 30.09.2013
mündliche Prüfung (Disputation) am: 03.12.2013

Druckjahr 2013

Vorveröffentlichungen der Dissertation

Teilergebnisse aus dieser Arbeit wurden mit Genehmigung der Fakultät für Lebenswissenschaften, vertreten durch den Mentor der Arbeit, in folgenden Beiträgen vorab veröffentlicht:

Publikationen

Zischka, M., Kuenne, C., Blom, J., Dabrowski, P. W., Linke, B., Hain, T., Nitsche, A., Goesmann, A., Larsen, J., Jensen, L. B., Witte, W. & Werner, G.: Complete Genome Sequence of the Porcine Isolate *Enterococcus faecalis* D32. JBacteriol. 194(19): 5490-1 (2012).

Boehme, H., Königsmark, C, Klare, I., Zischka, M. & Werner, G.; Cross-transmission rates of enterococcal isolates among newborns in a neonatal intensive care unit. Pediatr Rep. 4(1): e15 (2012).

Tagungsbeiträge

Zischka, M., Dabrowski, P. W., Fleige, C., Günther, C., Klare, I., Witte, W. & Werner, G.: Comparative Genomics of *Enterococcus faecalis* ST40: Differences between Commensal and Clincal Isolates. (Poster) 9th International Meeting on Microbial Epidemiological Markers (IMMEM-9), Wernigerode, Germany (2010).

Zischka, M., Dabrowski, P. W., Fleige, C., Klare, I., Schreiber, K., Witte, W. & Werner, G.: Comparative Genomics of *Enterococcus faecalis* ST40: Differences between Commensal and Clincal Isolates. (Poster) II. Summer School, Pathogen – Host Interactions at Cellular Barriers, Münster, Germany (2011).

Zischka, M., Dabrowski, P. W., Fleige, C., Klare, I., Schreiber, K., Witte, W. & Werner, G.: Comparative Genomics of *Enterococcus faecalis* ST40: Differences between Commensal and Clincal Isolates. (Poster) 5th European Conference on Prokaryotic and Fungal Genomics, Göttingen, Germany (2011).

Zischka, M., Voget, S., Dabrowski, P. W., Daniel, R., Nitsche, A., Sadowy, E., Ruiz-Garbajosa, P., Pérez, D. Q., Larsen, J, Jensen, L. B., Solheim, M., Boehme, H. & Werner, G.: Comparative Genomics of *Enterococcus faecalis* isolates of MLST type ST40: Are there differences between isolates of commensal and clinical origins?. (Poster) 10th International Meeting on Microbial Epidemiological Markers (IMMEM-10), Paris, France (2013).

Zischka, M., Wobser, D., Sakinc, T., Hauck, R., Hübner, H., Hafez, H. M., Larsen, J., Jensen, L. B. & Werner, G.: Comparative Assessment of the pathogenic potential of two highly related *Enterococcus faecalis* ST40 isolates: Differences between a porcine commensal and a human clinical isolate. (Poster) 10th International Meeting on Microbial Epidemiological Markers (IMMEM-10), Paris, France (2013).

Content

1 Abstract

1.1 Abstract

Enterococcus faecalis (*E. faecalis*) is a common colonizer of the animal and human gastrointestinal tracts, also used as a probiotic mixture in health care or as a starter culture in food fermentation. In contrast, *E. faecalis* is an opportunistic pathogen and one of the leading causes of nosocomial infections, especially of the urinary tract, bacteremia and/or endocarditis.

With the focus on niche adaptation, this thesis presents results of the genomic comparison of 42 *E. faecalis* isolates of the most frequent multilocus sequence type ST40, comprising strains of various clinical origins and colonization (humans/animals), which also originated from different countries and isolated over a period of nearly 50 years.

We resolved the complete genome sequence of a porcine commensal ST40 strain D32, which represents the first complete genome sequence of an animal *E. faecalis* isolate. It was further used as a template for detailed comparisons to high-quality draft genomes of 14 related ST40 isolates. By reflecting the close relationship, genomic and phylogenetic analyses suggest a high level of similarity regarding the core genome, which was also reflected by similar carbon utilization patterns, analyzed by BIOLOG MicroArray™ technology. Distribution of known and putative virulence-associated genes does not allow any differentiation between ST40 strains from a commensal (animal/human) and clinical background. Further analyses of mobile genetic elements (MGE) revealed a large pool for genomic diversity due to: (i) a modular structured pathogenicity island (PAI), varying independently of the core genome; (ii) a site-specifically integrated and previously unknown genomic island (GI; 138 kb) in D32, probably associated with exopolysaccharide synthesis; and (iii) a certain level of plasmid diversity and strain-specific phage patterns. Moreover, we used different cell-biological and animal experiments to compare the isolate D32 with a closely related clinical ST40 isolate UW7709, obtained from a patient with infective endocarditis and whose draft genome sequence was also generated within this project. The porcine colonizing strain D32 generally showed a greater capacity of

adherence and an increased pathogenic potential in combination with an even faster growth *in vivo* (not *in vitro*).

In general, these findings emphasized the crucial role of MGEs in niche adaptation by transferring virulence-associated features, which enable isolates of the commensal microflora to be a potential source of infections in humans.

1.2 Zusammenfassung

Enterococcus faecalis (*E. faecalis*) gehören zur natürlichen Flora des tierischen und menschlichen Verdauungstraktes, werden aber auch als Probiotika oder als Starterkulturen in der Lebensmittelfermentation eingesetzt. Als opportunistischer Krankheitserreger ist *E. faecalis* jedoch auch einer der häufigsten Ursachen für nosokomiale Infektionen, was insbesondere Harnwegsinfektionen, Bakteriämien und/oder Endokarditiden betrifft.

Grundlegend geht es in dieser Arbeit um den genomischen Vergleich von 42 eng verwandten *E. faecalis* Isolaten, die dem am weitesten verbreiteten MLST Sequenztyp ST40 angehören. Unsere Sammlung zeichnet sich durch eine breite Diversität aus und umfasst Stämme verschiedener klinischer Herkunft und Besiedlung (Mensch/Tier), die weltweit über einen Zeitraum von fast 50 Jahren gesammelt wurden und wodurch eine mögliche Anpassung an ökologische Nischen am ehesten nachvollzogen werden sollte.

Es ist uns gelungen die vollständige Genomsequenz des ST40 Stammes D32 darzustellen, der als Kommensale eines Schweins isoliert wurde und damit die als erstes veröffentlichte vollständige Genomsequenz eines tierischen *E. faecalis* Isolats repräsentiert. Diese Sequenzinformation nutzten wir dann als Grundlage für detaillierte Genomvergleiche mit den 14 ebenfalls sequenzierten und *de novo* assemblierten ST40 Isolaten. In diesen genomischen und phylogenetischen Analysen spiegelte sich die enge genetische Verwandtschaft durch ein stark konserviertes Kern- („core“) Genom wider, was zudem durch ähnliche Kohlenstoff-Verwertungsmuster in den durchgeführten BIOLOG MicroArray™ Analysen verdeutlicht werden konnte. Bereits beschriebene und vermeintliche virulenz-assoziierte Gene erlauben keine Differenzierung zwischen den ST40 Stämmen mit kommensalen (Tier/Mensch) und klinischen Hintergrund. Weitere Untersuchungen hinsichtlich des Vorkommens und der Zusammensetzung von mobilen genetischen Elementen (MGE) offenbarten jedoch einen umfangreichen Pool an genomischer Diversität, dargestellt durch: (i) eine modular aufgebaute Pathogenitätsinsel (PAI), deren Zusammensetzung unabhängig vom Kern-Genom variierte; (ii) im D32 eine positions-spezifisch integrierte und bislang unbeschriebene genomische Insel (GI;

138kb), die vermutlich mit der Synthese von Exopolysacchariden in Verbindung gebracht werden kann; sowie (iii) einen gewissen Grad an Plasmid-Diversität sowie Stamm-spezifisches Phagenmuster. Darüber hinaus haben wir zellbiologische Assays und verschiedene Tiermodelle verwendet, um dieses Isolat mit dem sehr eng verwandten klinischen ST40 Isolat UW7709 zu vergleichen, das von einem Patienten mit einer infektiösen Endokarditis isoliert wurde und während dieser Arbeit ebenfalls sequenziert wurde. Bei diesen Vergleichen zeigte der Schweine-kolonisierende Stamm D32 ein stärkeres Adhärenzverhalten und eine höhere Pathogenität kombiniert mit einem schnelleren *in vivo* (nicht aber *in vitro*) Wachstum.

Bezüglich der Anpassung an ökologische Nischen, weisen diese Erkenntnisse auf eine maßgebliche Rolle der MGE hin, durch die die Übertragung von virulenz-assoziierten Eigenschaften vermittelt wird und wodurch Isolate der Mikroflora als eine mögliche Quelle für nosokomiale Infektionen des Menschen befähigt werden.

2 Introduction

2.1 Genus *Enterococcus*

Belonging to the third-largest genus of lactic acid bacteria (LAB), enterococci are commensals of the gastrointestinal tracts (GIT) of animals and humans and also well adapted to survive in diverse environmental and animal-associated habitats (reviewed in (67, 100, 117, 165)).

Enterococci are Gram-positive, catalase-negative, non-spore-forming, facultative anaerobic bacteria, formerly classified as group D streptococci. In 1984, DNA-DNA and DNA-rRNA hybridization studies (210) resulted in the re-classification into the new genus *Enterococcus* (reviewed in (67, 165)).

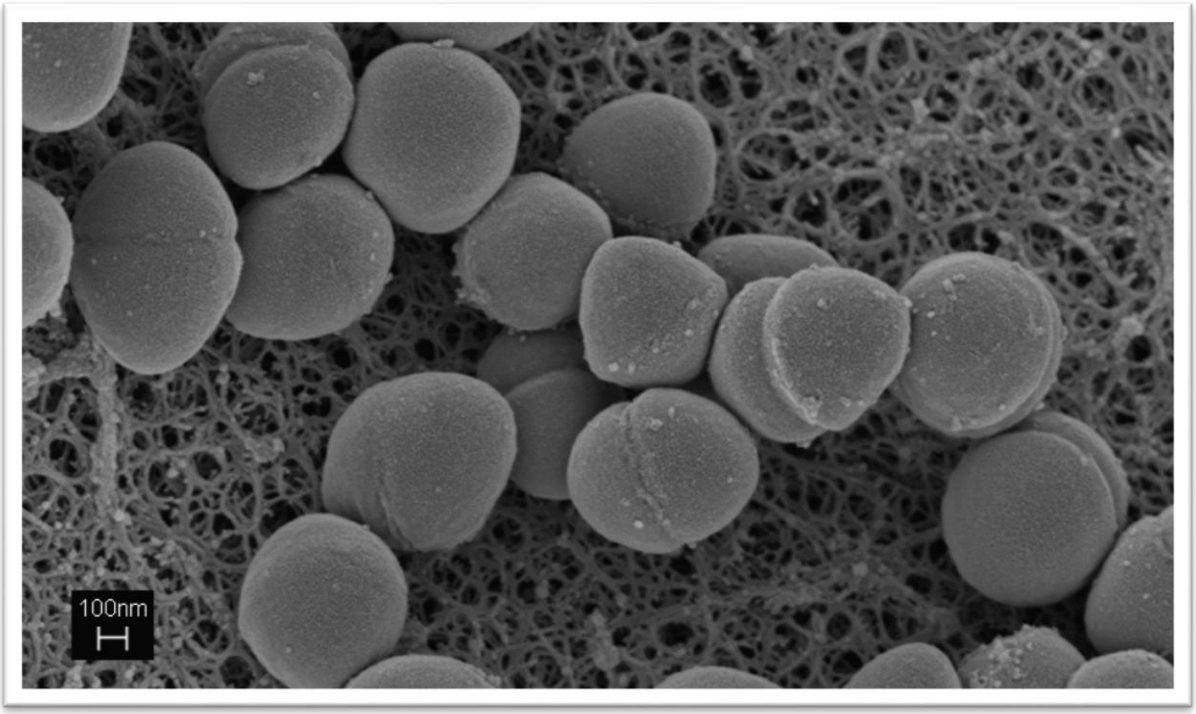

Figure 2.1: Scanning Electron microscopy of E. faecalis strain OG1RF (Image: G. Holland, Dr. N. Bannert, Robert Koch Institute, Berlin).

By now, more than 48 species of *Enterococcus* were described (http://www.bacterio.cict.fr/e/enterococcus.html), whereby *E. faecalis* and *E. faecium* have an outstanding position as common colonizers of the GIT and the cause of a wide range of infections, especially among hospitalized patients.

2.1.1 Ecology

Enterococci can grow at high salt concentrations, variable temperatures between 10 to 45°C. Also being resistant to desiccation, they occur in many natural habitats, like soil, water, sewage, plants and animals (reviewed in (64, 67)).

Enterococci play a crucial role as common colonizers of animals and humans. On the one hand, small numbers of enterococci occur in vaginal flora or on the skin and are rarely observed in oropharyngeal secretions (reviewed in (117)). But more important is their ability to colonize the gastrointestinal tracts of animals and humans, possible due to toleration and growth in the presence of 40% (w/v) bile acids. In healthy human feces, bacterial counts of *E. faecalis* range from 10^5 – 10^7 colony forming units (CFU) per gram and *E. faecium* counts range from 10^4 – 10^5 CFU per gram (reviewed in (64)). But in summary, human feces are mainly composed of anaerobic Gram-negative species ((186), reviewed in (117)). The suspected health-promoting effects explain, why some *E. faecalis* and E*. faecium* strains have been used as probiotics in health care (reviewed in (67, 278)).

Because of their further beneficial impact on ripening and aroma production of cheese and fermented meat, vegetables and olives, enterococci are also used as starter cultures or co-starter cultures in food fermentation. Thereby, production of a variety of bacteriocins with inhibitory activity against food spoilage or foodborne pathogens, such as *Listeria monocytogenes*, *Staphylococcus aureus*, *Vibrio cholerae*, *Clostridium* spp., and *Bacillus* spp., is a particularly advantageous (reviewed in (67, 79)).

On the contrary, enterococci are also opportunistic pathogens, especially associated with hospital-acquired infections. Thereby, *E. faecalis* is responsible for the major of

60 – 95% of nosocomial infections, while *E. faecium* is diagnosed in 5-40% of the cases (120). Hospitalized patients, especially premature newborns, immunocompromised and / or elderly patients, seem to have a greater incidence of enterococcal infections, particularly of surgical wounds, the urinary tract, bacteremia and/or endocarditis (reviewed in (64, 117, 278)). Moreover, enterococci are also able to survive for long periods on environmental surfaces and especially robustness on the surface of medical devices is one of the major problems, when preventing nosocomial transmission in hospital milieu (reviewed in (7)).

2.2 Antibiotic resistance

In context of enterococcal colonization of the gastrointestinal tract, antibiotic treatment plays a significant role. By destabilization of the intestinal microbial consortium, especially due to antibiotics with activity against anaerobic bacteria, new niches for colonization by resistant enterococci are opened ((78), reviewed in (7, 99, 120)). An association between predominantly colonization with vancomycin-resistant enterococci (VRE) was demonstrated, which could also be associated with its invasion into the bloodstream in combination with the spread within the host organism (259). Primarily, hospital milieu holds various risk factors for an infection: long period of hospitalization in combination with multiple antibiotic treatments, immunosuppression, surgical interventions and / or contact with colonized medical devices or infected patients and accordingly medical personnel (reviewed in (7, 99, 120)). In that context, it was demonstrated that intensive care units (ICU) are a reservoir for transmission of infections (76).

2.2.1 Intrinsic resistance

Intrinsic resistance mechanisms are naturally encoded on the host´s chromosome (reviewed in (3)).

A characteristic feature of enterococci is resistance to ß-lactams (particularly cephalosporins, semi-synthetic penicillins and monobactams) due to expression of

chromosomal-encoded penicillin binding proteins (PBPs; PBP5 in *E. faecium* and PBP4 in *E. faecalis*) with a low affinity to bind ß-lactam antibiotics (reviewed in (120)). Additionally in *E. faecalis*, tolerance to ß-lactams is also induced by removal of reactive oxygen species by superoxide dismutase activity (19).

Aminoglycosides act as 30S ribosome inhibitors and consequently inhibit protein synthesis (121). In enterococci, low-level intrinsic resistance to aminoglycosides is due to the low uptake of the drugs. To counteract, a combined therapy, consisting of cell wall active agents and aminoglycosides, is preferred to utilize bactericidal synergism (reviewed in (99)).

An ABC-efflux pump mechanism is suggested to be responsible for intrinsic resistance of *E. faecalis* to lincosamides and streptogramins of class A and B, like quinupristin/dalfopristin. Due to expression of a differently encoded ABC-efflux pump, *E. faecium* only show low-level resistance to streptogramins of class B (reviewed in (99)).

Only isolates of *E. gallinarum* and *E. casseliflavus* show low level intrinsic resistance to vancomycin, but are still susceptible for teicoplanin. In detail, expression of VanC phenotype is induced by replacing of the D-Ala ending of the peptidoglycan precursor to D-Ser resulted in a lower binding affinity to vancomycin (43).

Wide spectrum activity of fluoroquinolones does not apply to enterococci because resistance is generally encoded by the transmissible qnr gene (9).

2.2.2 Acquired resistance

Resistance to antibiotics is also evolved by sporadic mutations in genes targeted by the antibiotic, as well as, by incorporation of mobile genetic elements (MGE) acquired of other bacteria of the environment. In fact, horizontal gene transfer (HGT) of resistance determinants mainly occurs through transfer of plasmids, bacteriophages and transposons. Consequently, spread of multidrug resistance (MDR) is one of the biggest challenges nowadays (reviewed in (3, 99, 278)). In the following, a selection

of acquired resistance mechanisms against clinically relevant enterococci is described.

High-level resistance (HLR) to penicillins is associated with acquisition of ß-lactamases. The vast majority of resistance to ampicillin is found in *E. faecium*, but rarely in *E. faecalis*, and is associated with point mutations in the binding region of PBP5 (reviewed in (7, 99, 120)).

The synergistic therapy is limited due to the acquisition of mobile genetic elements, harboring genes that encode for HLR to aminoglycosides (especially gentamicin and streptomycin). Resistance to gentamicin bases on the enzymatically inactivation of gentamicin and its structural homologs, induced by the bifunctional 6´-aminoglycoside acetyltransferase 2´´ phosphotransferase enyzme. HLR to streptomycin is due to ribosomal mutations or antibiotic inactivation by adenylyltransferases Ant(6´)-Ia and Ant(3´´)-Ia ((63), reviewed in (8, 99)).

In 1988, the first vancomycin resistant clinical isolates of *E. faecium* were reported in France (134) and the United Kingdom (260). At the same time, *E. faecalis* V583 was the first vancomycin resistant clinical isolate reported in the US (202). Nowadays, vancomycin resistant enterococci (VRE) are widely distributed and especially acquired vancomycin resistance in clinical *E. faecium* isolates is a major problem in hospital milieu (284). In this context, highly transferable plasmids (like broad host-range Inc18 plasmid) play an important role in horizontal transfer of vancomycin determinants between enterococcal species (reviewed in (99)). However, presence of *vanA* resistance cluster in methicillin-resistant *S. aureus* (MRSA) was detected (reviewed in (185)), but Werner *et al*. also demonstrated that mobility across species- or genus-barriers seemed to be of lower frequency *in vitro* (281). Up to now, nine different vancomycin operons (*vanA*, *vanB*, *vanD*, *vanE*, *vanG*, *vanL*, *vanM*, *vanN* and the intrinsic *vanC* genotype) are described in enterococci, at which *vanA* and *vanB* gene clusters are most frequently (reviewed in (99)). Resistance mechanism bases on the modification of the C-terminus of the cell wall precursor, resulting in a less affinity to glycopeptides (reviewed in (43)).

Alternatively, the clinically relevant group of macrolide-lincosamide-streptogramin (MLS) antibiotics is characterized due to the similar antibacterial mechanism. Acquired resistance showed the following characteristics: (a) enzymatically methylation of rRNA, resulting from the expression of the erythromycin-resistant methylase (*erm*) genes; (b) presence of efflux pumps; or (c) enzymatically modification of the antibiotic, avoiding interaction to the ribosome (reviewed in (195)).

Furthermore, tetracyclines are the first broad spectrum class of antibiotics and they are frequently used in livestock production. The acquired resistance mechanisms are based on (a) the inhibition of protein synthesis by preventing the attachment of tRNA to the ribosome, especially encoded by *tetM* gene; (b) *tetL* encoded efflux pumps, which remove the drug out of the cell; or enzymatically deactivation of the tetracyclines (reviewed in (35, 195)).

2.3 Population structure and genomic diversity of *E. faecalis*

Nowadays, sequence-based tools, like multilocus sequence typing (MLST) (142) or multiple-locus variable-number tandem repeat analysis (MLVA) (257) in combination with genome sequencing, are the “gold-standard” to obtain insights into the population structure of enterococci to pursue adaption to ecological niches (287) (reviewed in (278)).

In 2006, Ruiz-Garbajosa and colleagues developed an MLST scheme for *E. faecalis*, based on sequencing of seven housekeeping genes. In comparison to the publicly available MLST database (http://efaecalis.mlst.net/), sequence of each locus resulted in a distinct allele number and combination of the allele numbers of all the seven loci assigned a sequence type (ST) (199).

MLST analysis of a diverse collection of 110 *E. faecalis* isolates revealed four major clonal complexes (CC; CC2, CC9, CC10 and CC21), combining closely related sequence types (ST) (199).

On the basis of this MLST scheme, widely distributed CC2 and CC9 were mainly characterized by containing hospital-associated strain types (125, 199, 200). But their characterization as high-risk enterococcal clonal complexes (HiRECCs) (133) is not

so strict, because isolates of these CCs were also found in feces of healthy infants (227), as well as, in pigs (68). Furthermore, other CCs – especially the CC40/ST40 – include strains of various clinical origins, from colonization and food (199). In this context, presence of antibiotic resistance and “virulence traits” can not only be correlated with adaption to hospital environment, because they were also found in livestock- and community-associated isolates (46, 128, 129, 227) and were spread over many diverse lineages of *E. faecalis* (129, 149). One important example is the so-called pathogenicity island (PAI), not limited to clinical strains (129, 149, 216). Probably, community could be a reservoir for transmission of *E. faecalis* clones. Further within this pool it is suggested, that MGEs, harboring genes with a proposed role in virulence, are spread between swine and humans (68, 129, 216). Types of MGEs with relevance in enterococci are discussed in section 2.6.

Until now, five complete genome sequences (24, 28, 71, 184, 300), and, numerous draft genome sequences of *E. faecalis* are publicly available (179, 181, 229, 267).
First, the VRE isolate V583, belonging to ST6/CC2, was completely sequenced in 2003. In addition to the occurrence of a large pathogenicity island (PAI), more than a quarter of the genome comprises of MGEs, including three plasmids and seven integrated putative phages. Vancomycin resistance is mediated by integration of a *vanB* conjugative transposon (184).
With a size of 2.74Mbp, the genome of the strain OG1RF, a derivate of the human colonizer OG1, was also sequenced (24). Probably due to the presence of the CRISPR-*cas* system, a bacterial defense mechanisms against invading DNA, this strain lacks plasmids, was well as, phages. But the putative role of CRISPR-*cas* will be described in part 2.5.1.4 in more detail. In comparison to V583, the OG1RF contains an inositol *iol* operon at the same *attL/R* site, which explained its ability to utilize m-inositol (27).
Furthermore, genome sequence of the commensal strain 62 (2.99Mbp), isolated from a healthy Norwegian infant, harbored genes involved in lactose and other carbohydrate metabolism, but also lacks virulence-associated traits. This suggested its adaption to the environment of the GIT (28).
During this thesis, the first complete genome sequence of an animal *E. faecalis* strain was resolved (300) and a detailed analysis of its sequence data will be presented.

At the beginning of 2013, the complete genome sequence of the probiotic *E. faecalis* Symbioflor 1 clone DSM 16431 was reported by Fritzenwanker *et al*. (71). With a genome size of 2.81Mbp, the absence of putative virulence traits and the previously described *vanB* transposon emphasize its non-pathogenic characteristics (53, 71).

2.4 Important aspects of metabolism of *E. faecalis*

Within the complex ecosystem of the intestine, enterococci are well adapted to the harsh conditions, where nutrients are limited. Thereby, a large spectrum of substrates, like diverse carbohydrates, organic acids, and amino acids, are catabolized to pyruvate. Catalyzed by the NADH-dependent L-(+)-lactate dehydrogenase (*ldh*), pyruvate is mainly reduced to lactate, the major end-product of LAB fermentation (reviewed in (107),(137)). But among enterococci, only *E. faecalis* is able to utilize pyruvate for growth (reviewed in (107)).

However, it was also demonstrated that certain conditions, probably such as the NADH/NAD ratio, can regulate a shift from homolactic to mixed-acid fermentation, where pyruvate is also fermented to other end-products, such as formate, ethanol, acetate, CO_2, diacetyl, acetoin, and 2,3-butanediol (116, 137, 153).

Hexoses and pentoses are primary key components of pyruvate formation. Especially substrates, like D-glucose, D-fructose, lactose, maltose, D-mannose, trehalose, sucrose, mannitol, and N-acetylglucoseamine, could be sensed and effectively transported into the bacterial cell by the phosphoenolpyruvate phosphotransferase system (PTS), where they are further channeled into glycolysis, Entner-Doudoroff, and pentose phosphate pathways, respectively (reviewed in (107)) (226). *E. faecalis* and other enterococci lack a tricarboxylic acid cycle and, consequently, enhanced pyruvate metabolism plays a key role within energy metabolism. Additionally, this also explains the disability to produce the porphyrin precursors resulting in the lack of heme synthesis (reviewed in (107)). Besides, only *E. faecalis* is able to ferment the sugar alcohol component glycerol to pyruvate in absence of oxygen, and not only under the ordinary aerobic and microaerophilic conditions (reviewed in (107)).

Organic acids, like malate and oxaloacetate, generated from citrate, aspartate or tartrate, can also be decarboxylated to pyruvate (reviewed in (137)). However, there

are several other potential possibilities for energy gain in *E. faecalis*, like catabolism of arginine and its derivate agmatine, oxidation of lactate and heme-dependent respiration by cytochrome *bd*, as well as, energy-yielding by ion transport (reviewed in (107)).

In context of the diverse microbial colonization of the intestine, the effective uptake of energy sources in combination with their efficient metabolism implicate bacterial fitness. On the other side, these mechanisms could also be used for regulation of expression of virulence genes. For example, activity of the major virulence regulator PrfA in *Listeria monocytogenes* is affected by the phosphorylation state of the PTS components ((54), reviewed in (188), (65)).

2.5 Pathogenicity of *E. faecalis*

In close association with the host immune system, the normal microflora represents the essential barrier defending several potential pathogens (62). But potential danger also lurks in their own lines – concretely in form of *E. faecalis*, for example. As an extremely robust opportunistic pathogen, *E. faecalis* is one of the leading causes of nosocomial infections (120), especially of the urinary tract, bacteremia and/or endocarditis.

2.5.1 Virulence determinants

According to Pillar *et al*., four steps from bacterial colonization up to the point of host damage have been described, including phases of (i) colonization, (ii) bacterial spread, (iii) persistence and growth, and (iv) tissue damage (186). Special environmental conditions could enable antibiotic resistant, opportunistic pathogens, like vancomycin resistant enterococci (VRE), to “overgrowth” normal commensal microbiota (259).

Several recent studies have identified putative enterococcal virulence traits. Their relevance in enhanced adherence was investigated in several cell culture assays (75, 94, 208, 248, 249) and their role in virulence was also estimated in various animal

infection models (Table 2.1) (reviewed in (41, 74, 90, 194, 218, 255), reviewed in (178, 207)).

At this point, importance of biofilm formation by *E. faecalis* should be emphasized because of its clinical relevance in enterococcal growth on medical devices, catheters, implants, or heart valves. These infections are extremely hard to treat because biofilms protect bacteria against antibiotics or host defense strategies, like phagocytosis (reviewed in (98, 178)).
In general, biofilms are a three-dimensional structured consortium of attached populations of microbes, surrounded by an extracellular polymeric substance (EPS) matrix. This EPS matrix consists of polysaccharides, proteins and extracellular DNA (eDNA) (reviewed in (73, 98)). Moreover, analyses of early biofilm formation by Barnes and colleagues also revealed a cell lysis-independent mechanism of eDNA release by living bacterial cells (13).
Mature biofilms are characterized by a concentration gradient of metabolic substrates and products, such as oxygen. Adaption to the local environment within the biofilm can be effected by various responses, like regulation of gene expression, genetic variation through mutation or recombination (reviewed in (236)).
In the following parts, the most important virulence factors, focused in this study, will be described and their role in biofilm formation will be discussed (Table 2.1)

2.5.1.1 Bacterial colonization and fitness

Components of the cell envelope play a crucial role in fitness and virulence, especially biofilm formation, because they enhance the bacterial ability to adhere to host cells and the extracellular matrix (ECM), as well as, to neighboring cells (reviewed in (178)).
For example, the enterococcal surface protein (Esp) is discussed to be one of the biofilm-enhancing factors (241) and seemed to be highly associated with the ability of *E. faecalis* to form biofilms on polystyrene surfaces (256), as well as, with the colonization of the urinary tract (218). But other data indicated that biofilm formation is independent form *esp* presence (60, 105, 124, 159). However, an advantage concerning to the bacterial fitness might be conceivable (51).

Furthermore, there are several other enterococcal adhesion factors, such as the members of the MSCRAMM (microbial surface component recognizing adhesive matrix molecule proteins) family, like aggregation substance and Ace (adhesion to collagen in *E. faecalis*), promoting adherence to the ECM. Furthermore, the enterococcal glycopolymers lipoteichoic acids (LTA) and peptidoglycan-attached wall teichoic acids (WTA) are responsible for binding to epithelial and endothelial cells, but also to biomaterials, and are also important for host cell invasion. It was also demonstrated that biochemical modifications resulted in a reduced sensitivity against cationic antimicrobial peptides by changes in the membrane charge (reviewed in (178, 194)).

Analyzes of pathogenicity, for example using a rat endocarditis and a murine urinary tract infection (UTI) model, described the role of endocarditis and biofilm associated pilus operon *ebpABC*, encoding pilus structures, in an increased attachment and biofilm formation (27, 221). Furthermore, expression of this locus could be controlled by RNA processing, as well as, the two regulators *ebpR* and *fsr* and could be enhanced by environmental conditions, like bicarbonate concentration (reviewed in (178)).

In summary, enriched presentation of surface-related structures seemed to be associated with virulence, demonstrated for strains of MLST CC2 (229).

2.5.1.2 *fsr*-regulated proteolytic activity

A complex interplay between the zinc metalloprotease gelatinase (GelE) and the serine protease (SprE) plays a major role in biofilm formation by causing cell lysis (6, 88, 251, 252). The co-located and co-expressed *gelE* and *sprE* genes are tightly regulated by the upstream *fsrABDC* quorum sensing locus (189, 251) and their relevance for virulence in *E. faecalis* was determined in different animal models (168, 220, 224, 255). GelE-mediated cell death resulted in eDNA release, which stabilizes the EPS biofilm (reviewed in (178)). Cell lysis is primary induced by modifying cell wall affinity of the proteolytically processed autolysin AtlA/Atn. However, autolysis is negatively affected by *sprE*, acting as an immunity protein against lysis (251, 252).

2.5.1.3 Toxicity by cytolysin

Both, hemolytic and bactericidal activities are induced by the quorum-sensing regulated cytolysin expression (84, 85). The mainly responsible cytolysin (*cyl*) operon is encoded within the *E. faecalis* PAI in close association with the *esp* gene (215, 217) or also on large pheromone-responsive plasmids (36, 110). Its role in contribution of virulence in *E. faecalis* was demonstrated in different infection models, ranging from *C. elegans* to rabbits (reviewed in (41)).

2.5.1.4 Strategies of self-protection against hosts defense mechanisms

Persistence due to evasion of the host immune system also plays a major role in virulence. Additionally to the formation of protective biofilms, especially encapsulation by capsular polysaccharides has been shown to cause resistance to complement-mediated opsonophagocytosis by masking LTA (87, 103, 106, 253, 254). There are two well-studied enterococcal cell wall polysaccharides: (i) a rhamnopolysaccharide Epa (244, 245, 293) and (ii) a MLST-specific capsular polysaccharide *cps* (87, 103, 150).

The former is supported for a key role in bacterial fitness. But nevertheless, behavior of tested mutants was demonstrated to be associated with pathogenicity, such as resistance to PMN-killing, biofilm formation, and virulence in a mouse peritonitis model, but needs more investigations (159, 194, 244, 245, 293). Two glycosyl transferases, which are encoded by *ef2167* and *ef2170* and are enriched in strains of MLST CC2, are suspected to have an effect to the structural diversity of Epa (194, 229).

Concerning the *E. faecalis* capsule**,** a serotyping scheme was defined by the presence of the 11 open-reading frames (ORF) of the *cps* locus (*cpsA* to *cpsK*) (87, 104). Strains of serotypes A and B possessed only the *cpsA* and *cpsB* genes, defined by the absence of a capsule (Maekawa/CPS type 1). Presence of capsular polysaccharides depends on the presence of *cpsC* to *cpsK* genes. Serodiversity between serotype C (Maekawa/CPS type 2) and D (Maekawa/CPS type 5) is attributed to the presence or absence of the putative glycosyltransferase encoded by *cpsF* gene (104, 141, 150, 253). In a large-scale study with respect to genetic

diversity of a diverse *E. faecalis* strain collection, CPS type 1 was most common, while CPS type 2 was associated with the accumulation of virulence traits and antibiotic resistances (150).

Table 2.1: Putative virulence factors present in *E. faecalis*.

Putative virulence factors	***Pathophysiology/Virulence***	***Reference(s)***
Secreted factors:		
Cytolysin (hemolysin/bacteriocin)	Lyses a broad range of eukaryotic and Gram-positive cells	(36, 40, 41)
Gelatinase / serine protease, regulated by *fsrABDC* quorum sensing locus	Biofilm formation, host tissue damage, immune evasion by degradation of complement peptide C3; Pathogenesis of Endocarditis	(25, 183, 190, 220, 255)
Autolysins: AtlA/Atn, AtlB, AtlC	Cell lysis and biofilm formation by releasing of eDNA	(83, 251, 252)
Reactive oxygen species	Extracellular superoxide and hydrogen peroxide; oxidative stress to damage other bacteria or host cells	(108, 109, 240)
Cell envelope bound factors:		
LPxTG surface proteins:		(Reviewed in (95))
(a) Aggregation substance, AS: Asa1, Asp1, Asc10	Promotes conjugation by directing aggregation, adherence to ECM, internalization; pathogenesis of endocarditis	(36, 97, 123, 176, 191, 197, 206, 211, 238, 263, 271, 277)
(b) Collagen-binding MSCRAMMs: Ace	Binding to collagen type I, collagen type IV, laminin and dentin; unclear relevance in endocarditis	(122, 169, 170, 193, 225)
(c) Enterococcal surface protein Esp	Biofilm enhancing factor; Role in murine UTI	(218, 241, 242, 256)
(d) Pili *ebpABC* locus	Three pilus subunits (EbpA, B and C) with a role in initial attachment during the process of biofim formation; assembly and cell wall anchoring by sortase SrtA; role in pathogenesis of endocarditis and UTI; antigenic in humans	(27, 38, 171, 173, 221, 223)
(e) *bee* locus	Biofilm formation (among 5% of *E.fs*)	(243)
(f) EF3314	Putative adhesion	(45)

Capsular polysaccharides, *cps* locus	Immune evasion due to resistance to complement and PMNs-mediated killing	(87, 103, 254)
Enterococcal rhamnopolysaccharide antigen Epa	Erythrocyte translocation, resistance to killing by PMNs and to infection by phages; biofilm formation; pathogenesis in a mouse peritonitis model; key role in host adaptation and fitness	(159, 194, 222, 244, 245, 293, 295)
Lipid-attached lipotechoic acids (LTA)	Attachment to epithelial and endothelial surfaces, as well as, to biomaterials; involved in host cell invasion; target of opsonic antibodies	(194, 247)
Peptidoglycan-attached wall teichoic acids (WTA)	Attachment to epithelial and endothelial surfaces, as well as, to biomaterials; involved in host cell invasion	(172, 194)
Glycolipids (like the *bgsA*-encoded gylcosyltransferase)	Biofilm formation, binding to colonic epithelial cells; pathogenesis in murine bacteremia model	(208, 248)

ECM, extracellular matrix; *E.fs*, *E. faecalis*; LPxTG, cell wall-anchored Leu-Pro-x-Thr-Gly proteins, where x denotes any amino acid; LTA, lipoteichoic acid; MSCRAMM, microbial surface component recognizing adhesive matrix molecules; PMNs, polymorphonuclear leukocytes; UTI, urinary tract infection; WTA, wall teichoic acid (Table modified and completed from (130, 178, 207)).

2.5.2 Short insights into the role of differential gene expression

Up to now, several *in vitro* transcriptome analyses, for example using DNA microarrays and RIVET, emphasized the role of the differential expression of putative virulence-associated genes controlled by diverse transcriptional regulators, like PerR (194), the PAI-encoded PerA ((140), reviewed in (178)), Fsr (reviewed in ((178)), AhrC (66), ebpR (27), or Rex factor (153, 268). But also, discrepancies between transcriptomic and proteomic data revealed further possibilities of regulation on a posttranscriptional or translational level (152). Thereby, a complex regulatory network is distinguished (56), being further regulated by environmental conditions, such as growing in the presence of bile (21, 228), blood (266), urine (267), metals (138, 192), or bicarbonate (27, 140).

2.6 Genome plasticity by exchange of MGEs

Enterococcal genomes evolutionary adapt to new niches, like hospital environment, by the exchange of genes by HGT and homologous recombination (reviewed in (262)). Thereby, acquisition and spread of virulence or resistance associated genes by MGE, such as bacteriophages, plasmids, genomic islands (GIs) and transposable elements, can result in a beneficial effect under certain circumstances (reviewed in (52, 92, 278)). Initial fitness costs are relativized over the time and beneficial effects of the plasmid-bacteria association may become dominantly (234).

Transposable elements, including transposons, insertions (IS) elements, and integrons, play a crucial role in genome plasticity because they move genes directly from one DNA site to another genomic location. Transposons in enterococci can be categorized as elements of Tn3-family, composite transposons and integrative conjugative elements (ICE). By an interplay of recombination and/or transposition, variability of such MGEs is increased, as well as, gene expression can be affected due to insertion into an ORF or into a promoter region (reviewed in (92, 278)).

Importantly, transmission of enterococci from animal source to humans, also being associated with infections, was demonstrated (68, 128, 129). In this context, conjugative and transferable elements play an important role in spread of resistance genes via lateral gene transfer (reviewed in (278)).

2.6.1 The pathogenicity island (PAI)

PAIs are large genomic regions (≥10 – 200kb), whose GC-content differs from the core genome. Their naming bases on the presence of one or more virulence-associated genes, which are normally absent in non-pathogenic strains. HGT and recombination seem to play a key role in its adaptive evolution, because PAIs are frequently integrated in transfer RNA (tRNA) genes and they also contain genes associated with mobility, like IS elements, integrases or transposases. However, characteristic segments of the PAI were also found in commensal, symbiotic and environmental bacteria (reviewed in (52, 86)).

E. faecalis MMH594, which caused a hospital outbreak in the mid-1980s, was the first enterococcal strain reported to contain a PAI, possessing a size of 153kb (215). Genomic analyses revealed 129 predicted ORF, encoding for several pathogenicity factors like cytolysin toxin, Esp, and aggregation substance (149, 215). The PAI of MMH594 seems to be a prototype from which strains like V586 and V583 evolved. The region, spanning the co-localized genes of the cytolysin operon and *esp*, was nearly identical. In V586, insertions interrupted the *cylB* gene, resulted in a Cyl-negative but Esp-positive phenotype. Whereas, V583 was phenotypically Cyl- and Esp-negative because of a spontaneous deletion of a 17,036bp DNA segment, which occurred in the strain V586 (215).

The *E. faecalis* PAI also contains genes encoding transcriptional regulators, such as quorum-sensing *fsrABDC* locus (described in part 2.5.1.2) or PerA (pathogenicity island-encoded). This *araC*-type regulator is suggested to coordinately regulate genes, involved in metabolism and pathogenicity, including biofilm formation (39, 86, 140, 189, 215). A number of additional factors within the PAI can influence the ability to colonize new niches within the host GI tract and might have an impact on pathogenesis. Genomic comparisons of the PAI-related genes of several enterococcal strains demonstrated the presence of genes associated with enhanced intestinal fitness, like due to the expression of a putative bile acid hydrolase (encoded by *cbh*) or of proteins with a function in DNA damage repair. Furthermore, other traits can contribute to survival under conditions of nutrient starvation or other stresses, like the general stress protein Gls24-like, PTS, or alternative metabolic enzymes, for example responsible for utilization of xylose ((149, 215), reviewed in (186)).

Contrasting the situation of Gram-negatives, the *E. faecalis* PAI shows a modular organization by defined gene clusters, categorized from regions A-F, and was found to be highly variable in gene content independently of clonal background (1, 149, 150, 216).

Representing a prime example (reviewed in (86)), the PAI in *E. faecalis* MMH594 has a GC-content of 32.3%, which varies to 37.38% of the remainder genome (reviewed in (186)). Additionally, the ends of the PAI contain phage-related integration and excision genes and were flanked by 10bp direct repeats (DR), resembling attachment sites *attL/R* for phage integrases (131, 215). Furthermore, several segments are flanked by multiple IS elements and conjugal transfer elements are also present.

These characteristics revealed that the PAI or segments of it could be mobilized. Although recombination is a key factor within the diversification of the core genome, it is suggested that the PAI evolves even faster most likely by HGT, which emphasized the variety of the PAI independently of the core genome (40, 149, 215). Previous studies demonstrated that segments, as well as, the PAI itself were transferable between *E. faecalis* isolates, as well as, between *E. faecalis* and *E. faecium* through conjugative mechanisms (40, 131, 145, 175), confirming the importance of mobile elements in the evolution from non-pathogenic to pathogenic *E. faecalis*.

2.6.2 Plasmids

As semi-autonomously replicating extra-chromosomal genetic elements, plasmids play a key role in bacterial adaptability and diversity of the gene pool within the species of many genera, mainly by HGT (reviewed in (250)). Further, stable inheritance can be facilitated by an acquired toxin-antitoxin (TA) system, a kind of selective killing machinery in case of plasmid loss (91, 162). Furthermore, Manson *et al*. demonstrated that plasmid integration into the chromosome occurs in a RecA-dependent manner (145).

2.6.2.1 Plasmid typing

By focusing on the phylogenetic relationship, enterococcal plasmids can be classified by several strategies; especially typing methods based on (i) the mode of replication (rolling cycle replication or theta-replicating plasmids) (reviewed in (278)), (ii) replication regions of various incompatibility (Inc) groups (reviewed in (30, 174)), (iii) homology of conserved areas of the replication initiation genes (*rep*) (114), or (iv) the specification of genes encoding for relaxases (37).

However, plasmids of the Inc18 group, like pIP501 (*rep*-family 1) and the multi-resistant plasmid pRE25 (*rep*-family 2), are broadly distributed among Gram-positive and partly Gram-negative bacteria, too (114, 127, 213, 246, 273); whereas, pheromone-responsive plasmids are characterized by a narrow host range (273). Also proposed as RepA_N plasmids (272), pheromone plasmids of *E. faecalis* are

classified to *rep*-family 8 and 9, represented by pAM373, as well as, pCF10 and pAD1 (114). Additionally, large plasmids, like the megaplasmid pLG1, are only described to be widespread in the hospital-associated *E. faecium* population (70, 132, 196).

In summery, classification of enterococcal plasmids is a complex matter, because (i) some of the *rep*-types are still unknown (92, 270), (ii) new plasmids are identified within whole genome sequencing projects (reviewed in (278)), and (iii) recombinatoric diversification resulted in mosaics of plasmid structures (69).

2.6.2.2 Benefits resulting from the acquisition of plasmids

Plasmids confer genomic flexibility, which enable bacteria to adapt to different ecological niches and to evade host defense strategies (reviewed in (278), (297)). Especially megaplasmids are described to confer fitness and a selective advantage due to (i) the expression of virulence-associated genes, such as LPxTG surface proteins or cytolysin, (ii) enzymes for the uptake and utilization of unusual carbon sources, as well as, (iii) the resistance to heavy metals and antibiotics (36, 95, 99, 110, 132, 192, 297).

2.6.3 CRISPR-*cas* – a prokaryotic immune system

Within the genomic variability, bacteria and archaea have also evolved a self-defense mechanism, clustered regularly interspaced short palindromic repeats (CRISPR), to limit HGT of mobile extra-chromosomal DNA elements, mainly like plasmids or bacteriophages (14, 29, 31, 101, 148). Widely distributed CRISPRs are typically characterized by several non-contiguous direct repeats, varying in size from 24 to 47bp, separated by stretches of variable sequences of spacers (81, 112, 160). By forming the CRISPR-*cas* system, six “core” CRISPR-associated genes *(cas1-6*), encoding for functional proteins with homology to nucleases, helicases, polymerases, and polynucleotide-binding proteins, can be found in multiple subtypes (reviewed in (101)).

By describing the spectrum of immunity, many CRISPR spacers showed sequence homology to MGEs, especially phages (230). During a kind of immunization process, the Cas complex recognizes and integrates a small segment of the exogenous DNA as a novel repeat-spacer unit at the leader end of the CRISPR array ((14), reviewed in (101)). This resulted in acquired immunity against the corresponding invading DNA, functioning via the RNA interference (RNAi) mechanism (reviewed in (101)).
The genome of *E. faecalis* OG1RF comprises only one phage remnant as part of the core genome and generally lacks mobile genetic elements (24, 150). Nevertheless, two CRISPR loci (CRISPR1 and CRISPR2) were described, while only CRISPR1 is associated with functional *cas* nuclease genes (24). However, over one quarter the genome of the clinical isolate V583 consists of MGE, but only harbors an orphan CRISPR2 locus, lacking the functional *cas* genes required for CRISPR defense (180, 184).

In the evolutionary context, composition of CRISPR arrays is extremely unstable, completely varying between closely related strains. Presumably by HGT, CRISPR loci evolved due to a process of adaption to rapidly changing repertoires of phages and plasmids (reviewed in (101), (136, 143, 230)). Furthermore, antibiotic usage seemed to have a negatively selective effect to CRISPR-associated immunity, reported by Palmer and Gilmore (180).

2.7 Objectives of this study

McBride *et al.* analyzed the genetic diversity among a collection of 106 *E. faecalis* strains isolated over the past 100 years, demonstrating that MLST ST40 is the most common sequence type (150).

According to these observations, the overall aim of this thesis is to characterize a heterogeneous *E. faecalis* ST40 strain collection, comprising randomly collected isolates of various clinical origins and colonization (humans/animals), which also originated from different countries and isolated over a period of many decades.

The main objectives are to identify microevolutionary changes coming along with niche adaptation and differences in pathogenic properties between highly related microorganisms.

More specifically, the following workflow is pursued:

(i) Analysis of the presence and expression of well-known virulence-associated markers, encoded within the *E. faecalis* pathogenicity island (PAI) and/or on the chromosome.

(ii) Investigation of plasmid content and their characterization.

(iii) On the basis of these previous characterizations, representative isolates should be chosen for *de novo* genome sequencing and comparison of these genome data sets among each other and with the publicly available *E. faecalis* complete genome sequences of V583 (184) and OG1RF (24) with the focus on niche adaptation.

(iv) Examination of utilization of carbon sources by using Biolog MicroArray™ technology.

(v) Investigation of the relationship between the genomic data and the *in vivo* pathogenic potential in selected animal models.

3 Materials and Methods

3.1 Materials

3.1.1 Chemicals

Table 3.1: Chemicals used in this study.

Chemicals	***Manufacturer***
Agarose	Sigma-Aldrich GmbH
Agarose	Life Technologies Corporation
Amino acids (nonessential)	Life Technologies Corporation
BIOLOG Redox Dye Mix D (100x)	BIOLOG Life Science Institute
Bromphenol blue (loading)	Sigma-Aldrich GmbH
Calcium chloride dihydrate ($CaCl_2 \cdot 2\ H_2O$)	Merck KGaA
Chloroform	Sigma-Aldrich GmbH
EDTA (Ethylenediaminetetraacetic acid)	Serva Electrophoresis GmbH
Ethanol (96%)	Merck KGaA
Ethidium Bromide (10mg/mL)	CARL ROTH GmbH & Co. KG
Fetal bovine serum	PAA - The Cell Culture Company
D-glucose	Merck KGaA
Distilled water	Sigma-Aldrich GmbH
Gelatin	Becton, Dickinson & Co.
Gram´s crystal violet	Merck KGaA
Heparin	Sigma-Aldrich GmbH
Hydrochloric acid 37% (HCl)	CARL ROTH GmbH & Co. KG
L-arginine	Sigma-Aldrich GmbH
Lysozyme	Sigma-Aldrich GmbH
Magnesium chloride ($MgCl_2$)	CARL ROTH GmbH & Co. KG
Magnesium chloride hexahydrate ($MgCl_2 \cdot 6\ H_2O$)	CARL ROTH GmbH & Co. KG
Maleic acid	CARL ROTH GmbH & Co. KG
N-Lauroylsarcosine	Sigma-Aldrich GmbH
Phenol/Chlorofom/Isoamyl alcohol (25:24:1)	CARL ROTH GmbH & Co. KG
Potassium chloride (KCl)	CARL ROTH GmbH & Co. KG
Potassium hydroxide (KOH)	Jenapharm Laborchemie
Potassium phosphate, monobasic (KH_2PO_4)	Merck KGaA
Proteinase K	AppliChem GmbH
Proteinase K	Sigma-Aldrich GmbH

RNaseI	Sigma-Aldrich GmbH
S1 nuclease	Takara Bio Inc.
*Sma*I	New England Biolabs Inc.
Sodium chloride (NaCl)	Sigma-Aldrich GmbH
Sodium dodecyl sulphate (SDS)	CARL ROTH GmbH & Co. KG
Sodium hydroxide (NaOH)	CARL ROTH GmbH & Co. KG
Sodium phosphate, dibasic ($Na_2HPO_4 \cdot 2\ H_2O$)	Merck KGaA
Tris(hydroxymethyl)aminomethane (Tris)	CARL ROTH GmbH & Co. KG
Tris-HCl	Merck KGaA
Tri-Sodium citrate	Merck KGaA
Trypsin	Life Technologies GmbH
Triton X-100	Sigma-Aldrich GmbH
Trypton	Becton, Dickinson & Co.
Tween 20	CARL ROTH GmbH & Co. KG

Table 3.2: Molecular markers and their sizes.

DNA Molecular Size markers	***Manufacturer***
GeneRuler 100bp DNA-Ladder Plus	Thermo Fisher Scientific Inc.
GeneRuler 1kb DNA-Ladder Plus	Thermo Fisher Scientific Inc.
DIG III DNA-Ladder	DIG III DNA-Ladder

3.1.2 Kits

Table 3.3: Kits used during this work.

Kit	***Manufacturer***
Cycle Sequencing Kit B3.1 (BigDye)	Applied Biosystems
DIG High-Prime	F. Hoffmann-La Roche AG
DIG Nucleic Acid Detection Kit	F. Hoffmann-La Roche AG
DNAeasy Blood and Tissue kit	QIAGEN GmbH
Expand Long Template PCR	F. Hoffmann-La Roche AG
Genomic Tipp 100 DNA isolation	QIAGEN GmbH
PCR Master Mix	Thermo Fisher Scientific Inc.
Quant-iT™ PicoGreen® dsDNA Assay Kit	Life Technologies GmbH

3.1.3 Media

Table 3.4: Media used for culturing of bacteria and cell-lines.

Medium	***Manufacturer***
BIOLOG IF-0a GN/GP Base inoculating fluid (1.2x)	BIOLOG Life Science Institute
Brain-Heart Infusion (BHI) agar	Oxoid GmbH
Brain-Heart Infusion (BHI) medium	Oxoid GmbH
Dubelco`s Modified Eagle`s Medium (DMEM)	Difco® labs
de Man, Rogosa and Sharpe (MRS) Agar	OXOID GmbH
de Man, Rogosa and Sharpe (MRS) Broth	OXOID GmbH
Mueller-Hinton (MH) Agar with sheep blood	OXOID GmbH
Nutrient Agar	OXOID GmbH
Nutrient Broth	Becton, Dickinson & Co.
Todd-Hewitt agar	OXOID GmbH
Tryptic Soy Agar (TSA)	Becton, Dickinson & Co
Tryptic Soy Broth (TSB)	Becton, Dickinson & Co

3.1.4 Standard solutions

Gram positive cell-lysis buffer

Tris, pH 8.0	20mM
EDTA	2mM
Triton X-100	1.2%
added before usage:	
Lysozym	20 mg/mL

Phosphate buffered saline (PBS)

NaCl	137mM
KCl	2.7mM
$Na_2HPO_4 \cdot 2\ H_2O$	10mM
KH_2PO_4	2mM
pH 7.4	

Tris-EDTA (TE) buffer

Tris-HCl	200mM
EDTA	20mM
pH 7.5	

TES buffer

Tris-HCl pH 8.0	10mM
Trypton pH 8.0	1mM

Tris-Borat-EDTA (TBE) buffer

Tris	10,78 g
Sodium EDTA (Celaplex III)	0,1 g
Boric acid	5,4 g
pH 8.0	

3.1.5 Software and Internet resources

Table 3.5: Software tools and publicly available web tool used for data analysis.

Program	***Manufacturer***	***Type of application***
AIDA Image Analyzer Version 3.52	Raytest	Evaluation of fluorometric analysis
Artemis 12	Sanger Institute	DNA sequence edition
BioNumerics Version 6.0	Applied Maths	PFGE analysis
BLAST Ring Image Generator (BRIG)	Sourceforge/Dice Holdings, Inc. (4)	Image generation of a multiple *E. faecalis* genome comparison
Celera Assembler Version 6.1	Celera Genomics, Inc. (156, 167)	Hybrid *de novo* assembly using reads gathered by 454 and long paired-end sequencing technologies
CRISPRFinder	Institut de Génétique et Microbiologie (82)	Web tool to identify clustered regularly interspaced short palindromic repeats (CRISPR)
DS Gene Software	Accelrys, Inc.	Analysis of DNA sequences; primer design
EDGAR	CeBiTec (20)	VENN diagram
EndNote® X5	Thomas Reuters	Reference library

GeCo	University Giessen (126)	Comparative genome analysis
GenDB	CeBiTec (155)	Genome annotation
GraphPad Prism 5.01 software package	GraphPad Software, Inc.	Statistical analysis
Kodon Software Version 3.61	Applied Maths	DNA sequence alignments and comparisons
Lasergene 8 (Seqman)	DNAStar	Evaluation of DNA sequences
MAUVE (progressive ~)	(47, 48)	Genome alignment
Microsoft office package Version 7 and Version 10	Microsoft	Word, Excel, PowerPoint
MiniMap	University Giessen (*Kuenne, C.T., unpublished software*)	Primer design for gap closing
Mira Assembler Version 3.4.0.1	Sourceforge/Dice Holdings, Inc. (33, 34)	Hybrid *de novo* assembly using reads generated by 454 and Illumina/Solexa sequencing technologies
Mugsy	(5)	MCL clustering and alignment
NCBI BLAST	NCBI (209)	Alignment search tool
NCBI ORF Finder	NCBI (209)	ORF Finder
Newbler Assembler Version 2.5.3	F. Hoffmann-La Roche AG	Assembly of data generated by 454 pyrosequencing
OmniLog Kinetic and Parametric analysis software version 2005	BIOLOG Life Science Institute	Analysis of Biolog MicroArray® data
PHAge Search Tool (PHAST)	Free Software Foundation, Inc. (299)	Identification of prophages integrated into the genome
Prophage Finder	(23)	Identification of integrated prophages
Quantity One Version 4.6.6	BioRad Laboratories	Documentation of gel images and Southern hybridization membranes
RAST Server	(10)	Genome annotation
RAxML	(233)	Generation of the phylogenetic tree
Sequin 9.0	NCBI	DNA sequence edition

3.1.6 Bacterial strains

Altogether 42 isolates of *E. faecalis* MLST type ST40 were collected from commensal and pathogenic (stool, blood, urine, swab) sources and originating from many different countries and years.

Table 3.6: *E. faecalis* ST40 strain collection used in this study.

Isolate	*Country (City)*	*Year*	*Origin*
UW1833 (U 09508/98)*	D (Berlin)	1998	H, U
UW5212	D (Köln)	2004	H, U
UW5744	D (Köln)	2004	H, U
UW6530	D (Augsburg)	2006	H, U
UW6756	D (Leezen)	2006	H, U
UW6724 (Ba7514)*	D (Wernigerode)	2006	H, C
UW6727 (Ba7517)*	D (Wernigerode)	2006	H, C
UW7775	D (Heidelberg)	2004	H, C
UW7776	D (Heidelberg)	2004	H, C
UW7777 (AK-EF 29)*	D (Heidelberg)	2004	H, C
UW7778	D (Heidelberg)	2004	H, C
UW7779 (AK-EF 92)*	D (Heidelberg)	2004	H, C
UW2860 (3803)*	D (Gera)	2000	H, B
UW2861	D (Gera)	2000	H, B
UW4340	D (Berlin)	2003	H, B
UW4889	D (Augsburg)	2004	H, B
UW5209	D (Augsburg)	2004	H, B
UW5213	D (Augsburg)	2004	H, B
UW5345	D (Augsburg)	2004	H, B
UW6149 (AB 5093-231)	D (Augsburg)	2005	H, B
UW7800 (ATCC 27275)	Unknown	≤1962	Unknown
UW7801 (ATCC 27959)*	USA (Iowa)	≤1975	A[1], M
UW7729 (LMGT 2333)*	IS (Reijkjavik)	1990	A[2], C
UW7730 (LMGT 3209)	GR (Athens)	<2004	F
UW7709 (5)*	DK	1997	H, E
UW7710	DK	Unknown (after 2000)	H, U
UW7742 (D1)*	DK	2001	A[3], C
UW7743 (D27)	DK	2001	A[3], C
UW7744 (D32)▲	DK	2001	A[3], C
UW7745 (D37)	DK	2001	A[3], C

UW7761 (DQ213/C003-e)*	Cuba (Havana)	2008	H, B
UW7753 (HC 24)*	ESP (Madrid)	2001	H, B
UW7780 (402/96)*	PL (Warsaw)	1996	H, C
UW7781	PL (Warsaw)	1996	H, PF
UW7782	PL (Warsaw)	1996	H, U
UW7784	PL (Grajewo)	1999	H, U
UW7785	PL (Zawiercie)	2000	H, W
UW7787	PL (Zamość)	2002	H, CSF
UW7788	PL (Bytom)	2003	H, B
UW7789	PL (Biała Podlaska)	2004	H, U
UW7790	PL (Wołomin)	2007	H, C
UW7791	PL (Maków Maz.)	2007	H, C

E. faecalis strain collection comprises 42 ST40 strains. * draft genomes; ▲ ST40 complete reference genome; A, animal ([1] cow, [2] fish, [3] pig); B, blood culture; C, colonizer; CSF, cerebrospinal fluid; E, endocarditis; F, food (cheese); H, human; M, bovine mastitis; PF, peritoneal fluid; U, urine; W, wound.

Table 3.7: Bacteria strains and plasmids used as references.

Strain	***MLST***	***Resistance***	***Plasmids***	***Description***	***References***
E. faecalis:					
V583	CC2 (ST6)	VAN	pTEF1, pTEF2 and pTEF3	ATCC700802; first sequences *E. faecalis* genome	(150, 184, 202)
MMH594	CC2 (ST6)			Contents the first identified complete PAI	(149, 150, 215)
OG1RF	ST1	RAM, FUS	Plasmid-free	ATCC 47077; mutant of OG1	(150, 166)
UW7770	ST6	VAN	85kb *vanA*	Epidemic strain	
UW1873		TET			
UW1965		ERY, STR			
UW18912		GEN			
E. faecium:					
64/3	ST21	RAM, FUS			(118)
Staphylococcus aureus:					
NCTC8325				Size marker in PFGE	

Plasmids:		
pAD1		Isolated from *E. faecalis* OG1::pAD1 (161)
pCF10		Isolated from *E. faecalis* OG1::pCF10 (58)
pRE25		Isolated from *E. faecalis* RE25::pRE25 (213)

CC, clonal complex; ST, sequence type; only antibiotic resistances relevant for this study are presented: ERY, erythromycin; FUS, fusidic acid; GEN, gentamicin; RAM, rifampicin; STR, streptomycin; TET, tetracycline; VAN, vancomycin

3.1.7 Cell-line

For adhesion studies, the human epithelial colorectal adenocarcinoma Caco-2 cell line, was used.

3.1.8 Animals

Table 3.8: Animals used for the assessment of the pathogenic potential.

Animal	***Company***	***Model***
BALB/c mouse (female; 5-6 weeks old)	Charles River Laboratories International, Inc.	Murine bacteremia
Chicken egg (day 5 and day 10-12 after fertilization)	VALO BioMedia GmbH	Chicken embryo infection
Galleria mellonella larva	Reptilienkosmos.de	*G. mellonella* infection

3.1.9 Consumables

Table 3.9: Devices and materials used in this study.

Consumables	***Manufacturer***
Centrifuge tubes (15mL, 50mL)	CARL ROTH GmbH & Co. KG
CO_2 Gene Compact sachets	Thermo Fisher Scientific Inc.
Eppendorf tubes (0.2, 0.5mL, 1.5mL, 2.0mL)	Eppendorf AG
Filter, Rotilabo® (0.22µm, 0.45µm)	CARL ROTH GmbH & Co. KG
LongSwabs, cotton, sterile	BIOLOG Life Science Institute
Nylon membranes	F. Hoffmann-La Roche AG GmbH
Petri plates	Sterilin Ltd.
Pipette tips (0.1µL, 0.5µL, 2µL, 100µL, 1000µL)	Eppendorf AG
PM panels (PM01, PM02)	BIOLOG Life Science Institute
Polystyrene cell culture microplates, 24-well	Greiner bio-one AG
Polystyrene microtiter plates flat bottom, 96-well	Greiner bio-one AG
Polystyrene semi-micro cuvette	Greiner bio-one AG
Polystyrene semi-micro cuvette	VWR
Reagent reservoirs, sterile	VWR
Syringes (5mL, 10mL)	CARL ROTH GmbH & Co. KG
Thermal paper, Mitsubishi	MS Laborgeräte GmbH
Whatman paper, 3MM	Whatman Ltd.

3.1.10 Equipment

Table 3.10: Instruments used during this work.

Equipment	***Manufacturer***
Autoclave, Biomedis	H+P Labortechnik
Biodocumentation luminescence detector ChemiDocXR	Bio-Rad Laboratories
Centrifuge Sartoris 3-30K (Rotor 19776-H)	Sigma-Aldrich GmbH
Centrifuge 5804R (Rotor F-34-6-38)	Eppendorf AG
Centrifuge 5417 R (Rotor FA)	Eppendorf AG
Centrifuge, mini spin plus (Rotor)	Eppendorf AG
Electrophoresis chambers, Sub Cell Mini And Mini Wide	Bio-Rad Laboratories
Electrophoresis Power supply	Bio-Rad Laboratories
ELISA reader, Sunrise	Tecan Group
Fluorescence reader, Fluorimeter FLA-200	Fujifilm

Freezer (-20°C), LIEBHERRcomfort	Liebherr-holding GmbH
Hamilton MICROLITER® syringe series 700 (10µL)	CARL ROTH GmbH & Co. KG
Hybridization oven and flasks, Techne	Biostep GmbH
Incubator	Binder GmbH
Incubator	Jamesway Incubator Company Inc.
Incubator, HERAcool	Thermo Scientific Inc.
Incubator shaker, Innova® 42	Eppendorf AG
Laminator	Severin Elektrogeräte GmbH
Mercury vapor lamp	MJR Norddeutsche Laborbau GmbH & Co. KG
Microbiological Safety Cabinet HERAsafe	Thermo Scientific Inc.
Microwave oven, Severin	CARL ROTH GmbH & Co. KG
Multicanal-pipette (8 and 12 canals), Research	Eppendorf AG
Multistep-pipette, Research pro	Eppendorf AG
OmniLog PM	BIOLOG Life Science Institute
pH-meter, HANNA instruments	neolab GmbH
Pipettes, Reference, variable	Eppendorf AG
Pipettes, Research, variable	Eppendorf AG
Pipettes, Research plus, variable	Eppendorf AG
Platform shaker, Heidolph Polymax 1040	neolab GmbH
Precision scale, Kern 440-43 N	Sartorius GmbH
Refrigerator, Bosch	Robert Bosch GmbH
Spectrophotometer, Biophotometer plus	Eppendorf AG
Spectrophotometer, NanoDrop®	Thermo Scientific Inc.
Spectrophotometer, NoaspecII	Pharmacia Biotech Inc.
Spectrophotometer, VP	Jouan S.A.
Thermocycler, Gene Amp 9700	Applied Biosystems
Thermocycler, SensoQuest	SensoQuest GmbH
Thermomixer, Comfort	Eppendorf AG
Thermal printer, Mitsubishi	Bio-Rad Laboratories
Turbidimeter	BIOLOG Life Science Institute
Ultraviolet irradiator, Bio-Link Cross linker BLX 365nm	Viler Lourmat
Vacuum blotter, TDNA, Model 230600	Appligene Oncor
Vacuum centrifuge, concentrator 5301	Eppendorf AG
Variable speed pump	Bio-Rad Laboratories
Vortex Genie 2	Scientific Industries
Water bath	GFL GmbH
Water purification system	SG Reinstwasser GmbH

3.1.11 Primer

All primers used in this study were purchased from Life Technologies Corporation and are listed in (Table 6.1 - Table 6.12).

3.2 Methods

3.2.1 Antibiotic resistance profile

Before starting this project, all ST40 strains were tested for their antibiotic susceptibilities by the routine laboratory of the RKI. According to the EUCAST clinical breakpoint table (version 2007), the following reference ranges (in micrograms per milliliter) for susceptibility (s) and resistance (r) were applied to the MIC tests: penicillin and ampicillin, s ≤ 8, r ≥ 16; gentamicin (high-level, HL), HLr ≥ 1024; streptomycin, HLr ≥ 512; glycopeptides, s ≤ 4, r ≥ 16; erythromycin and tetracycline, s ≤ 4, r ≥ 8; chloramphenicol, s ≤ 8, r ≥ 16 (285).

3.2.2 Cytolysin/hemolysin assay

According to Solheim *et al*., *in vitro* ß-hemolytic activity was qualitatively analyzed by the use of MH agar plates containing 5% human blood in combination with 1% glucose and 0.03% L-arginine. Overnight cultures were diluted 1:100 and spotted onto fresh plates. After incubation at 37°C overnight, zones of clearing around the colonies indicated production of cytolysin (227).

3.2.3 Gelatinase assay

In vitro gelatinase expression was determined using Todd-Hewitt agar plates containing 3% gelatin. Overnight cultures were diluted 1:100, spotted onto fresh plates and incubated at 37°C overnight. After plates were placed at 4°C for 5 hours (h), expression of gelatinase resulted in hydrolysis of gelatin, identified by zones of turbidity around the colonies (adapted from the protocol described in (227)).

3.2.4 Isolation of the whole cell DNA

Genomic DNA was isolated by using the DNAeasy Blood and Tissue kit following the manufacturer protocol with an additional step for an efficient lysis of the Gram positive cell wall.

1mL of an overnight culture in BHI broth at 37°C, was centrifuged and re-suspended into 180µL lysis buffer (not included into the kit), containing 1µL RNase. After incubation for 60 minutes (min) at 37°C, 25µL of the Proteinase K solution and 200µL Buffer AL were added and further incubated at 70°C for another 60min. Then 200µL of 96% ethanol were added, mixed and the whole content was pipetted into a DNAeasy Mini spin column. After a centrifugation step at 8,000rpm for 1min, 200µL of the washing buffer AW1 were added to the columns and centrifuged again. 200µL of buffer AW2 were added and centrifuged again at 14,000rpm for 3min. DNA was eluted from the column by incubating with 20µL of buffer AE for 1min at room temperature and centrifuging again at 8,000rpm for 1min. The final DNA concentration was determined using PicoGreen and could also be visualized by gel electrophoresis using 0.8% agarose.

3.2.5 Plasmid isolation

Preparation of plasmid DNA was done using the method of Woodford *et al*. (290) with some modifications (283)).

Cells were grown on BHI agar plate at 37°C and were re-suspended in 1mL of TES buffer. After centrifugation at 8,000rpm for 5min, the pellet was re-suspended and incubated for 60min at 37°C in 200µL of TES buffer containing 10mg/mL lysozyme and 1µL RNase. Afterwards, 400µL of 0,2N NaOH/1% SDS were added, the tube was inverted gently and then incubated at 56°C for 60min, again. For protein precipitation, 300µL of 3M potassium acetate were added. The tube was kept on ice for 20min and subsequently centrifuged at 15,000rpm for 15min. The supernatant was washed two times by adding one volume of phenol/chloroform/isoamyl alcohol (25:24:1) and once again with one volume of chloroform, inverting it 30 times, centrifuged it at 12,000rpm for 10min and collecting the upper, aqueous phase. Finally, the interphase would be clear. The plasmid DNA-containing phase was precipitated with two volumes of ethanol (96%) overnight at -20°C and was centrifuged at 14,000rpm for 10min at 4°C. The pellet was washed with 500µL of 70% ethanol, centrifuged, and finally dried at 37°C for 15 to 30min. Subsequently, the pellet was dissolved in 20µL water for 20min at room temperature. The final DNA

concentration was determined using PicoGreen and plasmid DNA could be visualized by gel electrophoresis using 0.8% agarose.

3.2.6 Determination of DNA concentration

DNA average concentration was determined by using a NanoDrop® spectrophotometer by using default measurement conditions for dsDNA quantification.

For a more specific quantification, DNA concentration was measured by an ultra-sensitive Quant-iT PicoGreen® system using the AIDA image Analyzer. First, a standard curve using the provided lambda DNA was prepared, as well as, appropriate dilutions of the samples, as shown in Table 3.11. 50µL of a prepared 1:200 solution of PicoGreen in TE were added into each flat-bottomed well (A1 until Bx) of a polystyrene black microtiter plate. Additionally, 50µL of each dilution A1 until A8 and B1 until Bx was diluted into the wells and the microtiter plate was scanned on a florescence reader at 480-520nm.

Table 3.11: Scheme for PicoGreen DNA quantification.

Tube	***Type***	***Amount – DNA***	***Amount - TE [µL]***	***Concentration [µg/mL]***
1		5µL lambda DNA	95	5.0
2		50µL of 1	50	2.5
A1	Standard	40µL of 2	60	1.0
A2	Standard	50µL of A1	50	0.5
A3	Standard	40µL of A2	60	0.25
A4	Standard	50µL of A3	50	0.1
A5	Standard	40µL of A4	60	0.05
A6	Standard	50µL of A5	50	0.025
A7	Standard	40µL of A6	60	0.01
A8	Standard	-	100	0.0
B1	DNA sample 1	1µL of DNA sample	99	unknown
B2	DNA probe 1	10µL of B1	90	unknown

(A) Standard curve preparation and (B) investigated sample dilutions are indicated.

3.2.7 Multilocus sequence typing (MLST)

On the basis of seven housekeeping genes, an *E. faecalis* MLST scheme was developed by Ruiz-Garbajosa and colleagues (199).

Primers used for amplification and sequencing of the gene fragments are listed in Table 6.1. After sequencing, sequences of the internal fragments of the seven loci were uploaded and compared with the MLST database (http://efaecalis.mlst.net/). According to the similarity to the database entries, each locus got an allele number and finally the sequence type (ST) arose from a combination of all of the allele numbers.

3.2.8 Pulse field gel electrophoresis and Southern hybridization

The Pulse field gel electrophoresis (PFGE) was used for molecular typing of *Enterococcus* and related Gram-positive bacteria (285). This method is generally based on an alternating electric field generated by hexagonal-arranged electrode pairs. Thus, DNA fragments of a few kilobases (kb) to some megabases (Mbp) are separated with a high resolution (164, 212).

In advance of this dissertation, clonal relatedness of the ST40 strain collection was analyzed via macrorestriction patterns, generated by several PFGE techniques.

a) *Sma*I PFGE

   Bacterial DNA fingerprints were generated by digestion of the DNA using the rare-cutting restriction endonuclease *Sma*I, which has a GC-rich recognition sequence (164, 165).

   All strains of the ST40 collection were prepared for macrorestriction analysis as previously described (285). By using the CHEF III apparatus, PFGE was done by medical technical assistants U. Geringer (RKI) and C. Günther (RKI) as described elsewhere (131, 279). Subsequently, Southern hybridization and immunological detection were practiced as described below. As an external size standard, *Sma*I-digested *S. aureus* NCTC8325 strain was used to calculate the fragment sizes applying BioNumerics version 6.0 software (164).

b) S1 nuclease PFGE

Briefly, plasmid content of the ST40 strains was analyzed after specific S1 nuclease digestion of the genomic DNA, as previously described (15, 70, 131). Subsequent Southern hybridization onto a nylon membrane and immunological detection, which were described in detail in the following part, were used to visualize the linearized plasmids as detectable bands on a faint genomic background (15). PFGE was done by medical technical assistant C. Fleige (RKI).

3.2.8.1 Vacuum Southern blotting

In general, DNA is first separated in an agarose gel (232). Then, the DNA fragments are transferred onto a nylon membrane using Southern blotting. The surface of the nylon membrane is positively charged, so that a stable complex with the negatively charged phosphate of the DNA backbone is formed (203, 231).

Here, Vacuum blotting was used to transfer DNA form plasmid preparation onto the nylon membrane. According to the instructions of the manufacturer of the Vacuum blotter device, the blot was constructed by placing the gel on the surface of the nylon membrane. The transfer was performed by adjusting the vacuum to 50mbar. The gel was completely covered with the Blot buffers I to III for respective 30min. Next, the whole blot was incubated with SSC for 120min. After the entire blot was disassembled, the DNA was cross-linked by 150mJoule of ultraviolet irradiation exposure for 30 seconds (s). Finally, the membrane was washed with water for 10min and was dried at room temperature.

Blot buffer I

HCl	0.25M

Blot buffer II

NaOH	0.5M
NaCl	1.5M

Blot buffer III

Tris	1M
NaCl	2M

SSC (stock solution, 20x)

NaCl	3M
Sodium citrate	0.3M

3.2.8.2 Probe labeling

Using PCR-based Digoxigenin- (DIG) High Prime system, DNA probes were non-radioactive labeled with alkali-labile DIG-11-dUTP. According to the manufacturer recommendations regarding the random primer labeling technique, 40µL of the PCR product were denatured at 96°C for 10min. After immediately cooling down on ice, 10µL of DIG High-Prime solution were added and incubated overnight at 37°C. The reaction was stopped by heating at 65°C for 10min. Before Southern hybridization, DNA probe was denatured by heating for 10min, followed by immediate cooling down on ice. Primers used in that study were listed in Table 6.9.

3.2.8.3 Southern hybridization

The previously to the nylon membrane blotted plasmid DNA was hybridized with the DIG-labeled DNA probe by using the DIG system kit. First, the nylon membrane was pre-hybridized by incubation with 25mL of Hybridization buffer I at 37°C for 2h. The solution was replaced with 12mL Hybridization buffer I containing 5µL freshly denatured probe and was incubated at 37°C for 12h. Then, the membrane was washed twice with 50mL SSC buffer I at room temperature for 5min, followed by twice washing with 50mL SSC buffer II at 37°C for 15min. During this process, dry out of the membrane had to be prevented. By doing this, transferred plasmid DNA was prepared for the final immunological detection.

Hybridization buffer I

SSC	5x
Blocking reagent	1x
N-lauroylsarcosine	0.1%
SDS	0.02%

Solution was heated at 50 – 70°C for 1h.

SSC buffer I

SSC	2x
SDS	0.1%

SSC buffer II

SSC	0.1x
SDS	0.1%

3.2.8.4 Immunochemical detection

Generally, immunochemical detection was performed by an enzyme-linked assay using Roche´s DIG Nucleic Acid Detection Kit.

Alkaline phosphatase-conjugated antibody binds selectively to the DIG-labeled DNA, whereby phosphatase activity could be detected with CDP-Star by chemiluminescence.

First, the membrane was washed briefly with Detection buffer I, where 0.3% Tween was previously added. To prevent undesired non-specific interactions with the antibody, membrane was incubated with 60mL Detection buffer II at room temperature for 30min. Then, 8µL of the anti-DIG antibody (1:10,000) were diluted in 40mL Detection buffer II and the membrane was incubated with this solution for 30min. The unbound antibody was removed by washing twice with 50mL of Detection buffer I for 15min and membrane was equilibrated for 2min with 20mL of Detection buffer III. After these steps, membrane was placed into a hybridization bag and 10.5µL CDP-Star solution in 1.5mL Detection buffer III was added. Air bubbles were removed and it was left 5min in darkness. After removing the CDP-Star solution, light

emission was documented within the ChemiDoc instrument by exposure within 10, 30, 60 and 120min.

The membrane was re-hybridized after removing the label. Therefor, the membrane was incubated twice with 50mL 0.2N NaOH with 0.1% SDS at 37°C for 30min. Then, a washing step with SSC solution (2x) followed. Before re-hybridization, the membrane was dried, in the end.

Blocking reagent (stock solution)

Blocking reagent (Roche) in Hybridization buffer I	10%

Detection buffer I

Maleic acid	0.1M
NaCl	0.15M
pH 7.5	

Detection buffer II

Blocking reagent (Roche)	1x
Detection buffer I	9x

Detection buffer III

Tris-HCl	0.1M
NaCl	0.1M
$MgCl_2$ x 6 H_2O	50mM
pH 9.5	

3.2.9 Polymerase chain reaction (PCR)

The standard PCR reactions were performed using PCR Master mix containing *Taq* Polymerase, nucleotides and PCR buffer. This PCR Master mix was mixed with primer pair, DNA template, and water to a final volume of 25µL, as presented in Table 3.12. Used primers are listed in section 6.

Table 3.12: Regular PCR reaction setting.

Substrate	***Amount***
PCR Master mix	12.5µL
Primer pair	Each 200nM
Genomic DNA (DNeasy)	10ng
Nuclease-free water	Up to 25µL

Cycling conditions were used in accordance to the manufacturer's instructions and were dependent on the annealing temperature of the used primer pair and expected amplicon size. In general, the following conditions were used: An initial denaturation step at 95°C, was followed by 30 to 35 cycles of denaturation (94°C for 30s), annealing (50-58°C for 30s) and extension (72°C for 30s), and finally one step of 10min at 72°C. Then the PCR amplificates were resolved in a 1.4% agarose gel and subsequently stained with ethidium bromide for 15min, washed for other 15min and finally visualized in UV light.

3.2.10 Long template PCR

According to Laverde-Gomez *et al*., long template PCR was used to amplify integration of a PAI at the known genomic integration site, as well as, to analyze its structure using MMH594 PAI as a reference (131, 149, 215).
Primers used in this study had been previously described in (131) and are listed in Table 6.7 and Table 6.8.
According to the manufacturer´s recommendations, two master mixes were prepared separately on ice and were mixed to a final volume of 50µL as presented in Table 3.13.

Table 3.13: Setting of long template PCR.

Master mix I	***Concentration***
dNTP mix	10mM
Primer – forward	300nM
Primer – reverse	300nM
Template DNA	300ng
Nuclease-free water	Up to 25µL
Master mix II	***Amount***
Buffer III (10x)	5µL
Expand Long Enzyme mix	0,75µL
Nuclease-free water	Up to 25µL

Cycling conditions were used as followed: After an initial denaturation step at 92°C for 2min, 10 cycles were run for 10s at 92°C, 30s at 60°C, followed by elongation with 10min at 68°C. Then, additional 25 cycles passed through with 10s at 92°C, 30s at 60°C and 10min at 68°C. Corresponding to the expected length of the amplicon, extension time of the elongation step was increased by 20s for each successive cycle. A temperature of 68°C for 10min was used for the final elongation step.

3.2.11 Sequencing

3.2.11.1 Amplicon Sequencing by Sanger ABI Big Dye technology

The classical method of determining DNA nucleotide sequences is Sanger sequencing, also described as chain termination method (205).
PCR products were amplified by using fluorescently labeled ddNTPs, lacking a 3´hydroxyl-group, which prevents a further elongation of the amplicon. Incorporation of ddNTPs occurs with the same probability just as the dNTPs, also contained in the used BigDye mix. By capillary electrophoresis, DNA fragments are separated by length and the respective fluorescence of the incorporated base is detected. Data analysis resulted in the corresponding electropherogram, which represents the final DNA sequence (according to http://www.lifetechnologies.com/de/en/home.html).

According to the recommendations of Applied Biosystems, PCR mix was prepared as presented in Table 3.14 and used primers are listed in section 6.

Table 3.14: Setting of sequencing PCR.

Substrate	***Amount***
PCR product	5ng
Primer (0.8µM)	2µL
BigDye	1µL
Nuclease-free water	Up to 10µL

PCR was done using the following cycling conditions: a 2min denaturation step at 96°C, following by 25 cycles with 10s at 96°C, 5s at 45°C - 60°C and 4min at 60°C. Amplicons were sequenced at the sequencing laboratory of the RKI in Berlin. Finally, Sanger reads were analyzed by SeqMan (Lasergene 5) or DS Gene software package.

3.2.11.2 *De novo* genome sequencing of selected *E. faecalis* ST40 strains

On the basis of the previous characterizations, 15 representative isolates were selected for *de novo* sequencing by Roche/GS-FLX 454 technology (Table 3.6; 12 isolates at the RKI and three isolates at GATC).

(i) Roche/454 FLX pyrosequencing

Roche/454 FLX pyrosequencing was chosen for *de novo* genome sequencing. Despite of the relatively error-prone raw data sequence (for example due to “InDel” errors), this NGS technology ensures long sequence reads. Until today, this sequencer can produce an average read length of 400bp (296).
In general, the process can be described as follows: First, a library of adapter-linked DNA fragments is constructed. During emulsion PCR as a key procedure, single-stranded DNA coupled to beads is clonally amplified. Then, beads are loaded into the picotiter plate (PTP) and pyrosequencing started, using Roche 454´s Titanium kit. Basically, this sequencing-by-synthesis technology uses bioluminescence to detect incorporation of a nucleotide by DNA polymerase (146, 147, 154, 296).

Finally, usage of this classical sequencing strategy revealed only two strains – D32 (UW7744) and UW7709 – with <100 genomic fragments.
Because no complete ST40 genome was previously sequenced, D32 was chosen to generate a template for a detailed genome comparison. This strain was isolated form pig feces in 2001 as part of the Danish Integrated Antimicrobial Resistance Monitoring and Research Programme (216, 300). Additional to the data of 454 sequencing, long paired-end (LPE) sequencing was used as a complementary technology.

(ii) LPE sequencing

Performed by the service platform of Eurofins MWG-Operon, an 8-kb LPE library was constructed and sequenced on Roche/GS-FLX 454 system. Generally, this means sequencing of the ends of two adaptor-linked DNA fragments, which were originally located approximately 8-kb apart from each other in the genome (113).

This sequencing approach was also used to resolve the additional genomes of both strains UW1833 and UW7709, in more detail. But until now, neither the gap closing nor the genome annotation is completely finished.

(iii) Assembly and Mapping

Eurofins MWG-Operon used Celera Assembler software for assembly and scaffolding. In detail, sequence information of the paired end reads was used to bridge gaps and to determine the orientation and relative position of the contigs derived from 454 pyrosequencing (113).
After receiving these data sets, contig orientation within the chromosomal scaffold was compared to that of *E. faecalis* strain V583 (184) by progressive Mauve alignment (48), which was done by C. Kuenne, staff of the working group of Dr. T. Hain at the Institute of Medical Microbiology of Giessen University.
A total number of 33 remaining gaps within the chromosomal scaffold, as well as, assembly ambiguities (“InDel” errors) were corrected by sequencing of PCR amplicons. Therefor, specific primer pairs, listed in Table 6.10 to Table 6.12, were

identified by MiniMap (*Kuenne, C.T., unpublished software*), which basically combines BLASTN and Primer3. The remaining five intra-chromosomal contigs were ordered and again orientated in comparison to the *E. faecalis* strain V583 (184) by progressive Mauve alignment (also done by C. Kuenne), again. Hereafter, intra-chromosomal gaps were closed, as well as, inversions within the sequence and overlapping regions were identified and corrected by sequencing.
Data management and sequence analysis were done with DS Gene as well as KODON software package.

(iv) Genome Annotation

Basically, ORF prediction and automatic annotation was performed by GenDB annotation pipeline (155) and RAST annotation services (10) at CeBiTec of the University of Bielefeld.
Subsequently, frame-shift mutations, modification of Start-/Stop codons and annotations were checked and manually corrected using online tools, like NCBI ORF Finder and BLAST comparisons (209) against completed and publicly available *E. faecalis* genomes.

A brief report about the complete genome sequence of this porcine *E. faecalis* isolate D32 was published in the Journal of Bacteriology (300), and whole sequence data have been deposited in GenBank under accession numbers CP003726 to CP003728.

(v) Illumina/Solexa sequencing

To improve the accuracy of the sequencing data, genomes of the 14 *E. faecalis* strains were additionally sequenced by using Illumina´s Genome Analyzer IIx at the department of “Genomic and Applied Microbiology” of the Georg-August University of Göttingen.
In each channel of the flow cell, solid-phase amplification produces randomly distributed, clonally amplified clusters of adapter-linked single DNA templates. Based on sequencing-by-synthesis approach, one of four fluorescently labeled nucleotides

is incorporated and emitted fluorescence of each cluster is imaged to identify the complementary base. To allow base-by-base sequencing, fluorophore is separated from the nucleotide by enzymatically cleaving after each sequencing cycle. That implies that raw error rates are greatly reduced (111, 154, 296).

(vi) Hybrid assembly

The hybrid assembly was done by Dr. S. Voget, staff of the working group of Prof. Dr. R. Daniel, at the department of “Genomic and Applied Microbiology” of the Georg-August University of Göttingen.
De novo sequences, generated by both Roche/454 FLX pyrosequencing and Illumina/Solexa sequencing, were assembled in a single run (hybrid assembly) by using Mira assembler software. Here, advantages of the individual sequencing methods are combined: 454 pyrosequencing generated long contigs and using Illumina/Solexa sequencing solved the problem concerning the homopolymers.

3.2.11.3 Genomic comparisons and phylogenetic analyses

Circular map (Figure 4.6), visualizing the *E. faecalis* ST40 genome comparison against the D32 reference genome, as well as, the phylogenetic tree (Figure 4.10) were generated by Dr. S. Voget, staff of the working group of Prof. Dr. R. Daniel at the department of “Genomic and Applied Microbiology” of the Georg-August University of Göttingen. The alignment was calculated with Mugsy (5) and only aligned regions present in all analyzed strains were extracted (“core genome”). These regions were concatenated and positions with gaps removed (201). The resulting core alignment (126.7 kb) was used to infer a Maximum Likelihood tree with RAxML (233). The GTRGAMMA model for nucleotide substitution and rate heterogeneity was utilized, bootstrap support values of 1000 replicates are shown at the nodes. M plutonius was used as an outgroup.

3.2.12 Biolog Phenotyping Microarrays

Biolog Phenotyping Microarrays (PM01 and PM02A MicroPlate™) were used to analyze the metabolic phenotype with focus on utilization of different carbon sources under aerobic conditions. In context of the BMBF “UroGenOmics” consortium (grant no: 0315833C), these assays were done in cooperation with the working group of Prof. Dr. D. Schomburg at Braunschweig University.

Aerobic conditions

Bacteria were incubated on fresh MH agar plates at 37°C for 24h. All microbial following steps were carried out under laminar flow to prevent contaminations. Using a sterile swab, bacteria were transferred into a sterile tube, containing 10mL IF-0a medium (1.2x), and cell suspension were adjusted to 81% transmittance by using the Biolog turbidimeter. Analog to the manufacturer´s recommendations, 20mL of the IF-0a Base (1.2x) were mixed with 0.24mL Redox Dye Mix D (100x) and 2.0mL of a 12x additive solution, containing 24mM $MgCl_2$ x $6H_2O$ and 12mM $CaCl_2$ x 2 H_2O. Finally, 1.76mL of cell suspension was added. 100µL of the final suspension was added to each well of the 96-well Biolog PM01 and PM02A plates. The panels were placed into the OmniLog instrument and incubated at 37°C for 72h, where the utilization of different carbon sources was measured spectrophotometrically and recorded every 15min over the whole incubation period. All assays were repeated for at least three times on different days.

Data evaluation

Data sets were evaluated by the OmniLog Kinetic and Parametric analysis software version 2005. The area under the kinetic curve (area values) was used to compare the utilization of different carbon sources between the strains. Calculation of the arithmetic averages with the corresponding standard deviations was done with Microsoft Excel. Color code, used in Table 4.13 and Table 4.14, was chosen according to Gripp *et al*. (80).

3.2.13 Growth kinetics

To determine the bacterial growth rates, overnight cultures were diluted 1:50 in TS broth and grown at 37°C with shaking. Optical density at 600nm was measured at different time points and the corresponding CFU were calculated by plating serial dilutions of the cultures onto LB agar plates in duplicate.

3.2.14 Biofilm plate assay

E. faecalis also play a significant role in the context of nosocomial infections. During the infections process, the formation of a slime matrix (biofilm) can be assigned an important role.

The potential of selected strains to produce biofilm on flat bottom polystyrene microtiter plates was tested by following the methodology previously described (11, 93, 248) with slight modifications. MH blood agar plate-grown bacteria were re-suspended in TS broth supplemented with 0.25% glucose to a concentration of 5 x 10^8 CFU/mL. 100µL of bacterial suspension was filled in triplicates to each well of the microtiter plate and incubated at 37°C for 24h. After incubation, bacteria were removed and the wells were washed with 200µL PBS for three times. The plates were dried for 1h at 60°C and stained by adding 100µL of 0.2% Gram´s crystal violet solution to each well. After 10min incubation step at room temperature, the stain was removed and the wells were washed again with 200µL PBS for three times. The plates were dried for 10min at 60°C and Gram´s crystal violet was re-suspended by adding 100µL ethanol and shaking for 30min. Finally, optical density (OD) of 595nm was measured in an ELISA reader. Biofilm plate assay for each of the strains was done in triplicate and repeated again.

Statistical analysis

Statistical comparisons were done by unpaired two-tailed t-test using GraphPad Prism 5.01 software package. A *P*-value of <0.05 was considered statistically significant.

3.2.15 Adherence assay

Adherence of Enterococci to the colonic epithelial cells is essential to colonize the gastrointestinal tract as a commensal, but it is also supposed to play an important role in biofilm formation and in translocation across the intestinal barrier.

In context of the BMBF “UroGenOmics” consortium (grant no: 0315833C), assays were done in cooperation with the working group of Prof. Dr. J. Hübner at Freiburg University.

Adherence to human epithelial colorectal adenocarcinoma Caco-2 cells was investigated using a protocol previously described (208, 248) with slight modifications. Caco-2 cells between the 15^{th} – 25^{th} passages were cultivated in 24-well plates to a density of 1 x 10^5 cells/well for 13 – 15 days. The confluent monolayers were incubated with a bacterial cell to epithelial cell ratio of 100:1, as well as, 1000:1 for 2h. After infection, Caco-2 cells were washed with PBS five times, and subsequently lysed with 0.25% Triton X-100 at 37°C for 20min. To quantitatively determine the amount of attached bacterial cells, lysates were diluted in PBS and plated onto LB agar plates.

Statistical analysis

Statistical comparisons were done by unpaired two-tailed t-test using GraphPad Prism 5.01 software package.

3.2.16 Animal models

Below, different animal models are presented which were used for a comparative assessment of the pathogenic potential of the selected enterococcal strains D32 and UW7709. Besides, *E. faecalis* strains V583 and OG1RF, as well as, *E. faecium* 64/3 served as controls.

3.2.16.1 Pathogenicity studies by using the model organism *Galleria mellonella*

Because of its simplicity, *G. mellonella* insect model is attractive to study bacteria to host interactions.

Assay of G. mellonella infection

Accordingly to previously described protocols (163, 182), assays were done with some modifications.

100µL of TSB overnight culture were added to 5mL of fresh TSB medium and were cultured at 37°C for 3h. After centrifugation for 5min at 8,000rpm, cell pellet was resuspended in 1mL sterile PBS. Cell concentration was photometrically measured and cell density of the inoculum was adjusted to 10^7 cells/500µL. Groups of 15 larvae with a weight of about 200mg were separated. Then, 5µL of the bacterial inoculum were microinjected at the base of the last proleg, corresponding to an infective dose of 10^5 CFU/larvae. A control group of larvae was infected with PBS only. The real infective dose was determined by serial dilution, which has been plated on PBS agar plates. Groups of infected larvae were kept per Petri dish at 37°C and the number of dead larvae was checked for a time interval of 18, 24, 42, 48, 66 and 70h. This experiment was repeated at least three times for each of the selected bacterial strain.

Statistical analysis

Using the nominal values of survival and dead, the diagram presented the death rates were calculated by Kaplan-Meier plot method in GraphPad Prism 5.01 software version.

3.2.16.2 Pathogenicity studies by using the chicken embryos as model organisms

In cooperation with the working group of Prof. Dr. H. M. Hafez at the Institute of Poultry Diseases of FU Berlin, pathogenicity of *E. faecalis* isolates was tested in a chicken embryo model (198, 291). By using embryonated chicken eggs, this model could be an interesting alternative in comparison to other complex model systems of

vertebrates. To test the functionality of this assay, infective doses were implemented into yolk sack at day five after fertilization and into allantoic cavity at day 10 to 12 after fertilization, respectively.

Assay of chicken embryo infection

Accordingly to the previously described protocol (198), overnight cultures of the *E. faecalis* isolates were used to generate a cell suspension with 10^7CFU/mL. Test groups of four eggs were separated and unfertilized eggs were sorted out by schiering using a mercury vapor lamp.

a) Infective dose into the yolk sack

At day five after fertilization, infective dose of 10^3 CFU was injected into the yolk sack. Therefore, surface of the eggs was disinfected with 70% ethanol and the eggshell was carefully opened at the blunt pole by the use of a needle. 0.2mL of the infective dose was injected with a sterile disposable syringe and the hole was sealed with liquid paraffin.

b) Infective dose into the allantoic cavity

At day 10 to 12 after fertilization, 0.2mL of each bacterial inoculum (~10^5 CFU) was injected into the allantoic cavity. For it, the surface of the eggs was disinfected with 70% ethanol and the eggshell was carefully opened at the blunt pole by the use of a needle. Finally, the hole was also sealed with liquid paraffin.

A control group of three eggs received saline solution only. Infected eggs were incubated at 37°C for four days. Every day, eggs were screened using the mercury vapor lamp and already dead embryos were discarded. At the end of the test, surviving embryos were killed by the storage at 4°C for 48h and all of the embryos were bacteriological screened.

Statistical analysis

Using the nominal values of survival and dead, the curve presented the death rates was constructed by Kaplan-Meier plot method in GraphPad Prism 5.01 software version.

3.2.16.3 Murine bacteremia model

Murine bacteremia model was used to evaluate the pathogenic potential of selected *E. faecalis* strains by analysis of bacterial growth in blood, liver, kidney and spleen after an intravenous infection via tail vein.
In context of the BMBF “UroGenOmics” consortium (grant no: 0315833C), these experiments were done in cooperation with the working group of Prof. Dr. J. Hübner at Freiburg University, wherein the previously described protocol has been used (105, 248). The animal assays described in the present study were reviewed and approved by the International Animal Care and Use Committee at Harvard University.

For preparation of the inoculum, bacteria were grown in TSB at 37°C overnight. Next, cell suspension was centrifuged and the cell pellet was dissolved in 5mL PBS, spun down again and resolved in 5mL of sterile 0.9% NaCl. Aliquots of 550µL were shock frozen and stored at -80°C.
Eight female six to eight weeks-old BALB/c mice were inoculated intravenously in the tail vein with 10^8 and $5x10^8$ CFU respectively. A control group of mice were injected with sterile saline only. Actual used inoculum was once verified by viable counts on TSA. 48h after infection, mice were sacrificed by CO_2 inhalation and exsanguination. Blood was obtained by cardiac puncture and 100µL were plated on TSA. Furthermore, liver, kidney and spleen were taken out and homogenized in TSB. To verify bacterial counts serial dilutions of these samples were also plated on TSA.
Statistical analysis
Statistical comparisons were done by Mann-Whitney test (non-parametric data) using GraphPad Prism 5.01 software package.

4 Results

4.1 Comparative genomics of *E. faecalis* ST40

Forty-two isolates of *E. faecalis* MLST type ST40 were collected from commensal and pathogenic sources (humans/animals) originating from different countries and years. A detailed listing of the ST40 strains with the corresponding background information is described in Table 3.6.

4.1.1 Pre-characterization of the ST40 strain collection

First of all, the strain collection was checked with respect to several phenotypic and genotypic characteristics, to select representative isolates for genome sequencing.

4.1.1.1 Genomic profile by *Sma*I macrorestriction patterns

Strains were typed by *Sma*I macrorestriction in PFGE identifying sub-clusters of closely related strains, which were independent from their geographical and temporal origin or clinical/non-clinical context (Figure 4.1).

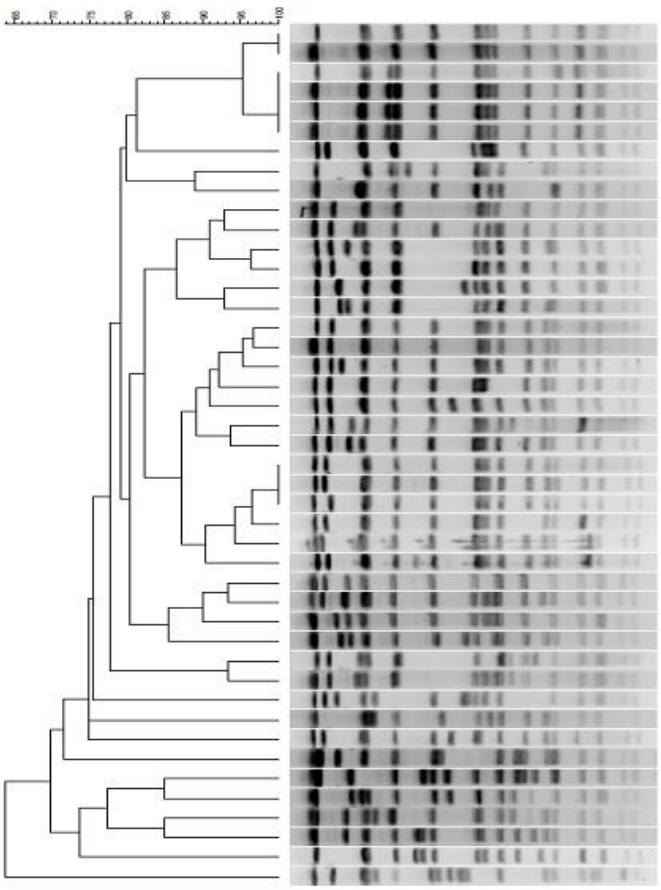

Isolate	Country	Year	Origin
UW6756	D (Leezen)	2006	U
UW7710	DK	-[5]	U
UW6530	D (Augsburg)	2006	U
UW6149	D (Augsburg)	2005	B
UW2860	D (Gera)	2000	B
UW2861	D (Gera)	2000	B
UW7714[1]	NL	2004	U
UW7778	D (Heidelberg)	2004	HC
UW4340	D (Berlin)	2003	B
UW5209	D (Augsburg)	2004	B
UW3107[2]	D (Berlin)	2000	B
UW6724	D (Wernigerode)	2006	HC
UW7761	Cuba (Havanna)	2008	B
UW7777	D (Heidelberg)	2004	HC
UW7780	PL (Warschau)	1996	HC
UW7782	PL (Warschau)	1996	U
UW5213	D (Augsburg)	2004	B
UW7785	PL (Zawiercie)	2000	W
UW7776	D (Heidelberg)	2004	HC
UW7775	D (Heidelberg)	2004	HC
UW7753	ESP (Madrid)	-[4]	B
UW7784	PL (Grajewo)	1999	U
UW7787	PL (Zamosc)	2002	CSF
UW7788	PL (Bytom)	2003	B
UW7790	PL (Wolomin)	2007	HC
UW5744	D (Köln)	2004	U
UW1833	D (Berlin)	1998	U
UW7779	D (Heidelberg)	2004	HC
ATCC 27275[3]	-[4]	<1962	-[4]
LMGT 2333[3]	IS (Reijkjavik)	1990	AC
LMGT 3209[3]	GR (Athen)	<2004	-[4]
D27[3]	DK	-[5]	AC
UW7781	PL (Warschau)	1996	PF
ATCC 27959[3]	USA (Iowa)	1975	M
UW6727	D (Wernigerode)	2006	HC
UW5345	D (Augsburg)	2004	B
UW7789	PL (Biala Podlaska)	2004	U
D32[3]	DK	-[5]	AC
D37[3]	DK	-[5]	AC
UW4889	D (Augsburg)	2004	B
UW7709	DK	-[5]	E
D1[3]	DK	-[5]	AC
UW7791	PL (Makow Maz)	2007	HC
UW5212	D (Köln)	2004	U

Figure 4.1: *Sma*I macrorestriction patterns in PFGE of 44 *E. faecalis* isolates.

Certain sub-clusters indicated a comparably high level of clonal relatedness. Displayed collection comprises 42 ST40 isolates and 2 isolates, belonging to the CC40 ([1] ST268 and [2] ST220). Sequenced isolates are marked with a blue square; [3] reference strain; [4] unknown; [5] unknown (after 2000); AC, animal colonizer; B, blood culture; CSF, cerebrospinal fluid; E, endocarditis; HC, human colonizer; M, bovine mastitis; PF, peritoneal fluid; U, urine; W, wound.

4.1.1.2 Antibiotic resistance profile

Distribution of phenotypic antibiotic susceptibilities was completed by determination of the corresponding genotype by PCR.

Table 4.1: Distribution of antibiotic resistances.

Antibiotic resistance	***Phenotype [%]***	***Resistance gene***	***Genotype [%]***
Vancomycin (VanA-type)	**2.4** (1/42)	*vanA*	**2.4** (1/42)
Erythromycin	**19.1** (8/42)	*ermB*	**21.4** (9/42)
Tetracycline	**81.0** (34/42)	*tetM*	**81.0** (34/42)
Streptomycin (high-level)	**28.6** (12/42)	*aadE*	**33.3** (14/42)
Gentamicin (high-level)	**2.4** (1/42)	*aac6'-aph2"*	**0** (0/42)

Broth microdilution assay was used to determine phenotypic antibiotic susceptibilities. Resistance genes (***aac6'-aph2", aadE***, *ermB*, *tetM*, *vanA*) were determined by PCR.

4.1.1.3 Assessment of putative virulence-associated markers

Presence and expression of putative virulence-associated genes encoded within the *E. faecalis* PAI (149) and/or on the chromosome were investigated by PCR and confirmed by phenotypic *in vitro* assays (Table 4.2). PAI associated aggregation substance *asc-10* gene was found in 16.7% of the isolates. Prevalence of the cytolysin (*cyl*) operon in 33.3% of the strains was associated with the evidence of β-hemolysis *in vitro* (Figure 4.2). The enterococcal surface protein (*esp*) gene was detected in 78.6% of the ST40 collection. All isolates harbored the *gelE* (gelatinase) and *fsr* (major accessory gene regulator) genes and showed *in vitro* gelatinase expression (Figure 4.3).

The capsule locus (*cps*) consists of 11 known open reading frames, namely *cpsA-K*. There are three known capsule operon polymorphisms: (1) *cps* type 2, which includes all 11 genes (e.g. V583); (2) *cps* type 5, which includes all genes except for *cpsF* (like strains of the CC9); and (3) *cps* type 1, where only *cpsA* and *cpsB* are present (e.g. OG1RF) (87, 141, 150). Capsule locus type 1 was verified for all ST40 isolates (Table 4.2).

Table 4.2: Presence of putative virulence factors.

Putative virulence factor	***Putative function***	***% of positive isolates***	***Comment***
Pathogenicity island			
asc-10 (EF0005)	Aggregation substance	**16.7** (7/42)	
cylM (EF0046)	Cytolysin subunit modifier	**33.3** (14/42)	Expression of ß-hemolysis *in vitro*
esp (EF0056)	Enterococcal surface protein	**78.6** (33/42)	
xyl kinase (EF0083)	Xylose kinase	**4.8** (2/42)	
gls24-like (EF0117)	General stress protein	**0** (0/42)	
Other			
gelE (EF1818)	Gelatinase/coccolysin	**100** (42/42)	Expression of gelatinase *in vitro*
fsrB (EF1821)	Accessory gene regulator B	**100** (42/42)	
cps type 1	Capsular polysaccharide	**100** (42/42)	

Presence of putative virulence-associated genes (in italics) was examined by PCR. Numbers in bold represent percentage of positive tested isolates, calculated from the number of the positive genotypes versus the whole strain collection (in parentheses).

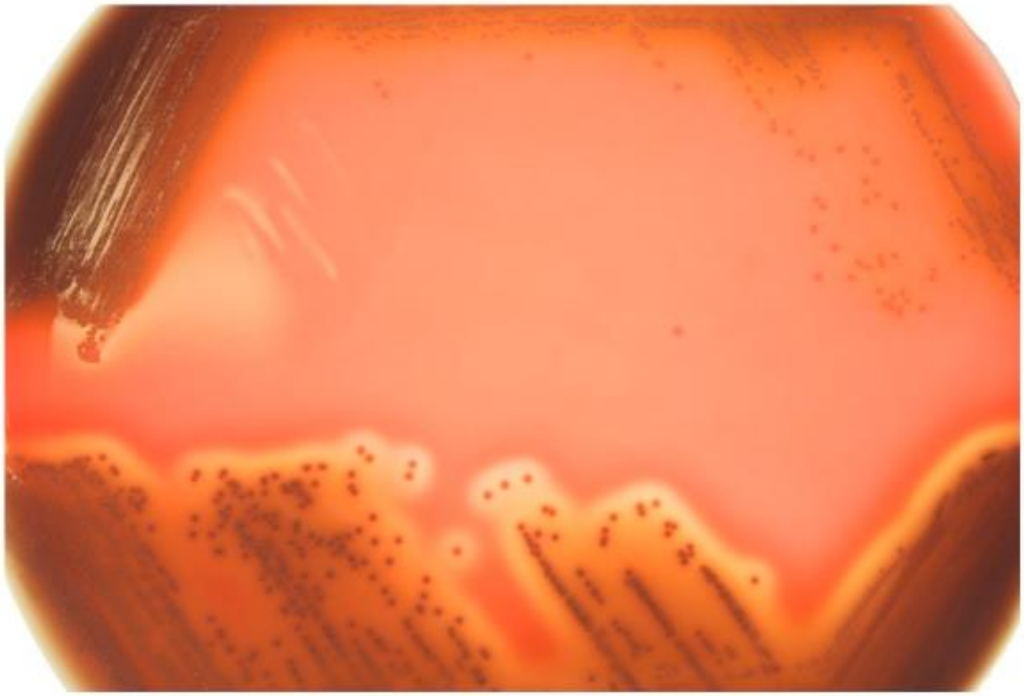

Figure 4.2: Hemolytic activity tested in human blood agar plates.

Human blood agar plate was used to show ß-hemolysis *in vitro*. Here, a representative example is shown: top, non-hemolytic strain OG1RF, bottom, hemolytic *E. faecalis* strain 3114.

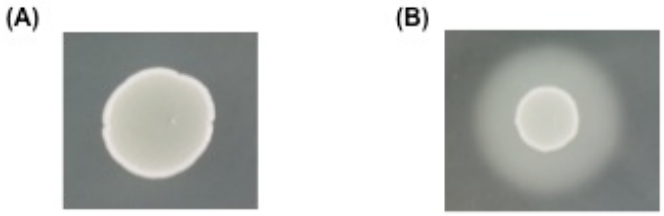

Figure 4.3: Expression of gelatinase *in vitro*.

Expression of gelatinase was visualized by hydrolysis of gelatin, indicated by turbid zones around the colony. Here, two examples are shown, which illustrate possible phenotypes in this experiment: (A) *E. faecium* 64/3 did not expressed gelatinase *in vitro*, (B) expression of an active metalloprotease GelE by *E. faecalis* strain UW7709.

We also tested the ability of the ST40 strains to form biofilms on polystyrene plates. *In vitro* biofilm formation was independently of the presence of putative biofilm-enhancing genes, like *esp* and *asc-10*, and was also inhomogeneous between closely related strains (data not shown). Because of high standard derivations, further studies are necessary.

4.1.1.4 Analysis of plasmid content

Results of plasmid isolation in combination with previously performed S1 nuclease PFGE indicated diversity in plasmid content, varying from none to two plasmids. To exemplify the S1 nuclease analyses, one of the gels is shown in Figure 4.4.

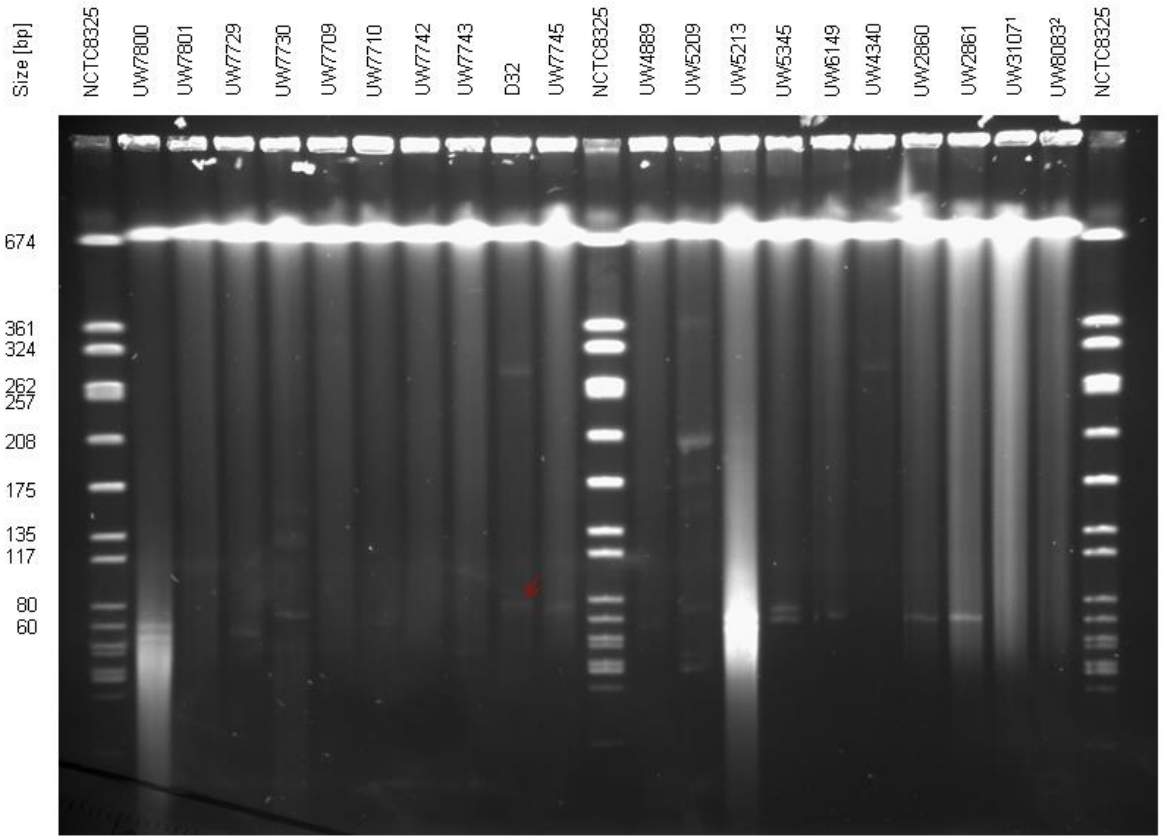

Figure 4.4: S1 nuclease analysis resolving plasmid content of 20 *E. faecalis* isolates.

This representative gel of S1 nuclease PFGE showed the presence of none to two linearized plasmids. Displayed collection comprises 18 ST40 isolates and 2 isolates, belonging to the CC40 ([1] ST220 and [2] ST268). A red arrow points at a plasmid of the sequenced E. faecalis strain D32, revealing its size of circa 75kb. The upper bands (migrating at an apparent size of 674kb), visible in all lanes, correspond to undigested chromosomal DNA.

The detailed properties of the plasmids of the 15 *de novo* sequenced ST40 strains are described in Table 4.11.

4.1.2 Genome sequencing strategies

4.1.2.1 *De novo* 454 genome sequencing of 15 representative *E. faecalis* ST40 isolates

On the basis of these previous characterizations, a subset of 15 strains (Figure 4.1), representing the diversity of the ST40 collection and some pairs of related isolates, was *de novo* sequenced by Roche GS FLX 454 technology (12 isolates at the Robert Koch Institute and 3 isolates at GATC). Genomic contigs were generated and assembled by using the Newbler assembler software (Table 4.3).

Table 4.3: Quality report of 454 sequencing data assembled with Newbler software.

Isolate	*Origin*	*GC content [%]*	*Number of contigs*	*Calculated genome size [bp]*	*Coverage [n-fold]*
UW6149	B	37.51	163	3,239,149	13.92
UW2860	B	37.51	104	3,062,478	15.78
UW6724	HC	37.31	298	3,050,235	10.04
UW7761	B	37.51	178	2,912,463	11.60
UW7777	HC	37.55	133	2,945,792	34.32
UW7780	HC	37.35	267	3,059,826	15.60
UW7753	B	37.32	148	3,158,895	13.54
UW1833	U	37.10	228	3,190,695	17.29
UW7779	HC	37.21	143	3,024,279	22.45
UW7729	AC	37.26	370	2,946,024	11.16
UW7801	M	37.51	218	2,900,593	10.55
UW6727	HC	37.02	236	3,275,508	18.39
UW7744 (D32)	AC	37.63	71	2,840,807	24.36
UW7709	E	37.26	94	2,921,715	23.13
UW7742	AC	37.34	124	2,889,018	22.59

Genomes were *de novo* sequenced and assembly was done with Newbler assembler software. Assembly of only two strains D32 and UW7709 resulted in less than 100 contigs. Genome size varied between 2.8 to 3.3Mbp, irrespective of the clinical or non-clinical background of the isolates. Coverage of the genomes was between 10 to 34-fold; AC, animal colonizer; B, blood culture; E, endocarditis; HC, human colonizer; M, bovine mastitis; U, urine.

Although in principle suitable for *de novo* genome assemblies, classical 454 sequencing revealed only two strains (D32 and UW7709) with less than 100 genomic fragments. Independent from a supposed pathogenic potential, the calculated

genome size varied from 2.8 to 3.3Mbp. For the majority of the genomes, only a low coverage of less than 20 was achieved. To improve the accuracy of the sequencing data, the following workflow was pursued:

(i) Representing the first finished ST40 genome, D32 was chosen to generate a template for a detailed genome comparison (see part 4.1.2.2).

(ii) Genomes of the other 14 *E. faecalis* strains were additionally sequenced by using Illumina´s Genome Analyzer IIx (see part 4.1.2.3).

4.1.2.2 Generation of a ST40 template for a detailed genome comparison

To resolve the complete genome of *E. faecalis* ST40 isolate D32, a classical short read library and a Long Paired End (LPE) library were prepared and 454 sequenced (see part 3.2.11.2). As previously described in part 4.1.2.1, *de novo* genome sequencing of D32 generated 71 contigs and also resulted in 125,952 reads with an average length of 392bp. Additional sequencing of an 8-kb LPE library generated 97,660 reads with an average read length of 346bp. Using Celera Assembler software, both data sets were assembled into three scaffolds. One chromosomal scaffold comprised of 28 contigs and the other two scaffolds suggested a plasmid origin. On the basis of the *E. faecalis* strain V583, chromosomal contigs were orientated by progressive Mauve alignment (48). Remaining gaps and assembly ambiguities (“InDel” errors) were resolved in detail and corrected by sequencing of PCR amplicons. ORF prediction and definition of the coding sequences (CDS) were performed by GenDB annotation pipeline (155). Frame-shift mutations, modification of Start-/Stop codons and annotations were checked and manually corrected using online tools, like NCBI ORF Finder and BLAST comparisons (209) against finished *E. faecalis* genomes (V583, OG1RF and 62).

4.1.2.3 Solexa sequencing and hybrid assembly strategy

For detailed comparisons with the D32 reference genome, quality and coverage of the 14 selected and already pyrosequenced ST40 strains had to be improved. For

that purpose, strains were additionally sequenced at the working group of Prof. Dr. Rolf Daniel (department of “Genomic and Applied Microbiology” of the Georg-August University of Göttingen) by using Illumina´s Solexa technology.

Generally, 454 pyrosequencing generates long reads, while the “InDel” problem in regions can be corrected by Solexa generated sequences. By using Mira assembler software (33, 34), reads of both sequencing strategies were hybrid assembled and thus, the even described advantages of both technologies were usefully combined (Table 4.4).

Table 4.4: Quality report of hybrid assemblies considering of 454 and Solexa sequencing data.

Isolate	*No. of assembled reads*	*Coverage (454) [n-fold]*	*Coverage (Solexa) [n-fold]*	*No. Scaffolds*	*Genome size [bp]*	*GC content [%]*
UW6149	5,060,490	12.78	166.36	72	3,011,563	37.46
UW2860	5,318,329	14.68	176.92	74	3,003,615	37.49
UW6724	1,232,615	9.91	39.94	38	3,085,224	37.33
UW7761	2,025,698	12.71	81.94	26	2,939,826	37.53
UW7777	1,504,959	24.05	45.28	24	2,999,678	37.43
UW7780	1,108,686	10.91	37.28	38	3,115,640	37.31
UW7753	1,424,574	11.14	39.48	67	3,119,011	37.09
UW1833	3,127,985	14.89	100.92	66	3,243,986	37.05
UW7779	1,412,336	18.92	37.1	45	3,070,536	37.20
UW7729	972,823	9.01	28.64	75	3,094,285	37.19
UW7801	1,478,988	10.79	56.72	26	2,933,628	37.52
UW6727	1,442,566	12.5	45.58	34	3,330,760	36.91
UW7709	2,403,224	12.98	90.18	36	2,928,951	37.30
UW7742	3,271,151	18.06	101.23	64	3,054,136	37.17

Genomes of 14 selected ST40 isolates were sequenced by using Solexa technology. Reads of 454 and Solexa sequencing were hybrid assembled by using Mira assembler software (33, 34) and resulted in an increase of coverage in combination with reduction of the number of large contigs.

4.1.3 Genomic characteristics of D32 in comparison to the already finished and publicly available *E. faecalis* genomes

The completed *E. faecalis* D32 circular chromosome contains of 2,987,450bp with a GC content of 37.49%. Finally, annotation of the chromosome created a total of

2,890 CDS, 62 tRNA-encoding genes, and four entire rRNA-encoding operons. The final annotated sequences were submitted in GenBank under the accession numbers CP003726 to CP003728 (300).

4.1.3.1 Chromosome

First analyses of the core genome of strain D32 did not reveal any specific features. Analog to the determination of the antibiotic profile (Table 4.1), high-level resistance to streptomycin (129) is chromosomally encoded by an aminoglycoside 6-adenyltransferase gene *aadK*.

We also used a Venn diagram, generated by the web application EDGAR (20), to illustrate homologies and differences between the finished and publicly available non-ST40 *E. faecalis* genomes.
Genome alignment, illustrated by Venn diagram (20) (Figure 4.5), showed a common gene pool of 2173 CDS, present in all of the finished *E. faecalis* genomes. This analysis also revealed that the number of unique CDS of the clinical strain V583 (184) was approximately two times higher than the counts of the commensal isolates 62 (28) and D32 (300), as well as, the probiotic Symbioflor 1 strain (71). As a derivate of the commensal isolate OG1, OG1RF strain (24) carried the minimal number of 140 unique CDS. Both commensal strains 62 and D32 shared significantly more CDS with the V583 chromosome, while the Symbioflor and OG1RF chromosomes overlapped less with the V583 chromosome.

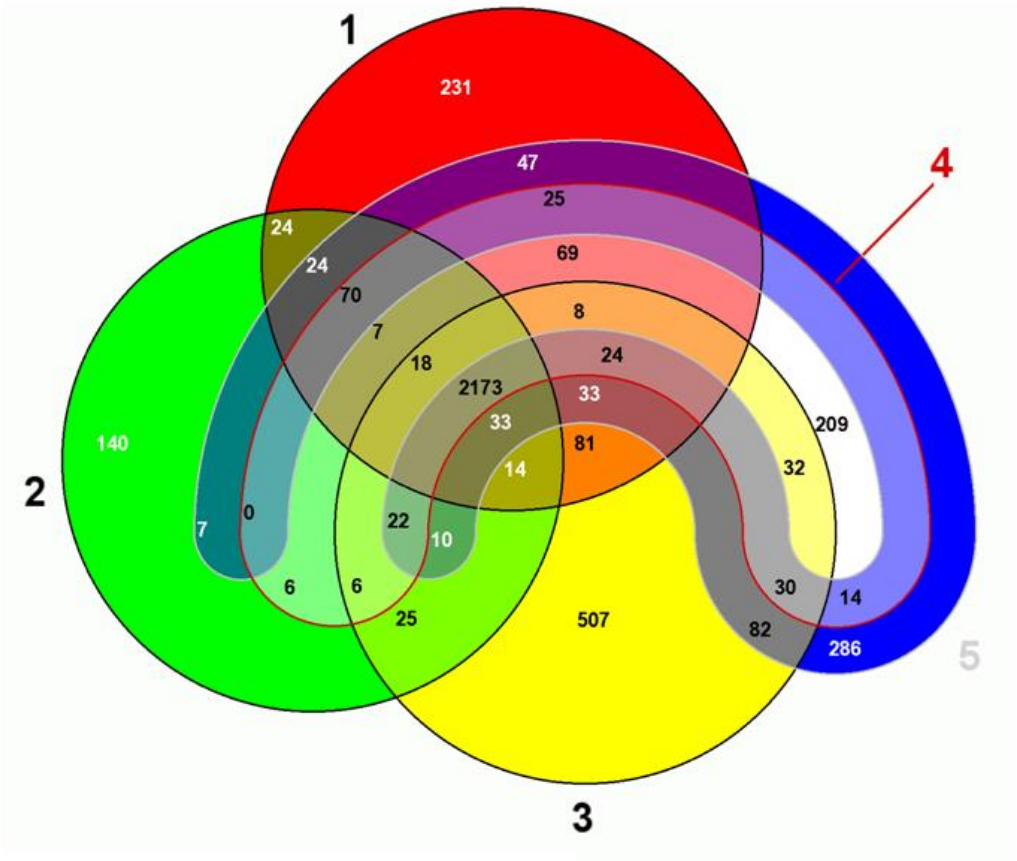

Figure 4.5: Comparative analysis of the finished and publicly available *E. faecalis* genomes.
EDGAR generated Venn diagram (20) facilitates visualizing core and strain-specific ("unique") genes. This comparative analysis only exploits CDS of the chromosomes without considering of plasmid genes, whereby all strains shared 2197 CDS; 1, *E. faecalis* strain 62 (28); 2, *E. faecalis* strain OG1RF (24); 3, *E. faecalis* V583 (184); 4, *E. faecalis* probiotic strain Symbioflor 1 Clone DSM 16431 (71); 5, *E. faecalis* strain D32 (300).

Genomic islands (GI)

Focusing of virulence-associated markers located on the PAI (location: 414203 – 449940, EFD32_0408 – EFD32_0443), analysis of genome data in conjunction with PCR results revealed that it only contained a bile acid hydrolase (*cbh*) and lactose metabolic pathway genes (*lacABCDEFG*). Utilization of lactose was also demonstrated by Biolog MicroArray™ analysis (part 4.2). In accordance to the original PAI in MMH594 (149, 215), the PAI of the D32 genome lacked common markers such as enterococcal surface protein gene (*esp*) and the cytolysin operon, which was also demonstrated by PCR and hemolytic activity test *in vitro* (part 4.1.1.3).

Additionally, a previously novel and uncharacterized GI with a size of 138kb (location: 1901082 – 2036659, EFD32_1828 – EFD32_1978) is integrated at the attachment site of the conjugative *vanB* transposon in V583 (EF_2282 – EF_2334) (184) and m-inositol (*iol*) operon in OG1RF (24), respectively (see parts 4.1.4.1 and 4.2). Genomic data of the probiotic strain Symbioflor indicated that neither the *iol* operon of the OG1RF nor the *vanB* transposon of V583 or the uncharacterized GI of the D32 strain are present (24, 53, 71).

We used SwissProt and BLASTP analyses to identify similarities to capulse-like genes encoded by the novel GI in D32, also described for *Streptococcus pneumonia*e and *Bacillus subtilis* (Table 4.5).

Table 4.5: SwissProt and BLASTP analyses of a putative capsule-encoding region within the *E. faecalis* D32 GI.

Locus Tag EFD32_	***annotated product name***	***SwissProt - best hits[a]***	***BLASTP - best hits[a] S. pneumoniae TIGR4***	***BLASTP - best hits[a] B. subtilis 168***
1891	UDP-glucose 6-dehydrogenase	UDP-glucose 6-dehydrogenase (0.0, 64%, 100%)	None	UDP-glucose dehydrogenase (2e-41, 29%, 86%)
1892	Glycosyl transferase, group 1 family protein	Glycosyltransferase Gtf1 (2e-07, 26%, 45%)	Group 1 glycosyl transferase (2e-08, 26%, 43%)	UDP-glucose: polyglycerol phosphate alpha-glucosyltransferase (1e-07, 30%, 36%)
1895	UDP-glucose 4-epimerase	UDP-glucose 4-epimerase (2e-163, 65%, 98%)	Capsular polysaccharide biosynthesis protein Cps4J (1e-169, 65%, 98%)	EpsC, UDP-sugar epimerase (1e-42, 35%, 88%)

1897	Undecaprenyl-phosphate galactosephosphotransferase	Undecaprenyl phosphate N,N'-diacetylbacillosamine 1-phosphate transferase (3e-77, 58%, 96%)[b]	Capsular polysaccharide biosynthesis protein Cps4E (4e-38, 47%, 91%)	Phosphotransferase (6e-78, 56%, 96%)[c]
1901	Putative tyrosine-protein phosphatase CapC	Tyrosine-protein phosphatase YwqE (3e-61, 41%, 100%)	Capsular polysaccharide biosynthesis protein Cps4B (9e-25, 27%, 88%)	YwqE, protein tyrosine-phosphatase (3e-63, 41%, 100%)
1902	Tyrosine-protein kinase YwqD	Tyrosine-protein kinase YwqD (2e-69, 50%, 93%)	Capsular polysaccharide biosynthesis protein Cps4D (5e-40, 38%, 88%)	YwqD, protein tyrosine kinase (2e-70; 50%, 93%)
1903	Capsular polysaccharide synthesis enzyme	Probable capsular polysaccharide biosynthesis protein YwqC (8e-42, 38%, 93%)	Transcriptional regulator (1e-70, 41%, 94%)	YwqC, modulator of YwqD protein tyrosine kinase activity (5e-41, 38%, 93%)
1904	Transcriptional regulator lytR	Transcriptional regulator LytR (3e-163, 72%, 96%)	Transcriptional regulator (1e-70, 41%, 94%)	Membrane-bound transcriptional regulator LytR (4e-81, 41%, 90%)

[a] Values in parentheses are E value, % identity, % query coverage; [b] second best hit: uncharacterized sugar transferase EpsL (7e-76, 56%, 96%); [c] second best hit: TuaA, putative undecaprenyl-phosphate N-acetylgalactosaminyl 1-phosphate transferase (4e-26, 40%, 69%).

Prophages

The web server PHAST (PHAge Search Tool) (299) was used to identify and graphically display integrated prophage structures in the D32 genome and both plasmids. Six prophage regions have been identified in D32 chromosome, of which three regions were intact, two regions were incomplete and also one questionable region was detected (Figure 4.6). Structures of prophages could not be identified in both plasmids.

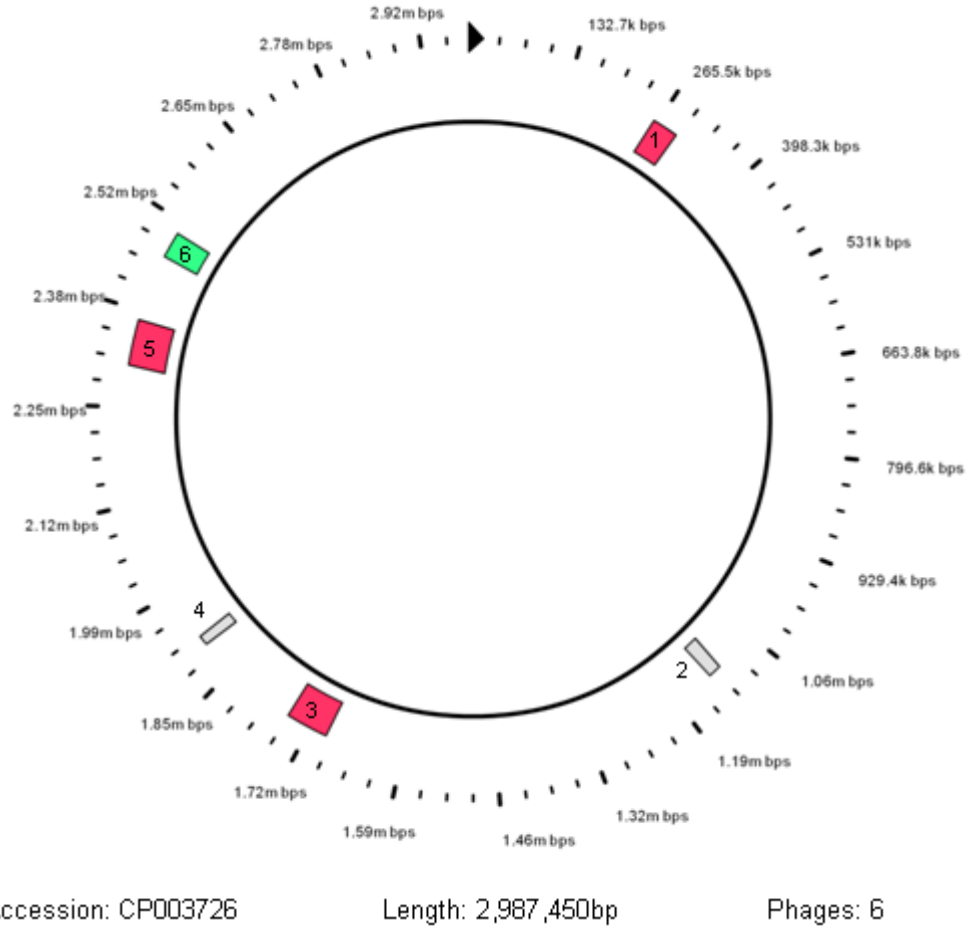

Figure 4.6: Circular D32 genome view with marked prophage regions.

By using PHAST (299), six putative prophage sequences (no. 1 – 6) were identified as part of the D32 chromosome. Red boxes indicate intact prophages; grey-colored boxes display incomplete prophages, while the green box symbolizes a questionable prophage.

Characteristics of the identified prophage regions are listed below (Table 4.6). In addition to the integration of *E. faecalis* temperate bacteriophages philFL4A and phiFL1A, comparison of sequence similarities indicated presence of Listeria phage B025 and Bacillus phage phBC6A52. The last one was also identified in the genomes of *E. faecalis* strains V583 and Symbioflor 1 by using PHAST (299).

Table 4.6: Characteristics of D32 prophages, predicted by PHAST (299).

Phage region	*Length [kb]*	*Completeness*	*No. of CDS*	*Position*	*Similarity (Accession no.)*	*GC content [%]*
1*	37.5	Intact	50	257732-295298	Enterococcus phage phiFL4A (NC_013644)	37.73
2	22.3	Incomplete	25	1116761-1139067	Enterococcus phage phiEf11 (NC_013696)	38.58
3*	60.2	Intact	54	1699388-1759670	Enterococcus phage phiFL1A (NC_013646)	34.90
4	17.1	Incomplete	18	1904479-1921631	Lactobacillus phage AQ113 (NC_019782)	30.29
5*	67.7	Intact	64	2310353-2378090	Listeria phage B025 (NC_009812)	35.98
6°	37.3	Questionable	50	2469609-2506979	Bacillus phage phBC6A52 (NC_004821)	35.06

After localization of start and end positions (*attL*/*attR*) of the six putative prophages (region no. 1 - 6), PHAST predicted whether the region contains an intact (red marked), an incomplete (grey marked) or a questionable prophage (green marked). By comparing the phage region with the database, the highest similarity to an already described bacteriophage was determined, automatically; * bacteriophages also identified by the web application Prophage Finder (23).

According to the results of PHAST search, additional usage of the web tool Prophage Finder (23) also revealed four putative prophages, integrated into the chromosome. These predicted prophages showed homologies to the prophage regions no. 1, 3, 5 and 6, also determined by PHAST.

PHAST analysis did not identify any attachment sites for prophage region no. 2, which was also defined as an incomplete phage, but also detected in public available and finished genomes of *E. faecalis* strains V583, OG1RF, 62 and Symbioflor 1, as a part of the chromosome. Additionally, integration of the incomplete prophage region no. 4 into the uncharacterized genomic island (GI; 138kb) was predicted. Both regions only represented fragments of prophage remnants and could be disregarded, finally.

4.1.3.2 Plasmids

As previously described, scaffolding also revealed two plasmid scaffolds. Plasmid EFD32pA contains of 12,893bp and 14 CDS were predicted. It could be characterized as an Inc18 broad-host-range plasmid according to the similarity of its putative replicase belonging to *rep*-family 1 genes (114, 272). Here, resistance to macrolide-lincosamide-streptogramin B antibiotics is encoded by an rRNA adenine N-6-methyltransferase gene (*ermB*).

For the larger plasmid EFD32pB, a size of 62,162bp was calculated and annotation resulted in 75 CDS. By using RAST server (10) and NCBI database (209), analyses revealed only a few sequence similarities, such as the autolysin N-acetylmuramoyl-L-alanine amidase (family A) or other genes associated with replication, stabilization and mobilization. According to the established Rep typing system (114), the plasmid family could not been unambiguously determined (see part 4.1.4.1).

There is a conflict regarding the size of one plasmid of D32. S1 nuclease PFGE indicated a size of 75kb (see Figure 4.4 and Table 4.11), while genome sequences suggested plasmid EFD32_pA with a size of 12,893bp and EFD32_pB with 62,162bp (see part 4.1.3.2). We suppose an assembly error and a combination of both scaffolds in to one (exactly 75kb) but could not confirm this by further analyses.

4.1.3.3 Presence of CRISPR loci and characterization of integrated spacers

Described as a bacterial adaptive immune system, CRISPR-*cas* system prevents integration of foreign DNA elements, like plasmids, transposons and viruses (14, 230).

By using the web application CRISPRFinder (82), two CRISPRs and one additional questionable structure (Table 4.7), lodged in CRISPR database (CRISPRdb) (81), were identified in the complete genome sequence of E. faecalis strain D32. Precisely formulated, CRISPR1 (NC_018221_1) possesses nine spacers (Figure 4.7), while CRISPR2 (NC_018221_2) composed of 13 spacers (Figure 4.8).

Table 4.7: CRISPRdb (81) revealed CRISPR loci in *E. faecalis* D32 genome.

CRISPR-ID	*Start position*	*End position*	*No. of spacer*	*DR consensus*
CRISPR1 (NC_018221_1)	498298	498926	9	GTTTTAGAGTCATGTTGTTTAGAATGGTACCAAAAC
CRISPR2 (NC_018221_2)	1772093	1772986	13	GTTTTGGTACCATTCTAAACAACATGACTCTAAAAC
CRISPR4 (NC_018221_4)	2098379	2098492	1	ACAACGTTCCCTTTGGTCACCTTGTGCTGTTC

Presence of two CRISPR loci (1 and 2) and one questionable structure (grey marked) was lodged in CRISPRdb. Database entries correlated to the results of PCR and sequencing, as described in Table 4.12.

```
# Sequence: NC_018221
# Description: Enterococcus faecalis D32 chromosome, complete genome.
# Length: 2987450
# Id: NC_018221
#
#================================================================================
# Crispr Rank in the sequence: 1
# Crispr_begin_position: 498298  Crispr_end_position: 498926
# DR: GTTTTAGAGTCATGTTGTTTAGAATGGTACCAAAAC       DR_length: 36   Number_of_spacers: 9
#================================================================================
Spacer_begin_position    Spacer_length   Spacer_sequence
               498334               30   GCACACACACGCTACTCACAGGCATTATAG

               498400               30   GTTTTCATTTAAGTAGTGCGCTTGATATGC

               498466               30   GTGCAACAAAAGAATATTGTTGTCAATGGT

               498532               30   ATCAGTTGTCGGGAAATTGCCGGAGCGTGG

               498598               30   TTCAAGAAAGCTATGGAAGTTCTGAAGCAA

               498664               30   TGGGGCTAAAGGTGTAGCACATCAAGTTTC

               498730               29   TAAAACAAGACGAAATGAGGAAATTAACA

               498795               30   TCATAGCAGACCAACCTGCTCCATCGCTTG

               498861               30   CAATGTAAATGCTCATTATGATTTACATAT
```

Figure 4.7: CRISPR1 locus of D32.

CRISPR1 locus (NC_018221_1), lodged in CRISPRdb (81), contained nine spacers. DR, directed repeats.

```
# Sequence: NC_018221
# Description: Enterococcus faecalis D32 chromosome, complete genome.
# Length: 2987450
# Id: NC_018221
#
#==========================================================================
# Crispr Rank in the sequence: 2
# Crispr_begin_position: 1772093         Crispr_end_position: 1772986
# DR: GTTTTGGTACCATTCTAAACAACATGACTCTAAAAC       DR_length: 36   Number_of_spacers: 13
#==========================================================================
Spacer_begin_position    Spacer_length   Spacer_sequence
              1772129               30   AAATTTTTTGAACTTAATGCAATTTCTTGA

              1772195               30   AAAACTTTTGACGGCTCTTTAGTCAACCCA

              1772261               30   GGAGAAATGTAGCTGCTGTTTTGACATTAG

              1772327               30   TGTTTCATCGTCCTTTCTATTTGGGAAGTG

              1772393               30   TTTGATAATCCAGAATCAACATCTTCACCA

              1772459               30   TTCTATTCTTGCCTTTGCCTTTAAATTAGC

              1772525               30   TTAGGATTGCATCACGCTCTACTTCAACAT

              1772591               30   GCAACTTTTGTTTTCTTTTCTTCTTTTGCT

              1772657               30   TACGAGCTCCCAACATACGTTGACGGTGCA

              1772723               30   AGCTTCAGTAAATTGGTTACACAAACCTCA

              1772789               30   AAGTACTCAGATCCAACAAGAAATCGATAA

              1772855               30   TCTTTGACAATATCATAATCCATGTGCTGA

              1772921               30   TCCGTTGTCTAATTCGATTAATTTCATCAT
```

Figure 4.8: CRISPR2 locus of D32.

CRISPR2 locus (NC_018221_2), lodged in CRISPRdb (81), contained 13 spacers. DR, directed repeats.

In the reference sequence D32, four annotated *CRISPR-associated* genes were identified in relation to CRISPR1 locus (Table 4.8).

Table 4.8: CRISPR-associated genes near to the CRISPR1 locus.

Locus_tag	***Start***	***End***	***Product***
EFD32_0487	492339	496352	CRISPR associated protein
EFD32_0488	496353	497219	CRISPR associated protein
EFD32_0489	497216	497545	CRISPR associated protein
EFD32_0490	497546	498205	CRISPR associated protein

Presence of *CRISPR-associated* genes was analyzed by CRISPR-Finder (82) and identified four genes in striking distance to the CRISPR1 locus. In contrast, the single CRISPR2 locus lacked functional *cas* genes.

By using publicly available CRISPRdb (81), BLAST comparisons (209) of both CRISPR loci only revealed similarities of five integrated spacers of the *cas*-deficient CRISPR2 locus to previously described enterococcal phages, as presented in Table 4.9.

Table 4.9: Similarity of CRISPR spacers to publicly available MGE.

CRISPR_ spacer-no.	***Spacer sequence***	***Seqeunce identity****	***Significant alignments of blastn***	***Area of identity***
CRISPR2_3	GGAGAAATGTAGC TGCTGTTTTGACAT TAG	30/30	gb|HQ426665.1| *Enterococcus faecalis* plasmid pLG2	pLG2-0017 hypothetical protein
CRISPR2_5	TTTGATAATCCAGA ATCAACATCTTCAC CA	26/30	gb|GQ452243.1| Enterococcus phage phiEf11, complete genome	PHIEF11_0019 putative phage tape measure protein
CRISPR2_7	TTAGGATTGCATCA CGCTCTACTTCAA CAT	29/30	gb|GQ478087.1| Enterococcus phage phiFL3B, complete genome	gp37 conserved hypothetical protein
		29/30	gb|GQ478086.1| Enterococcus phage phiFL3A, complete genome	gp34 transcriptional regulator
CRISPR2_9	TACGAGCTCCCAA CATACGTTGACGG TGCA	28/30	gb|JF731128.1| Enterococcus phage SAP6, complete genome	LPS glycosyltransferase
CRISPR2_13	TCCGTTGTCTAATT CGATTAATTTCATC AT	30/30	dbj|AB712291.1| Enterococcus phage BC-611 DNA, complete genome	efb53 hypothetical protein
		30/30	gb|JF731128.1| Enterococcus phage SAP6, complete genome	Intergenic region

BLAST comparisons of the spacer of D32 CRISPR loci (209). CRISPR spacers are numbered in consecutive order from left to right. Only spacers with sequence identities to mobile genetic elements are listed. * Sequence identity is shown as the number of bp with sequence identity in GenBank/total number of bp in this spacer.

Results of further investigations regarding the presence of CRISPR loci within the collection of the sequenced *E. faecalis* ST40 strains will be presented in part 4.1.4.4.

4.1.4 Comparative analysis of *E. faecalis* ST40 genomes

4.1.4.1 Comparative genome alignment

Comparisons of the 14 ST40 draft genomes against the D32 reference genome suggested a high level of genomic similarity regarding the core, irrespective of their geographical, temporal or clinical/non-clinical origin (Figure 4.9).

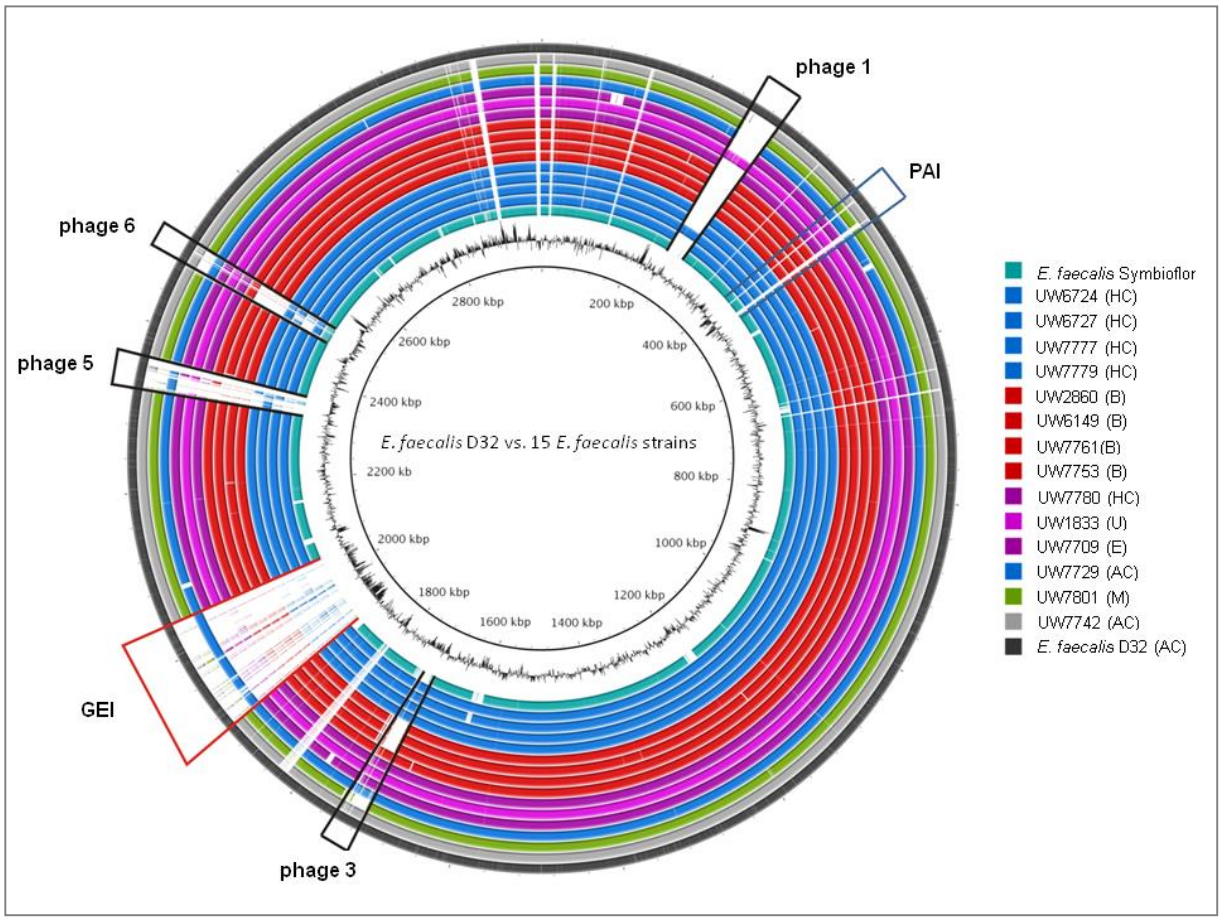

Figure 4.9: *E. faecalis* ST40 genome comparison against the D32 reference genome.

Generated by BRIG (4), the circular map illustrates the whole genome comparison of D32 against the other 14 sequenced ST40 isolates and the probiotic isolate Symbioflor 1 Clone DSM 16431 (71). The outer cycle (dark grey) represents the complete genome of the reference strain D32. The shade of color is geared to similarities in origin of the strains. The inner cycle illustrates the GC content of D32. Location of the PAI is illustrated by a blue colored box, while the red box indicates the presence of an uncharacterized and large genomic island (GI; 138kb). Additionally, black labels highlighted four identified prophages of D32; A, animal; B, blood culture; C, colonizer; E, endocarditis; H, human; M, bovine mastitis; U, urine.

Of note, genome comparisons also revealed that the probiotic Symbioflor 1 strain contains parts of the PAI (see Figure 4.9) (53, 184).

4.1.4.2 Phylogenetic analysis

Phylogenetic analysis was done by using concatenated nucleotide regions, represented in all aligned strains and after elimination of existing gaps. A phylogenetic tree resulting from an alignment of concatenated sequences, presented in all analyzed strains, is shown in Figure 4.10. It revealed a high level of genomic similarity of unrelated ST40 strains, despite their diverse origins and the time interval from 1975 to 2008.

When focusing on the ST40 isolates, the phylogenetic tree also showed an exceptional position of D32 in relation to the other sequenced ST40 isolates and furthermore, its close relationship to the other Danish porcine isolate UW7742.

Within the genomic homology, strains of a similar origin were not arranged in the same cluster. Especially, animal-associated strains were more diverse than human isolates. But, whole genome alignment suggests a minimal phylogenetic distance between the fish colonizing strain UW7729 and the isolate UW7801 from bovine mastitis.

When focusing on the human associated isolates, phylogenetic analyses also indicated a high genomic similarity between the human colonizing strain UW7779 and the urine isolate UW1833, as well as, the blood culture isolate UW7753 and the isolate UW7709, obtained from a patient with infective endocarditis.

As expected, the other completed and publicly available *E. faecalis* genomes branch separately, supporting their assessment to different sequence types and clonal complexes based on MLST.

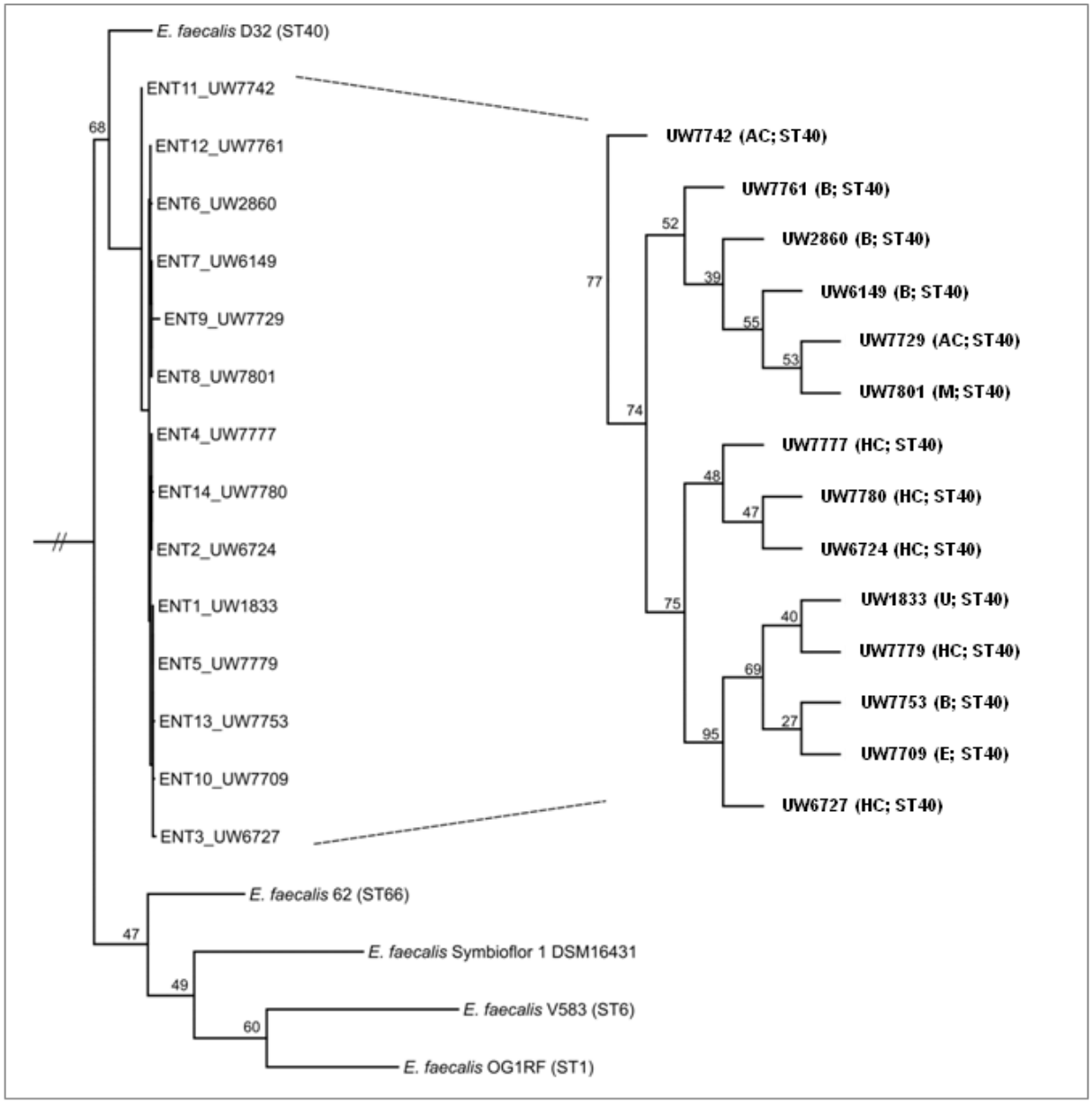

Figure 4.10: Phylogenetic relationship among selected *E. faecalis* strains based on whole genome alignments.

The alignment was calculated with Mugsy (5) and only aligned regions present in all analyzed strains were extracted. These regions were concatenated and positions with gaps removed (201). The resulting core alignment (126.7 kb) was used to infer a Maximum Likelihood tree with RAxML (233). The GTRGAMMA model for nucleotide substitution and rate heterogeneity was utilized, bootstrap support values of 1000 replicates are shown at the nodes. *Melissococcus plutonius* was used as an outgroup. Names of the ST40 isolates and their origin are indicated at the end of the branches; ST, sequence type; AC, animal colonizer; B, blood culture; E, endocarditis; HC, human colonizer; M, bovine mastitis; U, urine.

4.1.4.3 Analyses of MGE

Genomic islands

All isolates featured a modular structured pathogenicity island (PAI), which is flanked by phage-related integration and excision genes, as well as, varies independently of the core genome.

By using long template PCR, investigations regarding the structure of the PAI also confirmed results of genome analysis (Table 4.10).

Table 4.10: Screening of the *E. faecalis* PAI (215) by long PCR.

Region	*MMH594*	*OG1RF*	*UW6149*	*UW2860*	*UW6724*	*UW7761*	*UW7777*	*UW7780*	*UW7753*	*UW1833*	*UW7779*	*UW7729*	*UW7801*	*UW6727*	*D32*	*UW7709*	*UW7742*
1	+	-	+	+	+	+	+	+	+	+	+	+	+	+	+	+	+
2a	+	-	-	-	-	-	-	-	-	-	-	-	-	-	+	-	-
2b	+	-	-	-	-	-	-	-	-	-	-	-	-	-	-	-	-
2c	+	-	-	-	-	-	-	-	-	-	-	-	-	-	-	-	-
3a	+	-	-	-	+	-	-	+	+	+	+	-	-	-	-	+	-
3b	+	-	-	-	-	-	-	-	-	-	-	-	-	-	-	-	-
4a	+	-	-	-	-	-	-	-	-	-	-	+	-	-	-	-	-
4b	+	-	+	+	+	+	-	+	+	+	+	+	+	+	-	+	+
5a	+	-	-	-	-	-	-	-	-	-	-	+	-	-	-	-	-
5b	+	-	-	-	+	-	+	-	-	-	-	-	-	-	-	-	-
6a	+	-	-	-	-	-	-	-	-	-	-	-	-	-	-	-	-
6b	+	-	-	-	-	-	-	-	-	-	-	-	-	-	-	-	-
7a	+	-	-	-	-	-	-	-	-	-	-	-	-	-	-	-	+
7b	+	-	+	+	+	+	+	+	+	+	+	-	+	+	-	-	-
8a	+	-	-	-	-	-	-	-	-	-	-	-	-	-	-	-	-
8b	+	-	-	-	-	-	-	-	-	-	-	-	-	-	-	-	-
9	+	-	+	+	+	+	+	+	+	+	+	-	+	+	-	+	-
PAI*	+	+	+	+	+	+	+	+	+	+	+	+	+	+	+	+	+

Accordingly to (131), structure of the PAI based on the entire *E. faecalis* PAI of MMH594 (215) was analyzed by long template PCR, amplifying overlapping regions (Table 6.7 and Table 6.8). Positive results of amplification demonstrated a similar genomic structure compared to the prototype of the PAI. Structurally genomic differences, such as the absence of genes and/or the presence of additional insertions, were indicated by negative results. Integration of the PAI was additionally investigated by regular PCR (*).

Results of bidirectional BLAST showed that the uncharacterized GI (138kb; see part 4.1.3.1) of D32 was only verifiable in UW7729, an isolate originating from fish (Figure 4.9; data not shown in detail). Up until now, it is still unclear, whether the GI was additionally integrated with the inositol operon or instead of this because contig border was located at the end of the inositol operon .

Prophages

Comparison of the ST40 strains with the reference strain D32 indicated strain-specific phage patterns because of differences in prophage content independently of the strain background (Figure 4.9).

According to part 4.1.3.1, prophage 1, showing high similarity to the enterococcal phage phiFL4A (NC_013644), was also present in UW1833, isolated from urine, and in the human colonizing strain UW6727. In relation to D32, strains isolated from blood culture and bovine mastitis differed in prophage content, while the other ST40 isolates showed a relatively homogenous level of phage content. But, here it is noted that more detailed work is necessary to investigate the presence and the characteristics of other prophages, which differ from D32.

Plasmid content and classification

In the context of the 15 *de novo* sequenced strains, investigation of plasmid content indicated a certain level of diversity independently of the strain background (Table 4.11). Plasmids could be classified by the replication initiating gene *repA* of the corresponding replicase (*rep*) family (114, 272). Presence of *repA* of the well described *E. faecalis* plasmids pAD1, pCF10 and pRE25 was determined by Southern hybridization. Additionally, sequencing was used to review these results and to differentiate between the amplified conserved *repA* areas of the closely related pAD1 and pCF10.

The most dominant *rep*-family among the sequenced *E. faecalis* ST40 was *rep2* and *rep9* found in three (20%) and six isolates (40%), respectively. In addition, data also indicated the presence of plasmids of other *rep*-families, which were not investigated in detail.

Table 4.11: Plasmid content and the definition of the corresponding *rep*-families.

Isolate	*Origin*	*No.*	*Size [kb]*	*pAD1*	*pCF10*	*pRE25*	*Putative rep-family*
UW6149	B	1	65	+ (89%)	+ (94%)	-	9
UW2860	B	1	65	-	Undetermined	-	Unknown
UW6724	HC	2	70 / <60	+ (92%)	+ (96%)	-	9
UW7761	B	Ø					
UW7777	HC	Ø					
UW7780	HC	2	75 / 60	+ (92%)	+ (97%)	-	9
UW7753	B	2	70 / 60	+ (90%)	+ (95%)	+	9/2
UW1833	U	?	Unknown	-	-	+	2
UW7779	HC	2	75 / <60	-	-	+	2
UW7729	AC	1	<60	+ (95%)	+ (95%)	-	9
UW7801	M	Ø					
UW6727	HC	2	60 / <60	+ (88%)	+ (<90%)	-	9
D32	AC	2	75 / unknown	-	-	-	1/Unknown*
UW7709	E	Ø					
UW7742	AC	Ø					

Plasmid content was determined by plasmid profiling using (i) phenol-chloroform-based extraction (290) with subsequent agarose gel analysis and (ii) S1 nuclease PFGE. Approximate plasmid size was estimated from the S1 nuclease gel in accordance to the HARMONY protocol (164). Presence of the replication initiating gene (*repA*) of the corresponding plasmids pAD1, pCF10 and pRE25 was detected by Southern hybridization and checked by sequencing. Values in brackets indicated sequence identities in comparison to NCBI database. Based on PCR amplification and sequencing of conserved areas of the *rep* gene, plasmid *rep*-families were defined (114, 272). * Genomic characteristics of the plasmids EFD32pA and EFD32pB were described in part 4.1.3.2; A, animal; B, blood culture; C, colonizer; E, endocarditis; H, human; M, bovine mastitis; U, urine.

4.1.4.4 CRISPRs within the subset of sequenced *E. faecalis* ST40 strains

Within the subset of sequenced *E. faecalis* ST40 strains, presence of CRISPR1-*cas* and CRISPR2 was checked by PCR. CRISPR2 locus was also sequenced to characterize the integrated spacer (Table 4.12). Regarding to the two CRISPR loci identified in OG1RF (24, 102), our PCR results indicated that all of the selected ST40 genomes possess the CRISPR1-*cas* and CRISPR2 loci, lacking the functional *cas* genes. An exception represents the genome of UW7729, where only the CRISPR2 locus was present.

Table 4.12: Identification of CRISPR loci in selected *E. faecalis* ST40 strains by PCR.

Isolate	*cas_csn1*	*CRISPR1-cas*	*Size [bp]*	*CRISPR2*	*No. of spacer*
V583	-	-	773	-	0
OG1RF	+	+	1031	+	7
UW1833	+	+	870	+	4
UW6724	+	+	886	+	4
UW6727	+	+	857	+	4
UW7777	+	+	864	+	4
UW7779	+	+	892	+	4
UW2860	+	+	891	+	4
UW6149	+	+	892	+	4
UW7801	+	+	861	+	4
UW7729	-	-	927	+	5
UW7709	+	+	834	+	4
UW7742	+	+	988	+	6
D32	+	+	1432	+	13
UW7761	+	+	915	+	5
UW7753	+	+	860	+	4
UW7780	+	+	831	+	4

Analog to (180), presence of CRISPR loci corresponding to OG1RF CRISPR1-*cas* and CRISPR2 loci (24, 102) was checked by PCR. CRISPR2 locus was also sequenced to identify the integrated spacer. Analog to (102), existence of an empty CRISPR2 locus of the hospital-adapted V583 strain, also lacking the functional *cas* genes (102, 180) was demonstrated.

Our detailed analyses of CRISPR2 locus showed that all strains of the selected ST40 subgroup possessed three identical spacers, whereby two of those are also present in OG1RF (24) (data not shown).

4.2 Utilization of various carbon sources

We postulated that the different origins and habitats of the isolates may be reflected by minor, host-specific differences in their metabolic properties as described for isolates of *E. faecium* (298). To determine supposed differences in their metabolic profiles, Biolog MicroArray™ analyses were performed. Utilization of various carbon sources at aerobic conditions did not show significant differences between the 15 sequenced *E. faecalis* ST40 isolates. Additionally, this approach did not reveal any obvious association between origin or host and utilization of different carbon sources. For reasons of simplification, data values in Table 4.13 and Table 4.14 have been replaced by color codes. Tables with the complete, quantitative data sets and standard derivations are shown in Table 6.13 to Table 6.32.

Table 4.13: Aerobic utilization of carbon sources of Biolog MicroArray™ PM01.

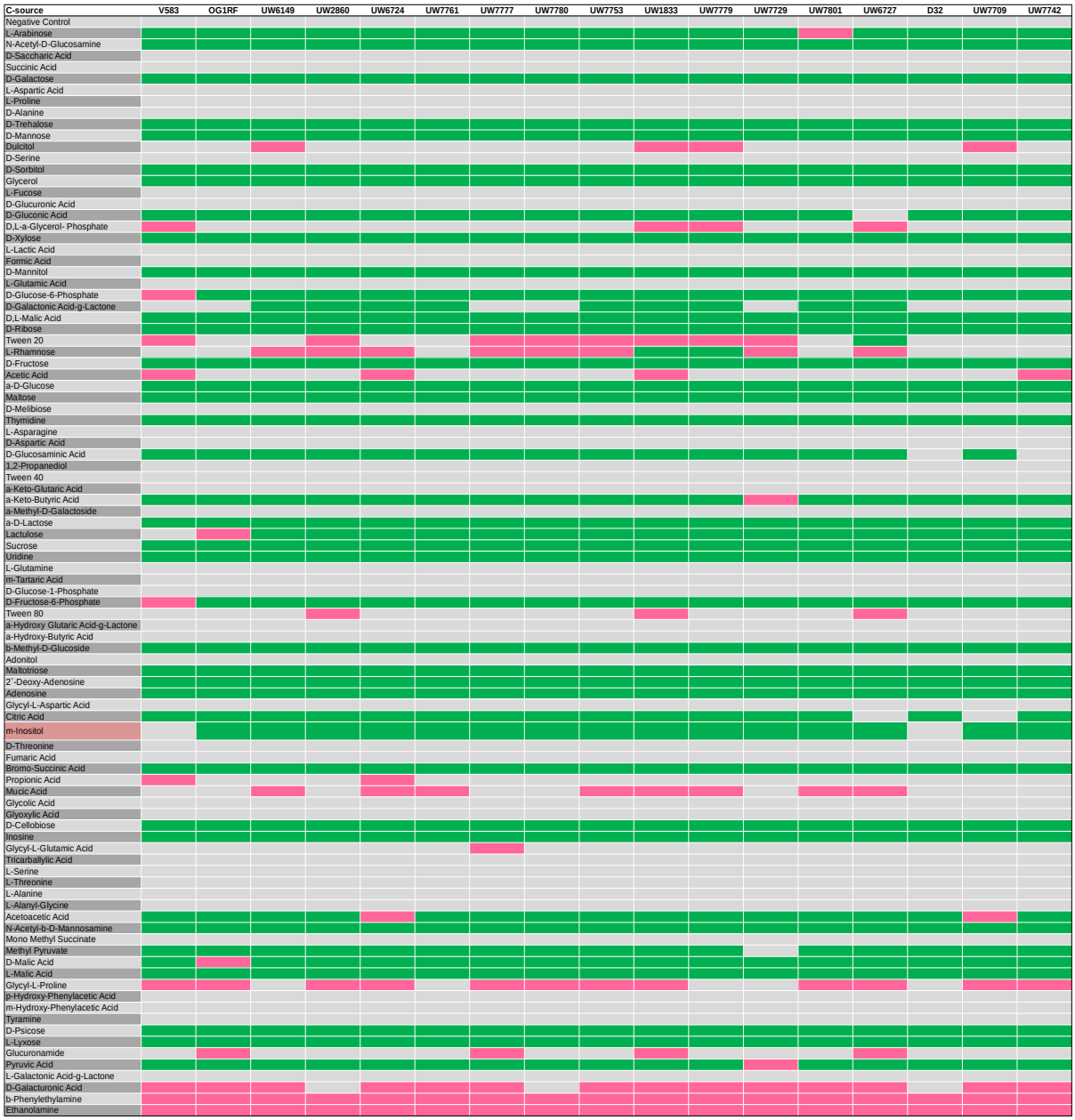

Mean area values were calculated of three independent experiments performed at 37°C for a 72h incubation time. For reasons of simplification, mean area values have been replaced by a color code. Grey color indicated no or only weak substrate utilization (mean area value below 10,000) and pink symbolized middle values (mean area value between 10,000 and 19,999). The green color represented strains with a high capability of utilization of the respective carbon source (mean area value greater or equal to 20,000). The red box highlighted m-Inositol as the carbon source of main interest.

Table 4.14: Aerobic utilization of carbon sources of Biolog MicroArray™ PM02.

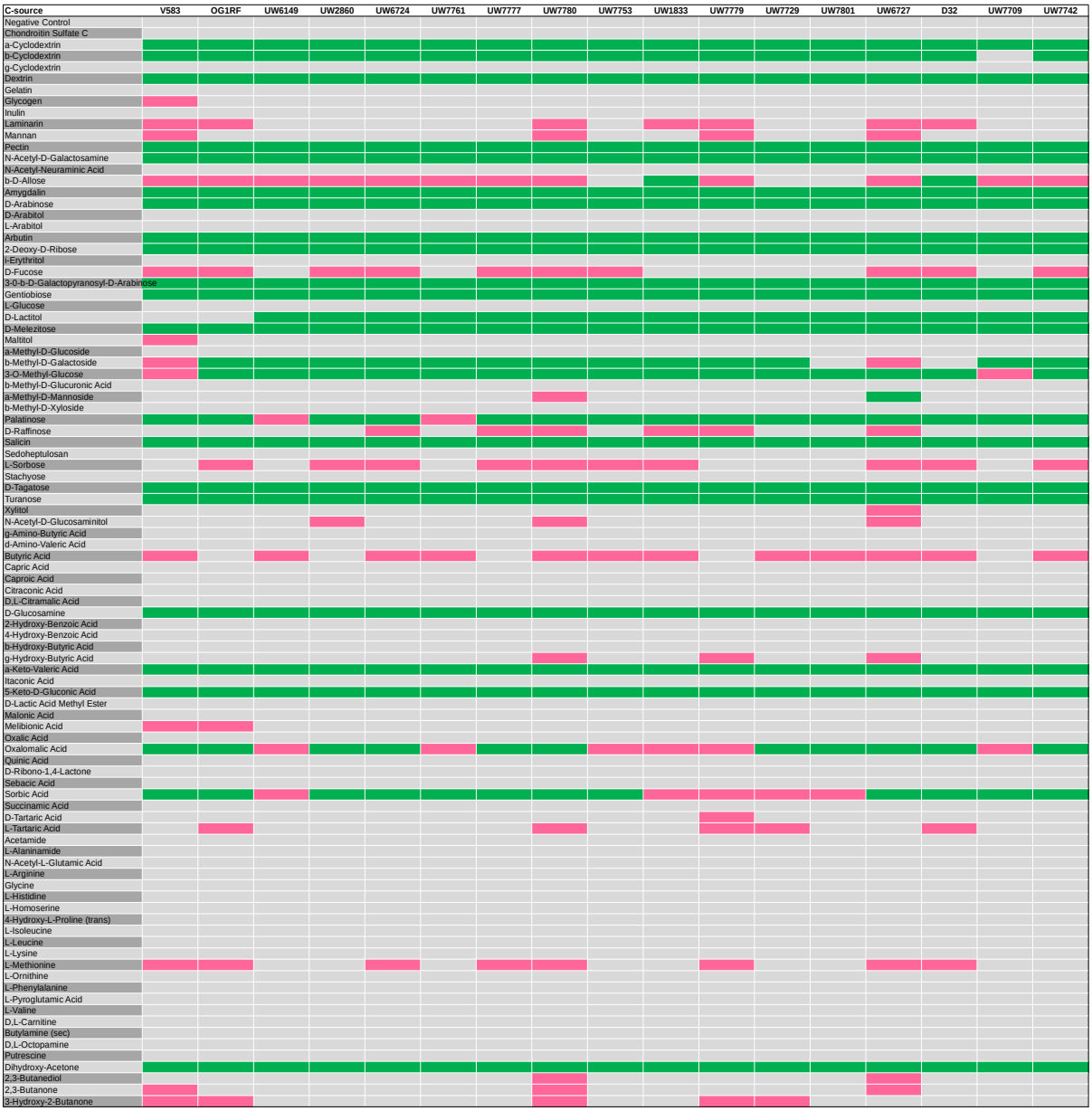

Mean area values were calculated of three independent experiments performed at 37°C for a 72h incubation time. For reasons of simplification, mean area values have been replaced by a color code. Grey color indicated no or only weak substrate utilization (mean area value below 10,000) and pink symbolized middle values (mean area value between 10,000 and 19,999). The green color represented strains with a high capability of utilization of the respective carbon source (mean area value greater or equal to 20,000).

In the following, the role of myo-inositol (m-inositol) will be reconsidered in more detail. Belonging to one of nine isomers of the inositol group, m-inositol is used as a sole carbon source by many soil and plant microorganisms by degradation into glyceraldehyde-3P (24).

As already described before, the novel and uncharacterized GI (138kb) of D32 was integrated at the attachment site of the conjugative *vanB* transposon in V583 (184). The genome sequence of OG1RF harbored the inositol operon at exactly this integration site, which consists of 10 genes (24). Presence of the inositol operon was also checked by PCR. In contrast to OG1RF, neither in the D32 nor the V583 genome the inositol operon was detected (Table 4.15). Accordingly, Biolog MicroArray™ analyses showed that only OG1RF, but not V583 and D32, was able to utilize m-inositol (Table 4.13).

Table 4.15: Evidence of the presence of the *iol* operon in combination of inositol utilization.

Strain	***iolR***	***iolB***	***iolG2***	***iolE***	***Inositol utilization***
V583	-	-	-	-	-
OG1RF	+	+	+	+	+
D32	-	-	-	-	-

Presence of selected genes of the inositol (*iol*) operon was tested by PCR and inositol utilization was further checked by Biolog MicroArray™ analysis. *iolR*, annotated as OG1_0175, the probable inositol regulator; *iolB*, myo-inositol catabolism protein; *iolG2*, inositol 2-dehydrogenase; *iolE*, myo-inositol catabolism protein.

For all the other sequenced strains, presence (but not the genomic localization) of the *iol* operon could be confirmed by PCR (data not shown) in combination with a positive result of inositol utilization in the Biolog MicroArray™ assay (Table 4.13).

4.3 Comparative assessment of the pathogenic potential of closely related *E. faecalis* isolates

Genomic comparisons revealed a high level of similarity between the porcine, commensal D32 and a human clinical endocarditis isolate UW7709, both from Denmark. Ability to adhere to human epithelial cells and to cause pathogenic effects in selected animal models was analyzed for these two related ST40 strains.

4.3.1 *In vitro* growth kinetics

Over a course of 24 hours, optical density and the corresponding bacterial counts were determined (Figure 4.11). Measurement of optical density suggested that D32 showed faster growth when compared to UW7709. But bacteria of D32 also showed an increased tendency to clump. We also determined the corresponding bacterial counts, showing comparatively similar growth rates of both *E. faecalis* strains D32 and UW7709.

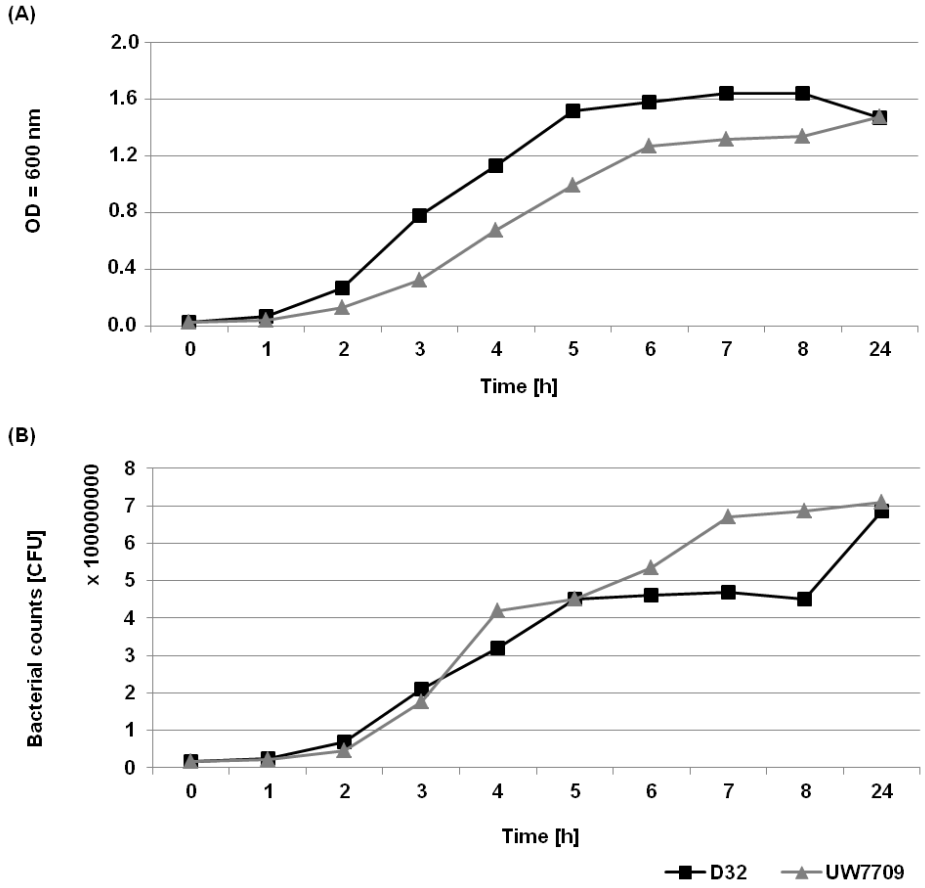

Figure 4.11: Comparative *in vitro* growth of *E. faecalis* strains D32 and UW7709.

Bacterial growth of both *E. faecalis* strains was analyzed by measuring the optical density (A) and determining the corresponding bacterial counts (B). Data are representative of at least three independent experiments with similar outcome.

4.3.2 *In vitro* biofilm formation

E. faecalis strain UW7709 showed a significantly enhanced biofilm production when compared with the strain D32 (Figure 4.12).

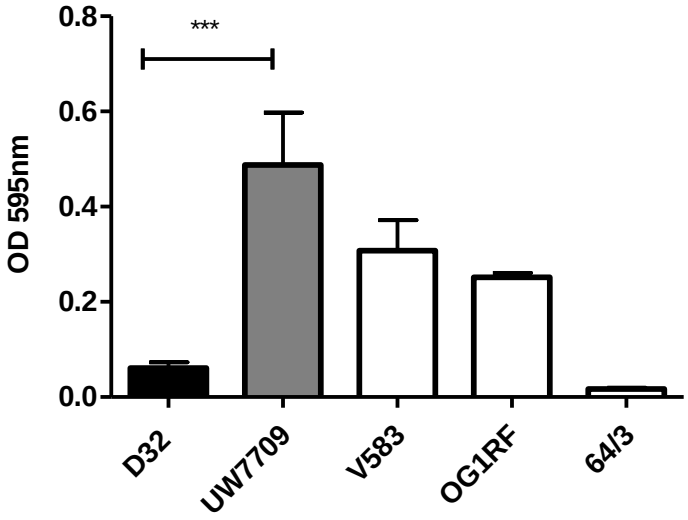

Figure 4.12: *In vitro* biofilm formation.

Biofilm formation of *E. faecalis* strains D32, UW7709 and the internal controls V583, OG1RF and *E. faecium* strain 64/3 on a synthetic surface was investigated by using polystyrene plates. After incubation in TSB for 24 hours, produced biofilms of adherent bacteria were stained with crystal violet. Bars represent the mean values of six or three (D32) replicates ± SEM. *** significant *P*-value < 0.0005, unpaired two-tailed t-test.

Results of biofilm formation were also compared to the corresponding genotype. Genomes of both strains harbored *fsrB* and *gelE* genes in combination with expression of an active metalloprotease GelE. No correlation between the presence of *esp* or other biofilm-enhancing factors (see Table 2.1), such as the *ebpABC* or *epa* locus, and the increase of biofilm formation was detected, because *esp* was absent in both genomes, while both genomes harbor the *ebp* and *epa* locus.

4.3.3 Adherence to Caco-2 cells

A monolayer of colonic epithelial cells (Caco-2) was incubated with *E. faecalis* strains D32 and UW7709 to test the potential of adhesion to human intestinal cells *in vitro*.
In summary, adherence of D32 to Caco-2 cells was approximately 1.5 times higher than adhesion of UW7709 (Figure 4.13).

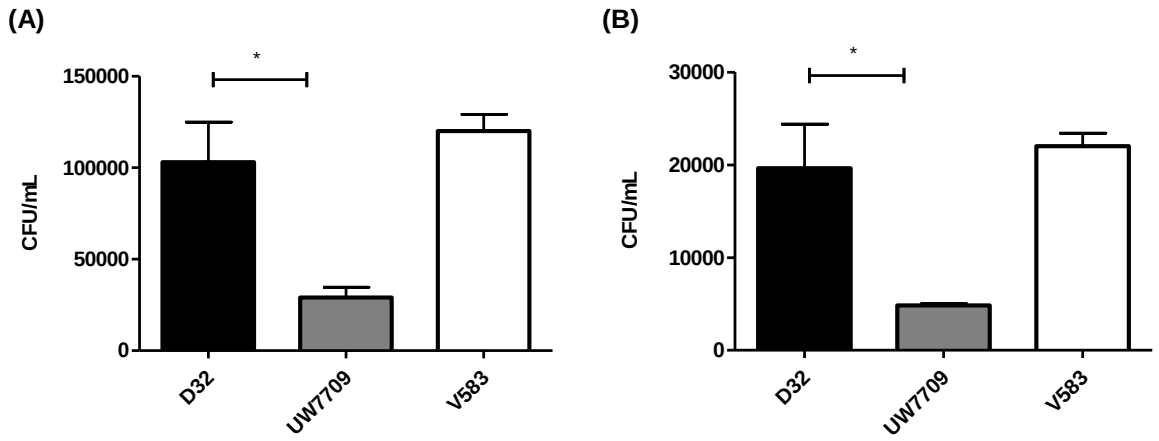

Figure 4.13: Adhesion ability to Caco-2 cells.

To analyze the potential of adhesion, a monolayer of Caco-2 cells was incubated with a bacterial cell to epithelial cell ratio of (A) 100:1 and (B) 1000:1 for two hours with the respective strain. Data represent the mean values ± SEM. * significant *P*-value < 0.05, unpaired two-tailed t-test.

4.3.4 Analysis of pathogenicity by using the model organism *G. mellonella*

The insect larvae *G. mellonella* is an alternative model to study bacteria-host interactions, also showing a complex immune reaction, consisting of both cellular and humoral responses (74, 163, 261).

In this assay, D32 was more rapidly lethal for *G. mellonella* and pathogenicity of D32 was generally increased in comparison to UW7709 (Figure 4.14).

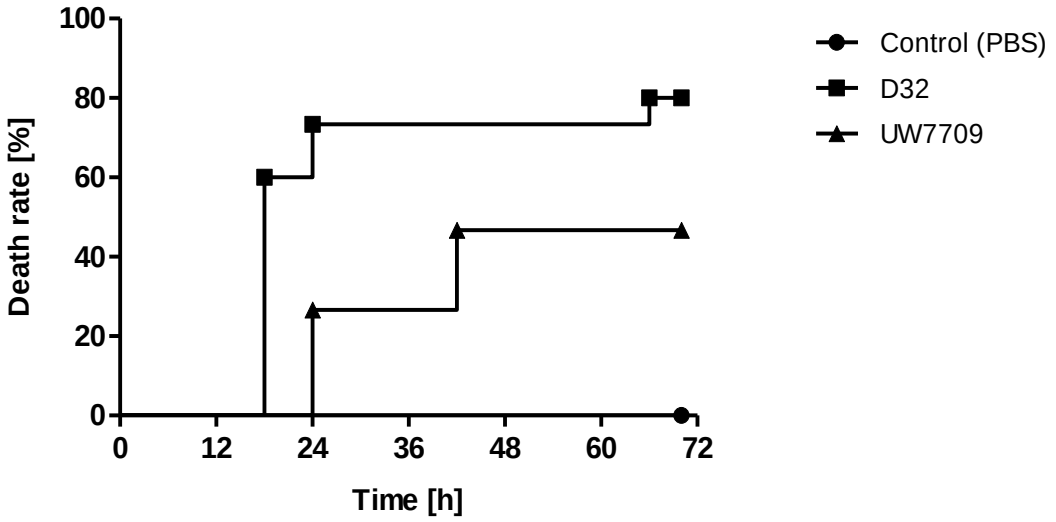

Figure 4.14: Pathogenicity of *E. faecalis* D32 and UW7709 in a *G. mellonella* model.

Death rates of *G. mellonella* larvae after injection with *E. faecalis* strains D32 (real infectious dose: 1.7 x 10^5 CFU per larvae) and UW7709 (real infectious dose: 2.8 x 10^5 CFU per larvae), respectively. PBS served as a negative control. One representative experiment of three independent experiments is shown. Data were analyzed by using Kaplan-Meier plot method.

4.3.5 Analysis of pathogenicity by using chicken embryos as model organisms

Two different infection methods were tested. The bacterial inoculum was injected into the:

a) Yolk sac at day five after fertilization (10^3 CFU per egg)
b) Allantois cavity at day 10 to 12 after fertilization (10^5 CFU per egg).

Independently of the strain background, infection of the yolk sac induced death of all embryos until the fifth day post infection. Embryos, infected with the enterococcal strain UW7709, died significantly later (Figure 4.15 (A)). After infection of the allantoic cavity, both strains were highly virulent, but only infection with D32 resulted in killing of all of the chicken embryos (Figure 4.15 (B)).
Additionally, *Enterococcus* spp. was identified in all screened death embryos with the exception of the negative control group.

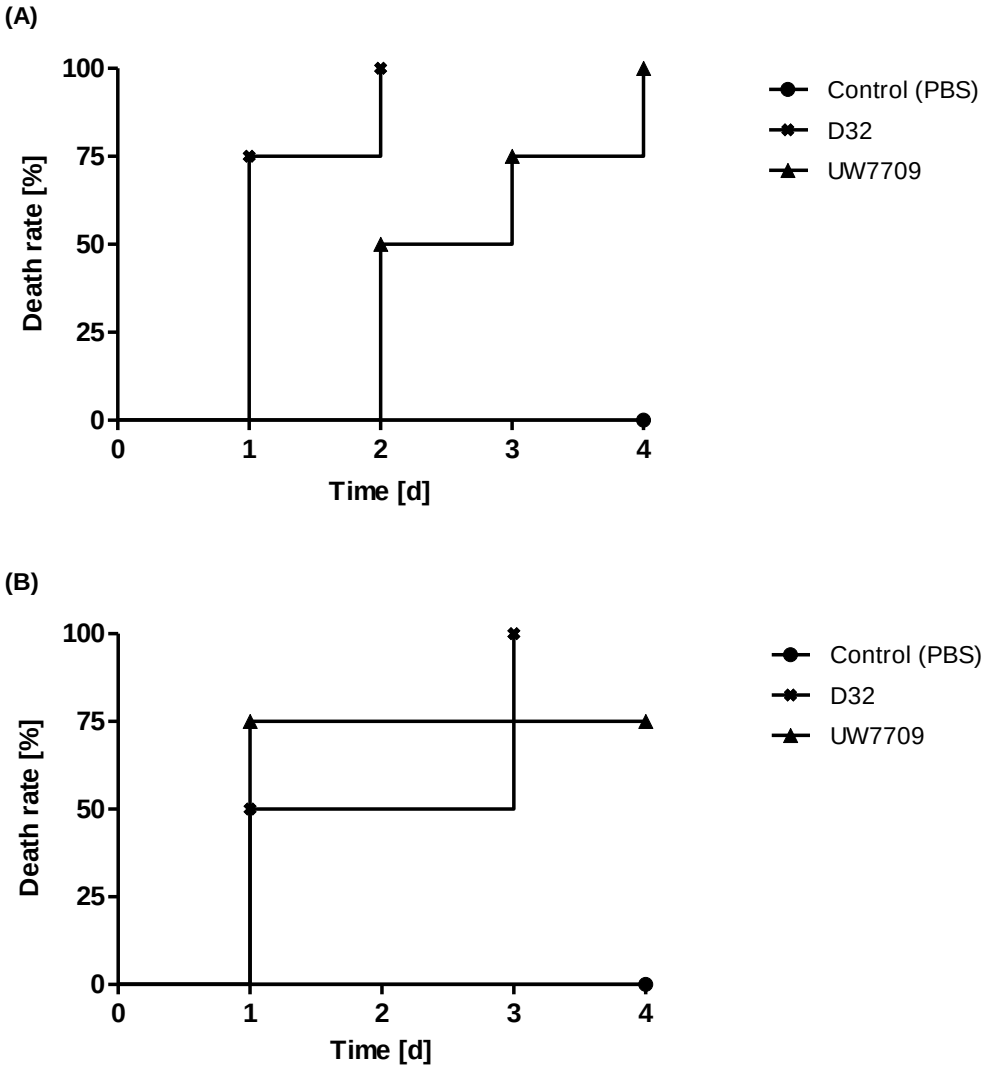

Figure 4.15: Killing of chicken embryos by *E. faecalis* strains D32 and UW7709.

Death rates of chicken embryos were tested after injection of an infectious dose of (A) 10^3 CFU per 0.2mL into the yolk sac and (B) 10^5 CFU per 0.2mL into the allantoic cavity. Survival of embryos was checked using the mercury vapor lamp over a period of four days. PBS served as a negative control. Data were analyzed by using Kaplan-Meier plot method.

4.3.6 Murine bacteremia model

Mice were infected with 5 x 10^8 CFU via the tail vein 48 hours before sacrifying. Bacterial counts were recovered from liver, kidneys, spleen and blood. D32 showed significantly enhanced growth rates in comparison to UW7709 (Figure 4.16 (A) and (B)).

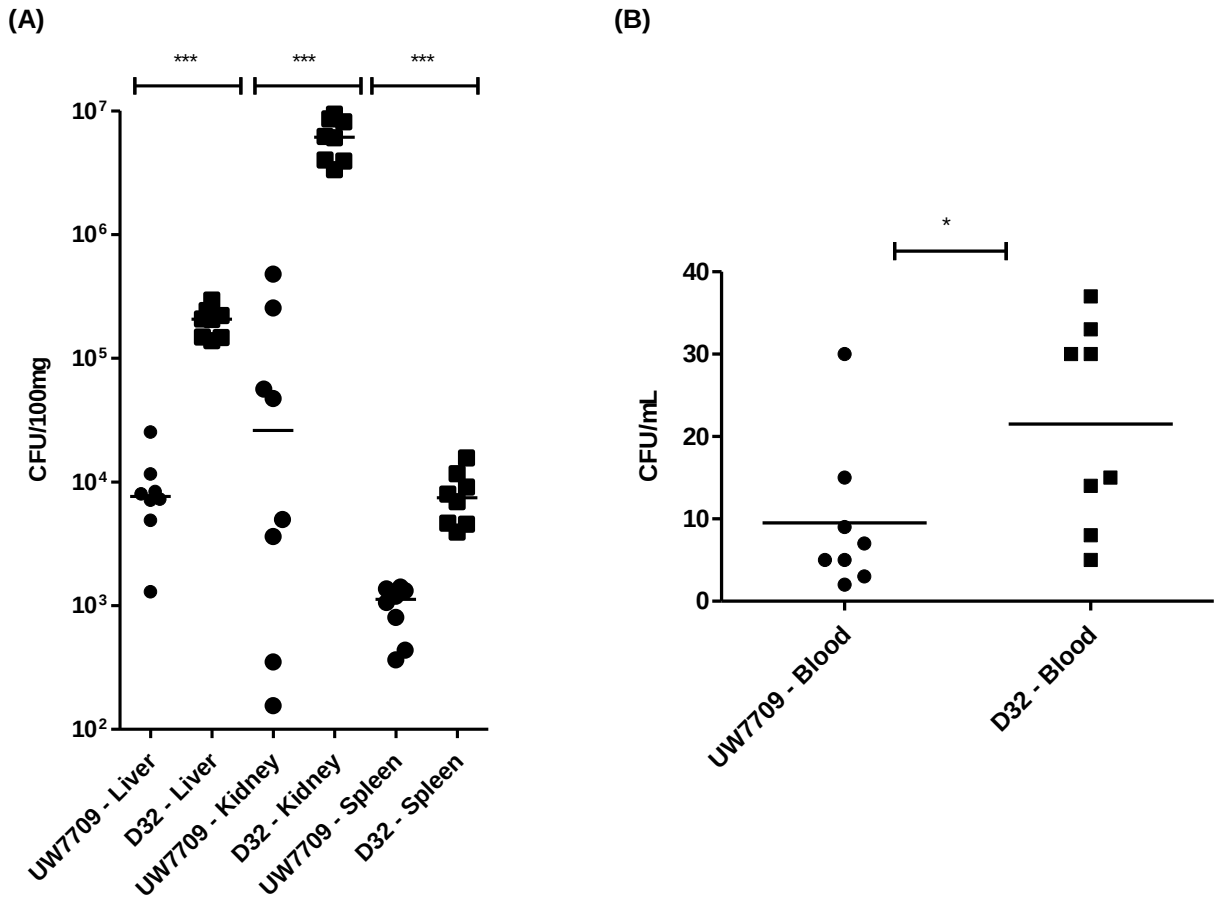

Figure 4.16: Growth rates of *E. faecalis* UW7709 and D32 in a mouse bacteremia model.

Eight female BALB/c mice were infected via the tail vein with *E. faecalis* strains UW7709 or D32 (5 x 10^8 CFU). After 48 hours, mice were sacrificed and bacterial counts in (A) liver, kidneys and spleen, as well as, in (B) blood were determined. Data represent the individual bacterial burdens and the geometric mean value. Asterisks indicate significant *P* values calculated by using Mann-Whitney test (* $P < 0.05$, *** $P < 0.0005$).

5 Discussion

5.1 Comparative genomic studies of *E. faecalis* ST40 strain collection

The “two-faced” *E. faecalis* is not only of relevance as part of the human and animal intestinal microbiota or as a probiotic in health care, but also as a leading cause of nosocomial infections, especially of the urinary tract, bacteremia and/or endocarditis. Based on multilocus sequence typing (MLST) in combination with phylogenetic analyses (eBURST), strains from distinct ecological backgrounds can be allocated to defined clonal complexes (CC) (199). Special clonal groups, such as CC2, CC9, and CC87, are also designed as high-risk enterococcal clonal complexes (HiRECCs) because they are preferentially associated with hospital infections and outbreaks, and are quite often multi-resistant (125, 133, 199, 262, 286). Epidemiological investigations of a diverse *E. faecalis* strain collection revealed that CC40/ST40 is the most common sequence type (ST), not showing a preferred host-specificity or any other characteristic (150).

In this study, a heterogeneous *E. faecalis* MLST ST40 strain collection, comprising randomly collected isolates of environmental and commensal/pathogenic sources (humans/animals) also originating from different countries and years, was examined for genomic and phenotypic characteristics. In enterococci, recombination and horizontal gene transfer (HGT) are suggested to be more relevant for genomic variability than single nucleotide polymorphism (SNP) mutations (278, 287)). Consequently, we supposed that additional to lineage-specific genes also genomic and phenotypic differences are present as a result of adaptation to the corresponding environments.

5.1.1 Genomic pre-characterization of the *E. faecalis* ST40 strain collection

*Sma*I macrorestriction patterns in combination with analyses of the presence and expression of so far described virulence-associated genes revealed a high level of similarity among the rather diverse collection of ST40 isolates. Thereby, strains of this clonal group did not show specific genomic characteristics or differences in relation to their origin in terms of host, context (commensal/clinical), time, and geography. As an example, I would like to point out the close, but also unclear relationship between the strain UW6724, isolated from the neonatology unit in Germany (Wernigerode), and the blood culture isolate UW7761, isolated from a patient in Cuba (Havanna) (see Figure 4.1). This suggests that genomic variability also might be limited as well among bacteria, showing a high level of recombination in general.

Corresponding to previous PCR-based screenings (214) and microarray-based comparative genomic hybridization (CGH) studies (1, 150, 227), our results further showed that previously described virulence-associated genes, including *fsrABDC*-regulated *gelE* (190), *cylM* (115), and *esp* (219), as well as, clinically relevant antibiotic resistance traits are also present in non-clinical strains (129). Formation of biofilm could not be correlated with the presence of already described and putative biofilm-associated genes, such as *esp* and *asc-10* (see Table 2.1).
According to McBride *et al*., all isolates of this most common sequence type ST40 are non-encapsulated and are characterized as cps type 1, consequently (150).

Moreover, I would like to point out another study, where a diverse *E. faecalis* strain collection of unrelated isolates isolated from bovine mastitis was molecularly characterized. Thereby, strains of ST40 predominated, which emphasizes its prevalence as a common and frequent sequence type without showing any preferred host-association (150, 280).

5.1.2 *De novo* sequencing strategy and generation of a ST40 reference genome

On the basis of these previous characterizations, a subset of 15 strains, representing the diversity of the collection, was chosen for *de novo* pyrosequencing by standard Roche 454 GS-FLX technology. But this strategy was limited due to a low coverage in combination with a high number of contigs (see Table 4.3) due to technological inconsistencies, which was still frequent at that time. Because no complete ST40 genome sequence had been publicly available, we decided to resolve the complete genome sequence of the pig commensal strain D32 (300) to use it as a ST40 template for detailed genome comparisons. After scaffolding by using an 8kb long-paired end (LPE) library, the remaining gaps and assembly ambiguities ("InDel" errors) were corrected by a Sanger-based process (300). We also gained experiences with the usage of the two different assembly software tools Newbler and Celera, generated two and one chromosomal scaffold, respectively. Usage of Celera resulted in a lesser extent of misassembled regions, while especially the assembly of repetitive sequences was more difficult for Newbler software (*Eurofins MWG-Operon, personal communication*).

For comparative genomics, including SNP-based phylogenies, we decided to additionally use Illumina sequencing technology, providing more accuracy and avoiding "InDel" errors. After Illumina sequencing of the remaining 14 *E. faecalis* ST40 strains and a subsequent hybrid assembly of both sequencing data sets (454 and Illumina), genomes of these strains could be mapped against the D32 reference genome. This strategy allowed a more detailed molecular analysis with respect to the structure of the pathogenicity island (PAI) and other mobile genetic elements (MGE), including plasmids and phages. This approach further reveals possible minor genomic differences between isolates of commensal and pathogenic origin and allows generation of the SNP-based phylogeny of the core and entire genome. Of note, detailed analysis of the genomic mapping against the D32 reference sequence was partially limited by the existence of intra-chromosomal gaps within the 14 *E. faecalis* genomes.

Sequencing technology platforms of the third generation are now available and could replace time-consuming gap closing approaches for “sequence polishing”. Especially, Pacific Biosciences´ single molecule real time technology (SMRT) is an ambitious tool, allowing cost- and time-efficiently sequencing with extra-long reads (up to 10,000bp) of high accuracy (>99.999%) ((151) and general information are presented on the website of Eurofins MWG (http://www.eurofinsgenomics.eu/en/home.aspx)). Thereby, quality of the draft genomes could be upgraded by using the software tool PBJelly, automated filling the existing gaps by using the generated long-reads in a reference-guided assembly process. But simultaneously, this emphasizes the importance regarding the excellent quality of the reference sequence (61). Other experiments in our group, when using PacBio for resolving the entire genome sequence of an *E. faecium* isolate, verified these predictions (*Werner, G., unpublished data*).

5.1.3 Comparative genomic studies

5.1.3.1 Conserved genomic backbone

Analog to the results of the pre-characterization, genome data also revealed a high degree of similarity. Regarding the presence of putative and described virulence-associated genes, genome data were in congruence to results of previous molecular typing. Furthermore, the close genomic relationship of the ST40 isolates was also reflected by phylogenetic analyses of the core genome DNA, suggesting a correlation between lineage-specific genes and MLST (52, 227). When comparing the phylogenetic tree and *Sma*I macrorestriction analysis, we have partially found overlapping results of clustered strains. For example, one cluster was composed of the human colonizing strain UW7779 and the urine isolate UW1833 (Figure 4.1 and Figure 4.10). In general, this genetic homogeneity was also reflected by similar patterns in the utilization of various carbon sources, tested by Biolog MicroArray™ analyses (see part 4.2).

Illustrated by Venn diagram (Figure 4.5), a genomic alignment of the five publicy available and completely closed *E. faecalis* genomes (24, 28, 71, 184, 300), revealed the presence of unique chromosomal genes, which might be acquired during niche

adaptation (181, 262). Notably, the number of unique CDS of the clinical strain V583 (184) was approximately two times higher than the counts of the commensal isolates 62 (28) and D32 (300), as well as, the probiotic Symbioflor 1 strain (71). As a derivate of the commensal isolate OG1, OG1RF strain carried the minimal number of 140 unique CDS compared to the other completed genomes, which are possibly explainable due to the lack of chromosomal integrated MGE, like the PAI or several prophages (24). Moreover, it might be interesting to analyze genes, which are only shared between V583 (184) and the commensal strains 62 (28) and D32 (300). But nevertheless, our comparisons of the chromosomes did not reveal a specific portfolio of hospital-associated *E. faecalis* V583 strain (184), which would explain its preferred hospital association in comparison to the commensal enterococcal strains. Relevance of transferred and integrated genetic elements must be considered and needs more attention (see 5.1.3.2).

A detailed analysis of the genome data of Symbioflor 1 strain showed the absence of putative virulence genes, like cytolysin and *esp* (53, 71). The relevance of present auxiliary traits, such as capsule formation or expression of aggregation substance, was associated with an advantage for colonization (53). Other studies demonstrated that adherence-promoted surface structures, especially enriched in strains of CC2, are supposed to play a crucial role in fitness and virulence, and especially in biofilm formation (178, 194, 229), which will be further discussed in the following section 5.1.3.2.

5.1.3.2 Genomic variability induced due to the acquisition of MGEs

Genomic “flexibility” plays a crucial role in adaption to and colonization of diverse ecological niches (49, 52). In this context, genomic variability is mainly realized by acquisition and loss of mobile elements, composing more than one quarter of the genome of *E. faecalis* V583 (184).

PAI and its genomic content

Comparable to the findings of McBride and co-workers (149), we could also demonstrate that all of the isolates featured a modular structured pathogenicity island, varying independently of the strain background and being flanked by putative

phage-related integrase and excisionase genes (215). Additionally, differences in GC-content and the presence of a characteristically large subset of mobility genes are associated with its foreign character, as well as, horizontal acquisition and gene loss (52, 144, 215, 216, 262)). Within several studies, transfer of virulence-associated determinants of the PAI, as well as, of the PAI itself were demonstrated and probably occurred via conjugative elements (40, 52, 131, 145, 175, 216, 262). Corresponding to the results of previous studies, the D32 PAI contains a bile acid hydrolase (*cbh*) and lactose metabolic pathway genes (*lac*ABCDEFG), but lacks common markers present in the original prototype of MMH594, associated with virulence, like *esp* and cytolysin operon (129, 215, 216, 300). Taken together, these results revealed that the PAI evolves by HGT and recombination in a much faster way than the relatively conserved core genome (149, 199, 262, 286). In case of D32, composition of the PAI suggested a putative niche adaptation to the pig´s intestine, may be indicated by selective pressure, like due the host immune response or, in some cases, antibiotics. Concrete examples are the presence of bile acid hydrolase (*cbh*) and lactose metabolic pathway genes (*lacABCDEFG*) (49, 52, 129, 144, 194, 216, 300).
Detailed analyses of the genetic components of the PAIs of the 14 *E. faecalis* ST40 draft genomes were limited by the existence of intra-chromosomal gaps. But, comparisons of PCR analyses with in *vitro* biofilm assays revealed that *esp* might be only one of the beneficial factors, involved in enhanced adhesion (60, 158).

Genomic islands (GI) – probably encoding for enterococcal exopolysaccharides
A so far unknown GI was identified to be integrated within the genome of the porcine commensal strain D32. Among several genes with unknown identity, a genomic cluster is encoded, probably associated with exopolysaccharid synthesis. Consisting of different sugars, the extracellular polysaccharides (EPS) are polymeric complex structures covalently bound to cell surface or released in its environment (44, 157). Generally, important conserved *E. faecalis* cell wall polysaccharides are the rhamnopolysaccharide Epa, encoded by the enterococcal polysaccharide biosynthesis locus *epa*, and the capsular polysaccharide Cps (*cps* cluster), consisting of galactose, glucose and phosphate (87, 89, 103, 181, 245, 292, 293). As already described before, we could demonstrate that all of the ST40 strains are non-encapsulated and are grouped as CPS type 1, representing the common CPS type

(150). Although presence of *cps* genes did not result in the expression of the corresponding capsule phenotype (75), genes related to cell surface structures are enriched in strains of CC2 (150, 227, 229, 267). In the context of fitness and host adaption, surface structures are thought to promote adhesion to human tissue cells (95, 194, 207, 239), enriched in strains of CC2 (184, 194, 229). First results of secretome analyses at the working group of Katharina Riedel at Greifswald University suggested differences in the extracellular proteome of both strains, D32 and UW7709 (*Zühlke, D., personal communication*). Eventually, differences within the secretome could explain why D32 showed significantly enhanced (i) adherence to human Caco-2 epithelial cells, as well as, (ii) growth rates in murine organs and blood, when compared to UW7709 (see part 5.2) (16, 22). In the working group of Prof. Johannes Hübner at Freiburg University, a rat endocarditis model was additionally established and here, D32 again showed enhanced growth rates at aortic values, comparable to murine bacteremia model (*Hübner, J., personal communication*).

The gastrointestinal tract (GIT) could be the starting point for a systemic infection when bacteria enter the blood stream and are dispersed inside the whole body, enabling the establishment of new sites of infection (7)). Intestinal overgrowth under specific conditions, such as antibiotic treatment, precedes systemic infections, especially involving members of *Enterococcus* (258, 259). For *E. faecalis*, relevant mechanisms for crossing the endothelial barrier of the GIT are not really understood, but capacity to invade depends on cell surface structures (32, 55). For example, *S. aureus* is suggested to use various strategies, such as transcytosis, paracytosis, phagocytic transport, and cytolytic toxin induced damage of the endothelium. However, attachment to the tissue cells plays a key role for bacterial entry into the blood stream (59, 207). Therefore, is might be interesting whether increased capacity of porcine commensal strain D32 to adhere to various endothelial cells, such as aortic values, is potentially associated with an increased capacity to infect the endocard, underlining the relevance of the normal intestinal microbial flora of humans and pigs as community reservoirs of clinical *E. faecalis* strains (129).
Deficiencies of the immune system and/or disturbance of the microbial flora of the gastrointestinal tract, especially by antibiotic long-term therapy, could increase the selective pressure for the colonization with enterococcal strains. A special feature is

that these strains acquired new traits by HGT, like antibiotic resistance traits or virulence genes, constituting an advantage for niche adaption (7, 77, 78, 120, 287). Especially acquisition of surface proteins, such as capsule formation, may also be an efficient strategy to evade the host immune system, by mediating resistance to phagocytosis (52, 87, 194, 244, 253, 267) and masking of lipoteichoic acids (LTA), which are targets of opsonic antibodies (17, 150, 208, 248, 253). This might result in an increased pathogenicity (163, 194), as it was described for D32 in the tested *Galleria mellonella* (*G. mellonella*) and the chicken embryo models.

Mass spectrometric analyzes of the secretome could be an useful approach to analyze the surface proteome in more detail, while a reference map of the membrane proteome of *E. faecalis* OG1X was previously provided by Maddalo and colleagues (139). Especially surface proteins, like LTA, peptidoglycan-attached wall teichoic acids (WTA), choline-binding proteins (CBP), putative microbial surface component recognizing adhesive matrix molecule proteins (MSCRAMMs), mucins and variation of glycosylation, have to be focused to get knowledge about their relevance in colonization and virulence (22, 95, 194, 208, 229, 239, 248, 249).

Because of the relatively conserved core genome of the ST40 strain collection, further investigations, concerning variations of the expression level of surface proteins dependent on host cell contact, could also be an interesting approach (177, 265). While *cps* and *epa* are down-regulated when growing in blood (266), the *fsr* quorum sensing system of *E. faecalis* directly mediates adherence to collagen (187). It is thought to control cell functions relevant for virulence (74), for example it regulates expression of the metalloprotease gelatinase GelE (190), while its activity correlates with reduced adhesion because of the cleavage of MSCRAMM Ace at the cell surface (169, 170, 187, 193). Expression of other surface proteins might also be regulated by cell-cell communication (289). Differential gene expression could also be controlled by environmental factors (96), such as the presence of bile (21, 228), blood (266), urine (267), metals (2, 138, 192), or bicarbonate (27, 140).
This complexity is also demonstrated by our results of *in vivo* biofilm formation (see part 5.2), where adhesion plays an important role (248, 249). In this study, increase of adherence of D32 could not be associated with enhanced biofilm formation *in vitro*,

corresponding to Larsen *et al.* (129). So far described regulators, such as Fsr (88), EbpR (26), EbrA (12), and PerA (140), suggested to have an influence to biofilm accumulation. But, Ballering and colleagues further concluded that other genes of the conserved core genome could also be involved in biofilm gene regulation (12).

More investigations, regarding the integration site of this novel GI, also showed that it is integrated within a conserved *attL*/*attR* attachment site, previously described as a "hot spot" for rearrangements or new integrations (24). It is suggested that two different integration events resulted in the presence of an *iol* operon in OG1RF and a conjugative *vanB* transposon in V583 (24, 184). This region is missing in the Symbioflor 1 strain (24, 53, 71). Our sequencing results demonstrated that all of the ST40 strains, with the exception of D32, harbor an *iol* operon comparable to OG1RF (24), coupled with identical phenotypes of myo-inositol utilization (seeTable 4.13). In general, metabolism of myo-inositol, abundant in nature, is suggested to be an auxiliary trait promoting fitness, also generally described for Lactobacilli (24, 294).
Furthermore, genome data in combination with results of Biolog MicroArray™ analyses of the strain UW7729, isolated from fish, suggested that the *iol* operon was co-integrated next to the novel GI. But the presence of intra-chromosomal gaps within this genomic region limited our possibilities to display the co-existence in more detail.

Other MGEs

Currently, there are no suitable software tools to filter out plasmid sequences, generated by 454 or the Illumina´s Solexa sequencing technology. Thus, "classical" molecular methods, such as plasmid isolation, analysis of the plasmid size by S1 nuclease PFGE in combination with PCR- and hybridization-based *rep*-typing, were used as meaningful approaches to improve data analysis. In combination with genomic mapping of the ST40 draft genomes against the D32 template, results revealed a high level of genomic diversity (270) and strain-specific phage patterns (see Figure 4.9 and Table 4.11). We propose that integration of bacteriophages might have a significant impact on niche adaptation. In this context, Duerkop *et al*. hypothesized that bacteriophages, especially a composition of different bacteriophages, cause bacterial dominance within the bacterial ecosystem, where

especially competition for nutrients plays a crucial role (57). Furthermore, the examination of the genomic integration sites would be an interesting approach. Here, integration of the bacteriophage into a promoter region might result in an increase of expression of putative virulence-associated genes (269). Additionally, surface-exposed WTA structures might be used as specific identification markers for bacteriophages, enabling HGT of virulence and resistance genes across genus–specific barriers of Gram-positive pathogens (288).

Using the rep-typing scheme, demonstrated that *rep*-types 2 and 9 were dominant and also offered some new plasmids (114, 272, 300). These results indicated that recombination and rearrangements of chromosomal and other plasmid DNA might contribute to mosaic-related structures, whereby an adaptation to changing environmental conditions is mediated (278).

Finally, there are several unanswered questions, regarding the presence and detailed analysis of additionally acquired genes or MGEs of the other ST40 strains, as well as, investigations regarding presence of plasmid stabilization systems (270).

5.1.3.3 CRISPR-*cas* – conferring bacterial adaptive immunity

Our studies highlighted the MGE-dependent genomic diversity of the *E. faecalis* ST40 strain collection. In this context, it is substantial to discuss the relevance of the CRISPR-*cas* system, mediating adaptive immunity against integration of bacteriophages and plasmids by taking up genetic material (101).
During this thesis, we mainly focused on CRISPR loci within the finished genome of *E. faecalis* strain D32. Detailed sequence analyses showed that only CRISPR1 locus is associated with four related *cas* genes, which are supposed to be responsible for recognition of foreign DNA and/or integration of new repeat-spacer units. Consequently, only CRISPR1 locus might be functional (101). Because of non-identical repeat sequences of CRISPR1-*cas* and CRISPR2 (see Table 4.7), interacting with Cas proteins, it is rather unlikely that both CRISPR loci are functionally linked (101, 180). Interestingly, the CRISPR2 locus occurred not only in the finished *E. faecalis* strains OG1RF and D32 but also in all of the sequenced *E.*

faecalis ST40 strains. As already described in (180), it is still unclear, whether CRISPR2-related *cas* genes have existed and have been lost over the time. In general, a functional analysis of the CRISPR2 locus might be an important approach. But nevertheless, a kind of dynamics in terms of the integrated spacers was also shown, when analyzing the CRISPR2 locus within the subset of sequenced ST40 strains. Conserved spacer sequences within this locus indicated their inheritance over time (101, 275), but minor variations also revealed a replacement of spacers as a consequence of niche adaptation and changing environmental conditions, probably acquired from the microbial ecosystem by HGT (136, 274, 275). Within a CRISPR-*cas* system, spacer acquisition needs to be regulated because integration is not only limited to new beneficial traits. Furthermore, it is more a balance of spacer addition and loss to guarantee fitness within the microbial ecosystem and to respond quickly to changing conditions (18, 135, 276). As a consequence of this obvious diversity within the ST40 strain collection, typing based on CRISPR locus would be complicated (180, 181).

Interestingly, we also noticed that the number of CRISPR2 spacers of the porcine commensal strain D32 sets apart from the other ST40 strains, raising further questions. Further analyzes, regarding homologies of the D32 CRISPR spacers, revealed that only one spacer, also belonging to CRISPR2 locus (CRISPR2_5; see Table 4.9), showed homologies to the *E. faecalis* phage phiEF11 (235). 38.5% of the phiEf11 phage components are detectable as remnants in the core genome of D32, as well as, other finished *E. faecalis* strains V583 (184), OG1RF (24), 62 (28) and Symbioflor 1 (71). But in contrast to D32, general analyses of the CRISPR-*cas* elements of these also finished genomes showed a lack of the corresponding, matching protospacer (see CRISPRdb; http://crispr.u-psud.fr/CRISPR-). Here, it could be hypothesized that these *E. faecalis* strains may have lost this spacer during the process of niche adaptation, which could ensure and optimize their fitness (136, 275).

Finally, genome data have a great potential for further more in-depth analyzes, especially with respect to the CRISPR1-*cas* integrated spacers of these closely-related *E. faecalis* ST40 strains. Further investigations, regarding the impact of the CRISPR-*cas* system on the regulation of surface genes, thought to be one way of

possible interaction between bacteria and eukaryotes, are possible (204). Moreover, it would be interesting to analyze whether individual phages or plasmids have already possessed strategies to circumvent this defense mechanism, like acquisition of mutations within the nucleic acid that matches to one of the CRISPR spacer ("proto-spacer") (136).

5.1.4 Aspects of "Functional Genomics"

Palmer and colleagues used Biolog MicroArray™ technology to identify species-specific biochemical traits of a diverse enterococcal strain collection, also including *E. faecalis* strains of various sequence types (181).
In the context of a relatively conserved core genome, we wanted to analyze possible differences within the ST40 strain collection, concerning the utilization of various carbon sources, which had never been tested in such a scope. But under aerobic conditions, Biolog MicroArray™ technology showed homogenous results of metabolic activity, not allowing a conclusion regarding to host- or environmental adaptation of metabolic characteristics.

By adaptation of the experimental conditions to the milieu of the gastrointestinal tract, we already tested changes within the metabolic profile, when using a microaerophilic atmosphere (80). First analyses revealed oxygen-dependence of some of the metabolic pathways, but also showed homogenous changes of carbon utilization patterns, when comparing the three tested ST40 isolates (D32, UW1833 and UW7709). However, this approach will need further tests and more intensive analyses.

5.2 Comparative assessment of the pathogenic potential of two highly related *E. faecalis* ST40 isolates

After analysis of the genome data sets, we compared microbiological, cell-biological and pathogenic properties of the porcine colonizing strain D32 (300), isolated in Denmark in 2001, and the clinical isolate UW7709, obtained from a patient with infective endocarditis in Denmark in 1997 (129). Results showed no obvious genomic differences between both strains, as well as, comparable *in vitro* aerobic metabolic profiles of carbon utilization, indicating the relevance of *in vivo* gene regulation.
In general, comparable *in vitro* growth rates exclude the possibility that differences in bacterial counts have an effect on the experimental design. When using a Caco-2 cell adherence assay, the commensal strain D32 showed a greater capacity to adhere to GIT-related epithelial cells. Comparable results were also achieved when testing adherence to uroepithelial cells (*Hübner, J., personal communication*). Despite the lowered host cell-dependent adherence, the clinical isolate UW7709 was able to form an increased biofilm at abiotic surfaces. Thereby, genome data of these both strains did not reveal any correlation between the presence of *esp* und the increase of biofilm formation, because *esp* was absent in both genomes (60, 105, 124, 129, 159). But in general, a supporting role during the process of infection cannot be clearly determined (51, 158). Furthermore, the role of differentially expression of LPxTG surface structures in combination with the relevance of other putative biofilm-associated genes might be causative but have not been investigated in greater details (178).

For studying bacteria-host interactions, we used different animal experiments:
(i) Galleria mellonella model organism
The use of larvae of the greater wax moth *G. mellonella* constitutes an attractive model because their immune system, showing both cellular and humoral responses, is comparable to those of vertebrates (42). Our results indicated that the D32 strain showed enhanced characteristics to evade the insect defense strategies (194, 261). According to this, *G. mellonella* might be used as a simple, cost- and time-efficient model for pre-tests, before using vertebrate model organisms (42), because of similar results when testing other model organisms, like chicken and mice (see below).

(ii) Chicken embryo model organism

We also tested death rates in a chicken embryo infectious model (198), by using different time points of infection. By infecting the yolk sac at an early time point of embryonic development, the embryo seemed to be more fragile because of the lower development status of defense mechanisms. These preliminary results showed that both infection models were suitable to assess differences in the pathogenic potential of nosocomial pathogens (for which it has not been used until now). To draw more general conclusions, further tests with various infectious doses in combination with a higher number of eggs would be necessary.

(iii) Murine bacteremia model

We demonstrated enhanced growth rates of the strain D32 in murine organs, liver, kidney, and spleen, by using the murine bacteremia model (105, 248). Of note, one important characteristic of colonization of organ-specific tissue cells is influenced by the ability for adhesion (95, 194). Consequently, we speculated that the D32 isolate should possess increased adherence properties, which should allow it to grow more rapidly in the tested organs. Curiously, it also showed enhanced growth at heart valves, which was expected to be characteristic of the strain UW7709, which was originally isolated from an endocarditis in humans (*Hübner, J., personal communication*).

Taken together, results of the tested animal models and cell culture assays (with the exception of the biofilm experiments) point into the same direction: The porcine commensal strain D32 generally showed a greater capacity to adhere, which might explain its increased pathogenic potential in the tested models in combination with an even faster growth *in vivo* (not *in vitro*).

Our detailed genomic comparisons emphasized the presence of a novel GI, only integrated into the genome of D32, as one distinctive feature, which might be one possibility to explain the different phenotypes. We speculate that the GI-encoded exopolysaccharides might increase adherence to host tissue cells and could provide one of the opportunities to evade the host immune response (181, 194). Consequently, it might be worth considering whether the excision of this GI or its integration into the genome of the clinical strain UW7709 would lead to different

results. Within the collection of the 15 sequenced ST40 strains, this GI is only present within the genome of the ST40 strain UW7729, isolated from fish. It would be worthwhile to include this strain in further analyses, such as the chicken embryo lethality assays.

5.3 Conclusions and further perspectives

The close evolutionary relationship is illustrated by the high level of similarity of the unrelated strains from the rather diverse *E. faecalis* ST40 strain collection. This implicates that the distribution of known and putative virulence-associated genes does not allow any differentiation between ST40 strains from a commensal and clinical background (animal/human). Results of comparative genomics also revealed differences, concerning probably horizontally acquired MGEs, which might have resulted in niche adaptation associated with dominance within the microbial habitat (49, 129, 181, 262, 286, 287).

Recombination-based *in vivo* expression technology (R-IVET) would be an useful approach to screen for genes *in vivo* activated during infection, such as genes encoded for cell surface structures, for example located within the novel GI (16, 22, 90). Knock–out of the novel GI and comparisons of the mutated and original strains under various test conditions (*in vitro* / *in vivo* models) could further allow a better understanding of the role of this supposed new GI.
A more detailed analysis of the proteome with the focus on secreted proteins might be a further objective to reveal differences not visible through genomic comparisons at the DNA level.

In the end, further work is warranted to analyze the structures of bacteriophages and plasmids in more detail. Studying of minor differences of the accessory genome could give insights in microevolution from commensal to pathogenic lifestyle in various animals and humans, and might help to trace possible transmission routes.

6 Appendix

Table 6.1: Primers used for Multilocus Sequence Typing (MLST).

Locus name	***Genbank Accession no.***	***Primer name***	***Primer sequence (5' → 3')***	***Reference***
aroE	EF_1561	aroE-1	TGGAAAACTTTACGGAGACAGC	(199), efaecalis.mlst.net
		aroE-2	GTCCTGTCCATTGTTCAAAAGC	
gdh	EF_1004	gdh-1	GGCGCACTAAAAGATATGGT	(199), efaecalis.mlst.net
		gdh-2	CCAAGATTGGGCAACTTCGTCCCA	
gki	EF_2788	gki-1	GATTTTGTGGGAATTGGTATGG	(199), efaecalis.mlst.net
		gki-2	ACCATTAAAGCAAAATGATCGC	
gyd	EF_1964	gyd-1	CAAACTGCTTAGCTCCAATGGC	(199), efaecalis.mlst.net
		gyd-2	CATTTCGTTGTCATACCAAGC	
pstS	EF_1705	pstS-1	CGGAACAGGACTTTCGC	(199), efaecalis.mlst.net
		pstS-2	ATTTACATCACGTTCTACTTGC	
xpt	EF_2365	xpt-1	AAAATGATGGCCGTGTATTAGG	(199), efaecalis.mlst.net
		xpt-2	AACGTCACCGTTCCTTCACTTA	
yqiL	EF_1364	yqiL-1	CAGCTTAAGTCAAGTAAGTGCCG	(199), efaecalis.mlst.net
		yqiL-2	GAATATCCCTTCTGCTTGTGCT	

Legend: *aroE*, shikimate-5-dehydrogenase; *gdh*, glucose-6-phosphate-dehydrogenase; *gki*, glucokinase; *gyd*, glyceraldehyde-3-phosphate dehydrogenase; *pstS*, phosphate ATP binding cassette transporter; *purK*, phosphoribosylaminoimidazol carboxylase ATPase subunit; *xpt*, xanthine phosphoribosyltransferase; *yqiL*, acetyl-coenzyme A acetyltransferase.

Table 6.2: Primers used for the analysis of the distribution of antibiotic resistances.

Locus name	*Antibitotic*	*Primer name*	*Primer sequence (5' → 3')*	*Amplicon [bp]*	*Reference*
vanA	vancomycin (vanA-type)	vanA I-1	TCTGCAATAGAGATAGCCGC	377	(119)
		vanA II-2	GGAGTAGCTATCCCAGCATT		
ermB	erythromycin	ermB-F	AGCCATGCGTCTGACATCTAT	341	(282)
		ermB-R	TGCTCATAAGTAACGGTACT		
tetM	tetracycline	tetM-F	GGTGAACATCATAGACACGC	401	(285)
		tetM-R	CTTGTTCGAGTTCCAATGC		
aacA-aphD	gentamicin	gen-F	TAATCCAAGAGCAATAAGGGC	227	(237)
		gen-R	GCCACACTATCATAACCACTA		
aadE	streptomycin	aadE-1	GCAGAACAGGATGAACGTATTCG	369	(50)
		aadE-2	ATCAGTCGGAACTATGTCCC		

Table 6.3: Primers used for screening of virulence-associated markers.

Locus name	*Genbank accession no.*	*Primer name*	*Primer sequence (5' → 3')*	*Amplicon [bp]*	*Reference*
asc10	EF0005	PAIasc10-1	GCCAAAGTGGAACGTTAAATG	345	(215), (*Werner, G., unpublished data*)
		PAIasc10-2	TCAATCCAGAAGGTCCTGTG		
cylM	EF0046	cylM-TQ1	GATGCGTATTACTGTTGTTAGAATGAGAT	150	(215), (*Werner, G., unpublished data*)
		cylM-TQ2	GAGTCTCCCTGTGATTCTGATATAGAGTT		
esp	EF0056	esp-TIM1	CTTTGATTCTTGGTTGTCGGATAC	475	(264)
		esp-TIM2	TCCAACTACCACGGTTTGTTTATC		
xyl kinase	EF0083	PAIefc-83F	GGAGCTGATAATGCTTGTGC	202	(131)
		PAIefc-83R	AAGAATTACCTGCTGCCAAC		
gls24-like	EF0117	gls24-F	TGAAGCAAATTCTCCAGTAGC	262	(215), (*Werner, G., unpublished data*)
		gls24-R	TGGAGTGGATGTTGAAGTAGG		
	AE016830.1	PAI164	ATGCCATGTTCAGCGAAGTTGCCAATTATC	*	(130, 131)
		PAI167	ATGTTGGTTGAAAGTTGCTTTTTGGCAAAC		
gelE	M37185.1	gelE-F	TATGACAATGCTTTTTGGGAT	213	(264)
		gelE-R	AGATGCACCCGAAATAATATA		
fsrB	EF_1821*	fsrB-1	GCATTGTTATCTATGTCGCCATACC	397	(150)
		fsrB-2	GGCTTAGTTCCCACACCATC		

Table 6.4: Primers used in this study for analysis of the capsule locus type.

Locus name	*Genbank accession no.*	*Primer name*	*Primer sequence (5' → 3')*	*Amplicon [bp]*	*Reference*
cpsA	EF_0095	cpsA-F	GTGTCTCCTGAAAAATCAGGCC	383	(87)
		cpsA-R	GTTAAAGTCAATGTAATGGGCTACC		
cpsB	EF_0094	cpsB-F	CTATCAAAACGATCTAAAATACCACC	619	(87)
		cpsB-R	GATTAACGTTATTAAGTTTTGAAGGCG		
cpsC	EF_0093	cpsC-F	CCAACGCTTTGCTTCTTGAATGAC	300	(150)
		cpsC-R	CCTGAATATCAATGTATTTGGGCAGTC		
cpsF	EF_0090	cpsF-F	GGCGATCTATTCTACCATCCGCGC	324	(87)
		cpsF-R	CCAAAGAAAGATATTTTGGATTGAG		

Table 6.5: Primers used for identification of CRISPR loci and characterization of the spacers, integrated in CRISPR2 locus.

Locus name	*Reference Sequence*	*Primer name*	*Primer sequence (5' → 3')*	*Amplicon [bp]*	*Reference*
CRISPR1-cas	AE016830.1	CRISPR1-cas-F	GCGATGTTAGCTGATACAAC	316	(180)
		CRISPR1-cas-R	CGAATATGCCTGTGGTGAAA		
CRISPR1 cas_csn	NC_017316.1	CRISPR1-cas_csn1-F	CAGAAGACTATCAGTTGGTG	783	(180)
		CRISPR1-cas_csn1-R	CCTTCTAAATCTTCTTCATAG		
CRISPR2	AE016830.1	CRISPR2-F	CTGGCTCGCTGTTACAGCT	variabel	(180)
		CRISPR2-R	GCCAATGTTACAATATCAAACA		
CRISPR3-cas	AE016830.1	CRISPR3-cas-F	GATCACTAGGTTCAGTTATTTC	225	(180)
		CRISPR3-cas-R	CATCGATTCATTATTCCTCCAA		

Table 6.6: Primers used for analysis of the presence of the inositol (*iol*) operon.

Locus name	*Reference Sequence*	*Primer name*	*Primer sequence (5' → 3')*	*Amplicon [bp]*	*Reference*
iolB	NC_017316.1	iolB-F	CCATCTGGCACGCCGACAGGA	363	This study
		iolB-R	GCCAGTGCACGTGATTACCGCTG		
iolG2	NC_017316.1	iolG2-F	GCGTTTGCCAGTCGGGCGAAA	465	This study
		iolG2-R	TGGTACAGGTGGGCTTCATGCGT		
iolE	NC_017316.1	iolE-F	ACGGATTGGCTTTGGCCGGATCT	363	This study
		iolE-R	TGGGGACAGGAGTCCAAACGACTG		
iolR	NC_017316.1	iolR-F	TCCCTAATCGCCACACTA	379	(24)
		iolR-R	TTGCTGAAAAAGCAGGAG		

Table 6.7: Primers used for the screening of the *E. faecalis* PAI (215) by long PCR - Part I.

Primer name	*Primer sequence (5' → 3')*	*Amplicon [bp]*	*Location (gbAF454824.1)*	*Reference*
PAI164	ATGCCATGTTCAGCGAAGTTGCCAATTATC	1548	C:427	(131)
1 PAI R	GGAAGATGGACGGTTGATGAAGCCTCAATATG			
2a PAI F	CAGTTGTCGAATACGATGCATGTCCCAGCC	9674	240:9913	(131)
2a PAI R	AAACCAAAGGAACCGAAACGGAAAAACTTAGCATGG			
2b PAI F	TTTAACCAGCCATGCTAAGTTTTTCCGTTTCGGTTC	6066	9869:15934	(131)
2b PAI R	TTTGAAATAATCTCCAACTTTTCCCCCGTTCCACAC			
2c PAI F	AACCATAAAAAGGAACGGAGGGAGCACAACAAAAGG	7697	14033:21999	(131)
2c PAI R	ACTTGCAGTGTGACTGTCTGTCGTAACTTCACC			
3a PAI F	CTCGTCCGTAACGATCTGTTTTATCGCCCTTATC	11645	21566:32079	(131)
3a PAI R	TCAAGTCCGTACAACAGGCACTTTCTTTATCAAGC			
3b PAI F	GAAGGCCGTTGCCAATTTTGCATTAGCTTGC	11411	31320:42730	(131)
3b PAI R	TCCTAAGCCTATGGTAAAACATGCTGGAGTTGTCTC			
4a PAI F	CAAGGTAGTGGAGATGTTCAGGCTGAGACAACAC	11079	42395:53473	(131)
4a PAI R	CGGATGTTACTTCTGCTGGACTTAAAACAATCCC			
4b PAI F	GGGATTGTTTTAAGTCCAGCAGAAGTAACATCCG	11561	53440:65000	(131)
4b PAI R	ACGCCAAGCACAAGGGATAAAGATTGCGAAAG			
5a PAI F	GGACGACCTTTATAGACGCCGTTTGCTTTCG	10629	64944:75572	(131)
5a PAI R	AGTCCCCTTTTTCTGCCATGACACCAGTTAAAATC			
5b PAI F	GCTGTGGTCAAGATAGATGGGAAAGAGATTGAGCG	11431	74158:85588	(131)
5b PAI R	GGATCTGAACCGTCTTGTGTCATAGTGTGCCAG			
6a PAI F	TGTAGCATACTGGCACACTATGACACAAGACGG	9115	85547:94661	(131)
6a PAI R	CGTGCCCCTAATTACCATAGAGATAGTCGCGTTG			
6b PAI F	TGGTAAACGCTGCTCCTGAAATGAAGAGTTTGAC	8432	93984:102421	(131)
6b PAI R	AGGTTTGATACGCAACTACCTTTCCCAACTGACG			

Table 6.8: Primers used for the screening of the *E. faecalis* PAI (215) by long PCR - Part II.

Primer name	*Primer sequence (5' → 3')*	*Amplicon [bp]*	*Location (gbAF454824.1)*	*Reference*
7a PAI F	TTTTGGGACAGGAACGCTATCAGTTAACGATTGC	10821	101954:113046	(131)
7a PAI R	CCTGCGGTCAAGCACAGTTGCCTTATCTTAG			
7b PAI F	ATTAAAGTCAAAAGAGACTGTTACTTGTGCGCCCTG	13858	113008:126865	(131)
7b PAI R	TCAGCAAACTAAGATAAGGCAACTGTGCTTGACC			
8a PAI F	TGCTTTAGTGGGTCGTACTAACGGAACAATAG	11008	125344:136351	(131)
8a PAI R	CAAACAACACGTCGTCGATCTTTACCTTG			
8b PAI F	CACCAATGCACATAATCAAACAATTCTAGGCGTAG	11048	135337:146384	(131)
8b PAI R	GTGGACAAGCACAGTCACAATTAGAAGCAATG			
9 PAI F	CATCATTTCTTCAGCAAATTGGTTGGCACGC	8298	146272:C	(131)
PAI167R	ATGTTGGTTGAAAGTTGCTTTTTGGCAAAC			

Table 6.9: Primers used for classification of the plasmids by amplification of the corresponding *repA* gene.

Primer name	*Reference sequence*	*Primer sequence (5' → 3')*	*Amplicon [bp]*	*Reference*
repCF10-1	*rep* of pCF10/pAD1	GCTCGATCARTTTTCAGAAG	201	(72)
repCF10-2		CGCAAACATTTGTCWATTTCTT		
repRE25-1	*rep* of pRE25	GAGAACCATCAAGGCGAAAT	630	(72)
repRE25-2		ACCAGAATAAGCACTACGTACAATCT		

Table 6.10: Primers used for gap closure of chromosomal contigs during *E. faecalis* D32 sequencing- Part I.

Primer name	*Primer sequence (5′ → 3′)*	*Reference*
Gap closure		
UW7744_01-F	TGATTCATTTCCCCGTCGTG	This study
UW7744_01-R	AAGGCCATTGAACCAGCAG	This study
UW7744_02-F	TTTAATGGAACTGCCCCCC	This study
UW7744_02-R	CGCTTTAATCTGTCGGCTTAG	This study
UW7744_04_05-F	TCCCCATTTTCAACATTGACTG	This study
UW7744_04_05-R	TGTGCAAACCCAGAATGTAATC	This study
UW7744_06-F	CAAATTATTGGCACCACATGG	This study
UW7744_06-R	TCAGAAGCAAAGGAAATCCTG	This study
UW7744_07_08-F	CATGATGGCGAACATGTCC	This study
UW7744_07_08-R	GTAGAAAGCTTGTGAGAAGTCC	This study
UW7744_09-F	ACCATTCCTAAAACTGACGC	This study
UW7744_09-R	GTTTATCCAATGGTGGAAACAC	This study
UW7744_10-F	CTAGCATTGGTGAACTAGCG	This study
UW7744_10-R	CAAGAGCTAGAATTGGTGACAG	This study
UW7744_12-F	TGTTCTATTTTCTATCGCGGG	This study
UW7744_12-R	TCACTCCTAACTACGCAGG	This study
UW7744_13-F	ATTGAAGGAGGACAATACGATG	This study
UW7744_13-R	TTCCATTCTTTGACACCGC	This study
UW7744_14-F	CTTGGAAAAACAGTGATTGTGG	This study
UW7744_14-R	CTGTATCAGTGGTCTCTGTTTG	This study
UW7744_15-F	GCAGGAATTGGTGTTTTAACC	This study
UW7744_15-R	ATTGAAGACGTAATGGCTGAG	This study
UW7744_16-F	CAGGATACATGCAACAGATGG	This study
UW7744_16-R	GTACGACATACACACCTTTCG	This study
UW7744_17-F	AGTATGACGAAGATGTTCTGC	This study
UW7744_17-R	ATACTGGAACAAGCTGTCAAG	This study
UW7744_18_F	AATCCAACTATTTGCATCCTCC	This study
UW7744_18_R	CATTACCTGCGACTCCAAAG	This study
UW7744_19-F	AGTTGATATTATCGGTTCCGC	This study
UW7744_19-R	TGTCCAATTAGTTCTGGATGTG	This study

Table 6.11: Primers used for gap closure of chromosomal contigs during *E. faecalis* D32 sequencing - Part II.

Primer name	*Primer sequence (5′ → 3′)*	*Reference*
UW7744_20-F	TGGTGATGTCCGTGAAAAAAC	This study
UW7744_20-R	ATGGTATGGCAATCCCTGC	This study
UW7744_21-F	TTTTCCTATGCCACAACTAGC	This study
UW7744_21-R	GCACAATCTTAACCATGATTGG	This study
UW7744_22-F	GTTATACGCAAGTAGCCGC	This study
UW7744_22-R	GCCAACGATAAACCAAAAACTG	This study
UW7744_23-F	AAGATAATCCGTTTGCGCC	This study
UW7744_23-R	GCTTTACTTATGCAAAACCCAG	This study
UW7744_24-F	GACGGAAGGCAAAACAATTAC	This study
UW7744_24-R	TGGTCTGGTGTTACTTTAACTG	This study
UW7744_25-F	TTGCCTTTCACTGTCCCAG	This study
UW7744_25-R	GGCCAACTTGCTGAAAAATTTG	This study
UW7744_26-F	TCTTTGAACGGTTCTATCGTG	This study
UW7744_26-R	AGGTTATTTAGCCATCACAGAC	This study
UW7744_27-F	GTTGTACGGACGGATTTAGAC	This study
UW7744_27-R	TGACGAAGAGTTAATGATTGCC	This study
UW7744_31b_32b-F	GGCATTTACAGCTAGTGATTCATC	This study
UW7744_31b_32b-R	GGCCTTAGTTTTTGGAACGATTC	This study
UW7744_33-F	CAGCAATTTTGGACAGAAAAGC	This study
UW7744_33-R	GGTGGCACTGTTACAATGC	This study
UW7744_4_1_1-F	AATGGCCGTTGTAGAACCAG	This study
UW7744_2_1-R	TCTTCATCAATGTTCGGACG	This study
UW7744_2_3-F	ACATTGTTGCTGCTGGTTTG	This study
UW7744_1_3-R	TTGCCACAAAAACACTCACC	This study
UW7744_7_1-F	CAACGCACAGAATACATGGG	This study
UW7744_5_1-R	ATTTCACCTGTCATTTCGGC	This study
UW7744_5_3-F	AAAGTGGCGGTGACAACAG	This study
UW7744_4_2_3-R	CCTTTCGCTTTCAACATTCAG	This study

Table 6.12: Primers used for gap closure of chromosomal contigs during *E. faecalis* D32 sequencing - Part III.

Primer name	*Primer sequence (5' → 3')*	*Reference*
UW7744_c5_1-F	AGCAAAGAAAGGTGTAAACTCC	This study
UW7744_c4.2_rc_1-R	TGGAAAGCCATTAGTAACCAAC	This study
UW7744_c4.2_rc_6-F	AAGTCACTCTTGGTTGGACGCC	This study
UW7744_c4.2_rest_6-R	TGAAGAAGGACAGCGCGGTATG	This study
UW7744_c1-7_R01_03-F	CAGAAAGCGTATTGCATCAAG	This study
UW7744_c1-7_R01_03-R	AAGCGCCTTTCACTCTTATG	This study
UW7744_c1-7_R02_02-F	TTAGTTGGGCACTCTAGCG	This study
UW7744_c1-7_R02_02-R	ACGAATGTTTTGAGAGTAGACC	This study
GI integration		
UW7744_5-Ende_02-F	CAGAACTCACCTCGTCTTTTAC	This study
UW7744_5-Ende_02-R	CGGTTGATACCTTTGATTTTGC	This study
UW7744_GI_05_01-F	CCCATTTATACTGGCAAATCGG	This study
UW7744_GI_05_01-R	GCAAAGGTAGCAGGAGTAAAAC	This study
UW7744_3-Ende_02-F	CTTTTCCTTGTGCAGAATCTTC	This study
UW7744_3-Ende_02-R	AACAAATTTCGCGCAACAG	This study
UW7744_GI_03_01-F	CAGACACATTGAGTAAAACAGC	This study
UW7744_GI_03_01-R	ATGGAAAGGATGTGCCTAATAC	This study

Table 6.13: Aerobic utilization of carbon sources of Biolog MicroArray™ PM01 - Part I.

C-source	*V583*	*OG1RF*	*UW6149*	*UW2860*	*UW6724*	*UW7761*	*UW7777*	*UW7780*	*UW7753*	*UW1833*	*UW7779*	*LMGT 2333*	*ATCC 27959*	*UW6727*	*D32*	*UW7709*	*D1*
Negative Control	0,00E+00	0,00E+00	0,00E+00	0,00E+00	0,00E+00	0,00E+00	0,00E+00	0,00E+00	0,00E+00	0,00E+00	0,00E+00	0,00E+00	0,00E+00	0,00E+00	0,00E+00	0,00E+00	0,00E+00
L-Arabinose	2,27E+04	2,72E+04	2,75E+04	3,36E+04	3,21E+04	2,77E+04	3,42E+04	3,54E+04	2,79E+04	2,74E+04	2,91E+04	2,55E+04	1,88E+04	2,33E+04	2,44E+04	3,36E+04	2,92E+04
N-Acetyl-D-Glucosamine	3,57E+04	4,16E+04	3,99E+04	4,44E+04	4,85E+04	4,13E+04	4,22E+04	4,67E+04	4,69E+04	4,02E+04	3,72E+04	4,13E+04	4,11E+04	4,37E+04	4,14E+04	5,49E+04	4,38E+04
D-Saccharic Acid	7,36E+02	1,20E+01	2,09E+02	3,67E+00	1,04E+02	8,00E+00	9,67E+00	7,40E+01	4,44E+02	6,42E+02	1,86E+02	3,07E+01	7,90E+01	1,09E+02	1,07E+01	4,70E+01	6,67E-01
Succinic Acid	5,98E+02	2,80E+01	9,27E+01	0,00E+00	1,51E+02	0,00E+00	0,00E+00	3,47E+01	2,69E+02	2,92E+02	3,49E+02	0,00E+00	9,70E+01	3,24E+02	4,97E+01	2,17E+01	0,00E+00
D-Galactose	4,68E+04	5,14E+04	5,30E+04	5,64E+04	5,53E+04	5,03E+04	5,14E+04	5,26E+04	5,26E+04	4,79E+04	4,61E+04	5,00E+04	5,19E+04	5,12E+04	5,15E+04	5,53E+04	5,13E+04
L-Aspartic Acid	8,46E+02	1,49E+02	4,29E+02	2,37E+01	1,92E+02	0,00E+00	3,20E+02	2,66E+02	2,41E+02	1,25E+03	4,13E+02	4,33E+01	1,84E+02	7,20E+02	7,07E+01	8,03E+01	1,70E+01
L-Proline	5,54E+02	4,27E+01	5,97E+01	1,00E+00	6,37E+01	0,00E+00	8,33E+00	3,00E+01	1,60E+02	5,85E+02	3,37E+02	5,00E+00	6,43E+01	3,62E+02	5,43E+01	1,17E+01	3,33E-01
D-Alanine	1,03E+03	5,52E+02	2,15E+02	6,53E+01	3,07E+02	4,33E+00	1,13E+02	1,07E+02	2,93E+02	1,08E+03	5,95E+02	3,00E+00	1,34E+02	5,71E+02	1,63E+02	1,25E+02	9,00E+00
D-Trehalose	4,19E+04	4,49E+04	4,96E+04	5,24E+04	5,01E+04	4,37E+04	4,80E+04	4,91E+04	4,85E+04	4,57E+04	4,39E+04	4,56E+04	5,00E+04	4,99E+04	4,72E+04	5,43E+04	4,62E+04
D-Mannose	4,47E+04	4,84E+04	5,03E+04	5,49E+04	5,57E+04	4,82E+04	5,08E+04	5,18E+04	4,89E+04	4,90E+04	4,60E+04	4,78E+04	4,81E+04	5,29E+04	5,44E+04	5,87E+04	4,91E+04
Dulcitol	9,10E+03	7,94E+03	1,11E+04	6,87E+03	8,30E+03	6,21E+03	6,89E+03	5,30E+03	6,91E+03	1,13E+04	1,16E+04	6,70E+03	7,30E+03	9,15E+03	5,09E+03	1,06E+04	5,86E+03
D-Serine	6,55E+03	3,87E+03	6,39E+03	6,06E+03	3,46E+03	5,78E+02	4,39E+03	4,45E+03	4,76E+03	7,12E+03	3,65E+03	3,60E+03	2,71E+03	3,41E+03	2,44E+03	2,84E+03	2,51E+03
D-Sorbitol	4,54E+04	4,85E+04	5,10E+04	5,43E+04	5,29E+04	4,75E+04	4,86E+04	5,25E+04	5,27E+04	4,86E+04	4,42E+04	4,86E+04	5,06E+04	5,00E+04	4,59E+04	5,66E+04	5,25E+04
Glycerol	4,68E+04	5,33E+04	5,12E+04	5,59E+04	5,43E+04	5,10E+04	5,21E+04	5,24E+04	5,25E+04	4,80E+04	4,70E+04	4,87E+04	5,36E+04	5,01E+04	4,73E+04	4,86E+04	4,77E+04
L-Fucose	2,36E+03	2,22E+03	6,43E+03	2,20E+03	1,25E+03	5,07E+01	2,57E+03	1,38E+03	2,81E+03	7,45E+03	2,75E+03	4,97E+02	1,42E+03	4,43E+03	1,80E+03	5,79E+02	4,49E+02
D-Glucuronic Acid	1,19E+03	9,36E+02	7,77E+02	4,50E+01	5,60E+02	0,00E+00	1,71E+02	6,38E+02	8,78E+02	1,98E+03	1,09E+03	4,27E+01	4,15E+02	9,52E+02	1,79E+02	1,20E+02	5,00E+01
D-Gluconic Acid	4,46E+04	4,58E+04	5,14E+04	5,56E+04	5,18E+04	4,73E+04	4,93E+04	5,13E+04	5,12E+04	4,55E+04	4,23E+04	4,63E+04	4,77E+04	1,52E+03	4,68E+04	5,75E+04	5,22E+04
D,L-a-Glycerol-Phosphate	1,06E+04	4,27E+03	5,61E+03	5,30E+03	5,02E+03	4,13E+03	6,26E+03	6,68E+03	7,10E+03	1,17E+04	1,08E+04	7,65E+03	3,92E+03	1,17E+04	3,62E+03	2,07E+03	5,23E+03
D-Xylose	2,83E+04	2,53E+04	2,46E+04	2,50E+04	3,09E+04	2,13E+04	2,31E+04	2,32E+04	2,59E+04	2,33E+04	2,80E+04	2,02E+04	2,27E+04	2,46E+04	2,26E+04	2,66E+04	2,29E+04

Table 6.14: Aerobic utilization of carbon sources of Biolog MicroArray™ PM01 - Part II.

C-source	*V583*	*OG1RF*	*UW6149*	*UW2860*	*UW6724*	*UW7761*	*UW7777*	*UW7780*	*UW7753*	*UW1833*	*UW7779*	*LMGT 2333*	*ATCC 27959*	*UW6727*	*D32*	*UW7709*	*D1*
L-Lactic Acid	8,01E+02	6,97E+01	9,43E+01	0,00E+00	5,43E+01	0,00E+00	2,77E+01	5,03E+01	7,90E+01	3,86E+02	8,40E+01	4,67E+00	5,57E+01	6,43E+01	1,97E+01	9,67E+00	1,00E+00
Formic Acid	1,37E+03	4,02E+02	7,13E+02	3,33E-01	1,63E+03	1,67E+00	1,85E+02	1,89E+02	2,74E+02	7,28E+02	7,16E+02	3,07E+01	1,72E+02	2,74E+02	6,57E+01	2,18E+02	3,70E+01
D-Mannitol	3,66E+04	4,28E+04	4,51E+04	4,60E+04	4,56E+04	3,88E+04	4,64E+04	4,56E+04	4,25E+04	4,09E+04	3,65E+04	3,99E+04	4,51E+04	4,93E+04	4,65E+04	5,44E+04	3,96E+04
L-Glutamic Acid	5,19E+03	5,03E+03	6,25E+03	2,30E+03	5,01E+03	3,11E+03	4,77E+03	2,32E+03	4,64E+03	7,81E+03	6,96E+03	3,54E+03	3,95E+03	5,57E+03	3,76E+03	7,15E+03	2,14E+03
D-Glucose-6-Phosphate	1,27E+04	4,52E+04	4,96E+04	4,60E+04	4,98E+04	4,81E+04	4,70E+04	5,03E+04	4,95E+04	4,73E+04	4,57E+04	4,78E+04	5,35E+04	4,76E+04	4,54E+04	4,78E+04	5,00E+04
D-Galactonic Acid-g-Lactone	6,30E+02	0,00E+00	4,86E+04	5,38E+04	5,11E+04	4,71E+04	2,47E+02	3,47E+01	4,98E+04	4,49E+04	4,31E+04	0,00E+00	5,02E+04	4,87E+04	0,00E+00	1,33E+00	0,00E+00
D,L-Malic Acid	5,58E+04	5,92E+04	5,82E+04	6,03E+04	5,84E+04	5,56E+04	5,78E+04	5,85E+04	5,82E+04	5,51E+04	5,31E+04	5,67E+04	5,84E+04	5,68E+04	5,67E+04	5,64E+04	5,80E+04
D-Ribose	5,22E+04	5,46E+04	5,53E+04	5,76E+04	5,71E+04	5,18E+04	5,31E+04	5,35E+04	5,58E+04	5,08E+04	5,21E+04	5,24E+04	5,50E+04	5,27E+04	5,20E+04	5,25E+04	5,35E+04
Tween 20	1,46E+04	7,23E+03	6,29E+03	1,21E+04	8,59E+03	7,83E+03	1,33E+04	1,36E+04	1,04E+04	1,70E+04	1,48E+04	1,08E+04	8,22E+03	2,16E+04	7,27E+03	5,94E+03	8,85E+03
L-Rhamnose	2,72E+03	6,56E+03	1,27E+04	1,08E+04	1,05E+04	7,71E+03	1,58E+04	1,46E+04	1,25E+04	2,75E+04	2,17E+04	1,17E+04	8,41E+03	1,31E+04	3,69E+03	2,23E+03	1,23E+03
D-Fructose	4,15E+04	3,64E+04	4,65E+04	5,21E+04	4,86E+04	4,34E+04	4,70E+04	5,00E+04	4,83E+04	4,35E+04	4,03E+04	4,50E+04	4,69E+04	5,02E+04	4,40E+04	5,76E+04	4,48E+04
Acetic Acid	1,18E+04	5,38E+03	8,44E+03	5,36E+03	1,01E+04	5,08E+03	7,18E+03	5,34E+03	7,63E+03	1,13E+04	7,21E+03	7,99E+03	6,44E+03	7,03E+03	5,64E+03	8,30E+03	1,02E+04
a-D-Glucose	3,62E+04	3,81E+04	3,94E+04	4,44E+04	4,90E+04	3,99E+04	4,16E+04	4,60E+04	4,06E+04	3,55E+04	3,66E+04	4,12E+04	4,04E+04	4,45E+04	4,11E+04	5,43E+04	4,08E+04
Maltose	3,72E+04	3,73E+04	4,36E+04	4,82E+04	4,80E+04	3,96E+04	4,38E+04	4,60E+04	4,41E+04	4,02E+04	3,78E+04	4,05E+04	4,43E+04	4,48E+04	4,25E+04	5,18E+04	4,23E+04
D-Melibiose	2,48E+03	2,25E+03	3,50E+03	2,15E+03	2,74E+03	7,34E+02	2,66E+03	1,93E+03	3,23E+03	7,45E+03	5,02E+03	1,77E+03	1,46E+03	5,63E+03	1,12E+03	2,62E+03	1,56E+03
Thymidine	4,21E+04	4,24E+04	4,75E+04	4,35E+04	4,60E+04	4,22E+04	4,40E+04	4,28E+04	4,56E+04	4,52E+04	4,29E+04	4,44E+04	4,66E+04	4,29E+04	4,18E+04	3,97E+04	4,16E+04
L-Asparagine	4,45E+03	5,66E+03	4,71E+03	4,44E+03	4,70E+03	1,60E+03	4,32E+03	4,32E+03	5,22E+03	5,36E+03	4,21E+03	3,11E+03	4,76E+03	6,97E+03	3,77E+03	2,15E+03	3,49E+03
D-Aspartic Acid	1,59E+03	9,96E+02	3,49E+02	2,15E+02	7,45E+02	2,37E+01	4,68E+02	7,24E+02	1,49E+03	8,43E+02	9,44E+02	7,60E+01	8,26E+02	1,17E+03	3,08E+02	4,16E+02	8,50E+01
D-Glucosaminic Acid	4,70E+04	5,32E+04	5,54E+04	5,77E+04	5,74E+04	5,22E+04	5,43E+04	5,64E+04	5,64E+04	5,14E+04	4,85E+04	5,43E+04	5,63E+04	5,39E+04	5,46E+03	4,97E+04	4,36E+03

Table 6.15: Aerobic utilization of carbon sources of Biolog MicroArray™ PM01 - Part III.

C-source	*V583*	*OG1RF*	*UW6149*	*UW2860*	*UW6724*	*UW7761*	*UW7777*	*UW7780*	*UW7753*	*UW1833*	*UW7779*	*LMGT 2333*	*ATCC 27959*	*UW6727*	*D32*	*UW7709*	*D1*
1,2-Propanediol	7,45E+02	4,73E+01	1,41E+02	5,33E+00	8,87E+01	0,00E+00	8,33E+00	1,05E+02	1,25E+02	5,02E+02	4,22E+02	3,33E+00	2,99E+02	1,21E+03	2,03E+01	3,67E+00	0,00E+00
Tween 40	5,01E+03	6,82E+02	1,54E+02	4,43E+02	6,45E+02	0,00E+00	7,22E+02	6,17E+02	6,83E+02	2,88E+03	2,92E+03	3,20E+01	3,62E+02	4,35E+03	1,18E+02	1,83E+03	2,30E+01
a-Keto-Glutaric Acid	1,62E+03	2,76E+02	8,60E+02	4,60E+01	8,95E+02	2,00E+00	1,14E+02	4,18E+02	6,08E+02	1,32E+03	1,91E+03	7,77E+01	2,28E+02	1,01E+03	1,51E+02	1,65E+02	7,33E+00
a-Keto-Butyric Acid	4,33E+04	4,65E+04	4,50E+04	4,39E+04	4,27E+04	4,29E+04	4,32E+04	4,31E+04	4,41E+04	4,25E+04	4,24E+04	1,05E+04	4,50E+04	4,57E+04	4,24E+04	4,39E+04	4,44E+04
a-Methyl-D-Galactoside	8,72E+02	2,79E+02	3,93E+02	2,73E+02	5,30E+02	0,00E+00	8,30E+02	5,30E+02	5,04E+02	1,78E+03	1,69E+03	6,90E+01	4,11E+02	8,77E+02	1,16E+02	1,62E+02	2,61E+02
a-D-Lactose	4,04E+04	4,58E+04	4,13E+04	4,81E+04	4,65E+04	3,97E+04	4,36E+04	4,71E+04	4,36E+04	3,95E+04	3,86E+04	4,06E+04	4,33E+04	4,54E+04	4,31E+04	5,23E+04	4,16E+04
Lactulose	9,91E+03	1,71E+04	5,25E+04	5,49E+04	5,34E+04	4,76E+04	5,07E+04	5,20E+04	5,03E+04	4,80E+04	4,72E+04	5,12E+04	5,29E+04	5,18E+04	4,74E+04	5,63E+04	4,97E+04
Sucrose	4,57E+04	5,41E+04	5,68E+04	5,75E+04	5,62E+04	5,26E+04	5,36E+04	5,28E+04	5,44E+04	5,17E+04	4,87E+04	5,22E+04	5,67E+04	5,42E+04	5,45E+04	5,88E+04	5,48E+04
Uridine	4,39E+04	4,78E+04	5,05E+04	4,75E+04	4,78E+04	4,48E+04	4,69E+04	4,50E+04	4,83E+04	4,57E+04	4,59E+04	4,19E+04	5,02E+04	4,61E+04	4,49E+04	4,35E+04	4,63E+04
L-Glutamine	4,91E+03	3,46E+03	2,56E+03	2,75E+03	4,36E+03	1,83E+03	3,82E+03	3,49E+03	3,79E+03	4,77E+03	3,92E+03	2,57E+03	4,33E+03	4,21E+03	2,22E+03	2,80E+03	3,56E+03
m-Tartaric Acid	2,12E+03	2,55E+02	3,07E+02	5,10E+01	7,45E+02	5,67E+00	1,85E+02	5,49E+02	7,75E+02	1,21E+03	6,85E+02	1,80E+02	4,80E+02	4,29E+02	4,13E+01	1,06E+02	2,46E+02
D-Glucose-1-Phosphate	3,43E+03	1,79E+03	1,54E+03	7,25E+02	1,19E+03	3,33E+02	1,59E+03	2,42E+03	1,89E+03	3,24E+03	2,43E+03	2,80E+02	8,34E+02	2,54E+03	6,83E+02	3,99E+02	1,11E+03
D-Fructose-6-Phosphate	1,27E+04	5,24E+04	5,24E+04	5,36E+04	5,28E+04	5,01E+04	5,13E+04	5,18E+04	5,18E+04	4,93E+04	4,75E+04	5,09E+04	5,40E+04	5,00E+04	5,03E+04	4,98E+04	5,18E+04
Tween 80	5,84E+03	3,34E+03	6,11E+03	1,02E+04	4,96E+03	5,27E+03	9,37E+03	8,99E+03	7,33E+03	1,17E+04	9,52E+03	6,61E+03	5,57E+03	1,61E+04	3,31E+03	2,40E+03	6,70E+03
a-Hydroxy Glutaric Acid-g-Lactone	8,27E+02	4,33E+00	6,67E+01	1,07E+01	1,51E+02	6,67E+00	1,00E+01	8,87E+01	5,57E+01	7,42E+02	1,86E+02	6,00E+00	8,97E+01	9,87E+01	1,67E+00	3,83E+01	7,67E+00
a-Hydroxy-Butyric Acid	8,70E+02	4,82E+02	2,39E+02	6,30E+01	4,94E+02	5,00E+00	2,52E+02	5,41E+02	3,40E+02	5,78E+02	9,36E+02	7,47E+01	2,36E+02	5,75E+02	3,73E+01	2,97E+01	1,56E+02
b-Methyl-D-Glucoside	4,62E+04	3,97E+04	4,49E+04	4,61E+04	4,77E+04	3,96E+04	4,33E+04	5,19E+04	4,29E+04	4,13E+04	4,07E+04	4,00E+04	4,32E+04	4,72E+04	4,15E+04	5,00E+04	4,25E+04
Adonitol	1,34E+03	1,51E+03	1,12E+03	4,73E+02	1,69E+03	1,03E+01	4,11E+02	4,11E+02	1,01E+03	1,19E+03	2,43E+03	1,55E+02	1,69E+03	1,84E+03	2,55E+02	5,24E+02	9,11E+02
Maltotriose	4,09E+04	4,12E+04	4,77E+04	5,11E+04	5,10E+04	4,26E+04	4,76E+04	4,99E+04	4,60E+04	4,47E+04	4,15E+04	4,44E+04	4,78E+04	4,91E+04	4,66E+04	5,35E+04	4,55E+04

Table 6.16: Aerobic utilization of carbon sources of Biolog MicroArray™ PM01 - Part IV.

C-source	*V583*	*OG1RF*	*UW6149*	*UW2860*	*UW6724*	*UW7761*	*UW7777*	*UW7780*	*UW7753*	*UW1833*	*UW7779*	*LMGT 2333*	*ATCC 27959*	*UW6727*	*D32*	*UW7709*	*D1*
2`-Deoxy-Adenosine	4,35E+04	4,10E+04	4,75E+04	4,52E+04	4,93E+04	4,58E+04	4,66E+04	4,46E+04	4,64E+04	4,59E+04	4,49E+04	4,60E+04	4,99E+04	4,59E+04	4,35E+04	3,97E+04	4,60E+04
Adenosine	3,58E+04	3,61E+04	3,90E+04	3,78E+04	4,35E+04	3,85E+04	3,93E+04	3,64E+04	4,28E+04	4,21E+04	3,96E+04	3,92E+04	4,34E+04	3,62E+04	3,62E+04	4,22E+04	3,99E+04
Glycyl-L-Aspartic Acid	9,10E+03	6,75E+03	7,09E+03	5,09E+03	7,25E+03	4,36E+03	6,71E+03	7,23E+03	7,59E+03	8,99E+03	6,85E+03	6,51E+03	7,53E+03	6,24E+03	4,56E+03	6,20E+03	7,12E+03
Citric Acid	4,98E+04	5,36E+04	5,45E+04	5,51E+04	5,49E+04	5,22E+04	5,21E+04	4,10E+04	5,38E+04	5,11E+04	5,07E+04	5,19E+04	5,60E+04	4,34E+03	5,15E+04	1,99E+03	5,39E+04
m-Inositol	6,28E+03	5,43E+04	5,55E+04	5,74E+04	5,62E+04	5,08E+04	5,30E+04	5,43E+04	5,52E+04	5,32E+04	4,82E+04	5,14E+04	5,42E+04	5,30E+04	1,54E+03	4,96E+04	5,47E+04
D-Threonine	9,45E+02	8,37E+01	3,62E+02	1,37E+01	2,77E+02	0,00E+00	3,13E+01	2,26E+02	3,26E+02	6,97E+02	3,40E+02	1,17E+01	1,86E+02	3,21E+02	5,40E+01	7,30E+01	3,33E-01
Fumaric Acid	2,58E+02	6,67E-01	8,33E+00	3,33E-01	0,00E+00	0,00E+00	0,00E+00	6,00E+00	1,53E+01	0,00E+00	6,67E-01	0,00E+00	4,00E+00	1,67E+00	0,00E+00	0,00E+00	0,00E+00
Bromo-Succinic Acid	4,28E+04	4,11E+04	4,61E+04	4,47E+04	4,43E+04	4,45E+04	4,25E+04	3,87E+04	4,62E+04	3,74E+04	4,13E+04	4,27E+04	4,57E+04	4,43E+04	3,33E+04	4,68E+04	4,66E+04
Propionic Acid	1,29E+04	4,88E+03	7,93E+03	1,91E+03	1,02E+04	7,77E+02	7,69E+03	8,07E+03	4,05E+03	9,69E+03	6,37E+03	1,50E+03	3,84E+03	4,25E+03	1,87E+03	6,29E+03	7,27E+03
Mucic Acid	3,61E+03	1,87E+03	1,03E+04	7,67E+03	1,19E+04	1,01E+04	2,53E+03	2,51E+03	1,17E+04	1,38E+04	1,55E+04	1,29E+03	1,16E+04	1,64E+04	5,63E+02	7,47E+02	1,96E+03
Glycolic Acid	2,34E+03	2,40E+03	1,84E+03	1,13E+03	2,84E+03	6,76E+02	2,22E+03	2,24E+03	1,34E+03	2,46E+03	1,83E+03	9,13E+02	2,01E+03	2,35E+03	6,50E+02	2,51E+03	1,53E+03
Glyoxylic Acid	2,78E+03	2,08E+03	1,28E+03	6,12E+02	2,53E+03	1,07E+02	2,20E+03	2,02E+03	1,28E+03	1,44E+03	2,60E+03	5,30E+02	2,01E+03	2,60E+03	6,59E+02	2,24E+03	1,32E+03
D-Cellobiose	3,90E+04	3,76E+04	4,27E+04	4,63E+04	4,76E+04	4,02E+04	4,38E+04	4,56E+04	4,41E+04	4,03E+04	3,92E+04	4,06E+04	4,53E+04	4,58E+04	4,24E+04	5,18E+04	4,14E+04
Inosine	3,36E+04	3,84E+04	4,30E+04	4,01E+04	4,44E+04	4,08E+04	4,29E+04	3,98E+04	4,26E+04	4,14E+04	4,00E+04	3,97E+04	4,45E+04	3,75E+04	3,68E+04	4,16E+04	3,46E+04
Glycyl-L-Glutamic Acid	8,77E+03	8,30E+03	9,18E+03	8,38E+03	9,16E+03	6,10E+03	1,03E+04	8,75E+03	8,46E+03	8,70E+03	8,34E+03	7,56E+03	8,93E+03	9,35E+03	6,84E+03	8,15E+03	7,75E+03
Tricarballylic Acid	2,65E+03	1,56E+03	2,09E+03	7,94E+02	2,95E+03	4,67E+02	2,08E+03	1,67E+03	1,54E+03	2,38E+03	2,08E+03	1,13E+03	1,79E+03	1,56E+03	5,47E+02	7,81E+02	1,63E+03
L-Serine	6,68E+03	4,98E+03	3,83E+03	4,30E+03	4,30E+03	1,14E+03	4,15E+03	4,45E+03	4,73E+03	7,49E+03	5,29E+03	4,11E+03	3,22E+03	4,78E+03	3,95E+03	2,48E+03	3,31E+03
L-Threonine	2,71E+03	1,64E+03	6,60E+02	7,30E+02	1,33E+03	2,43E+01	1,38E+03	1,35E+03	1,95E+03	2,69E+03	3,11E+03	3,53E+02	1,48E+03	1,91E+03	4,59E+02	2,06E+02	1,16E+03
L-Alanine	2,27E+03	2,83E+02	2,23E+02	1,09E+02	6,78E+02	0,00E+00	4,19E+02	7,22E+02	7,56E+02	8,86E+02	1,35E+03	9,83E+01	4,63E+02	9,49E+02	1,22E+02	1,40E+02	4,67E+01

Table 6.17: Aerobic utilization of carbon sources of Biolog MicroArray™ PM01 - Part V.

C-source	*V583*	*OG1RF*	*UW6149*	*UW2860*	*UW6724*	*UW7761*	*UW7777*	*UW7780*	*UW7753*	*UW1833*	*UW7779*	*LMGT 2333*	*ATCC 27959*	*UW6727*	*D32*	*UW7709*	*D1*
L-Alanyl-Glycine	1,70E+03	4,84E+02	3,22E+02	1,24E+02	6,74E+02	3,33E-01	4,25E+02	9,81E+02	3,91E+02	8,18E+02	3,68E+02	5,47E+01	3,89E+02	9,56E+02	1,19E+02	1,51E+02	1,14E+02
Acetoacetic Acid	2,80E+04	2,49E+04	2,32E+04	2,36E+04	1,98E+04	2,43E+04	2,61E+04	2,39E+04	2,57E+04	3,16E+04	2,74E+04	2,40E+04	2,24E+04	2,96E+04	2,29E+04	1,76E+04	2,57E+04
N-Acetyl-b-D-Mannosamine	4,85E+04	5,37E+04	5,17E+04	5,08E+04	5,53E+04	4,74E+04	5,24E+04	5,28E+04	5,09E+04	4,77E+04	4,68E+04	4,80E+04	5,04E+04	5,31E+04	5,03E+04	5,65E+04	4,83E+04
Mono Methyl Succinate	5,07E+03	4,15E+03	4,49E+03	2,57E+03	5,25E+03	2,57E+03	5,11E+03	3,89E+03	3,89E+03	4,88E+03	9,15E+03	2,62E+03	5,07E+03	6,98E+03	1,71E+03	3,99E+03	3,25E+03
Methyl Pyruvate	4,90E+04	5,29E+04	5,32E+04	5,21E+04	5,12E+04	4,95E+04	5,15E+04	5,01E+04	5,03E+04	4,97E+04	4,72E+04	9,09E+03	5,41E+04	5,16E+04	4,85E+04	5,24E+04	5,29E+04
D-Malic Acid	2,61E+04	1,83E+04	3,16E+04	2,27E+04	2,61E+04	2,59E+04	2,95E+04	2,97E+04	2,77E+04	2,60E+04	2,74E+04	2,73E+04	2,47E+04	3,11E+04	2,22E+04	2,38E+04	3,20E+04
L-Malic Acid	5,97E+04	6,30E+04	6,36E+04	6,33E+04	6,34E+04	6,10E+04	6,30E+04	6,07E+04	6,30E+04	5,91E+04	5,98E+04	6,05E+04	6,52E+04	6,22E+04	5,99E+04	6,33E+04	6,32E+04
Glycyl-L-Proline	1,02E+04	1,05E+04	9,05E+03	1,05E+04	1,13E+04	8,42E+03	1,08E+04	1,12E+04	1,11E+04	1,05E+04	9,77E+03	8,85E+03	1,22E+04	1,04E+04	9,27E+03	1,05E+04	1,12E+04
p-Hydroxy-Phenylacetic Acid	5,45E+03	3,90E+03	4,04E+03	3,54E+03	5,63E+03	2,93E+03	4,54E+03	5,36E+03	4,99E+03	3,57E+03	4,84E+03	3,46E+03	5,87E+03	4,22E+03	2,69E+03	4,95E+03	5,38E+03
m-Hydroxy-Phenylacetic Acid	3,27E+03	3,43E+03	2,31E+03	2,35E+03	3,91E+03	1,37E+03	3,67E+03	4,10E+03	2,87E+03	2,37E+03	2,98E+03	1,73E+03	3,85E+03	3,15E+03	1,06E+03	3,40E+03	3,13E+03
Tyramine	4,77E+03	4,27E+03	2,21E+03	3,56E+03	3,95E+03	2,34E+03	4,94E+03	4,93E+03	3,23E+03	3,87E+03	3,92E+03	1,60E+03	4,60E+03	8,25E+03	1,82E+03	3,19E+03	3,26E+03
D-Psicose	3,18E+04	4,00E+04	5,05E+04	5,08E+04	3,94E+04	2,92E+04	4,29E+04	4,21E+04	3,42E+04	3,69E+04	3,76E+04	2,85E+04	3,45E+04	4,57E+04	3,91E+04	3,11E+04	2,83E+04
L-Lyxose	4,44E+04	4,82E+04	4,47E+04	4,71E+04	5,41E+04	4,43E+04	4,84E+04	4,82E+04	4,65E+04	4,31E+04	5,01E+04	3,79E+04	4,62E+04	4,81E+04	4,68E+04	4,81E+04	4,52E+04
Glucuronamide	9,05E+03	1,09E+04	8,78E+03	7,58E+03	9,43E+03	5,68E+03	1,07E+04	8,53E+03	7,79E+03	1,06E+04	8,30E+03	5,06E+03	9,28E+03	1,06E+04	7,05E+03	9,05E+03	8,07E+03
Pyruvic Acid	5,38E+04	5,77E+04	5,90E+04	5,84E+04	5,43E+04	5,78E+04	5,81E+04	5,73E+04	5,78E+04	5,59E+04	5,59E+04	1,84E+04	6,08E+04	5,79E+04	5,48E+04	5,62E+04	5,97E+04
L-Galactonic Acid-g-Lactone	4,02E+03	4,46E+03	4,20E+03	2,41E+03	5,35E+03	1,92E+03	4,46E+03	3,43E+03	2,69E+03	4,75E+03	3,92E+03	1,90E+03	5,07E+03	5,50E+03	1,40E+03	4,47E+03	4,51E+03
D-Galacturonic Acid	1,48E+04	1,18E+04	1,57E+04	7,34E+03	1,37E+04	1,24E+04	1,28E+04	9,39E+03	1,39E+04	1,93E+04	1,73E+04	1,17E+04	1,53E+04	1,28E+04	8,84E+03	1,90E+04	1,40E+04
b-Phenylethylamine	1,90E+04	1,64E+04	1,51E+04	1,15E+04	1,72E+04	1,34E+04	1,81E+04	1,49E+04	1,41E+04	1,85E+04	1,75E+04	1,42E+04	1,64E+04	1,88E+04	1,34E+04	1,76E+04	1,48E+04
Ethanolamine	1,58E+04	1,53E+04	1,45E+04	1,02E+04	1,52E+04	1,13E+04	1,45E+04	1,23E+04	1,28E+04	1,40E+04	1,59E+04	1,06E+04	1,56E+04	1,40E+04	1,05E+04	1,52E+04	1,21E+04

Table 6.18: Standard derivations of Biolog MicroArray™ PM01 analyzes - Part I.

C-source	*V583*	*OG1RF*	*UW6149*	*UW2860*	*UW6724*	*UW7761*	*UW7777*	*UW7780*	*UW7753*	*UW1833*	*UW7779*	*LMGT 2333*	*ATCC 27959*	*UW6727*	*D32*	*UW7709*	*D1*
Negative Control	0,0E+00	0,0E+00	0,0E+00	0,0E+00	0,0E+00	0,0E+00	0,0E+00	0,0E+00	0,0E+00	0,0E+00	0,0E+00	0,0E+00	0,0E+00	0,0E+00	0,0E+00	0,0E+00	0,0E+00
L-Arabinose	2,4E+03	1,4E+03	1,3E+04	5,8E+02	2,5E+03	6,6E+03	1,1E+03	1,3E+03	5,4E+03	4,9E+03	4,1E+03	9,8E+03	6,7E+03	8,9E+02	7,2E+02	9,7E+03	6,7E+03
N-Acetyl-D-Glucosamine	3,1E+03	5,7E+03	7,2E+02	4,1E+03	2,1E+03	5,8E+03	6,3E+02	3,2E+03	3,9E+03	5,2E+03	4,8E+03	3,8E+03	4,7E+03	1,1E+03	4,1E+03	1,4E+03	2,7E+03
D-Saccharic Acid	8,8E+02	9,1E+00	2,8E+02	3,9E+00	1,5E+02	8,6E+00	1,4E+01	1,0E+02	6,3E+02	4,1E+02	1,3E+02	4,3E+01	1,1E+02	1,4E+02	1,4E+01	5,5E+01	9,4E-01
Succinic Acid	7,1E+02	3,5E+01	1,3E+02	0,0E+00	2,1E+02	0,0E+00	0,0E+00	4,9E+01	3,8E+02	2,4E+02	2,5E+02	0,0E+00	1,4E+02	3,6E+02	7,0E+01	3,1E+01	0,0E+00
D-Galactose	1,4E+03	3,8E+03	2,2E+03	1,8E+03	1,3E+03	2,3E+02	3,7E+03	3,4E+03	1,5E+03	3,6E+03	4,6E+03	1,6E+03	1,8E+03	3,1E+03	2,3E+03	1,5E+03	3,7E+03
L-Aspartic Acid	8,8E+02	1,2E+02	5,8E+02	1,5E+01	2,7E+02	0,0E+00	3,2E+02	3,6E+02	2,0E+02	4,5E+02	4,0E+02	6,0E+01	2,6E+02	4,8E+02	7,7E+01	1,1E+02	2,3E+01
L-Proline	7,4E+02	3,3E+01	7,0E+01	8,2E-01	8,6E+01	0,0E+00	6,5E+00	4,2E+01	2,1E+02	3,4E+02	2,8E+02	7,1E+00	9,1E+01	2,9E+02	6,5E+01	1,6E+01	4,7E-01
D-Alanine	9,1E+02	7,6E+02	2,8E+02	6,1E+01	4,1E+02	6,1E+00	9,9E+01	1,5E+02	3,5E+02	2,6E+02	6,2E+02	3,6E+00	1,9E+02	4,8E+02	1,2E+02	1,5E+02	1,3E+01
D-Trehalose	3,8E+02	2,9E+03	2,0E+03	2,0E+03	1,7E+03	1,1E+03	4,0E+03	4,3E+03	1,8E+03	3,1E+03	3,5E+03	1,5E+03	1,7E+03	1,8E+03	3,2E+03	9,5E+02	3,0E+03
D-Mannose	6,3E+02	3,2E+03	3,0E+03	9,0E+02	3,1E+03	8,0E+02	4,8E+03	3,8E+03	2,3E+03	3,7E+03	6,9E+03	1,1E+03	6,1E+03	2,1E+03	2,5E+03	1,8E+03	3,8E+03
Dulcitol	4,0E+03	3,6E+03	1,1E+03	1,7E+03	4,1E+03	3,0E+03	3,8E+03	2,5E+03	1,8E+03	1,9E+03	1,4E+03	4,0E+03	8,8E+02	7,6E+02	7,7E+02	1,4E+03	2,1E+03
D-Serine	2,8E+03	1,5E+03	4,8E+03	2,0E+03	2,6E+03	7,2E+02	1,5E+03	1,7E+03	2,7E+03	1,4E+03	9,5E+02	2,9E+03	1,0E+03	1,4E+03	1,2E+03	2,7E+03	2,4E+02
D-Sorbitol	1,7E+03	3,6E+03	2,0E+03	1,4E+03	3,2E+03	2,6E+03	3,4E+03	3,8E+03	1,4E+03	3,0E+03	2,9E+03	9,4E+02	1,4E+03	1,5E+03	4,0E+03	1,7E+03	5,7E+02
Glycerol	2,1E+03	3,2E+03	2,8E+03	2,2E+03	4,2E+02	1,8E+03	4,5E+03	2,6E+03	2,2E+03	2,3E+03	1,7E+03	6,5E+03	1,0E+03	3,4E+03	2,6E+03	7,8E+02	1,4E+03
L-Fucose	7,4E+02	1,5E+03	3,6E+03	7,5E+02	1,6E+03	6,3E+01	6,3E+02	1,2E+03	2,0E+03	2,8E+03	1,0E+03	3,6E+02	2,0E+03	1,4E+03	3,5E+02	7,7E+02	5,6E+02
D-Glucuronic Acid	7,8E+02	7,3E+02	1,1E+03	3,3E+01	7,9E+02	0,0E+00	5,0E+01	9,0E+02	6,7E+02	6,9E+02	8,0E+02	3,9E+01	5,9E+02	4,3E+02	1,9E+02	1,7E+02	7,1E+01
D-Gluconic Acid	1,4E+03	2,4E+03	1,8E+03	1,1E+03	2,8E+03	1,4E+03	3,0E+03	3,7E+03	2,0E+03	2,3E+03	4,7E+03	2,1E+03	1,7E+03	1,3E+02	3,8E+03	3,0E+03	2,5E+03
D,L-a-Glycerol-Phosphate	1,6E+03	2,3E+03	2,9E+03	2,7E+03	3,3E+03	1,5E+03	2,9E+03	2,3E+03	1,1E+03	3,1E+03	3,9E+03	2,9E+03	3,4E+03	2,2E+03	7,2E+02	1,3E+03	3,3E+03
D-Xylose	4,3E+03	3,7E+03	4,3E+03	4,0E+02	1,1E+04	3,4E+03	4,5E+03	3,4E+03	3,4E+03	1,3E+03	5,9E+03	2,2E+03	4,5E+03	5,8E+02	9,1E+02	1,4E+03	1,8E+03

Table 6.19: Standard derivations of Biolog MicroArray™ PM01 analyzes - Part II.

C-source	*V583*	*OG1RF*	*UW6149*	*UW2860*	*UW6724*	*UW7761*	*UW7777*	*UW7780*	*UW7753*	*UW1833*	*UW7779*	*LMGT 2333*	*ATCC 27959*	*UW6727*	*D32*	*UW7709*	*D1*
L-Lactic Acid	1,1E+03	6,0E+01	1,2E+02	0,0E+00	6,9E+01	0,0E+00	2,9E+01	7,1E+11	1,1E+22	4,2E+22	8,4E+11	5,2E+00	7,9E+11	7,7E+11	2,8E+11	6,9E+00	1,4E+00
Formic Acid	1,8E+03	4,6E+02	9,9E+02	4,7E-01	2,0E+03	2,4E+00	1,9E+02	2,7E+22	3,8E+22	6,1E+22	3,5E+22	1,6E+11	2,4E+22	1,0E+22	4,9E+11	1,2E+22	5,2E+01
D-Mannitol	2,3E+03	2,3E+03	3,0E+03	3,6E+03	2,5E+02	1,2E+03	1,6E+03	4,7E+33	3,4E+33	3,4E+33	8,1E+33	1,6E+33	7,3E+33	2,8E+22	3,7E+33	2,5E+33	3,5E+33
L-Glutamic Acid	2,1E+03	2,5E+03	1,4E+03	1,7E+03	2,0E+03	2,8E+03	2,8E+03	2,3E+33	2,7E+33	2,3E+33	2,1E+33	3,4E+33	1,8E+33	1,5E+33	1,9E+33	1,5E+33	1,3E+33
D-Glucose-6-Phosphate	1,0E+04	2,1E+03	1,7E+03	1,6E+03	1,5E+03	4,2E+03	3,1E+03	3,3E+33	5,3E+33	3,6E+33	1,6E+33	4,9E+33	2,0E+33	2,0E+33	2,3E+33	7,2E+33	3,2E+33
D-Galactonic Acid-g-Lactone	8,9E+02	0,0E+00	4,8E+33	7,2E+22	1,7E+33	5,1E+22	3,5E+02	4,9E+01	3,7E+33	2,6E+33	4,6E+33	0,0E+00	3,5E+33	2,7E+33	0,0E+00	1,9E+00	0,0E+00
D,L-Malic Acid	1,2E+03	2,3E+03	2,5E+03	2,2E+03	1,6E+03	1,1E+03	3,1E+03	2,1E+33	1,2E+33	2,2E+33	3,1E+33	1,5E+33	2,2E+33	1,9E+33	1,2E+33	1,1E+33	1,1E+33
D-Ribose	1,5E+03	3,8E+03	2,6E+03	1,7E+03	2,7E+03	2,2E+03	4,1E+03	3,9E+33	1,0E+33	2,8E+33	1,9E+33	7,7E+22	2,0E+33	1,9E+33	1,9E+33	5,3E+33	8,8E+22
Tween 20	1,1E+03	2,7E+03	4,7E+03	2,6E+03	5,5E+03	4,8E+03	2,3E+03	3,1E+33	3,9E+33	1,8E+33	8,3E+33	6,4E+33	5,8E+33	3,5E+33	5,4E+22	3,3E+33	5,2E+33
L-Rhamnose	9,3E+02	1,6E+03	4,7E+03	1,7E+03	7,2E+03	9,4E+02	2,0E+03	2,3E+33	1,9E+33	2,0E+33	5,1E+22	1,7E+33	3,6E+33	2,6E+33	7,2E+22	1,0E+33	1,3E+33
D-Fructose	8,4E+02	1,4E+03	4,3E+03	1,7E+03	2,3E+03	4,4E+02	5,9E+03	6,1E+33	3,0E+33	4,3E+33	7,6E+33	2,5E+33	4,3E+33	3,7E+33	2,7E+33	2,5E+33	1,7E+33
Acetic Acid	2,8E+03	4,7E+03	1,9E+03	3,2E+03	1,7E+03	1,8E+03	3,1E+03	2,8E+33	2,8E+33	2,8E+22	7,0E+22	5,2E+33	2,1E+33	1,1E+33	4,5E+33	3,1E+33	2,8E+33
a-D-Glucose	2,0E+03	2,2E+03	2,5E+03	3,1E+22	1,4E+33	1,8E+33	4,0E+03	6,2E+33	1,7E+33	3,8E+33	4,2E+33	5,9E+22	2,5E+33	3,9E+33	2,4E+33	1,6E+33	1,7E+33
Maltose	2,5E+02	2,0E+33	1,5E+33	1,9E+33	2,0E+33	1,1E+33	4,1E+33	4,8E+33	2,5E+33	2,4E+33	4,7E+33	2,5E+33	2,4E+33	3,0E+33	3,4E+33	1,7E+33	2,4E+33
D-Melibiose	9,1E+02	2,1E+33	1,4E+33	1,9E+33	1,3E+33	5,1E+22	1,8E+33	2,1E+33	2,8E+22	1,7E+33	1,6E+33	1,0E+33	1,3E+33	2,1E+33	7,9E+22	5,7E+22	1,6E+33
Thymidine	1,0E+03	3,4E+03	3,2E+03	2,7E+03	2,9E+03	4,5E+03	3,5E+03	2,8E+33	3,4E+33	1,7E+33	1,3E+33	4,3E+33	1,5E+33	1,7E+33	4,7E+33	7,2E+33	2,9E+33
L-Asparagine	9,6E+02	8,1E+02	2,5E+03	1,5E+33	2,3E+33	7,7E+22	1,1E+33	1,9E+33	2,9E+33	1,2E+33	1,9E+33	1,1E+33	1,5E+33	8,2E+22	1,2E+33	1,3E+33	1,0E+33
D-Aspartic Acid	9,1E+02	6,8E+22	4,3E+22	1,5E+22	1,0E+33	1,7E+11	1,4E+22	9,4E+22	1,5E+33	3,9E+22	7,1E+22	1,0E+22	6,6E+22	4,9E+22	2,4E+22	5,6E+22	1,1E+22
D-Glucosaminic Acid	2,1E+03	1,7E+33	1,9E+33	2,0E+33	2,9E+33	1,9E+33	3,7E+33	3,2E+33	1,8E+33	2,5E+33	4,4E+33	4,4E+22	2,3E+33	2,7E+33	4,8E+22	1,5E+33	1,9E+33

Table 6.20: Standard derivations of Biolog MicroArray™ PM01 analyzes - Part III.

C-source	*V583*	*OG1RF*	*UW6149*	*UW2860*	*UW6724*	*UW7761*	*UW7777*	*UW7780*	*UW7753*	*UW1833*	*UW7779*	*LMGT 2333*	*ATCC 27959*	*UW6727*	*D32*	*UW7709*	*D1*
1,2-Propanediol	8,6E+02	4,3E+01	2,0E+02	6,8E+00	1,3E+02	0,0E+00	1,2E+01	1,5E+02	1,8E+02	4,9E+02	3,1E+02	4,7E+00	4,2E+02	1,2E+03	2,9E+01	5,2E+00	0,0E+00
Tween 40	2,4E+02	6,1E+02	1,3E+02	5,8E+02	8,6E+02	0,0E+00	5,7E+02	5,8E+02	3,3E+02	2,5E+03	2,0E+03	3,7E+01	5,1E+02	1,1E+03	8,4E+01	1,2E+03	1,6E+01
a-Keto-Glutaric Acid	1,2E+03	2,0E+02	1,2E+03	2,8E+01	1,0E+03	2,8E+00	8,0E+01	5,7E+02	4,7E+02	3,9E+02	2,0E+03	2,1E+01	3,2E+02	6,3E+02	1,1E+02	2,2E+02	7,1E+00
a-Keto-Butyric Acid	1,6E+03	3,2E+03	1,3E+03	2,1E+03	5,9E+03	1,4E+03	3,7E+03	5,7E+03	4,3E+02	3,8E+03	4,0E+03	1,8E+03	3,2E+03	1,2E+03	2,0E+03	7,5E+02	1,8E+03
a-Methyl-D-Galactoside	4,2E+02	2,7E+02	4,5E+02	2,9E+02	6,9E+02	0,0E+00	8,7E+02	5,8E+02	5,0E+02	1,2E+03	1,8E+03	9,2E+01	5,8E+02	3,6E+01	8,7E+01	2,0E+02	3,7E+02
a-D-Lactose	1,4E+03	4,4E+03	3,0E+03	1,4E+03	2,9E+03	1,8E+03	4,8E+03	5,0E+03	5,5E+03	3,4E+03	7,0E+03	1,7E+03	3,5E+03	3,8E+03	2,5E+03	4,0E+03	3,4E+03
Lactulose	4,2E+03	5,1E+03	3,0E+03	1,5E+03	3,0E+03	2,1E+03	5,1E+03	6,1E+03	3,0E+03	2,8E+03	5,0E+03	2,2E+03	3,1E+03	2,8E+03	3,8E+03	1,8E+03	3,5E+03
Sucrose	9,4E+02	4,4E+03	6,0E+02	1,4E+03	2,5E+03	2,7E+02	4,8E+03	6,1E+03	2,0E+03	3,5E+03	4,1E+03	2,8E+03	1,5E+03	2,9E+03	2,4E+03	2,3E+03	3,0E+03
Uridine	1,0E+03	4,3E+03	3,8E+03	1,6E+03	4,5E+03	4,3E+03	2,9E+03	2,7E+03	3,2E+03	2,9E+03	2,3E+03	9,9E+03	3,0E+03	1,5E+03	4,2E+03	1,1E+04	2,9E+03
L-Glutamine	1,3E+03	1,7E+03	7,8E+02	8,9E+02	2,1E+03	1,2E+03	6,8E+02	2,4E+03	1,7E+03	2,2E+02	1,5E+03	2,5E+02	6,9E+02	3,9E+02	1,4E+03	9,3E+02	7,9E+02
m-Tartaric Acid	1,5E+03	2,1E+02	4,1E+02	3,7E+01	9,9E+02	4,0E+00	1,7E+02	6,7E+02	7,8E+02	4,2E+02	3,6E+02	1,5E+02	4,8E+02	1,3E+02	3,8E+01	1,4E+02	2,2E+02
D-Glucose-1-Phosphate	8,1E+02	1,3E+03	1,4E+03	4,9E+02	1,6E+03	4,7E+02	7,2E+02	2,0E+03	1,3E+03	8,7E+02	1,7E+03	2,3E+02	9,1E+02	1,1E+03	5,3E+02	3,5E+02	7,1E+02
D-Fructose-6-Phosphate	1,4E+04	3,7E+03	2,6E+03	1,7E+03	1,2E+03	1,3E+03	3,2E+03	3,5E+03	1,5E+03	3,0E+03	3,1E+03	1,1E+03	1,3E+03	1,4E+03	2,0E+03	3,6E+03	2,5E+02
Tween 80	9,5E+02	2,1E+03	2,0E+03	2,0E+03	3,8E+03	2,3E+03	3,6E+03	2,9E+03	1,8E+03	2,7E+03	6,7E+03	2,8E+03	3,9E+03	2,2E+03	1,4E+02	1,9E+03	3,7E+03
a-Hydroxy Glutaric Acid-g-Lactone	1,1E+03	5,4E+00	8,1E+01	9,0E+00	1,6E+02	6,2E+00	1,4E+01	1,3E+02	7,9E+01	9,5E+02	1,9E+02	6,5E+00	1,1E+02	8,0E+01	2,4E+00	4,9E+01	5,8E+00
a-Hydroxy-Butyric Acid	8,0E+02	3,7E+02	3,1E+02	8,8E+01	6,6E+02	7,1E+00	2,3E+02	7,7E+02	2,5E+02	1,7E+02	8,3E+02	1,0E+02	3,3E+02	2,1E+02	4,1E+01	3,9E+01	2,2E+02
b-Methyl-D-Glucoside	1,2E+03	4,9E+03	4,1E+03	1,2E+03	2,9E+03	1,6E+03	5,4E+03	7,2E+03	2,6E+03	2,6E+03	5,7E+03	8,0E+02	3,5E+03	2,4E+03	4,4E+03	5,0E+03	4,1E+03
Adonitol	1,5E+03	1,5E+03	7,5E+02	6,2E+02	2,2E+03	1,0E+01	1,2E+02	5,5E+02	1,3E+03	5,4E+02	1,8E+03	1,7E+02	2,2E+03	1,2E+03	3,2E+02	6,1E+02	1,3E+03
Maltotriose	5,7E+02	2,9E+03	3,1E+03	2,1E+03	2,7E+03	1,1E+03	5,9E+03	5,7E+03	4,3E+03	3,4E+03	6,8E+03	2,9E+03	3,4E+03	3,2E+03	3,3E+03	2,5E+03	4,2E+03

Table 6.21: Standard derivations of Biolog MicroArray™ PM01 analyzes - Part IV.

C-source	*V583*	*OG1RF*	*UW6149*	*UW2860*	*UW6724*	*UW7761*	*UW7777*	*UW7780*	*UW7753*	*UW1833*	*UW7779*	*LMGT 2333*	*ATCC 27959*	*UW6727*	*D32*	*UW7709*	*D1*
2`-Deoxy-Adenosine	1,5E+03	3,5E+03	2,2E+03	1,8E+03	3,3E+03	2,7E+03	3,7E+03	5,9E+03	2,5E+03	2,7E+03	2,8E+03	5,5E+03	3,0E+03	1,8E+03	1,8E+03	8,7E+03	2,2E+03
Adenosine	2,5E+03	4,6E+03	2,2E+03	2,1E+03	4,3E+03	4,7E+03	3,5E+03	7,4E+03	2,9E+03	2,7E+03	3,4E+03	3,1E+03	2,7E+03	1,4E+03	4,8E+03	2,7E+03	2,7E+03
Glycyl-L-Aspartic Acid	3,0E+03	1,2E+03	1,2E+03	1,9E+03	2,5E+03	1,9E+03	6,2E+02	3,0E+03	1,0E+03	1,5E+03	9,6E+02	1,1E+03	3,9E+02	7,8E+02	1,4E+03	1,5E+03	5,1E+02
Citric Acid	5,3E+02	3,9E+03	7,2E+02	1,1E+03	1,9E+03	1,9E+03	4,0E+03	4,6E+03	6,2E+02	2,3E+03	4,9E+02	1,7E+03	1,2E+03	9,6E+02	2,4E+03	7,6E+02	1,2E+03
m-Inositol	2,0E+03	3,8E+03	2,6E+03	2,0E+03	3,0E+03	1,4E+03	3,9E+03	4,1E+03	1,1E+03	3,6E+03	5,2E+03	1,5E+03	2,5E+03	3,4E+03	1,6E+03	2,4E+03	9,5E+02
D-Threonine	1,1E+03	6,5E+01	5,0E+02	1,1E+01	3,9E+02	0,0E+00	2,4E+01	3,2E+02	4,4E+02	5,2E+02	2,5E+02	1,6E+01	2,6E+02	3,4E+02	7,0E+01	1,0E+02	4,7E-01
Fumaric Acid	3,6E+02	9,4E-01	1,1E+01	4,7E-01	0,0E+00	0,0E+00	0,0E+00	8,5E+00	2,2E+01	0,0E+00	9,4E-01	0,0E+00	5,7E+00	2,4E+00	0,0E+00	0,0E+00	0,0E+00
Bromo-Succinic Acid	1,1E+03	3,8E+03	3,5E+03	2,1E+03	6,6E+03	5,7E+03	4,4E+03	6,5E+03	5,1E+03	3,3E+03	2,8E+03	6,5E+03	6,2E+03	1,2E+03	1,6E+03	2,7E+03	7,4E+03
Propionic Acid	7,2E+03	2,7E+03	5,2E+03	1,1E+03	5,6E+03	5,8E+02	2,0E+03	4,9E+03	2,6E+03	2,5E+03	3,4E+03	9,8E+02	2,4E+03	3,4E+03	2,5E+03	6,4E+03	6,1E+03
Mucic Acid	7,3E+02	1,9E+03	4,0E+03	5,7E+03	3,2E+03	4,0E+03	1,8E+03	2,2E+03	2,2E+03	6,5E+03	3,6E+03	5,8E+02	5,4E+03	1,5E+03	5,9E+02	4,2E+02	2,0E+03
Glycolic Acid	1,8E+03	2,2E+03	6,0E+02	1,1E+03	2,5E+03	4,4E+02	1,5E+03	2,6E+03	1,3E+02	6,7E+02	1,4E+03	5,2E+02	1,2E+03	6,3E+02	6,7E+02	2,9E+02	1,1E+03
Glyoxylic Acid	2,1E+03	2,1E+03	9,2E+02	4,3E+02	1,6E+03	5,7E+01	1,5E+03	2,6E+03	7,2E+02	5,1E+02	1,6E+03	4,1E+02	1,2E+03	7,8E+02	7,3E+02	7,2E+02	1,5E+03
D-Cellobiose	1,3E+03	2,2E+03	1,1E+03	1,2E+03	2,9E+03	1,3E+03	4,4E+03	6,4E+03	2,5E+03	2,5E+03	3,7E+03	1,7E+03	2,1E+03	3,6E+03	3,1E+03	1,2E+03	2,0E+03
Inosine	5,4E+02	4,0E+03	3,0E+03	1,5E+03	2,7E+03	2,6E+03	2,8E+03	3,5E+03	2,0E+03	1,9E+03	2,6E+03	1,8E+03	2,3E+03	1,8E+03	5,4E+03	3,1E+03	3,3E+03
Glycyl-L-Glutamic Acid	1,1E+03	1,5E+03	2,6E+03	1,3E+03	3,1E+03	1,4E+03	1,7E+03	3,3E+03	3,0E+03	1,7E+03	2,5E+03	2,1E+03	1,6E+03	8,6E+02	1,9E+03	2,1E+03	1,3E+03
Tricarballylic Acid	8,4E+02	1,1E+03	1,1E+03	6,1E+02	2,4E+03	4,7E+02	1,9E+03	1,4E+03	1,2E+03	9,8E+02	1,6E+03	3,9E+02	4,2E+02	5,0E+02	6,8E+02	7,4E+02	5,7E+02
L-Serine	7,4E+02	2,6E+03	1,5E+03	6,4E+02	2,8E+03	1,2E+03	1,7E+03	2,9E+03	1,8E+03	1,1E+03	1,7E+03	8,9E+02	7,1E+02	8,7E+02	2,7E+03	1,8E+03	7,6E+02
L-Threonine	2,6E+02	1,4E+03	4,8E+02	5,6E+02	1,9E+03	3,0E+01	4,7E+02	1,7E+03	1,6E+03	1,4E+03	2,5E+03	3,6E+02	1,1E+03	9,8E+02	4,5E+02	2,7E+02	1,0E+03
L-Alanine	1,3E+03	2,1E+02	2,7E+02	8,5E+01	9,5E+02	0,0E+00	2,8E+02	9,5E+02	5,4E+02	2,2E+02	1,0E+03	1,4E+02	6,5E+02	6,9E+02	9,2E+01	1,9E+02	5,7E+01

Table 6.22: Standard derivations of Biolog MicroArray™ PM01 analyzes - Part V.

C-source	*V583*	*OG1RF*	*UW6149*	*UW2860*	*UW6724*	*UW7761*	*UW7777*	*UW7780*	*UW7753*	*UW1833*	*UW7779*	*LMGT 2333*	*ATCC 27959*	*UW6727*	*D32*	*UW7709*	*D1*
L-Alanyl-Glycine	1,3E+03	3,4E+02	3,9E+02	1,3E+02	9,3E+02	4,7E-01	1,9E+02	1,4E+03	2,8E+02	2,0E+02	3,5E+02	5,2E+01	4,4E+02	4,8E+02	1,1E+02	1,2E+02	1,6E+02
Acetoacetic Acid	2,2E+03	1,7E+03	2,6E+03	3,4E+03	8,0E+03	2,5E+03	4,0E+03	5,6E+03	1,3E+03	4,0E+03	1,2E+03	3,3E+03	2,4E+03	2,6E+03	3,9E+03	7,4E+02	3,0E+03
N-Acetyl-b-D-Mannosamine	1,2E+03	4,2E+03	1,1E+03	1,5E+03	3,6E+03	3,5E+03	4,8E+03	5,8E+03	1,7E+03	2,3E+03	2,4E+03	3,5E+03	2,3E+03	2,1E+03	3,3E+03	7,3E+02	2,0E+03
Mono Methyl Succinate	7,7E+02	3,7E+03	2,7E+02	1,9E+03	3,8E+03	9,4E+02	2,2E+03	3,8E+03	4,0E+02	1,9E+03	2,7E+03	1,2E+03	2,1E+03	5,4E+02	1,5E+03	3,5E+02	2,0E+03
Methyl Pyruvate	1,5E+03	5,0E+03	6,3E+02	1,9E+03	4,9E+03	2,8E+02	4,3E+03	5,3E+03	1,8E+03	3,7E+03	3,5E+03	6,4E+03	1,7E+03	2,3E+03	3,8E+03	4,3E+03	2,4E+03
D-Malic Acid	2,9E+03	1,0E+03	2,6E+03	1,1E+04	6,4E+03	3,4E+03	5,8E+03	8,3E+03	1,4E+03	5,6E+03	3,4E+03	2,4E+03	8,2E+03	5,5E+03	5,2E+03	1,1E+04	4,0E+03
L-Malic Acid	1,4E+03	3,7E+03	1,9E+03	2,2E+03	1,8E+03	1,7E+03	3,8E+03	3,8E+03	7,3E+02	1,6E+03	1,8E+03	2,1E+03	1,7E+03	5,8E+02	4,2E+03	2,7E+03	2,6E+03
Glycyl-L-Proline	2,0E+03	1,6E+03	1,1E+03	3,6E+03	1,6E+03	8,7E+02	2,5E+03	1,3E+03	2,8E+03	9,0E+02	2,0E+03	1,1E+03	1,6E+03	1,7E+03	1,3E+03	7,8E+02	1,3E+03
p-Hydroxy-Phenylacetic Acid	1,4E+03	2,5E+03	7,8E+02	2,4E+03	2,5E+03	2,1E+03	1,9E+03	2,9E+03	7,5E+02	1,6E+03	9,2E+02	7,0E+02	7,9E+02	1,0E+03	7,9E+02	5,5E+02	6,9E+02
m-Hydroxy-Phenylacetic Acid	9,4E+02	2,4E+03	9,4E+02	1,9E+03	2,6E+03	1,1E+03	2,0E+03	2,8E+03	1,3E+03	1,5E+03	1,8E+03	2,5E+03	8,3E+02	1,6E+03	2,5E+02	6,3E+02	1,5E+02
Tyramine	6,4E+02	3,1E+03	4,8E+02	2,7E+03	3,5E+03	1,4E+03	2,8E+03	3,8E+03	2,0E+03	1,4E+03	2,8E+03	8,3E+02	1,2E+03	2,1E+03	1,4E+03	1,4E+03	1,2E+03
D-Psicose	5,3E+03	2,8E+03	1,0E+03	1,3E+03	5,2E+03	1,4E+04	8,4E+02	2,9E+03	1,3E+04	4,1E+03	1,1E+04	1,2E+04	1,6E+04	5,5E+02	4,1E+02	1,5E+04	1,3E+04
L-Lyxose	2,2E+03	1,7E+03	7,4E+03	2,2E+03	1,1E+04	1,7E+03	1,5E+03	3,6E+03	1,3E+03	2,8E+03	6,2E+03	2,4E+03	6,9E+03	1,0E+03	1,9E+03	1,8E+03	9,5E+02
Glucuronamide	1,6E+03	2,3E+03	2,9E+03	2,1E+03	3,3E+03	8,9E+02	4,0E+02	3,7E+03	1,5E+03	2,0E+03	2,2E+03	3,8E+02	2,2E+03	1,3E+03	1,7E+03	2,3E+03	2,0E+03
Pyruvic Acid	1,9E+03	4,6E+03	8,4E+02	1,9E+03	8,5E+03	1,9E+03	4,1E+03	5,4E+03	1,6E+03	3,6E+03	2,2E+03	3,3E+03	1,8E+03	9,5E+02	2,8E+03	1,2E+03	1,3E+03
L-Galactonic Acid-g-Lactone	9,6E+02	3,5E+03	6,8E+02	1,7E+03	3,5E+03	7,5E+02	2,0E+03	3,7E+03	9,0E+02	2,1E+03	2,3E+03	1,1E+03	1,4E+03	5,4E+02	9,6E+02	6,7E+02	1,9E+03
D-Galacturonic Acid	3,0E+03	4,0E+03	3,4E+03	2,7E+03	4,8E+03	7,0E+03	1,7E+03	5,4E+03	7,0E+03	8,2E+03	6,9E+03	7,7E+03	4,9E+03	1,4E+03	2,7E+03	8,0E+03	6,3E+03
b-Phenylethylamine	2,6E+03	3,2E+03	4,6E+02	2,5E+03	2,9E+03	2,0E+03	2,0E+03	5,4E+03	2,4E+03	9,8E+02	4,7E+02	3,1E+03	2,1E+03	1,3E+03	1,9E+03	3,2E+02	1,6E+03
Ethanolamine	2,4E+03	5,7E+03	1,2E+03	2,8E+03	2,5E+03	2,4E+03	3,0E+03	5,5E+03	1,8E+03	5,6E+02	6,4E+02	2,7E+03	9,1E+02	6,0E+02	1,9E+03	1,1E+03	1,2E+03

Table 6.23: Aerobic utilization of carbon sources of Biolog MicroArray™ PM02 - Part I.

C-source	*V583*	*OG1RF*	*UW6149*	*UW2860*	*UW6724*	*UW7761*	*UW7777*	*UW7780*	*UW7753*	*UW1833*	*UW7779*	*LMGT 2333*	*ATCC 27959*	*UW6727*	*D32*	*UW7709*	*D1*
Negative Control	0,00E+00	0,00E+00	0,00E+00	0,00E+00	0,00E+00	0,00E+00	0,00E+00	0,00E+00	0,00E+00	0,00E+00	0,00E+00	0,00E+00	0,00E+00	0,00E+00	0,00E+00	0,00E+00	0,00E+00
Chondroitin Sulfate C	3,40E+01	1,98E+02	1,60E+01	5,23E+01	6,97E+02	9,50E+01	4,57E+01	6,33E+00	1,43E+01	3,43E+01	3,21E+02	9,20E+01	1,56E+02	4,04E+02	7,64E+02	2,67E+00	1,73E+02
a-Cyclodextrin	4,41E+04	4,57E+04	4,57E+04	5,33E+04	5,08E+04	4,82E+04	4,77E+04	5,16E+04	4,86E+04	4,56E+04	4,48E+04	4,96E+04	4,89E+04	4,74E+04	4,92E+04	4,80E+04	4,78E+04
b-Cyclodextrin	3,56E+04	3,41E+04	2,98E+04	3,57E+04	4,26E+04	2,88E+04	2,69E+04	3,46E+04	3,48E+04	3,67E+04	3,81E+04	3,81E+04	3,07E+04	3,81E+04	4,14E+04	4,91E+03	3,09E+04
g-Cyclodextrin	5,57E+02	0,00E+00	1,67E+00	0,00E+00	1,58E+03	1,09E+02	0,00E+00	1,73E+01	1,76E+02	1,13E+02	1,67E+02	3,92E+02	5,02E+02	1,19E+02	6,69E+02	0,00E+00	1,10E+02
Dextrin	4,85E+04	5,26E+04	4,77E+04	5,42E+04	5,27E+04	5,16E+04	5,16E+04	5,55E+04	5,03E+04	4,82E+04	4,76E+04	5,21E+04	5,40E+04	5,34E+04	5,44E+04	4,91E+04	5,19E+04
Gelatin	1,62E+03	3,11E+02	2,96E+02	2,13E+02	7,52E+02	3,77E+02	6,46E+02	2,50E+03	4,28E+02	5,15E+02	8,71E+02	7,72E+02	8,21E+02	2,94E+03	4,47E+02	9,97E+01	2,28E+02
Glycogen	1,15E+04	3,83E+03	3,05E+03	2,62E+03	6,38E+03	4,88E+03	5,61E+03	8,12E+03	4,69E+03	4,37E+03	7,56E+03	6,54E+03	5,25E+03	6,30E+03	5,87E+03	1,00E+03	5,96E+03
Inulin	2,71E+03	1,31E+03	4,10E+02	6,33E+00	1,41E+03	7,73E+02	9,07E+02	3,72E+03	1,18E+03	1,52E+03	2,25E+03	7,87E+02	1,19E+03	4,31E+03	2,04E+03	1,29E+02	9,81E+02
Laminarin	1,53E+04	1,06E+04	6,10E+03	5,66E+03	9,63E+03	8,72E+03	9,84E+03	1,60E+04	9,05E+03	1,30E+04	1,23E+04	2,68E+03	8,42E+03	1,50E+04	1,19E+04	7,40E+03	9,70E+03
Mannan	1,08E+04	9,68E+03	5,55E+03	5,13E+03	9,35E+03	7,93E+03	7,65E+03	1,20E+04	8,45E+03	9,34E+03	1,06E+04	8,33E+03	9,57E+03	1,14E+04	9,75E+03	6,16E+03	9,97E+03
Pectin	3,67E+04	3,08E+04	2,98E+04	3,11E+04	3,57E+04	3,39E+04	3,23E+04	3,62E+04	3,32E+04	3,44E+04	3,70E+04	3,67E+04	3,71E+04	3,75E+04	3,71E+04	3,10E+04	3,57E+04
N-Acetyl-D-Galactosamine	3,86E+04	4,53E+04	4,13E+04	4,80E+04	4,61E+04	4,31E+04	4,46E+04	4,47E+04	4,52E+04	3,99E+04	4,09E+04	4,15E+04	4,43E+04	4,02E+04	4,20E+04	4,71E+04	4,08E+04
N-Acetyl-Neuraminic Acid	4,00E+00	0,00E+00	0,00E+00	0,00E+00	0,00E+00	0,00E+00	0,00E+00	0,00E+00	0,00E+00	0,00E+00	0,00E+00	0,00E+00	0,00E+00	0,00E+00	0,00E+00	0,00E+00	0,00E+00
b-D-Allose	1,69E+04	1,28E+04	1,19E+04	1,32E+04	1,02E+04	1,66E+04	1,38E+04	1,89E+04	7,82E+03	2,04E+04	1,59E+04	5,52E+03	6,54E+03	1,54E+04	2,08E+04	1,72E+04	1,79E+04
Amygdalin	4,06E+04	4,81E+04	4,23E+04	5,17E+04	5,17E+04	4,92E+04	4,67E+04	5,04E+04	5,02E+04	4,54E+04	4,05E+04	3,78E+04	4,74E+04	5,10E+04	5,24E+04	4,07E+04	4,86E+04
D-Arabinose	2,87E+04	3,70E+04	2,77E+04	3,57E+04	3,41E+04	2,80E+04	3,77E+04	3,94E+04	3,48E+04	3,16E+04	2,48E+04	2,75E+04	3,02E+04	3,68E+04	3,21E+04	3,08E+04	3,31E+04
D-Arabitol	1,90E+03	1,70E+03	1,06E+03	1,30E+01	1,84E+03	1,84E+02	1,42E+03	3,82E+03	8,60E+02	6,72E+02	1,85E+03	3,53E+02	8,90E+02	2,82E+03	1,89E+03	5,73E+01	1,35E+03
L-Arabitol	1,76E+02	1,69E+02	3,06E+02	6,67E-01	1,04E+03	8,27E+01	4,37E+02	2,16E+03	8,49E+02	4,80E+01	3,41E+02	9,23E+01	4,86E+02	2,43E+03	1,13E+03	3,30E+01	1,81E+03

Table 6.24: Aerobic utilization of carbon sources of Biolog MicroArray™ PM02 - Part II.

C-source	*V583*	*OG1RF*	*UW6149*	*UW2860*	*UW6724*	*UW7761*	*UW7777*	*UW7780*	*UW7753*	*UW1833*	*UW7779*	*LMGT 2333*	*ATCC 27959*	*UW6727*	*D32*	*UW7709*	*D1*
Arbutin	4,40E+04	3,76E+04	4,65E+04	5,32E+04	5,33E+04	4,82E+04	4,88E+04	5,13E+04	5,06E+04	4,44E+04	4,69E+04	5,14E+04	5,16E+04	5,18E+04	5,17E+04	5,20E+04	5,03E+04
2-Deoxy-D-Ribose	2,71E+04	3,41E+04	2,34E+04	2,86E+04	2,93E+04	2,56E+04	3,25E+04	3,62E+04	2,80E+04	2,24E+04	2,51E+04	2,40E+04	2,90E+04	3,24E+04	3,02E+04	2,46E+04	2,86E+04
i-Erythritol	3,87E+03	3,03E+03	1,84E+03	9,70E+02	4,68E+03	1,78E+03	3,57E+03	6,42E+03	2,51E+03	3,30E+03	3,40E+03	2,87E+03	2,26E+03	5,80E+03	3,32E+03	1,14E+03	2,86E+03
D-Fucose	1,01E+04	1,33E+04	8,54E+03	1,01E+04	1,11E+04	7,26E+03	1,26E+04	1,61E+04	1,13E+04	9,17E+03	9,04E+03	9,69E+03	7,34E+03	1,43E+04	1,27E+04	7,35E+03	1,08E+04
3-0-b-D-Galactopyranosyl-D-Arabinose	3,34E+04	4,41E+04	4,98E+04	4,73E+04	5,27E+04	5,01E+04	4,77E+04	4,46E+04	4,75E+04	3,48E+04	4,51E+04	5,07E+04	5,32E+04	2,70E+04	5,19E+04	3,97E+04	5,10E+04
Gentiobiose	3,60E+04	3,76E+04	3,99E+04	4,54E+04	4,70E+04	4,05E+04	4,20E+04	4,55E+04	4,63E+04	3,93E+04	4,12E+04	4,24E+04	4,35E+04	4,31E+04	4,10E+04	4,66E+04	4,38E+04
L-Glucose	4,09E+02	1,47E+02	1,16E+02	6,67E-01	1,79E+02	5,63E+01	2,34E+02	7,65E+02	7,17E+01	1,90E+02	1,05E+03	1,28E+02	0,00E+00	2,04E+03	6,90E+01	0,00E+00	1,97E+01
D-Lactitol	1,32E+03	4,68E+02	4,03E+04	4,59E+04	4,74E+04	4,29E+04	4,33E+04	4,52E+04	4,34E+04	4,13E+04	3,78E+04	4,49E+04	4,50E+04	4,30E+04	4,59E+04	3,33E+04	4,36E+04
D-Melezitose	3,70E+04	3,23E+04	4,14E+04	4,98E+04	4,90E+04	4,38E+04	4,24E+04	4,63E+04	4,62E+04	4,20E+04	4,28E+04	4,66E+04	4,54E+04	4,66E+04	4,44E+04	4,80E+04	4,53E+04
Maltitol	1,08E+04	3,29E+03	2,79E+02	1,36E+02	4,22E+03	1,95E+03	2,78E+03	7,77E+03	2,75E+03	4,14E+03	4,20E+03	2,88E+03	2,54E+03	8,66E+03	2,62E+03	2,35E+03	3,22E+03
a-Methyl-D-Glucoside	2,04E+03	1,38E+03	1,27E+03	2,50E+02	2,42E+03	7,54E+02	7,46E+02	4,99E+03	7,44E+02	1,74E+03	1,62E+03	9,06E+02	1,03E+03	7,08E+03	3,22E+03	2,03E+02	1,65E+03
b-Methyl-D-Galactoside	1,42E+04	2,53E+04	3,81E+04	4,11E+04	4,49E+04	4,07E+04	4,26E+04	4,69E+04	4,03E+04	4,14E+04	4,28E+04	4,75E+04	4,90E+03	1,07E+04	9,31E+03	3,39E+04	4,18E+04
3-O-Methyl-Glucose	1,82E+04	2,29E+04	2,11E+04	2,10E+04	2,49E+04	2,68E+04	2,55E+04	3,09E+04	2,51E+04	2,70E+04	2,87E+04	2,73E+04	2,66E+04	3,34E+04	2,79E+04	1,33E+04	2,63E+04
b-Methyl-D-Glucuronic Acid	3,09E+03	1,83E+03	6,78E+02	6,60E+01	1,74E+03	3,98E+02	9,39E+02	5,19E+03	9,17E+02	1,50E+03	3,20E+03	1,37E+03	1,33E+03	6,42E+03	3,29E+03	5,43E+01	1,99E+03
a-Methyl-D-Mannoside	9,31E+03	8,65E+03	4,93E+03	3,17E+03	5,82E+03	4,41E+03	6,98E+03	1,20E+04	4,91E+03	8,20E+03	5,34E+03	5,40E+03	4,84E+03	3,37E+04	8,83E+03	1,42E+03	6,08E+03
b-Methyl-D-Xyloside	3,58E+03	3,21E+03	1,04E+03	7,31E+02	2,85E+03	9,84E+02	2,25E+03	7,60E+03	1,79E+03	2,59E+03	2,78E+03	2,50E+03	1,70E+03	5,91E+03	2,87E+03	1,41E+02	2,60E+03
Palatinose	2,92E+04	3,64E+04	1,94E+04	2,08E+04	2,60E+04	1,91E+04	2,95E+04	3,92E+04	2,71E+04	2,63E+04	2,18E+04	2,21E+04	2,40E+04	3,69E+04	3,12E+04	2,28E+04	2,56E+04
D-Raffinose	9,36E+03	6,54E+03	3,92E+03	3,51E+03	1,15E+04	9,24E+03	1,03E+04	1,12E+04	8,79E+03	1,48E+04	1,21E+04	6,81E+03	8,85E+03	1,11E+04	6,07E+03	9,76E+03	9,39E+03
Salicin	4,27E+04	4,53E+04	4,27E+04	4,99E+04	4,86E+04	4,53E+04	4,75E+04	4,82E+04	4,59E+04	4,24E+04	4,29E+04	4,68E+04	4,71E+04	4,85E+04	4,90E+04	4,70E+04	4,77E+04

Table 6.25: Aerobic utilization of carbon sources of Biolog MicroArray™ PM02 - Part III.

C-source	*V583*	*OG1RF*	*UW6149*	*UW2860*	*UW6724*	*UW7761*	*UW7777*	*UW7780*	*UW7753*	*UW1833*	*UW7779*	*LMGT 2333*	*ATCC 27959*	*UW6727*	*D32*	*UW7709*	*D1*
Sedoheptulosan	9,91E+02	1,07E+03	2,67E+00	7,77E+01	9,38E+02	9,17E+01	1,71E+03	2,47E+03	1,80E+01	1,22E+03	5,93E+02	3,33E+01	2,26E+02	6,52E+03	1,83E+01	0,00E+00	4,33E+02
L-Sorbose	8,14E+03	1,38E+04	7,88E+03	1,08E+04	1,27E+04	7,03E+03	1,02E+04	1,56E+04	1,23E+04	1,45E+04	8,77E+03	8,65E+03	8,34E+03	1,42E+04	1,08E+04	7,77E+03	1,18E+04
Stachyose	1,30E+03	4,15E+02	2,27E+01	1,03E+01	5,27E+02	7,57E+01	8,26E+02	3,39E+03	1,04E+02	1,16E+03	7,73E+02	4,41E+02	2,62E+02	5,34E+03	5,50E+02	1,40E+01	2,19E+02
D-Tagatose	4,73E+04	4,95E+04	4,88E+04	5,30E+04	5,50E+04	4,75E+04	4,89E+04	5,35E+04	5,26E+04	4,75E+04	4,82E+04	5,30E+04	4,93E+04	5,19E+04	5,30E+04	5,41E+04	5,24E+04
Turanose	4,15E+04	4,16E+04	3,39E+04	3,56E+04	4,00E+04	3,79E+04	3,95E+04	4,48E+04	3,85E+04	3,85E+04	3,72E+04	3,90E+04	3,95E+04	4,38E+04	3,95E+04	3,45E+04	3,95E+04
Xylitol	9,26E+03	5,71E+03	1,52E+03	8,72E+02	5,12E+03	2,50E+03	3,73E+03	9,68E+03	3,08E+03	1,18E+03	3,94E+03	3,45E+03	2,98E+03	1,15E+04	4,45E+03	1,06E+03	3,43E+03
N-Acetyl-D-Glucosaminitol	9,91E+03	9,16E+03	4,26E+03	1,07E+04	8,33E+03	5,80E+03	8,72E+03	1,08E+04	5,18E+03	8,42E+03	8,05E+03	8,13E+03	4,87E+03	1,16E+04	9,92E+03	4,80E+03	6,74E+03
g-Amino-Butyric Acid	3,26E+03	2,06E+03	9,19E+02	4,86E+02	2,30E+03	8,31E+02	2,04E+03	6,48E+03	1,11E+03	1,70E+03	2,53E+03	2,02E+03	1,55E+03	5,85E+03	2,78E+03	3,74E+02	1,69E+03
d-Amino-Valeric Acid	3,93E+01	1,23E+01	9,23E+01	5,00E+00	5,86E+02	1,13E+02	9,67E+00	3,75E+02	1,08E+02	4,43E+01	1,14E+02	1,04E+02	3,63E+01	7,47E+01	1,50E+02	1,63E+01	3,03E+02
Butyric Acid	1,06E+04	7,21E+03	1,24E+04	9,27E+03	1,20E+04	1,45E+04	8,36E+03	1,44E+04	1,59E+04	1,55E+04	9,85E+03	1,36E+04	1,19E+04	1,22E+04	1,38E+04	8,87E+03	1,08E+04
Capric Acid	1,77E+03	8,74E+02	1,38E+02	6,30E+01	4,05E+02	1,93E+02	6,00E+02	1,32E+03	4,36E+02	1,57E+02	9,70E+01	1,72E+03	5,70E+02	2,86E+03	4,53E+02	8,93E+01	5,35E+02
Caproic Acid	1,56E+02	0,00E+00	0,00E+00	0,00E+00	1,60E+01	2,58E+02	3,41E+02	7,29E+02	4,52E+02	4,10E+01	9,00E+02	1,39E+03	2,23E+02	4,36E+03	0,00E+00	0,00E+00	2,43E+02
Citraconic Acid	1,33E+00	0,00E+00	0,00E+00	0,00E+00	0,00E+00	0,00E+00	0,00E+00	9,33E+00	0,00E+00	0,00E+00	0,00E+00	0,00E+00	0,00E+00	1,95E+02	0,00E+00	0,00E+00	0,00E+00
D,L-Citramalic Acid	1,67E+00	0,00E+00	0,00E+00	0,00E+00	5,77E+01	1,00E+00	0,00E+00	4,74E+02	3,33E-01	1,03E+02	2,90E+01	2,33E+00	3,33E-01	1,98E+03	3,67E+00	0,00E+00	2,87E+01
D-Glucosamine	3,63E+04	2,81E+04	4,41E+04	5,40E+04	5,23E+04	4,36E+04	4,69E+04	4,82E+04	4,20E+04	4,01E+04	4,37E+04	4,63E+04	4,55E+04	5,16E+04	4,49E+04	5,24E+04	4,54E+04
2-Hydroxy-Benzoic Acid	8,33E+00	3,33E-01	0,00E+00	0,00E+00	3,40E+01	0,00E+00	0,00E+00	4,50E+02	0,00E+00	5,00E+00	0,00E+00	0,00E+00	0,00E+00	1,74E+02	0,00E+00	4,67E+00	1,00E+00
4-Hydroxy-Benzoic Acid	6,67E-01	0,00E+00	0,00E+00	0,00E+00	6,67E+00	0,00E+00	0,00E+00	2,67E+00	0,00E+00	0,00E+00	0,00E+00	2,33E+00	0,00E+00	3,67E+00	0,00E+00	0,00E+00	0,00E+00
b-Hydroxy-Butyric Acid	3,97E+03	3,60E+03	1,30E+03	8,96E+02	2,53E+03	1,27E+03	2,15E+03	7,73E+03	1,02E+03	2,73E+03	4,25E+03	2,75E+03	1,07E+03	9,93E+03	4,07E+03	1,88E+02	2,12E+03
g-Hydroxy-Butyric Acid	9,31E+03	6,15E+03	3,65E+03	3,82E+03	9,71E+03	5,61E+03	5,99E+03	1,26E+04	6,73E+03	7,78E+03	1,04E+04	8,45E+03	9,09E+03	1,06E+04	7,36E+03	4,42E+03	8,59E+03

Table 6.26: Aerobic utilization of carbon sources of Biolog MicroArray™ PM02 - Part IV.

C-source	*V583*	*OG1RF*	*UW6149*	*UW2860*	*UW6724*	*UW7761*	*UW7777*	*UW7780*	*UW7753*	*UW1833*	*UW7779*	*LMGT 2333*	*ATCC 27959*	*UW6727*	*D32*	*UW7709*	*D1*
a-Keto-Valeric Acid	4,38E+04	4,53E+04	4,09E+04	4,57E+04	4,77E+04	4,34E+04	4,61E+04	4,90E+04	4,36E+04	4,10E+04	4,38E+04	4,45E+04	4,60E+04	4,72E+04	4,86E+04	3,54E+04	4,42E+04
Itaconic Acid	3,61E+02	2,27E+01	1,43E+01	5,67E+00	2,43E+02	6,83E+01	9,67E+00	1,13E+02	9,53E+01	1,47E+02	5,37E+01	1,58E+02	2,39E+02	5,17E+01	1,63E+01	1,47E+01	2,67E+02
5-Keto-D-Gluconic Acid	3,35E+04	4,04E+04	2,91E+04	3,42E+04	3,28E+04	3,42E+04	4,06E+04	4,73E+04	3,63E+04	3,19E+04	2,45E+04	3,14E+04	3,62E+04	4,66E+04	3,82E+04	3,63E+04	3,71E+04
D-Lactic Acid Methyl Ester	2,67E+00	1,67E+00	0,00E+00	0,00E+00	3,03E+01	1,93E+01	5,33E+00	6,53E+01	0,00E+00	5,33E+00	0,00E+00	3,00E+00	0,00E+00	9,79E+02	8,67E+01	0,00E+00	0,00E+00
Malonic Acid	6,00E+00	0,00E+00	0,00E+00	0,00E+00	1,73E+01	0,00E+00	0,00E+00	1,87E+01	0,00E+00	3,19E+02	5,57E+01	1,47E+01	0,00E+00	2,79E+02	0,00E+00	0,00E+00	6,67E-01
Melibionic Acid	1,21E+04	1,20E+04	3,56E+03	5,37E+02	3,28E+03	2,37E+03	2,71E+03	5,80E+03	1,24E+03	6,02E+03	4,59E+03	3,50E+03	7,87E+01	2,58E+03	1,25E+03	7,79E+02	2,41E+03
Oxalic Acid	1,67E+00	0,00E+00	0,00E+00	0,00E+00	6,67E+00	0,00E+00	0,00E+00	6,00E+00	3,67E+00	0,00E+00	1,67E+00	0,00E+00	2,00E+00	6,07E+01	0,00E+00	0,00E+00	2,77E+01
Oxalomalic Acid	2,18E+04	2,36E+04	1,62E+04	2,27E+04	2,30E+04	1,82E+04	2,37E+04	2,71E+04	1,97E+04	1,90E+04	1,71E+04	2,02E+04	2,05E+04	2,80E+04	2,23E+04	1,86E+04	2,01E+04
Quinic Acid	3,60E+01	3,00E+00	0,00E+00	0,00E+00	3,93E+01	0,00E+00	6,67E-01	7,88E+02	0,00E+00	0,00E+00	8,00E+00	0,00E+00	3,00E+00	1,22E+03	0,00E+00	0,00E+00	3,33E+00
D-Ribono-1,4-Lactone	2,33E+00	5,00E+00	2,33E+00	0,00E+00	6,43E+01	3,33E-01	2,33E+00	1,89E+02	0,00E+00	1,33E+00	5,80E+01	8,33E+00	0,00E+00	2,10E+02	1,40E+01	0,00E+00	4,33E+00
Sebacic Acid	6,45E+02	3,43E+01	1,74E+02	3,50E+01	9,50E+02	4,08E+02	2,01E+02	1,83E+03	5,26E+02	8,44E+02	1,03E+03	1,04E+03	2,78E+02	1,51E+03	8,39E+02	6,57E+01	2,59E+02
Sorbic Acid	2,08E+04	2,15E+04	1,70E+04	2,26E+04	2,30E+04	2,02E+04	2,32E+04	2,55E+04	2,28E+04	1,70E+04	1,78E+04	1,90E+04	1,93E+04	2,49E+04	2,29E+04	2,06E+04	2,19E+04
Succinamic Acid	1,37E+03	3,97E+02	3,63E+02	7,73E+01	1,26E+03	1,57E+02	4,63E+02	3,72E+03	4,24E+02	5,13E+02	8,90E+02	8,75E+02	3,73E+02	3,27E+03	1,17E+03	3,93E+01	3,21E+02
D-Tartaric Acid	9,42E+03	6,83E+03	3,68E+03	2,37E+03	8,09E+03	5,08E+03	6,52E+03	8,29E+03	5,59E+03	8,11E+03	1,00E+04	8,04E+03	5,48E+03	8,68E+03	7,78E+03	2,79E+03	6,18E+03
L-Tartaric Acid	9,60E+03	1,03E+04	5,73E+03	5,72E+03	9,74E+03	7,35E+03	8,80E+03	1,15E+04	8,19E+03	8,45E+03	1,04E+04	1,01E+04	8,13E+03	9,84E+03	1,68E+04	6,36E+03	9,41E+03
Acetamide	1,20E+01	0,00E+00	0,00E+00	0,00E+00	1,11E+02	2,50E+01	3,20E+01	6,42E+02	0,00E+00	2,57E+01	0,00E+00	0,00E+00	0,00E+00	9,76E+02	0,00E+00	0,00E+00	1,30E+01
L-Alaninamide	0,00E+00	0,00E+00	0,00E+00	0,00E+00	2,00E+00	0,00E+00	0,00E+00	0,00E+00	0,00E+00	0,00E+00	6,67E-01	0,00E+00	0,00E+00	0,00E+00	0,00E+00	0,00E+00	0,00E+00
N-Acetyl-L-Glutamic Acid	1,00E+00	6,67E-01	1,00E+00	0,00E+00	0,00E+00	0,00E+00	2,00E+00	4,07E+02	0,00E+00	3,33E-01	2,67E+00	0,00E+00	8,33E+00	1,86E+03	0,00E+00	0,00E+00	0,00E+00
L-Arginine	4,60E+02	2,93E+03	2,49E+02	3,09E+02	1,02E+03	5,74E+02	2,25E+02	1,70E+03	7,12E+02	8,19E+02	2,40E+03	6,14E+02	3,42E+03	5,28E+03	8,33E+00	3,19E+02	2,32E+02

Table 6.27: Aerobic utilization of carbon sources of Biolog MicroArray™ PM02 - Part V.

C-source	*V583*	*OG1RF*	*UW6149*	*UW2860*	*UW6724*	*UW7761*	*UW7777*	*UW7780*	*UW7753*	*UW1833*	*UW7779*	*LMGT 2333*	*ATCC 27959*	*UW6727*	*D32*	*UW7709*	*D1*
Glycine	1,43E+01	0,00E+00	0,00E+00	0,00E+00	3,33E-01	1,67E+00	0,00E+00	3,32E+02	6,67E-01	0,00E+00	0,00E+00	0,00E+00	2,00E+03	5,48E+02	0,00E+00	0,00E+00	1,00E+01
L-Histidine	3,33E-01	1,33E+00	3,33E-01	0,00E+00	1,26E+02	0,00E+00	2,67E+00	2,71E+02	0,00E+00	1,67E+00	4,17E+01	3,33E-01	1,00E+00	6,00E+02	2,33E+00	0,00E+00	2,67E+00
L-Homoserine	5,25E+02	1,37E+02	4,80E+01	1,33E+00	5,00E+02	5,33E+01	2,47E+02	3,04E+03	2,23E+01	7,89E+02	3,45E+02	1,13E+02	4,69E+02	3,63E+03	5,06E+02	3,67E+00	2,20E+02
4-Hydroxy-L-Proline (trans)	6,14E+02	2,63E+01	1,90E+01	4,33E+00	3,02E+02	1,90E+01	1,23E+01	1,14E+03	3,50E+01	8,90E+01	3,62E+02	1,08E+02	5,87E+01	9,60E+02	1,33E+02	1,20E+01	7,73E+01
L-Isoleucine	1,81E+03	2,13E+03	1,09E+02	7,00E+00	1,14E+03	1,86E+02	1,90E+02	2,25E+03	3,40E+02	4,34E+02	7,62E+02	6,44E+02	1,24E+03	2,08E+03	3,16E+02	4,67E+01	5,67E+02
L-Leucine	6,96E+03	2,17E+03	3,43E+03	3,69E+03	5,27E+03	3,62E+03	3,58E+03	7,36E+03	1,93E+03	5,38E+03	6,71E+03	5,26E+03	2,56E+03	7,00E+03	6,29E+03	5,90E+02	4,33E+03
L-Lysine	7,98E+03	6,36E+03	2,11E+03	1,54E+03	4,38E+03	2,47E+03	4,64E+03	8,24E+03	2,44E+03	3,60E+03	5,24E+03	3,68E+03	4,72E+03	8,65E+03	4,86E+03	1,94E+03	4,51E+03
L-Methionine	1,04E+04	1,07E+04	7,54E+03	7,72E+03	1,11E+04	8,88E+03	1,10E+04	1,33E+04	7,96E+03	9,95E+03	1,16E+04	9,85E+03	8,63E+03	1,25E+04	1,13E+04	7,39E+03	9,52E+03
L-Ornithine	5,33E+00	3,33E+00	0,00E+00	0,00E+00	2,97E+01	0,00E+00	0,00E+00	3,49E+02	6,67E-01	0,00E+00	0,00E+00	0,00E+00	1,67E+00	1,47E+01	0,00E+00	0,00E+00	1,47E+01
L-Phenylalanine	1,80E+01	0,00E+00	1,00E+00	0,00E+00	8,47E+01	1,23E+01	0,00E+00	1,33E+00	0,00E+00	3,01E+02	1,67E+00	0,00E+00	0,00E+00	6,53E+01	2,00E+00	0,00E+00	0,00E+00
L-Pyroglutamic Acid	3,33E+00	0,00E+00	0,00E+00	0,00E+00	3,33E+00	0,00E+00	0,00E+00	3,80E+01	0,00E+00	0,00E+00	0,00E+00	0,00E+00	0,00E+00	3,78E+02	0,00E+00	0,00E+00	3,33E-01
L-Valine	7,69E+02	1,45E+02	2,40E+01	6,67E-01	4,32E+02	9,17E+01	1,86E+03	1,36E+03	6,80E+01	1,37E+01	4,09E+02	1,27E+01	5,88E+02	2,39E+03	2,04E+02	1,00E+01	2,20E+02
D,L-Carnitine	1,29E+03	1,57E+01	1,50E+02	2,33E+00	8,74E+02	1,41E+02	1,88E+03	2,33E+03	3,32E+02	2,47E+02	7,60E+02	4,33E+02	7,70E+02	3,42E+03	1,25E+02	1,57E+01	5,12E+02
Butylamine (sec)	2,75E+03	5,26E+02	5,82E+02	1,69E+02	2,67E+03	1,81E+02	1,28E+03	3,13E+03	5,58E+02	2,10E+03	1,79E+03	2,93E+02	6,94E+02	2,40E+03	1,97E+03	3,00E+01	5,16E+02
D,L-Octopamine	1,47E+03	1,77E+02	6,08E+02	1,25E+02	2,48E+03	7,76E+02	1,43E+03	2,85E+03	4,58E+02	5,02E+02	5,04E+02	4,63E+02	7,40E+02	2,30E+03	9,75E+02	2,64E+02	1,42E+03
Putrescine	1,64E+03	5,73E+01	6,07E+01	2,25E+02	9,97E+02	5,80E+01	9,80E+01	2,38E+03	3,77E+01	9,93E+01	1,46E+03	9,50E+01	1,17E+03	2,24E+03	3,16E+02	3,23E+01	1,61E+02
Dihydroxy-Acetone	4,23E+04	5,01E+04	3,78E+04	4,36E+04	4,34E+04	4,14E+04	4,60E+04	5,25E+04	4,18E+04	3,67E+04	3,71E+04	4,10E+04	4,64E+04	4,75E+04	4,70E+04	4,43E+04	4,31E+04
2,3-Butanediol	7,96E+03	6,90E+03	3,33E+03	2,47E+03	6,97E+03	4,33E+03	6,22E+03	1,10E+04	3,51E+03	4,03E+03	7,61E+03	4,72E+03	4,84E+03	1,28E+04	7,44E+03	1,79E+03	6,08E+03
2,3-Butanone	1,04E+04	9,38E+03	5,00E+03	4,70E+03	9,14E+03	5,10E+03	8,99E+03	1,25E+04	5,11E+03	5,51E+03	7,50E+03	8,65E+03	8,64E+03	1,14E+04	8,31E+03	5,19E+03	6,75E+03
3-Hydroxy-2-Butanone	1,05E+04	1,15E+04	7,62E+03	6,69E+03	9,88E+03	7,60E+03	8,76E+03	1,16E+04	6,64E+03	9,60E+03	1,11E+04	1,02E+04	8,61E+03	9,95E+03	9,98E+03	5,52E+03	8,79E+03

Table 6.28: Standard derivations of Biolog MicroArray™ PM02 analyzes - Part I.

C-source	*V583*	*OG1RF*	*UW6149*	*UW2860*	*UW6724*	*UW7761*	*UW7777*	*UW7780*	*UW7753*	*UW1833*	*UW7779*	*LMGT 2333*	*ATCC 27959*	*UW6727*	*D32*	*UW7709*	*D1*
Negative Control	0,0E+00	0,0E+00	0,0E+00	0,0E+00	0,0E+00	0,0E+00	0,0E+00	0,0E+00	0,0E+00	0,0E+00	0,0E+00	0,0E+00	0,0E+00	0,0E+00	0,0E+00	0,0E+00	0,0E+00
Chondroitin Sulfate C	1,9E+01	2,8E+02	1,2E+01	6,6E+01	3,7E+02	9,2E+01	6,0E+01	9,0E+00	2,0E+01	3,0E+01	4,3E+02	1,3E+02	1,9E+02	5,1E+02	5,6E+02	3,8E+00	2,5E+02
a-Cyclodextrin	9,3E+02	2,8E+03	8,0E+03	2,3E+03	2,4E+03	3,5E+03	2,8E+03	2,3E+03	2,6E+03	1,3E+03	3,0E+03	4,5E+02	7,3E+02	3,0E+03	9,3E+02	2,1E+03	2,4E+03
b-Cyclodextrin	3,7E+03	2,2E+03	6,6E+03	3,0E+03	3,0E+03	2,3E+03	6,1E+02	2,5E+03	1,6E+03	2,9E+03	3,8E+03	2,3E+03	4,3E+03	1,8E+03	5,8E+02	9,3E+02	2,4E+03
g-Cyclodextrin	5,8E+02	0,0E+00	2,4E+00	0,0E+00	1,5E+03	1,5E+02	0,0E+00	2,5E+01	2,5E+02	1,5E+02	2,3E+02	5,5E+02	7,1E+02	1,7E+02	8,3E+02	0,0E+00	1,6E+02
Dextrin	3,1E+03	1,1E+03	7,4E+03	1,6E+03	1,8E+03	2,9E+03	1,0E+03	8,3E+02	1,4E+03	1,8E+03	4,5E+03	2,3E+03	6,9E+02	3,1E+03	1,8E+03	1,9E+03	2,6E+03
Gelatin	1,7E+03	1,4E+02	3,3E+02	4,6E+01	5,3E+02	1,3E+02	3,4E+02	2,0E+03	2,6E+02	1,5E+02	7,4E+02	6,8E+02	6,0E+02	2,3E+03	9,0E+01	9,1E+01	1,6E+02
Glycogen	2,1E+03	1,3E+03	2,2E+03	1,1E+03	1,4E+03	2,6E+02	5,7E+02	3,8E+03	1,9E+03	3,7E+03	1,6E+03	1,3E+03	2,4E+03	4,5E+03	2,0E+03	5,9E+02	1,5E+03
Inulin	1,6E+03	1,4E+03	4,5E+02	4,9E+00	8,6E+02	6,0E+02	6,6E+02	2,3E+03	1,0E+03	1,1E+03	5,9E+02	5,6E+02	1,4E+03	4,5E+03	2,2E+03	1,4E+02	8,6E+02
Laminarin	6,0E+02	2,3E+03	4,6E+03	2,8E+03	5,1E+02	9,1E+02	1,7E+03	4,2E+03	2,9E+03	5,7E+03	3,2E+03	2,0E+03	3,6E+02	5,8E+03	2,8E+03	3,5E+03	1,1E+03
Mannan	2,9E+03	1,5E+03	3,4E+03	9,9E+02	1,6E+03	1,9E+03	6,4E+02	3,4E+03	2,3E+03	1,0E+03	1,5E+03	2,0E+03	2,1E+03	4,3E+03	2,6E+03	3,3E+03	2,2E+03
Pectin	2,6E+03	1,4E+03	7,6E+03	2,4E+03	1,1E+03	2,3E+03	3,5E+03	3,0E+03	2,2E+03	4,9E+03	3,2E+03	4,0E+03	4,4E+03	9,7E+02	2,9E+03	2,9E+03	2,0E+03
N-Acetyl-D-Galactosamine	2,6E+03	2,3E+03	7,3E+03	1,3E+03	2,8E+02	1,6E+03	4,2E+03	5,3E+03	2,9E+03	3,9E+03	4,6E+03	3,7E+03	8,3E+02	2,1E+03	4,4E+03	2,7E+03	2,8E+02
N-Acetyl-Neuraminic Acid	5,7E+00	0,0E+00	0,0E+00	0,0E+00	0,0E+00	0,0E+00	0,0E+00	0,0E+00	0,0E+00	0,0E+00	0,0E+00	0,0E+00	0,0E+00	0,0E+00	0,0E+00	0,0E+00	0,0E+00
b-D-Allose	4,1E+03	7,5E+03	7,0E+03	6,9E+03	6,5E+03	2,0E+03	7,6E+03	3,3E+03	6,7E+03	4,5E+03	7,5E+02	7,6E+03	8,9E+03	9,6E+03	3,3E+03	1,6E+03	1,1E+03
Amygdalin	9,4E+03	3,2E+03	5,8E+03	1,8E+03	2,8E+03	3,2E+03	4,3E+03	3,1E+03	3,7E+03	3,8E+03	7,9E+03	2,0E+04	2,5E+03	1,1E+03	1,5E+03	1,8E+04	1,6E+03
D-Arabinose	1,0E+04	6,2E+02	1,2E+04	2,0E+03	9,1E+03	3,0E+03	1,3E+03	1,4E+03	3,7E+03	5,5E+03	4,9E+03	8,5E+03	6,1E+03	3,6E+03	4,6E+03	3,8E+03	4,7E+03
D-Arabitol	2,1E+03	1,9E+03	1,4E+03	1,4E+01	1,6E+03	1,8E+02	8,9E+02	2,9E+03	9,7E+02	7,6E+02	2,4E+03	2,1E+02	7,3E+02	3,3E+03	4,8E+02	1,5E+01	1,0E+03
L-Arabitol	1,5E+02	7,8E+01	3,9E+02	9,4E-01	1,3E+03	7,6E+01	5,2E+02	1,6E+03	7,5E+02	5,8E+01	4,3E+02	6,0E+01	3,5E+02	2,4E+03	1,2E+03	4,4E+01	8,7E+02

Table 6.29: Standard derivations of Biolog MicroArray™ PM02 analyzes - Part II.

C-source	*V583*	*OG1RF*	*UW6149*	*UW2860*	*UW6724*	*UW7761*	*UW7777*	*UW7780*	*UW7753*	*UW1833*	*UW7779*	*LMGT 2333*	*ATCC 27959*	*UW6727*	*D32*	*UW7709*	*D1*
Arbutin	1,6E+03	2,0E+03	8,3E+03	2,4E+03	1,7E+03	2,4E+03	4,7E+03	4,3E+03	3,3E+03	5,7E+03	5,1E+03	2,0E+03	1,4E+03	1,6E+03	3,7E+02	3,5E+03	3,0E+03
2-Deoxy-D-Ribose	9,1E+03	1,6E+03	9,8E+03	4,6E+03	6,7E+03	3,5E+03	2,0E+03	2,4E+03	3,3E+03	3,4E+03	6,2E+03	4,6E+03	2,5E+03	2,8E+03	1,5E+03	3,2E+03	4,2E+03
i-Erythritol	1,6E+03	6,4E+02	1,6E+03	4,3E+02	1,5E+03	1,3E+03	1,3E+03	2,3E+03	7,1E+02	2,6E+03	2,9E+03	1,4E+03	6,4E+02	3,5E+03	7,4E+02	8,1E+02	2,5E+02
D-Fucose	7,4E+03	4,5E+02	6,2E+03	1,7E+03	4,8E+03	3,1E+03	1,6E+03	1,4E+03	4,4E+03	5,5E+03	5,1E+03	4,9E+03	4,3E+03	4,3E+03	1,5E+03	4,6E+03	3,4E+03
3-0-b-D-Galactopyranosyl-D-Arabinose	9,3E+03	6,5E+03	7,1E+03	2,2E+03	5,7E+02	2,6E+03	6,7E+03	2,3E+03	1,3E+03	9,1E+03	4,2E+03	4,4E+03	6,2E+02	5,9E+03	4,4E+03	1,8E+03	2,6E+03
Gentiobiose	4,2E+03	5,9E+03	7,0E+03	1,4E+03	1,5E+03	1,1E+03	4,1E+03	5,4E+03	2,8E+03	3,0E+03	4,9E+03	4,1E+03	2,0E+02	2,7E+03	3,5E+03	3,5E+03	1,4E+03
L-Glucose	5,5E+02	1,3E+02	1,6E+02	9,4E-01	2,0E+02	8,0E+01	3,3E+02	8,1E+02	7,1E+01	2,7E+02	1,5E+03	1,8E+02	0,0E+00	2,7E+03	4,9E+01	0,0E+00	1,8E+01
D-Lactitol	8,9E+02	3,7E+02	8,2E+03	4,3E+02	3,3E+03	3,6E+03	4,7E+03	4,1E+03	3,3E+03	3,5E+03	4,6E+03	2,4E+03	9,8E+02	6,5E+02	1,7E+03	1,6E+03	3,2E+03
D-Melezitose	4,2E+03	4,7E+03	8,8E+03	7,6E+02	2,9E+03	2,3E+03	7,0E+03	7,6E+03	2,7E+03	4,6E+03	4,4E+03	1,7E+03	2,9E+03	2,8E+03	3,2E+03	3,3E+03	2,4E+03
Maltitol	1,6E+03	2,6E+03	1,8E+02	1,4E+02	2,3E+03	1,6E+03	3,5E+03	3,7E+03	3,7E+03	2,7E+03	2,1E+03	1,7E+03	2,5E+03	7,6E+03	3,0E+03	3,1E+03	3,6E+03
a-Methyl-D-Glucoside	1,7E+03	4,9E+02	9,2E+02	1,8E+02	1,9E+03	7,2E+02	7,8E+02	2,3E+03	6,0E+02	1,8E+03	1,6E+03	1,1E+03	3,6E+02	4,3E+03	1,4E+03	2,6E+02	1,4E+02
b-Methyl-D-Galactoside	5,8E+03	2,6E+03	8,1E+03	2,8E+03	3,1E+03	4,8E+03	2,0E+03	2,5E+03	3,1E+03	4,5E+03	4,5E+03	4,4E+03	1,1E+03	5,6E+03	2,4E+03	3,6E+03	4,4E+03
3-O-Methyl-Glucose	1,2E+04	4,2E+03	7,3E+03	4,7E+03	2,1E+03	2,2E+03	3,2E+03	4,7E+03	2,1E+03	4,5E+03	4,7E+03	3,5E+03	1,9E+03	5,1E+03	2,8E+03	6,0E+03	1,2E+03
b-Methyl-D-Glucuronic Acid	3,6E+03	9,8E+02	7,4E+02	2,8E+01	1,5E+03	3,4E+02	8,6E+02	2,4E+03	9,2E+02	1,3E+03	2,0E+03	1,2E+03	7,3E+02	4,0E+03	3,0E+03	2,4E+01	8,4E+02
a-Methyl-D-Mannoside	7,1E+03	2,5E+03	3,5E+03	1,4E+03	3,1E+03	2,4E+03	2,0E+03	3,8E+03	2,0E+03	5,2E+03	6,2E+03	3,7E+03	3,4E+03	4,5E+03	2,3E+03	9,6E+02	2,5E+03
b-Methyl-D-Xyloside	3,5E+03	9,2E+02	1,1E+03	6,7E+02	7,9E+02	8,3E+01	8,4E+02	3,1E+03	8,2E+02	1,6E+03	2,7E+03	1,5E+03	1,3E+03	4,7E+03	1,8E+03	6,0E+01	5,5E+02
Palatinose	8,8E+03	1,8E+03	1,1E+04	8,1E+03	6,1E+03	4,1E+03	8,3E+03	5,5E+03	1,8E+03	3,7E+03	4,5E+03	4,3E+03	6,0E+03	1,2E+04	6,4E+03	3,6E+03	4,9E+03
D-Raffinose	4,4E+03	2,0E+03	2,8E+03	7,9E+02	1,6E+03	3,9E+03	9,3E+02	3,7E+03	5,8E+03	5,5E+03	2,4E+03	8,8E+02	3,1E+03	6,5E+03	1,5E+03	4,6E+03	5,0E+03
Salicin	4,0E+03	1,7E+03	8,7E+03	8,6E+02	3,6E+03	3,4E+03	3,3E+03	3,3E+03	3,3E+03	2,7E+03	4,1E+03	2,8E+03	2,0E+03	1,4E+03	1,7E+03	4,2E+03	4,1E+03

Table 6.30: Standard derivations of Biolog MicroArray™ PM02 analyzes - Part III.

C-source	*V583*	*OG1RF*	*UW6149*	*UW2860*	*UW6724*	*UW7761*	*UW7777*	*UW7780*	*UW7753*	*UW1833*	*UW7779*	*LMGT 2333*	*ATCC 27959*	*UW6727*	*D32*	*UW7709*	*D1*
Sedoheptulosan	8,2E+02	1,5E+03	3,8E+00	1,1E+02	1,2E+03	1,3E+02	1,3E+03	3,1E+03	2,5E+01	1,7E+03	8,3E+02	3,0E+01	2,5E+02	5,1E+03	2,3E+01	0,0E+00	3,4E+02
L-Sorbose	3,0E+03	9,7E+02	5,1E+03	3,0E+03	3,6E+03	2,8E+03	2,5E+03	2,5E+03	1,4E+03	5,0E+03	4,0E+03	1,5E+03	7,2E+02	5,8E+03	1,9E+03	1,5E+03	2,4E+03
Stachyose	1,5E+03	3,7E+02	2,3E+01	1,4E+01	6,0E+02	4,4E+01	8,6E+02	2,1E+03	7,0E+01	1,5E+03	8,5E+02	6,0E+02	3,1E+02	5,3E+03	6,7E+02	1,5E+01	1,7E+02
D-Tagatose	2,7E+03	5,4E+03	1,0E+04	6,5E+03	3,2E+03	4,6E+03	7,6E+03	5,0E+03	2,9E+03	3,9E+03	5,2E+03	1,7E+03	5,7E+03	4,0E+03	3,8E+03	4,0E+03	2,8E+03
Turanose	4,4E+03	1,6E+03	6,2E+03	2,7E+03	1,7E+03	2,0E+03	1,6E+03	2,8E+03	1,3E+03	3,3E+03	2,4E+03	8,4E+02	1,2E+03	5,5E+03	1,9E+03	2,2E+03	1,4E+03
Xylitol	3,9E+03	3,3E+03	1,1E+03	1,2E+03	2,2E+03	1,4E+03	1,8E+03	3,4E+03	1,4E+03	1,6E+03	4,3E+03	2,3E+03	5,4E+02	5,2E+03	4,3E+02	8,6E+02	9,3E+02
N-Acetyl-D-Glucosaminitol	6,1E+03	1,0E+03	3,3E+03	2,7E+03	5,1E+03	3,4E+03	1,5E+03	1,8E+03	2,4E+03	5,3E+03	4,4E+03	5,1E+03	1,8E+03	3,1E+03	1,4E+03	3,4E+03	3,3E+03
g-Amino-Butyric Acid	3,0E+03	1,1E+03	1,0E+03	3,3E+02	1,9E+03	7,6E+02	1,0E+03	2,3E+03	7,3E+02	1,8E+03	2,3E+03	1,4E+03	5,9E+02	4,8E+03	1,1E+03	1,9E+02	9,8E+02
d-Amino-Valeric Acid	2,3E+01	9,5E+00	1,1E+02	4,1E+00	4,2E+02	1,6E+02	9,7E+00	5,0E+02	1,4E+02	5,0E+01	1,1E+02	1,1E+02	3,9E+01	1,0E+02	1,8E+02	1,9E+01	3,2E+02
Butyric Acid	4,2E+03	1,1E+03	8,0E+03	1,5E+03	5,2E+03	2,0E+03	8,0E+02	3,6E+03	8,8E+03	5,0E+03	4,3E+03	2,8E+03	4,4E+03	3,2E+03	5,1E+03	5,2E+03	4,5E+03
Capric Acid	2,3E+03	7,6E+02	4,8E+01	4,5E+01	4,1E+02	1,6E+02	8,1E+02	6,5E+02	5,3E+02	8,1E+01	8,1E+01	2,3E+03	6,2E+02	4,0E+03	4,8E+02	1,2E+02	6,6E+02
Caproic Acid	1,4E+02	0,0E+00	0,0E+00	0,0E+00	1,4E+01	3,6E+02	4,8E+02	9,5E+02	6,4E+02	3,7E+01	9,5E+02	2,0E+03	3,0E+02	2,7E+03	0,0E+00	0,0E+00	3,4E+02
Citraconic Acid	1,9E+00	0,0E+00	0,0E+00	0,0E+00	0,0E+00	0,0E+00	0,0E+00	1,3E+01	0,0E+00	0,0E+00	0,0E+00	0,0E+00	0,0E+00	2,7E+02	0,0E+00	0,0E+00	0,0E+00
D,L-Citramalic Acid	2,4E+00	0,0E+00	0,0E+00	0,0E+00	7,7E+01	1,4E+00	0,0E+00	6,6E+02	4,7E-01	1,5E+02	3,6E+01	1,7E+00	4,7E-01	2,7E+03	2,6E+00	0,0E+00	4,1E+01
D-Glucosamine	4,3E+03	2,2E+03	1,1E+04	5,0E+02	4,4E+03	6,2E+03	7,5E+03	6,3E+03	6,5E+03	5,4E+03	6,5E+03	5,8E+03	2,6E+03	2,8E+03	5,2E+03	5,2E+03	6,1E+03
2-Hydroxy-Benzoic Acid	1,2E+01	4,7E-01	0,0E+00	0,0E+00	4,8E+01	0,0E+00	0,0E+00	6,3E+02	0,0E+00	7,1E+00	0,0E+00	0,0E+00	0,0E+00	2,4E+02	0,0E+00	6,6E+00	1,4E+00
4-Hydroxy-Benzoic Acid	9,4E-01	0,0E+00	0,0E+00	0,0E+00	9,4E+00	0,0E+00	0,0E+00	3,8E+00	0,0E+00	0,0E+00	0,0E+00	3,3E+00	0,0E+00	5,2E+00	0,0E+00	0,0E+00	0,0E+00
b-Hydroxy-Butyric Acid	3,5E+03	1,4E+03	1,1E+03	5,6E+02	2,1E+03	1,1E+03	7,5E+02	3,5E+03	6,9E+02	3,0E+03	3,1E+03	2,7E+03	9,9E+02	4,4E+03	2,1E+03	2,1E+02	1,2E+03
g-Hydroxy-Butyric Acid	2,2E+03	8,4E+02	2,4E+03	2,2E+03	2,4E+03	1,9E+03	1,5E+03	3,5E+03	3,3E+03	3,8E+03	3,7E+03	6,4E+02	4,0E+03	3,8E+03	1,2E+03	2,9E+03	2,8E+03

Table 6.31: Standard derivations of Biolog MicroArray™ PM02 analyzes - Part IV.

C-source	*V583*	*OG1RF*	*UW6149*	*UW2860*	*UW6724*	*UW7761*	*UW7777*	*UW7780*	*UW7753*	*UW1833*	*UW7779*	*LMGT 2333*	*ATCC 27959*	*UW6727*	*D32*	*UW7709*	*D1*
a-Keto-Valeric Acid	3,7E+03	1,9E+03	7,2E+03	2,0E+03	3,2E+03	3,1E+03	3,2E+03	3,2E+03	2,4E+03	3,2E+03	5,6E+03	4,9E+03	8,2E+02	4,3E+03	1,5E+03	1,8E+03	1,4E+03
Itaconic Acid	4,6E+02	3,3E+00	9,0E+00	8,0E+00	2,7E+02	6,1E+01	1,4E+01	1,1E+02	1,3E+02	1,9E+02	6,5E+01	2,2E+02	3,3E+02	7,2E+01	1,2E+01	2,0E+01	3,7E+02
5-Keto-D-Gluconic Acid	1,0E+04	2,3E+03	1,1E+04	1,8E+03	6,6E+03	3,7E+03	6,3E+03	3,6E+03	9,7E+02	4,4E+03	1,2E+04	6,4E+03	1,0E+04	8,6E+03	4,0E+03	1,0E+03	1,5E+03
D-Lactic Acid Methyl Ester	3,8E+00	2,4E+00	0,0E+00	0,0E+00	4,3E+01	1,6E+01	7,5E+00	9,2E+01	0,0E+00	7,5E+00	0,0E+00	3,6E+00	0,0E+00	1,3E+03	1,1E+02	0,0E+00	0,0E+00
Malonic Acid	8,5E+00	0,0E+00	0,0E+00	0,0E+00	2,3E+01	0,0E+00	0,0E+00	2,6E+01	0,0E+00	4,5E+02	7,9E+01	2,1E+01	0,0E+00	3,9E+02	0,0E+00	0,0E+00	9,4E-01
Melibionic Acid	4,4E+03	4,1E+03	3,8E+03	6,9E+02	2,2E+03	2,0E+03	1,4E+03	1,3E+03	4,5E+02	6,7E+03	3,7E+03	2,9E+03	6,6E+01	3,0E+03	1,6E+03	7,9E+02	8,3E+02
Oxalic Acid	1,2E+00	0,0E+00	0,0E+00	0,0E+00	9,4E+00	0,0E+00	0,0E+00	8,5E+00	5,2E+00	0,0E+00	2,4E+00	0,0E+00	2,8E+00	8,6E+01	0,0E+00	0,0E+00	3,9E+01
Oxalomalic Acid	6,3E+03	7,2E+02	9,7E+03	2,2E+03	8,3E+03	6,5E+03	1,4E+03	2,5E+03	5,3E+03	7,2E+03	5,1E+03	4,7E+03	4,1E+03	1,6E+03	2,9E+03	5,9E+03	5,7E+03
Quinic Acid	5,1E+01	4,2E+00	0,0E+00	0,0E+00	5,1E+01	0,0E+00	9,4E-01	1,1E+03	0,0E+00	0,0E+00	9,3E+00	0,0E+00	4,2E+00	1,7E+03	0,0E+00	0,0E+00	4,7E+00
D-Ribono-1,4-Lactone	3,3E+00	7,1E+00	3,3E+00	0,0E+00	9,0E+01	4,7E-01	3,3E+00	2,6E+02	0,0E+00	1,9E+00	7,9E+01	1,0E+01	0,0E+00	2,9E+02	1,9E+01	0,0E+00	5,4E+00
Sebacic Acid	3,2E+02	4,4E+01	1,3E+02	3,6E+01	1,1E+03	4,2E+02	2,2E+02	1,4E+03	3,1E+02	1,2E+03	9,9E+02	1,2E+03	3,3E+02	1,8E+03	5,4E+02	4,8E+01	2,5E+02
Sorbic Acid	5,5E+03	4,5E+03	9,2E+03	3,4E+03	4,2E+03	2,9E+03	1,7E+03	2,5E+03	2,4E+03	2,7E+03	4,7E+03	5,6E+03	1,4E+03	3,6E+03	1,1E+03	2,1E+03	2,5E+03
Succinamic Acid	1,5E+03	1,7E+02	4,1E+02	7,8E+01	1,5E+03	1,2E+02	3,9E+02	2,4E+03	4,6E+02	6,9E+02	1,1E+03	8,0E+02	3,4E+02	3,5E+03	6,9E+02	2,0E+01	1,2E+02
D-Tartaric Acid	8,2E+02	2,2E+02	2,6E+03	8,4E+02	2,0E+03	1,3E+03	1,1E+03	2,2E+03	1,4E+03	4,3E+03	1,9E+03	2,3E+03	8,3E+02	3,4E+03	1,3E+03	1,4E+03	2,3E+02
L-Tartaric Acid	4,5E+02	6,3E+02	3,9E+03	1,1E+03	1,2E+03	2,3E+02	1,8E+02	1,7E+03	1,2E+03	4,1E+03	1,4E+03	1,5E+03	1,0E+03	3,9E+03	9,3E+03	6,4E+02	3,6E+02
Acetamide	1,4E+01	0,0E+00	0,0E+00	0,0E+00	1,6E+02	3,4E+01	4,5E+01	9,1E+02	0,0E+00	3,6E+01	0,0E+00	0,0E+00	0,0E+00	1,4E+03	0,0E+00	0,0E+00	1,8E+01
L-Alaninamide	0,0E+00	0,0E+00	0,0E+00	0,0E+00	2,8E+00	0,0E+00	0,0E+00	0,0E+00	0,0E+00	0,0E+00	9,4E-01	0,0E+00	0,0E+00	0,0E+00	0,0E+00	0,0E+00	0,0E+00
N-Acetyl-L-Glutamic Acid	1,4E+00	9,4E-01	1,4E+00	0,0E+00	0,0E+00	0,0E+00	2,8E+00	5,8E+02	0,0E+00	4,7E-01	3,8E+00	0,0E+00	1,2E+01	2,2E+03	0,0E+00	0,0E+00	0,0E+00
L-Arginine	2,5E+02	1,2E+03	7,1E+01	3,8E+02	7,7E+02	7,8E+02	2,4E+02	1,8E+03	9,0E+02	6,5E+02	1,4E+03	4,8E+02	2,3E+03	3,6E+03	1,0E+01	4,3E+02	3,2E+02

Table 6.32: Standard derivations of Biolog MicroArray™ PM02 analyzes - Part V.

C-source	*V583*	*OG1RF*	*UW6149*	*UW2860*	*UW6724*	*UW7761*	*UW7777*	*UW7780*	*UW7753*	*UW1833*	*UW7779*	*LMGT 2333*	*ATCC 27959*	*UW6727*	*D32*	*UW7709*	*D1*
Glycine	1,2E+01	0,0E+00	0,0E+00	0,0E+00	4,7E-01	2,4E+00	0,0E+00	4,7E+02	9,4E-01	0,0E+00	0,0E+00	0,0E+00	2,8E+03	7,8E+02	0,0E+00	0,0E+00	1,4E+01
L-Histidine	4,7E-01	1,9E+00	4,7E-01	0,0E+00	1,7E+02	0,0E+00	1,9E+00	3,8E+02	0,0E+00	2,4E+00	5,7E+01	4,7E-01	1,4E+00	8,4E+02	2,1E+00	0,0E+00	2,5E+00
L-Homoserine	5,0E+02	8,0E+01	3,4E+01	1,9E+00	4,6E+02	4,7E+01	2,4E+02	3,1E+03	1,8E+01	1,1E+03	2,6E+02	1,1E+02	3,3E+02	3,9E+03	5,3E+02	3,3E+00	2,1E+02
4-Hydroxy-L-Proline (trans)	4,3E+02	2,7E+01	2,5E+01	6,1E+00	3,9E+02	2,0E+01	7,9E+00	1,5E+03	1,3E+01	1,2E+02	4,1E+02	1,1E+02	4,3E+01	1,2E+03	8,3E+01	1,4E+01	9,4E+01
L-Isoleucine	1,6E+03	2,8E+03	9,3E+01	2,2E+00	8,1E+02	2,2E+02	1,3E+02	2,5E+03	3,9E+02	5,5E+02	2,7E+02	5,6E+02	1,2E+03	2,0E+03	1,8E+02	4,8E+01	6,9E+02
L-Leucine	2,9E+03	5,3E+02	2,4E+03	4,5E+02	2,9E+03	2,4E+03	2,1E+03	1,5E+03	1,2E+03	4,4E+03	4,2E+03	4,1E+03	4,1E+02	4,0E+03	8,1E+02	3,0E+02	2,3E+03
L-Lysine	2,6E+03	1,3E+03	1,6E+03	9,9E+02	1,8E+03	8,1E+02	1,4E+03	2,3E+03	1,3E+03	2,9E+03	2,6E+03	1,8E+03	2,6E+03	5,0E+03	1,5E+03	9,1E+02	1,0E+03
L-Methionine	1,8E+03	1,6E+03	5,4E+03	1,6E+03	2,3E+03	2,5E+03	2,9E+03	2,0E+03	3,2E+03	3,4E+03	3,6E+03	2,8E+03	8,2E+02	3,0E+03	1,3E+03	1,1E+03	2,3E+03
L-Ornithine	7,5E+00	4,7E+00	0,0E+00	0,0E+00	4,2E+01	0,0E+00	0,0E+00	4,9E+02	9,4E-01	0,0E+00	0,0E+00	0,0E+00	2,4E+00	2,1E+01	0,0E+00	0,0E+00	2,1E+01
L-Phenylalanine	2,5E+01	0,0E+00	1,4E+00	0,0E+00	1,1E+02	1,7E+01	0,0E+00	1,2E+00	0,0E+00	4,3E+02	2,4E+00	0,0E+00	0,0E+00	9,2E+01	2,8E+00	0,0E+00	0,0E+00
L-Pyroglutamic Acid	4,7E+00	0,0E+00	0,0E+00	0,0E+00	4,7E+00	0,0E+00	0,0E+00	5,4E+01	0,0E+00	0,0E+00	0,0E+00	0,0E+00	0,0E+00	5,4E+02	0,0E+00	0,0E+00	4,7E-01
L-Valine	7,3E+02	1,9E+02	2,3E+01	9,4E-01	2,2E+02	1,3E+02	2,6E+03	1,8E+03	9,6E+01	1,9E+01	5,1E+02	1,3E+01	6,6E+02	3,3E+03	2,8E+02	1,3E+01	3,1E+02
D,L-Carnitine	1,1E+03	1,4E+01	1,9E+02	3,3E+00	7,5E+02	2,0E+02	2,6E+03	2,2E+03	3,9E+02	2,5E+02	8,3E+02	3,9E+02	6,2E+02	3,4E+03	1,5E+02	1,7E+01	6,2E+02
Butylamine (sec)	1,9E+03	1,3E+02	6,9E+02	1,4E+02	1,9E+03	2,5E+02	9,4E+02	1,9E+03	4,1E+02	2,7E+03	1,9E+03	3,9E+02	5,0E+02	3,2E+03	1,2E+03	3,0E+01	5,4E+02
D,L-Octopamine	1,3E+03	2,2E+02	5,2E+02	9,0E+01	1,8E+03	1,4E+02	8,8E+02	1,8E+03	1,8E+02	7,1E+02	5,0E+02	3,6E+02	6,2E+02	2,0E+03	6,4E+02	1,5E+02	6,0E+02
Putrescine	2,0E+03	4,5E+01	5,7E+01	2,7E+01	9,3E+02	4,8E+01	5,5E+01	2,8E+03	2,7E+01	1,1E+02	1,1E+03	5,2E+01	1,0E+03	2,0E+03	3,1E+02	1,7E+01	1,5E+02
Dihydroxy-Acetone	7,3E+03	2,5E+03	1,1E+04	1,6E+03	4,6E+03	3,0E+03	6,6E+02	3,4E+03	2,7E+03	5,1E+03	7,2E+03	5,2E+03	4,0E+03	4,8E+03	1,5E+03	2,4E+03	2,5E+03
2,3-Butanediol	3,0E+03	1,9E+03	2,3E+03	1,4E+03	2,2E+03	1,0E+03	2,0E+03	2,6E+03	1,4E+03	2,9E+03	3,8E+03	2,4E+03	1,6E+03	3,6E+03	9,2E+02	9,5E+02	1,4E+03
2,3-Butanone	4,3E+03	1,6E+03	3,4E+03	1,4E+03	1,8E+03	2,0E+03	4,7E+02	3,2E+03	1,9E+03	6,8E+02	9,3E+02	4,4E+03	2,3E+03	4,4E+03	1,4E+03	1,6E+03	1,6E+03
3-Hydroxy-2-Butanone	2,8E+03	8,1E+02	5,3E+03	1,4E+03	1,7E+03	2,9E+03	9,5E+02	2,1E+03	2,5E+03	3,6E+03	4,6E+03	5,1E+03	1,7E+03	2,7E+03	7,9E+02	1,6E+03	3,1E+03

7 List of Abbreviations

C. elegans	*Caenorhabditis elegans*
E. faecalis	*Enterococcus faecalis*
E. faecium	*Enterococcus faecium*
G. mellonella	*Galleria mellonella*
S. aureus	*Staphylococcus aureus*
Taq	*Thermus aquaticus*

°C	Centigrade
g, mg, µg, ng	Gram, milligram, microgram, nanogram
h, min, s	Hour, minute, second
L, mL, µL	Liter, mililiter, microliter
M, mM, µM,	Molar, milimolar, micromolar
Mbp, kb, bp	Megabase pairs, kilobase pairs, base pairs
%	Percent
Rpm	Revolutions per minute
w/v	Weight per volume

CU	Cuba
D	Germany
DK	Denmark
ESP	Spain
GR	Greece
IS	Iceland
JP	Japan
N	Norway
NL	Netherlands
PL	Poland
US	United States
USA	United States of America

A	Deoxyadenosine
C	Deoxycytidine
G	Deoxyguanosine
T	Deoxythymidine

Ala	Alanine
ATP	Adenosine-5'-triphosphate
BLAST	Basic Local Alignment Search Tool
CFU	Colony forming units
CO2	Carbon dioxide
DB	Data base
DNA	Deoxyribonucleic acid
dNTPs	2´-Deoxyribonucleosid triphosphate
ddNTPs	2´,3´-Dideoxyribonucleosid triphosphate
ELISA	Enzyme Linked Immunosorbent Assay
et al.	*et alii*
Fig.	Figure
Inc	Incompatibility
InDel	Insertion/deletion
LB	Lysogeny broth
MRSA	Multi-resistant *Staphylococcus aureus*
NAD(H)	Nicotinamide adenine dinucleotide
NGS	Next generation sequencing
No	Number
PCR	Polymerase chain reaction
RKI	Robert Koch Institute
RNA	Ribonucleic acid
RNAi	RNA interference
Ser	Serine
Tab.	Table
tRNA	Transfer-RNA
UV	Ultraviolet

8 List of Figures

9 List of Tables

10 References

1. **Aakra, A., O. L. Nyquist, L. Snipen, T. S. Reiersen, and I. F. Nes.** 2007. Survey of genomic diversity among Enterococcus faecalis strains by microarray-based comparative genomic hybridization. Appl Environ Microbiol **73:**2207-2217.
2. **Abrantes, M. C., J. Kok, and F. Lopes Mde.** 2013. EfaR is a major regulator of *Enterococcus faecalis* manganese transporters and influences processes involved in host colonization and infection. Infect Immun. **81:**935-944.
3. **Alekshun, M. N., and S. B. Levy.** 2007. Molecular mechanisms of antibacterial multidrug resistance. Cell **128:**1037-1050.
4. **Alikhan, N. F., N. K. Petty, N. L. Ben Zakour, and S. A. Beatson.** 2011. BLAST Ring Image Generator (BRIG): simple prokaryote genome comparisons. BMC Genomics **12:**402.
5. **Angiuoli, S. V., and S. L. Salzberg.** 2011. Mugsy: fast multiple alignment of closely related whole genomes. Bioinformatics. **27:**334-342.
6. **Arciola, C. R., L. Baldassarri, D. Campoccia, R. Creti, V. Pirini, J. Huebner, and L. Montanaro.** 2008. Strong biofilm production, antibiotic multi-resistance and high *gelE* expression in epidemic clones of *Enterococcus faecalis* from orthopaedic implant infections. Biomaterials. **29:**580-586.
7. **Arias, C. A., and B. E. Murray.** 2012. The rise of the *Enterococcus*: beyond vancomycin resistance. Nat Rev Microbiol. **10:**266-278.
8. **Arias, C. A. A. a., and B. E. Murray.** 2009. Antibiotic-Resistant Bugs in the 21st Centurey - A Clinical Super-Challenge. The New England Journal of Medicine **360:**439-443.
9. **Arsene, S., and R. Leclercq.** 2007. Role of a *qnr* -like gene in the intrinsic resistance of *Enterococcus faecalis* to fluoroquinolones. Antimicrobial Agents and Chemotherapy **51:**3254-3258.
10. **Aziz, R. K., D. Bartels, A. A. Best, M. DeJongh, T. Disz, R. A. Edwards, K. Formsma, S. Gerdes, E. M. Glass, M. Kubal, F. Meyer, G. J. Olsen, R. Olson, A. L. Osterman, R. A. Overbeek, L. K. McNeil, D. Paarmann, T. Paczian, B. Parrello, G. D. Pusch, C. Reich, R. Stevens, O. Vassieva, V. Vonstein, A. Wilke, and O. Zagnitko.** 2008. The RAST Server: rapid annotations using subsystems technology. BMC Genomics **9:**75.
11. **Baldassarri, L., L. Bertuccini, M. G. Ammendolia, G. Gherardi, and R. Creti.** 2001. Variant esp gene in vancomycin-sensitive Enterococcus faecium. Lancet **357:**1802.
12. **Ballering, K. S., C. J. Kristich, S. M. Grindle, A. Oromendia, D. T. Beattie, and G. M. Dunny.** 2009. Functional genomics of Enterococcus faecalis: multiple novel genetic determinants for biofilm formation in the core genome. Journal of bacteriology **191:**2806-2814.
13. **Barnes, A. M., K. S. Ballering, R. S. Leibman, C. L. Wells, and G. M. Dunny.** 2012. *Enterococcus faecalis* produces abundant extracellular structures containing DNA in the absence of cell lysis during early biofilm formation. MBio. **3:**e00193-00112.

14. **Barrangou, R., C. Fremaux, H. Deveau, M. Richards, P. Boyaval, S. Moineau, D. A. Romero, and P. Horvath.** 2007. CRISPR provides acquired resistance against viruses in prokaryotes. Science **315:**1709-1712.
15. **Barton, B. M., G. P. Harding, and A. J. Zuccarelli.** 1995. A general method for detecting and sizing large plasmids. Anal.Biochem. **226:**235-240.
16. **Benachour, A., T. Morin, L. Hébert, A. Budin-Verneuil, A. Le Jeune, Y. Auffray, and V. Pichereau.** 2009. Identification of secreted and surface proteins from *Enterococcus faecalis*. Can J Microbiol. **55:**967-974.
17. **Bentley, S. D., D. M. Aanensen, A. Mavroidi, D. Saunders, E. Rabbinowitsch, M. Collins, K. Donohoe, D. Harris, L. Murphy, M. A. Quail, G. Samuel, I. C. Skovsted, M. S. Kaltoft, B. Barrell, P. R. Reeves, J. Parkhill, and B. G. Spratt.** 2006. Genetic analysis of the capsular biosynthetic locus from all 90 pneumococcal serotypes. PLoS Genet. **2:**e31.
18. **Bikard, D., and L. A. Marraffini.** 2012. Innate and adaptive immunity in bacteria: mechanisms of programmed genetic variation to fight bacteriophages. Curr Opin Immunol. **24:**15-20.
19. **Bizzini, A., C. Zhao, Y. Auffray, and A. Hartke.** 2009. The Enterococcus faecalis superoxide dismutase is essential for its tolerance to vancomycin and penicillin. The Journal of antimicrobial chemotherapy **64:**1196-1202.
20. **Blom, J., S. P. Albaum, D. Doppmeier, A. Pühler, F. J. Vorhölter, M. Zakrzewski, and A. Goesmann.** 2009. EDGAR: a software framework for the comparative analysis of prokaryotic genomes. BMC Bioinformatics **10:**154.
21. **Bøhle, L. A., E. M. Færgestad, E. Veiseth-Kent, H. Steinmoen, I. F. Nes, V. G. Eijsink, and G. Mathiesen.** 2010. Identification of proteins related to the stress response in Enterococcus faecalis V583 caused by bovine bile. Proteome science **8:**37.
22. **Bøhle, L. A., T. Riaz, W. Egge-Jacobsen, M. Skaugen, Ø. L. Busk, V. G. Eijsink, and G. Mathiesen.** 2011. Identification of surface proteins in Enterococcus faecalis V583. BMC Genomics **12:**135.
23. **Bose, M., and R. D. Barber.** 2006. Prophage Finder: a prophage loci prediction tool for prokaryotic genome sequences. In Silico Biol. **6:**223-227.
24. **Bourgogne, A., D. A. Garsin, X. Qin, K. V. Singh, J. Sillanpaa, S. Yerrapragada, Y. Ding, S. Dugan-Rocha, C. Buhay, H. Shen, G. Chen, G. Williams, D. Muzny, A. Maadani, K. A. Fox, J. Gioia, L. Chen, Y. Shang, C. A. Arias, S. R. Nallapareddy, M. Zhao, V. P. Prakash, S. Chowdhury, H. Jiang, R. A. Gibbs, B. E. Murray, S. K. Highlander, and G. M. Weinstock.** 2008. Large scale variation in Enterococcus faecalis illustrated by the genome analysis of strain OG1RF. Genome Biol **9:**R110.
25. **Bourgogne, A., S. G. Hilsenbeck, G. M. Dunny, and B. E. Murray.** 2006. Comparison of OG1RF and an isogenic fsrB deletion mutant by transcriptional analysis: the Fsr system of Enterococcus faecalis is more than the activator of gelatinase and serine protease. Journal of bacteriology **188:**2875-2884.
26. **Bourgogne, A., K. V. Singh, K. A. Fox, K. J. Pflughoeft, B. E. Murray, and D. A. Garsin.** 2007. EbpR is important for biofilm formation by activating expression of the endocarditis and biofilm-associated pilus operon (*ebpABC*) of *Enterococcus faecalis* OG1RF. The Journal of Bacteriology **189:**6490-6493.
27. **Bourgogne, A., L. C. Thomson, and B. E. Murray.** 2010. Bicarbonate enhances expression of the endocarditis and biofilm associated pilus locus, ebpR-ebpABC, in Enterococcus faecalis. BMC Microbiol **10:**17.

28. **Brede, D. A., L. G. Snipen, D. W. Ussery, A. J. Nederbragt, and I. F. Nes.** 2011. Complete genome sequence of the commensal Enterococcus faecalis 62, isolated from a healthy Norwegian infant. Journal of bacteriology **193:**2377-2378.
29. **Brouns, S. J., M. M. Jore, M. Lundgren, E. R. Westra, R. J. Slijkhuis, A. P. Snijders, M. J. Dickman, K. S. Makarova, E. V. Koonin, and J. van der Oost.** 2008. Small CRISPR RNAs guide antiviral defense in prokaryotes. Science. **321:**960-964.
30. **Carattoli, A.** 2009. Resistance plasmid families in Enterobacteriaceae. Antimicrob Agents Chemother **53:**2227-2238.
31. **Carte, J., R. Wang, H. Li, R. M. Terns, and M. P. Terns.** 2008. Cas6 is an endoribonuclease that generates guide RNAs for invader defense in prokaryotes. Genes Dev. **22:**3489-3496.
32. **Chang, Y. C., Z. Wang, L. A. Flax, D. Xu, J. D. Esko, V. Nizet, and M. J. Baron.** 2011. Glycosaminoglycan binding facilitates entry of a bacterial pathogen into central nervous systems. PLoS Pathog. **7:**e1002082.
33. **Chevreux, B.** 2005. MIRA: An Automated Genome and EST Assembler. Ph.D. The Ruprecht-Karls-University, http://www.chevreux.org/projects_mira.html.
34. **Chevreux, B., T. Pfisterer, B. Drescher, A. J. Driesel, W. E. Müller, T. Wetter, and S. Suhai.** 2004. Using the miraEST assembler for reliable and automated mRNA transcript assembly and SNP detection in sequenced ESTs. Genome Res. **14:**1147-1159.
35. **Chopra, I., and M. Roberts.** 2001. Tetracycline antibiotics: mode of action, applications, molecular biology, and epidemiology of bacterial resistance. Microbiol Mol Biol Rev. **65:**232-260.
36. **Chow, J. W., L. A. Thal, M. B. Perri, J. A. Vazquez, S. M. Donabedian, D. B. Clewell, and M. J. Zervos.** 1993. Plasmid-associated hemolysin and aggregation substance production contribute to virulence in experimental enterococcal endocarditis. Antimicrobial Agents and Chemotherapy **37:**2474-2477.
37. **Clewell, D. B., K. E. Weaver, G. M. Dunny, T. M. Coque, M. V. Francia, and F. Hayes.** 2013. Extrachromosomal and mobile elements in Enterococci: transmission, maintenance, and epidemiology. In: Gilmore, M.S. (Ed.), The Enterococci.; ASM Press.
38. **Cobo Molinos, A., H. Abriouel, N. B. Omar, R. L. Lopez, and A. Galvez.** 2008. Detection of *ebp* (endocarditis- and biofilm-associated pilus) genes in enterococcal isolates from clinical and non-clinical origin. Int J Food Microbiol **126:**123-126.
39. **Coburn, P. S., A. S. Baghdayan, G. T. Dolan, and N. Shankar.** 2008. An AraC-type transcriptional regulator encoded on the Enterococcus faecalis pathogenicity island contributes to pathogenesis and intracellular macrophage survival. Infect Immun **76:**5668-5676.
40. **Coburn, P. S., A. S. Baghdayan, G. T. Dolan, and N. Shankar.** 2007. Horizontal transfer of virulence genes encoded on the Enterococcus faecalis pathogenicity island. Mol Microbiol **63:**530-544.
41. **Coburn, P. S., and M. S. Gilmore.** 2003. The Enterococcus faecalis cytolysin: a novel toxin active against eukaryotic and prokaryotic cells. Cellular Microbiology **5:**661-669.

42. **Cook, S. M., and J. D. McArthur.** 2013. Developing *Galleria mellonella* as a model host for human pathogens. Virulence. **4:**350-353.
43. **Courvalin, P.** 2006. Vancomycin resistance in gram-positive cocci. Clin Infect.Dis. **42:**S25-34.
44. **Cozzone, A. J.** 2005. Role of protein phosphorylation on serine/threonine and tyrosine in the virulence of bacterial pathogens. J Mol Microbiol Biotechnol. **9:**198-213.
45. **Creti, R., F. Fabretti, S. Koch, J. Huebner, D. A. Garsin, L. Baldassarri, L. Montanaro, and C. R. Arciola.** 2009. Surface protein EF3314 contributes to virulence properties of *Enterococcus faecalis*. Int J Artif Organs. **32:**611-620.
46. **Creti, R., M. Imperi, L. Bertuccini, F. Fabretti, G. Orefici, R. Di Rosa, and L. Baldassarri.** 2004. Survey for virulence determinants among *Enterococcus faecalis* isolated from different sources. J Med Microbiol. **53:**13-20.
47. **Darling, A. C., B. Mau, F. R. Blattner, and N. T. Perna.** 2004. Mauve: multiple alignment of conserved genomic sequence with rearrangements. Genome research **14:**1394-1403.
48. **Darling, A. E., B. Mau, and N. T. Perna.** 2010. progressiveMauve: multiple genome alignment with gene gain, loss and rearrangement. PloS one **5:**e11147.
49. **de Regt, M. J., W. van Schaik, M. van Luit-Asbroek, H. A. Dekker, E. van Duijkeren, C. J. Koning, M. J. Bonten, and R. J. Willems.** 2012. Hospital and community ampicillin-resistant *Enterococcus faecium* are evolutionarily closely linked but have diversified through niche adaptation. PLoS One. **7:**e30319.
50. **Derbise, A., S. Aubert, and S. N. El.** 1997. Mapping the regions carrying the three contiguous antibiotic resistance genes aadE , sat4 , and aphA -3 in the genomes of staphylococci. Antimicrobial Agents and Chemotherapy **41:**1024-1032.
51. **Di Rosa, R., R. Creti, M. Venditti, R. D'Amelio, C. R. Arciola, L. Montanaro, and L. Baldassarri.** 2006. Relationship between biofilm formation, the enterococcal surface protein (Esp) and gelatinase in clinical isolates of *Enterococcus faecalis* and *Enterococcus faecium*. FEMS Microbiol Lett. **256:**145-150.
52. **Dobrindt, U., B. Hochhut, U. Hentschel, and J. Hacker.** 2004. Genomic islands in pathogenic and environmental microorganisms. Nat Rev Micro **2:**414-424.
53. **Domann, E., T. Hain, R. Ghai, A. Billion, C. Kuenne, K. Zimmermann, and T. Chakraborty.** 2007. Comparative genomic analysis for the presence of potential enterococcal virulence factors in the probiotic Enterococcus faecalis strain Symbioflor 1. International journal of medical microbiology : IJMM **297:**533-539.
54. **Donskey, C. J.** 2004. The role of the intestinal tract as a reservoir and source for transmission of nosocomial pathogens. Clin.Infect.Dis. **39:**219-226.
55. **Doran, K. S., E. J. Engelson, A. Khosravi, H. C. Maisey, I. Fedtke, O. Equils, K. S. Michelsen, M. Arditi, A. Peschel, and V. Nizet.** 2005. Blood-brain barrier invasion by group B Streptococcus depends upon proper cell-surface anchoring of lipoteichoic acid. J Clin Invest. **115:**2499-2507.
56. **Dørum, G., L. Snipen, M. Solheim, and S. Saebo.** 2011. Smoothing gene expression data with network information improves consistency of regulated genes. Stat Appl Genet Mol Biol. **10**.

57. **Duerkop, B. A., C. V. Clements, D. Rollins, J. L. Rodrigues, and L. V. Hooper.** 2012. A composite bacteriophage alters colonization by an intestinal commensal bacterium. Proc Natl Acad Sci U S A. **109:**17621-17626.
58. **Dunny, G. M., M. H. Antiporta, and H. Hirt.** 2001. Peptide pheromone-induced transfer of plasmid pCF10 in *Enterococcus faecalis*: probing the genetic and molecular basis for specificity of the pheromone response. Peptides **22:**1529-1539.
59. **Edwards, A. M., and R. C. Massey.** 2011. How does Staphylococcus aureus escape the bloodstream? Trends Microbiol **19:**184-190.
60. **Elhadidy, M., and A. Elsayyad.** 2013. Uncommitted role of enterococcal surface protein, Esp, and origin of isolates on biofilm production by *Enterococcus faecalis* isolated from bovine mastitis. J Microbiol Immunol Infect. **46:**80-84.
61. **English, A. C., S. Richards, Y. Han, M. Wang, V. Vee, J. Qu, X. Qin, D. M. Muzny, J. G. Reid, K. C. Worley, and R. A. Gibbs.** 2012. Mind the gap: upgrading genomes with Pacific Biosciences RS long-read sequencing technology. PLoS One. **7:**e47768.
62. **Fanaro, S., R. Chierici, P. Guerrini, and V. Vigi.** 2003. Intestinal microflora in early infancy: composition and development. Acta Paediatr Suppl. **91:**48-55.
63. **Ferretti, J. J., ., K. S. Gilmore, and P. Courvalin.** 1986. Nucleotide sequence analysis of the gene specifying the bifunctional 6'-aminoglycoside acetyltransferase 2''-aminoglycoside phosphotransferase enzyme in *Streptococcus faecalis* and identification and cloning of gene regions specifying the two activities. J Bacteriol. **167:**631-638.
64. **Fisher, K., and C. Phillips.** 2009. The ecology, epidemiology and virulence of Enterococcus. Microbiology **155:**1749-1757.
65. **Flint, H. J., P. Louis, K. P. Scott, and S. H. Duncan.** 2007. Commensal Bacteria in Health and Disease., p. 101 - 115. *In* K. A. Brogden, F. C. Minion, N. Cornick, T. B. Stanton, Q. Zhang, L. K. Nolan, and M. J. Wannemuehler (ed.), Virulence Mechanisms of Bacterial Pathogens, vol. 4. ASM Press, Washington, DC 20036-2904.
66. **Frank, K. L., P. S. Guiton, A. M. Barnes, D. A. Manias, O. N. Chuang-Smith, P. L. Kohler, A. R. Spaulding, S. J. Hultgren, P. M. Schlievert, and G. M. Dunny.** 2013. AhrC and Eep are biofilm infection-associated virulence factors in *Enterococcus faecalis*. Infect Immun. **81:**1696-1708.
67. **Franz, C. M., M. Huch, H. Abriouel, W. Holzapfel, and A. Gálvez.** 2011. Enterococci as probiotics and their implications in food safety. Int J Food Microbiol. **151:**125 - 140.
68. **Freitas, A. R., T. M. Coque, C. Novais, A. M. Hammerum, C. H. Lester, M. J. Zervos, S. Donabedian, L. B. Jensen, M. V. Francia, F. Baquero, and L. Peixe.** 2011. Human and swine hosts share vancomycin-resistant Enterococcus faecium CC17 and CC5 and Enterococcus faecalis CC2 clonal clusters harboring Tn1546 on indistinguishable plasmids. J Clin Microbiol **49:**925-931.
69. **Freitas, A. R., C. Novais, A. P. Tedim, M. V. Francia, F. Baquero, L. Peixe, and T. M. Coque.** 2013. Microevolutionary events involving narrow host plasmids influences local fixation of vancomycin-resistance in Enterococcus populations. PLoS One. **8:**e60589.
70. **Freitas, A. R., A. P. Tedim, C. Novais, P. Ruiz-Garbajosa, G. Werner, J. A. Laverde-Gomez, R. Canton, L. Peixe, F. Baquero, and T. M. Coque.** 2010.

Global spread of colonization-virulence *hylEfm* gene in megaplasmids of CC17 *Enterococcus faecium* polyclonal sub-cluster. Antimicrobial Agents and Chemotherapy **54** 2660-2665.

71. **Fritzenwanker, M., C. Kuenne, A. Billion, T. Hain, K. Zimmermann, A. Goesmann, T. Chakraborty, and E. Domann.** 2013. Complete Genome Sequence of the Probiotic Enterococcus faecalis Symbioflor 1 Clone DSM 16431. Genome Announc. **1:**e00165-00112.
72. **Garcia-Migura, L., E. Liebana, and L. B. Jensen.** 2007. Transposon characterization of vancomycin-resistant Enterococcus faecium (VREF) and dissemination of resistance associated with transferable plasmids. Journal of Antimicrobial Chemotherapy **60:**263-268.
73. **Garsin, D. A., and R. J. Willems.** 2010. Insights into the biofilm lifestyle of enterococci. Virulence. **1:**219-221.
74. **Gaspar, F., N. Teixeira, L. Rigottier-Gois, P. Marujo, C. Nielsen-LeRoux, M. T. Crespo, M. d. F. Lopes, and P. Serror.** 2009. Virulence of Enterococcus faecalis dairy strains in an insect model: the role of fsrB and gelE. Microbiology **155:**3564-3571.
75. **Gaspar, F. B., N. Montero, E. Akary, N. Teixeira, R. Matos, B. Gonzalez-Zorn, M. T. Barreto Crespo, P. Serror, and F. Silva Lopes Mde.** 2012. Incongruence between the *cps* type 2 genotype and host-related phenotypes of an *Enterococcus faecalis* food isolate. Int J Food Microbiol. **158:**120-125.
76. **Gastmeier, P., F. Schwab, S. Barwolff, H. Ruden, and H. Grundmann.** 2006. Correlation between the genetic diversity of nosocomial pathogens and their survival time in intensive care units. J.Hosp.Infect. **62:**181-186.
77. **Gilmore, M. S., P. Coburn, S. R. Nallapareddy, and B. E. Murray.** 2002. Enterococcal Virulence., p. 301-354. *In* M. S. Gilmore (ed.), The Enterococci: Pathogenesis, Molecular Biology, and Antibiotic Resistance., vol. 1. ASM Press, Washington, DC 20036-2904.
78. **Gilmore, M. S., and J. J. Ferretti.** 2003. Microbiology. The thin line between gut commensal and pathogen. Science **299:**1999-2002.
79. **Giraffa, G.** 2003. Functionality of enterococci in dairy products. Int.J.Food Microbiol. **88:**215-222.
80. **Gripp, E., D. Hlahla, X. Didelot, F. Kops, S. Maurischat, K. Tedin, T. Alter, L. Ellerbroek, K. Schreiber, D. Schomburg, T. Janssen, P. Bartholomäus, D. Hofreuter, S. Woltemate, M. Uhr, B. Brenneke, P. Grüning, G. Gerlach, L. Wieler, S. Suerbaum, and C. Josenhans.** 2011. Closely related *Campylobacter jejuni* strains from different sources reveal a generalist rather than a specialist lifestyle. BMC Genomics **12:**584.
81. **Grissa, I., G. Vergnaud, and C. Pourcel.** 2007. The CRISPRdb database and tools to display CRISPRs and to generate dictionaries of spacers and repeats. BMC Bioinformatics **8:**172.
82. **Grissa, I., G. Vergnaud, and C. Pourcel.** 2007. CRISPRFinder: a web tool to identify clustered regularly interspaced short palindromic repeats. Nucleic Acids Res **35:**W52-57.
83. **Guiton, P. S., C. S. Hung, K. A. Kline, R. Roth, A. L. Kau, E. Hayes, J. Heuser, K. W. Dodson, M. G. Caparon, and S. J. Hultgren.** 2009. Contribution of autolysin and Sortase A during *Enterococcus faecalis* DNA-dependent biofilm development. Infect Immun. **77:**3626-3638.

84. **Haas, W., and M. S. Gilmore.** 1999. Molecular nature of a novel bacterial toxin: the cytolysin of *Enterococcus faecalis*. Med Microbiol Immunol **187:**183-190.
85. **Haas, W., B. D. Shepard, and M. S. Gilmore.** 2002. Two-component regulator of Enterococcus faecalis cytolysin responds to quorum-sensing autoinduction. Nature **415:**84-87.
86. **Hacker, J., and J. B. Kaper.** 2000. Pathogenicity islands and the evolution of microbes. Annu Rev Microbiol.
87. **Hancock, L. E., and M. S. Gilmore.** 2002. The capsular polysaccharide of Enterococcus faecalis and its relationship to other polysaccharides in the cell wall. Proc Natl Acad Sci U S A **99:**1574-1579.
88. **Hancock, L. E., and M. Perego.** 2004. The Enterococcus faecalis fsr two-component system controls biofilm development through production of gelatinase. Journal of bacteriology **186:**5629-5639.
89. **Hancock, L. E., B. D. Shepard, and M. S. Gilmore.** 2003. Molecular Analysis of the Enterococcus faecalis Serotype 2 Polysaccharide Determinant. Journal of bacteriology **185:**4393-4401.
90. **Hanin, A., I. Sava, Y. Bao, J. Huebner, A. Hartke, Y. Auffray, and N. Sauvageot.** 2010. Screening of in vivo activated genes in *Enterococcus faecalis* during insect and mouse infections and growth in urine. PloS one **5:**e11879.
91. **Hayes, F.** 2003. Toxins-antitoxins: plasmid maintenance, programmed cell death, and cell cycle arrest. Science **301:**1496-1499.
92. **Hegstad, K., T. Mikalsen, T. M. Coque, G. Werner, and A. Sundsfjord.** 2010. Mobile genetic elements and their contribution to the emergence of antimicrobial resistant *Enterococcus faecalis* and *Enterococcus faecium*. Clin Microbiol.Infect **16:**541-554.
93. **Heikens, E., M. J. M. Bonten, and R. J. L. Willems.** 2007. Enterococcal surface protein Esp is important for biofilm formation of Enterococcus faecium E1162. The Journal of Bacteriology **189:**8233-8240.
94. **Heikens, E., M. Leendertse, L. M. Wijnands, M. van Luit-Asbroek, M. J. Bonten, T. van der Poll, and R. J. Willems.** 2009. Enterococcal surface protein Esp is not essential for cell adhesion and intestinal colonization of Enterococcus faecium in mice. BMC Microbiol **9:**19.
95. **Hendrickx, A. P., R. J. Willems, M. J. Bonten, and W. van Schaik.** 2009. LPxTG surface proteins of enterococci. Trends Microbiol **17:**423-430.
96. **Hew, C. M., M. Korakli, and R. F. Vogel.** 2007. Expression of virulence-related genes by Enterococcus faecalis in response to different environments. Systematic and applied microbiology **30:**257-267.
97. **Hirt, H., P. M. Schlievert, and G. M. Dunny.** 2002. In vivo induction of virulence and antibiotic resistance transfer in Enterococcus faecalis mediated by the sex pheromone-sensing system of pCF10. Infection and Immunity **70:**716-723.
98. **Høiby, N., T. Bjarnsholt, M. Givskov, S. Molin, and O. Ciofu.** 2010. Antibiotic resistance of bacterial biofilms. International Journal of Antimicrobial Agents **35:**322-332.
99. **Hollenbeck, B. L., and L. B. Rice.** 2012. Intrinsic and acquired resistance mechanisms in enterococcus. Virulence **3:**421-433.

100. **Holzapfel, W. H., R. Geisen, and U. Schillinger.** 1995. Biological preservation of foods with reference to protective cultures, bacteriocins and food-grade enzymes. Int J Food Microbiol. **24:**343-362.
101. **Horvath, P., and R. Barrangou.** 2010. CRISPR/Cas, the immune system of bacteria and archaea. Science **327:**167-170.
102. **Horvath, P., A. C. Coute-Monvoisin, D. A. Romero, P. Boyaval, C. Fremaux, and R. Barrangou.** 2009. Comparative analysis of CRISPR loci in lactic acid bacteria genomes. Int J Food Microbiol **131:**62-70.
103. **Huebner, J., Y. Wang, W. A. Krueger, L. C. Madoff, G. Martirosian, S. Boisot, D. A. Goldmann, D. L. Kasper, A. O. Tzianabos, and G. B. Pier.** 1999. Isolation and chemical characterization of a capsular polysaccharide antigen shared by clinical isolates of *Enterococcus faecalis* and vancomycin-resistant *Enterococcus faecium*. Infect Immun. **67:**1213-1219.
104. **Hufnagel, M., L. E. Hancock, S. Koch, C. Theilacker, M. S. Gilmore, and J. Huebner.** 2004. Serological and genetic diversity of capsular polysaccharides in Enterococcus faecalis. J Clin Microbiol **42:**2548-2557.
105. **Hufnagel, M., S. Koch, R. Creti, L. Baldassarri, and J. Huebner.** 2004. A putative sugar-binding transcriptional regulator in a novel gene locus in *Enterococcus faecalis* contributes to production of biofilm and prolonged bacteremia in mice. J.Infect.Dis. **189:**420-430.
106. **Hufnagel, M., A. Kropec, C. Theilacker, and J. Huebner.** 2005. Naturally acquired antibodies against four *Enterococcus faecalis* capsular polysaccharides in healthy human sera. Clin Diagn Lab Immunol. **12:**930-934.
107. **Huycke, M. M.** 2002. Physiology of Enterococci., p. 133-175. *In* M. S. Gilmore (ed.), The Enterococci: Pathogenesis, Molecular Biology, and Antibiotic Resistance., vol. 1. ASM Press, Washington, DC 20036-2904.
108. **Huycke, M. M., V. Abrams, and D. R. Moore.** 2002. Enterococcus faecalis produces extracellular superoxide and hydrogen peroxide that damages colonic epithelial cell DNA. Carcinogenesis **23:**529-536.
109. **Huycke, M. M., W. Joyce, and M. F. Wack.** 1996. Augmented production of extracellular superoxide by blood isolates of Enterococcus faecalis. J.Infect.Dis. **173:**743-746.
110. **Ike, Y., D. B. Clewell, R. A. Segarra, and M. S. Gilmore.** 1990. Genetic analysis of the pAD1 hemolysin/bacteriocin determinant in *Enterococcus faecalis*: Tn917 insertional mutagenesis and cloning. J Bacteriol. **172:**155-163.
111. **Illumina, I.** 2010. Illumina Sequencing Technology - Highest data accuracy, simple workflow, and a broad range of applications. , Technology Spotlight: Illumina® Sequencing. Illumina, Inc.
112. **Jansen, R., J. D. Embden, W. Gaastra, and L. M. Schouls.** 2002. Identification of genes that are associated with DNA repeats in prokaryotes. Mol Microbiol. **43:**1565-1575.
113. **Jarvie, T., and T. Harkins.** 2008. *De novo* assembly and genomic structural variation analysis with genome sequencer FLX 3K long-tag paired end reads. Biotechniques. **44:**829-831.
114. **Jensen, L. B., L. Garcia-Migura, A. J. Valenzuela, M. Lohr, H. Hasman, and F. M. Aarestrup.** 2010. A classification system for plasmids from enterococci and other Gram-positive bacteria. J Microbiol Methods **80:**25-43.
115. **Jett, B. D., H. G. Jensen, R. E. Nordquist, and M. S. Gilmore.** 1992. Contribution of the pAD1-encoded cytolysin to the severity of experimental Enterococcus faecalis endophthalmitis. Infection and Immunity **60:**2445-2452.

116. **Jönsson, M., Z. Saleihan, I. F. Nes, and H. Holo.** 2009. Construction and characterization of three lactate dehydrogenase-negative *Enterococcus faecalis* V583 mutants. Appl Environ Microbiol. **75:**4901-4903.
117. **Kayser, F. H.** 2003. Safety aspects of enterococci from the medical point of view. International Journal of Food Microbiology **88:**255-262.
118. **Klare, I., E. Collatz, S. Al-Obeid, J. Wagner, A. C. Rodloff, and W. Witte.** 1992. Glycopeptide resistance in Enterococcus faecium from colonizations and infections in intensive care patients from Berlin hospitals and a transplantation centre. ZAC Zeitschrift für antimikrobielle antineoplastische Chemotherapie (German) **10:**45-53.
119. **Klare, I., C. Konstabel, S. Mueller-Bertling, G. Werner, B. Strommenger, C. Kettlitz, S. Borgmann, B. Schulte, D. Jonas, A. Serr, A. Fahr, U. Eigner, and W. Witte.** 2005. Spread of ampicillin/vancomycin-resistant Enterococcus faecium of the epidemic-virulent clonal complex-17 carrying the genes esp and hyl in German hospitals. European Journal of Clinical Microbiology & Infectious Diseases **24:**815-825.
120. **Klare, I., W. Witte, C. Wendt, and G. Werner.** 2012. Vancomycin-resistente Enterokokken (VRE). Aktuelle Daten und Trends zur Resistenzentwicklung. Bundesgesundheitsblatt Gesundheitsforschung Gesundheitsschutz. **55:**1387–1400.
121. **Kohanski, M. A., D. J. Dwyer, and J. J. Collins.** 2010. How antibiotics kill bacteria: from targets to networks. Nature reviews. Microbiology **8:**423-435.
122. **Kowalski, W. J., E. L. Kasper, J. F. Hatton, B. E. Murray, S. R. Nallapareddy, and M. J. Gillespie.** 2006. Enterococcus faecalis adhesin, ace, mediates attachment to particulate dentin. J.Endod. **32:**634-637.
123. **Kreft, B., R. Marre, U. Schramm, and R. Wirth.** 1992. Aggregation substance of Enterococcus faecalis mediates adhesion to cultured renal tubular cells. Infection and Immunity **60:**25-30.
124. **Kristich, C. J., Y. H. Li, D. G. Cvitkovitch, and G. M. Dunny.** 2004. Esp-Independent Biofilm Formation by Enterococcus faecalis. Journal of bacteriology **186:**154-163.
125. **Kuch, A., R. J. Willems, G. Werner, T. M. Coque, A. M. Hammerum, A. Sundsfjord, I. Klare, P. Ruiz-Garbajosa, G. S. Simonsen, M. van Luit-Asbroek, W. Hryniewicz, and E. Sadowy.** 2012. Insight into antimicrobial susceptibility and population structure of contemporary human *Enterococcus faecalis* isolates from Europe. The Journal of antimicrobial chemotherapy **Epub ahead of print**.
126. **Kuenne, C. T., R. Ghai, T. Chakraborty, and T. Hain.** 2007. GECO--linear visualization for comparative genomics. Bioinformatics. **23:**125-126.
127. **Kurenbach, B., C. Bohn, J. Prabhu, M. Abudukerim, U. Szewzyk, and E. Grohmann.** 2003. Intergeneric transfer of the Enterococcus faecalis plasmid pIP501 to Escherichia coli and Streptomyces lividans and sequence analysis of its tra region. Plasmid **50:**86-93.
128. **Larsen, J., H. C. Schonheyder, C. H. Lester, S. S. Olsen, L. J. Porsbo, L. Garcia-Migura, L. B. Jensen, M. Bisgaard, and A. M. Hammerum.** 2010. Porcine-origin gentamicin-resistant Enterococcus faecalis in Humans, Denmark. Emerg.Infect.Dis. **16:**682-684.
129. **Larsen, J., H. C. Schønheyder, K. V. Singh, C. H. Lester, S. S. Olsen, L. J. Porsbo, L. Garcia-Migura, L. B. Jensen, M. Bisgaard, B. E. Murray, and A.**

M. Hammerum. 2011. Porcine and Human Community Reservoirs of Enterococcus faecalis, Denmark. Emerg.Infect.Dis. **17**.
130. **Laverde Gomez, J. A.** 2011. Horizontally Transferable Elements among Enterococci. Dissertation (Dr. rer. nat.). Technischen Universität Carolo-Wilhelmina zu Braunschweig.
131. **Laverde Gomez, J. A., A. P. Hendrickx, R. J. Willems, J. Top, I. Sava, J. Huebner, W. Witte, and G. Werner.** 2011. Intra- and interspecies genomic transfer of the *Enterococcus faecalis* pathogenicity island. PloS one **6:**e16720.
132. **Laverde Gomez, J. A., W. van Schaik, A. R. Freitas, T. M. Coque, K. E. Weaver, M. V. Francia, W. Witte, and G. Werner.** 2011. A multiresistance megaplasmid pLG1 bearing a *hylEfm* genomic island in hospital *Enterococcus faecium* isolates. International journal of medical microbiology : IJMM **301:**165-175.
133. **Leavis, H. L., M. J. Bonten, and R. J. Willems.** 2006. Identification of high-risk enterococcal clonal complexes: global dispersion and antibiotic resistance. Curr Opin Microbiol **9:**454-460.
134. **Leclercq, R., E. Derlot, J. Duval, and P. Courvalin.** 1988. Plasmid-mediated resistance to vancomycin and teicoplanin in Enterococcus faecium N.Engl.J.Med. **319:**157-161.
135. **Levin, B. R.** 2010. Nasty viruses, costly plasmids, population dynamics, and the conditions for establishing and maintaining CRISPR-mediated adaptive immunity in bacteria. PLoS Genet. **6:**e100117.
136. **Levin, B. R., S. Moineau, M. Bushman, and R. Barrangou.** 2013. The population and evolutionary dynamics of phage and bacteria with CRISPR-mediated immunity. PLoS Genet. **9:**e1003312.
137. **Liu, S. Q.** 2003. Practical implications of lactate and pyruvate metabolism by lactic acid bacteria in food and beverage fermentations. Int J Food Microbiol. **83:**115-131.
138. **Low, Y. L., N. S. Jakubovics, J. C. Flatman, H. F. Jenkinson, and A. W. Smith.** 2003. Manganese-dependent regulation of the endocarditis-associated virulence factor EfaA of *Enterococcus faecalis*. J Med Microbiol. **52:**113-119.
139. **Maddalo, G., P. Chovanec, F. Stenberg-Bruzell, H. V. Nielsen, M. I. Jensen-Seaman, L. L. Ilag, K. A. Kline, and D. O. Daley.** 2011. A reference map of the membrane proteome of *Enterococcus faecalis*. Proteomics **11:**3935-3941.
140. **Maddox, S. M., P. S. Coburn, N. Shankar, and T. Conway.** 2012. Transcriptional Regulator PerA Influences Biofilm-Associated, Platelet Binding, and Metabolic Gene Expression in *Enterococcus faecalis*. PloS one **7:**e34398.
141. **Maekawa, S., M. Yoshioka, and Y. Kumamoto.** 1992. Proposal of a new scheme for the serological typing of *Enterococcus faecalis* strains. Microbiol Immunol. **36:**671-681.
142. **Maiden, M. C., J. A. Bygraves, E. Feil, G. Morelli, J. E. Russell, R. Urwin, Q. Zhang, J. Zhou, K. Zurth, D. A. Caugant, I. M. Feavers, M. Achtman, and B. G. Spratt.** 1998. Multilocus sequence typing: a portable approach to the identification of clones within populations of pathogenic microorganisms. Proc Natl Acad Sci U S A. **95:**3140-3145.
143. **Makarova, K. S., N. V. Grishin, S. A. Shabalina, Y. I. Wolf, and E. V. Koonin.** 2006. A putative RNA-interference-based immune system in prokaryotes: computational analysis of the predicted enzymatic machinery,

functional analogies with eukaryotic RNAi, and hypothetical mechanisms of action. Biol Direct. **1:**7.

144. **Manson, J. M., and M. S. Gilmore.** 2006. Pathogenicity island integrase cross-talk: a potential new tool for virulence modulation. Mol.Microbiol. **61:**555-559.
145. **Manson, J. M., L. E. Hancock, and M. S. Gilmore.** 2010. Mechanism of chromosomal transfer of Enterococcus faecalis pathogenicity island, capsule, antimicrobial resistance, and other traits. Proc Natl Acad Sci U S A **107:**12269-12274.
146. **Mardis, E. R.** 2008. Next-generation DNA sequencing methods. Annu Rev Genomics Hum Genet. **9:**387-402.
147. **Margulies, M., M. Egholm, W. E. Altman, S. Attiya, J. S. Bader, L. A. Bemben, J. Berka, M. S. Braverman, Y. J. Chen, Z. Chen, S. B. Dewell, L. Du, J. M. Fierro, X. V. Gomes, B. C. Godwin, W. He, S. Helgesen, C. H. Ho, G. P. Irzyk, S. C. Jando, M. L. Alenquer, T. P. Jarvie, K. B. Jirage, J. B. Kim, J. R. Knight, J. R. Lanza, J. H. Leamon, S. M. Lefkowitz, M. Lei, J. Li, K. L. Lohman, H. Lu, V. B. Makhijani, K. E. McDade, M. P. McKenna, E. W. Myers, E. Nickerson, J. R. Nobile, R. Plant, B. P. Puc, M. T. Ronan, G. T. Roth, G. J. Sarkis, J. F. Simons, J. W. Simpson, M. Srinivasan, K. R. Tartaro, A. Tomasz, K. A. Vogt, G. A. Volkmer, S. H. Wang, Y. Wang, M. P. Weiner, P. Yu, R. F. Begley, and J. M. Rothberg.** 2005. Genome sequencing in microfabricated high-density picolitre reactors. Nature. **437:**376-380.
148. **Marraffini, L. A., and E. J. Sontheimer.** 2008. CRISPR interference limits horizontal gene transfer in staphylococci by targeting DNA. Science. **322:**1843-1845.
149. **McBride, S. M., P. S. Coburn, A. S. Baghdayan, R. J. Willems, M. J. Grande, N. Shankar, and M. S. Gilmore.** 2009. Genetic variation and evolution of the pathogenicity island of Enterococcus faecalis. Journal of bacteriology **191:**3392-3402.
150. **McBride, S. M., V. A. Fischetti, D. J. Leblanc, R. C. Moellering, Jr., and M. S. Gilmore.** 2007. Genetic diversity among Enterococcus faecalis. PloS one **2:**e582.
151. **McCarthy, A.** 2010. Third generation DNA sequencing: pacific biosciences' single molecule real time technology. Chem Biol. **17:**675-676.
152. **Mehmeti, I., E. M. Faergestad, M. Bekker, L. Snipen, I. F. Nes, and H. Holo.** 2012. Growth rate-dependent control in *Enterococcus faecalis*: effects on the transcriptome and proteome, and strong regulation of lactate dehydrogenase. Appl Environ Microbiol. **78:**170-176.
153. **Mehmeti, I., M. Jönsson, E. M. Fergestad, G. Mathiesen, I. F. Nes, and H. Holo.** 2011. Transcriptome, proteome, and metabolite analyses of a lactate dehydrogenase-negative mutant of Enterococcus faecalis V583. Appl Environ Microbiol **77:**2406-2413.
154. **Metzker, M. L.** 2010. Sequencing technologies - the next generation. Nature reviews. Genetics **11:**31-46.
155. **Meyer, F., A. Goesmann, A. C. McHardy, D. Bartels, T. Bekel, J. Clausen, J. Kalinowski, B. Linke, O. Rupp, R. Giegerich, and A. Pühler.** 2003. GenDB--an open source genome annotation system for prokaryote genomes. Nucleic Acids Res. **31:**2187-2195.

156. **Miller, J. R., A. L. Delcher, S. Koren, E. Venter, B. P. Walenz, A. Brownley, J. Johnson, K. Li, C. Mobarry, and G. Sutton.** 2008. Aggressive assembly of pyrosequencing reads with mates. Bioinformatics **24:**2818-2824.
157. **Minic, Z., C. Marie, C. Delorme, J. M. Faurie, G. Mercier, D. Ehrlich, and P. Renault.** 2007. Control of EpsE, the phosphoglycosyltransferase initiating exopolysaccharide synthesis in *Streptococcus thermophilus*, by EpsD tyrosine kinase. J Bacteriol. **189:**1351-1357.
158. **Mohamed, J. A., and D. B. Huang.** 2007. Biofilm formation by enterococci. J Med Microbiol **56:**1581-1588.
159. **Mohamed, J. A., W. Huang, S. R. Nallapareddy, F. Teng, and B. E. Murray.** 2004. Influence of origin of isolates, especially endocarditis isolates, and various genes on biofilm formation by Enterococcus faecalis. Infect Immun **72:**3658-3663.
160. **Mojica, F. J., C. Ferrer, G. Juez, and F. Rodríguez-Valera.** 1995. Long stretches of short tandem repeats are present in the largest replicons of the Archaea *Haloferax mediterranei* and *Haloferax volcanii* and could be involved in replicon partitioning. Mol Microbiol. **17:**85-93.
161. **Mori, M., Y. Sakagami, M. Narita, A. Isogai, M. Fujino, C. Kitada, R. A. Craig, D. B. Clewell, and A. Suzuki.** 1984. Isolation and structure of the bacterial sex pheromone, cAD1, that induces plasmid transfer in *Streptococcus faecalis*. FEBS Lett. **178:**97-100.
162. **Moritz, E. M., and P. J. Hergenrother.** 2007. Toxin-antitoxin systems are ubiquitous and plasmid-encoded in vancomycin-resistant enterococci. Proc Natl Acad Sci U S A **104:**311-316.
163. **Mukherjee, K., B. Altincicek, T. Hain, E. Domann, A. Vilcinskas, and T. Chakraborty.** 2010. Galleria mellonella as a model system for studying Listeria pathogenesis. Appl Environ Microbiol **76:**310-317.
164. **Murchan, S., M. E. Kaufmann, A. Deplano, R. de Ryck, M. Struelens, C. Elsberg Zinn, V. Fussing, S. Salmenlinna, J. Vuopio-Varkila, N. El Solh, C. Cuny, W. Witte, P. T. Tassios, N. Legakis, W. van Leeuwen, A. van Belkum, A. Vindel, I. Laconcha, J. Garaizar, S. Haeggman, B. Olsson-Liljequist, U. Ransjo, G. Coombes, and B. Cookson.** 2003. Harmonization of Pulsed-Field Gel Electrophoresis Protocols for Epidemiological Typing of Strains of Methicillin-Resistant *Staphylococcus aureus*: a Single Approach Developed by Consensus in 10 European Laboratories and Its Application for Tracing the Spread of Related Strains. J Clin Microbiol. **41:**1574–1585.
165. **Murray, B. E.** 1990. The life and times of the Enterococcus. Clinical Microbiology Reviews **3:**46-65.
166. **Murray, B. E., K. V. Singh, R. P. Ross, J. D. Heath, G. M. Dunny, and G. M. Weinstock.** 1993. Generation of restriction map of *Enterococcus faecalis* OG1 and investigation of growth requirements and regions encoding biosynthetic function. Journal of bacteriology **175:**5216-5223.
167. **Myers, E. W., G. G. Sutton, A. L. Delcher, I. M. Dew, D. P. Fasulo, M. J. Flanigan, S. A. Kravitz, C. M. Mobarry, K. H. Reinert, K. A. Remington, E. L. Anson, R. A. Bolanos, H. H. Chou, C. M. Jordan, A. L. Halpern, S. Lonardi, E. M. Beasley, R. C. Brandon, L. Chen, P. J. Dunn, Z. Lai, Y. Liang, D. R. Nusskern, M. Zhan, Q. Zhang, X. Zheng, G. M. Rubin, M. D. Adams, and J. C. Venter.** 2000. A whole-genome assembly of Drosophila. Science **287:**2196-2204.

168. **Mylonakis, E., M. Engelbert, X. Qin, C. D. Sifri, B. E. Murray, F. M. Ausubel, M. S. Gilmore, and S. B. Calderwood.** 2002. The *Enterococcus faecalis fsrB* gene, a key component of the *fsr* quorum-sensing system, is associated with virulence in the rabbit endophthalmitis model. Infection and Immunity **70:**4678-4681.
169. **Nallapareddy, S. R., X. Qin, G. M. Weinstock, M. Hook, and B. E. Murray.** 2000. Enterococcus faecalis adhesin, ace, mediates attachment to extracellular matrix proteins collagen type IV and laminin as well as collagen type I. Infection and Immunity **68:**5218-5224.
170. **Nallapareddy, S. R., K. V. Singh, R. W. Duh, G. M. Weinstock, and B. E. Murray.** 2000. Diversity of ace, a gene encoding a microbial surface component recognizing adhesive matrix molecules, from different strains of Enterococcus faecalis and evidence for production of ace during human infections. Infection and Immunity **68:**5210-5217.
171. **Nallapareddy, S. R., K. V. Singh, J. Sillanpaa, D. A. Garsin, M. Hook, S. L. Erlandsen, and B. E. Murray.** 2006. Endocarditis and biofilm-associated pili of Enterococcus faecalis. The Journal of clinical investigation **116:**2799-2807.
172. **Neuhaus, F. C., and J. Baddiley.** 2003. A continuum of anionic charge: structures and functions of D-alanyl-teichoic acids in gram-positive bacteria. Microbiology and Molecular Biology Reviews **67:**686-723.
173. **Nielsen, H. V., A. L. Flores-Mireles, A. L. Kau, K. A. Kline, J. S. Pinkner, F. Neiers, S. Normark, B. Henriques-Normark, M. G. Caparon, and S. J. Hultgren.** 2013. Pilin and sortase residues critical for endocarditis- and biofilm-associated pilus biogenesis in *Enterococcus faecalis*. J Bacteriol. **[Epub ahead of print]**.
174. **Novick, R. P.** 1987. Plasmid incompatibility. Microbiol Rev. **51:**381-395.
175. **Oancea, C., I. Klare, W. Witte, and G. Werner.** 2004. Conjugative transfer of the virulence gene, esp, among isolates of Enterococcus faecium and Enterococcus faecalis. The Journal of antimicrobial chemotherapy **54:**232-235.
176. **Olmsted, S. B., S. M. Kao, L. J. van Putte, J. C. Gallo, and G. M. Dunny.** 1991. Role of the pheromone-inducible surface protein Asc10 in mating aggregate formation and conjugal transfer of the Enterococcus faecalis plasmid pCF10. The Journal of Bacteriology **173:**7665-7672.
177. **Orihuela, C. J., J. N. Radin, J. E. Sublett, G. Gao, D. Kaushal, and E. Tuomanen.** 2004. Microarray analysis of pneumococcal gene expression during invasive disease. Infect Immun. **72:**5582-5596.
178. **Paganelli, F. L., R. J. Willems, and H. L. Leavis.** 2012. Optimizing future treatment of enterococcal infections: attacking the biofilm? Trends Microbiol. **20:**40-49.
179. **Palmer, K. L., K. Carniol, J. M. Manson, D. Heiman, T. Shea, S. Young, Q. Zeng, D. Gevers, M. Feldgarden, B. Birren, and M. S. Gilmore.** 2010. High-quality draft genome sequences of 28 *Enterococcus sp*. isolates. Journal of bacteriology **192:**2469-2470.
180. **Palmer, K. L., and M. S. Gilmore.** 2010. Multidrug-resistant enterococci lack CRISPR-cas. MBio. **1:**e00227-00210.
181. **Palmer, K. L., P. Godfrey, A. Griggs, V. N. Kos, J. Zucker, C. Desjardins, G. Cerqueira, D. Gevers, S. Walker, J. Wortman, M. Feldgarden, B. Haas, B. Birren, and M. S. Gilmore.** 2012. Comparative genomics of enterococci:

variation in *Enterococcus faecalis*, clade structure in *E. faecium*, and defining characteristics of *E. gallinarum* and *E. casseliflavus*. MBio. **3:**e00318-00311.

182. **Park, S. Y., K. M. Kim, J. H. Lee, S. J. Seo, and I. H. Lee.** 2007. Extracellular gelatinase of Enterococcus faecalis destroys a defense system in insect hemolymph and human serum. Infect Immun. **75:**1861-1869.
183. **Park, S. Y., Y. P. Shin, C. H. Kim, H. J. Park, Y. S. Seong, B. S. Kim, S. J. Seo, and I. H. Lee.** 2008. Immune evasion of *Enterococcus faecalis* by an extracellular gelatinase that cleaves C3 and iC3b. J Immunol. **181:**6328-6336.
184. **Paulsen, I. T., L. Banerjei, G. S. Myers, K. E. Nelson, R. Seshadri, T. D. Read, D. E. Fouts, J. A. Eisen, S. R. Gill, J. F. Heidelberg, H. Tettelin, R. J. Dodson, L. Umayam, L. Brinkac, M. Beanan, S. Daugherty, R. T. DeBoy, S. Durkin, J. Kolonay, R. Madupu, W. Nelson, J. Vamathevan, B. Tran, J. Upton, T. Hansen, J. Shetty, H. Khouri, T. Utterback, D. Radune, K. A. Ketchum, B. A. Dougherty, and C. M. Fraser.** 2003. Role of mobile DNA in the evolution of vancomycin-resistant Enterococcus faecalis. Science **299:**2071-2074.
185. **Perichon, B., and P. Courvalin.** 2009. VanA-type vancomycin-resistant Staphylococcus aureus. Antimicrobial Agents and Chemotherapy **53:**4580-4587.
186. **Pillar, C. M., and M. S. Gilmore.** 2004. Enterococcal virulence - pathogenicity island of *E. faecalis*. Front Biosci. **9:**2335-2346.
187. **Pinkston, K. L., P. Gao, D. Diaz-Garcia, J. Sillanpää, S. R. Nallapareddy, B. E. Murray, and B. R. Harvey.** 2011. The Fsr Quorum-Sensing System of *Enterococcus faecalis* Modulates Surface Display of the Collagen-Binding MSCRAMM Ace through Regulation of *gelE*. J Bacteriol. **193:**4317-4325.
188. **Poncet, S., E. Milohanic, A. Mazé, J. Nait Abdallah, F. Aké, M. Larribe, A. E. Deghmane, M. K. Taha, M. Dozot, X. De Bolle, J. J. Letesson, and J. Deutscher.** 2009. Correlations between carbon metabolism and virulence in bacteria. Contrib.Microbiol. **16:**88-102.
189. **Qin, X., K. V. Singh, G. M. Weinstock, and B. E. Murray.** 2001. Characterization of fsr , a regulator controlling expression of gelatinase and serine protease in Enterococcus faecalis OG1RF. The Journal of Bacteriology **183:**3372-3382.
190. **Qin, X., K. V. Singh, G. M. Weinstock, and B. E. Murray.** 2000. Effects of Enterococcus faecalis fsr genes on production of gelatinase and a serine protease and virulence. Infection and Immunity **68:**2579-2586.
191. **Rakita, R. M., N. N. Vanek, K. Jacques-Palaz, M. Mee, M. M. Mariscalco, G. M. Dunny, M. Snuggs, W. B. Van Winkle, and S. I. Simon.** 1999. Enterococcus faecalis bearing aggregation substance is resistant to killing by human neutrophils despite phagocytosis and neutrophil activation. Infection and Immunity **67:**6067-6075.
192. **Reyes-Jara, A., M. Latorre, G. Lopez, A. Bourgogne, B. E. Murray, V. Cambiazo, and M. Gonzalez.** 2010. Genome-wide transcriptome analysis of the adaptive response of Enterococcus faecalis to copper exposure. Biometals : an international journal on the role of metal ions in biology, biochemistry, and medicine **23:**1105-1112.
193. **Rich, R. L., B. Kreikemeyer, R. T. Owens, S. LaBrenz, S. V. Narayana, G. M. Weinstock, B. E. Murray, and M. Hook.** 1999. Ace is a collagen-binding MSCRAMM from Enterococcus faecalis. J.Biol.Chem. **274:**26939-26945.

194. **Rigottier-Gois, L., A. Alberti, A. Houel, J. F. Taly, P. Palcy, J. Manson, D. Pinto, R. C. Matos, L. Carrilero, N. Montero, M. Tariq, H. Karsens, C. Repp, A. Kropec, A. Budin-Verneuil, A. Benachour, N. Sauvageot, A. Bizzini, M. S. Gilmore, P. Bessières, J. Kok, J. Huebner, F. Lopes, B. Gonzalez-Zorn, A. Hartke, and P. Serror.** 2011. Large-scale screening of a targeted Enterococcus faecalis mutant library identifies envelope fitness factors. PLoS One. **6:**e29023.
195. **Roberts, M. C.** 2011. Environmental macrolide-lincosamide-streptogramin and tetracycline resistant bacteria. Front Microbiol. **2:**40.
196. **Rosvoll, T. C., B. L. Lindstad, T. M. Lunde, K. Hegstad, B. Aasnaes, A. M. Hammerum, C. H. Lester, G. S. Simonsen, A. Sundsfjord, and T. Pedersen.** 2012. Increased high-level gentamicin resistance in invasive *Enterococcus faecium* is associated with *aac(6')Ie-aph(2")Ia*-encoding transferable megaplasmids hosted by major hospital-adapted lineages. FEMS Immunol Med Microbiol. **66:**166-176.
197. **Rozdzinski, E., R. Marre, M. Susa, R. Wirth, and A. Muscholl-Silberhorn.** 2001. Aggregation substance-mediated adherence of Enterococcus faecalis to immobilized extracellular matrix proteins. Microb.Pathog. **30:**211-220.
198. **Rudolph, B.** 2004. Untersuchungen zu *Enterococcus faecalis* als möglicher Faktor zur Entstehung der amyloiden Arthropathie der braunen Legehenne. Inaugural-Dissertation. Freien Universität Berlin.
199. **Ruiz-Garbajosa, P., M. J. M. Bonten, D. A. Robinson, J. Top, S. R. Nallapareddy, C. Torres, T. M. Coque, R. Canton, F. Baquero, B. E. Murray, R. del Campo, and R. J. L. Willems.** 2006. Multilocus Sequence Typing Scheme for Enterococcus faecalis Reveals Hospital-Adapted Genetic Complexes in a Background of High Rates of Recombination. Journal of Clinical Microbiology **44:**2220-2228.
200. **Ruiz-Garbajosa, P., T. M. Coque, R. Cantón, R. J. Willems, F. Baquero, and R. Del Campo.** 2007. High-risk clonal complexes CC2 and CC9 are widely distributed among *Enterococcus faecalis* hospital isolates recovered in Spain. Enferm Infecc Microbiol Clin. **25:**513-518.
201. **Sahl, J. W., M. N. Matalka, and D. A. Rasko.** 2012. Phylomark, a tool to identify conserved phylogenetic markers from whole-genome alignments. Appl Environ Microbiol. **78:**4884-4892.
202. **Sahm, D. F., J. Kissinger, M. S. Gilmore, P. R. Murray, R. Mulder, J. Solliday, and B. Clarke.** 1989. In vitro susceptibility studies of vancomycin-resistant *Enterococcus faecalis*. Antimicrob Agents Chemother. **33:**1588-1591.
203. **Sambrook, J., E. Fritsch, and T. Maniatis.** 1989. Molecular Cloning, a Laboratory Manual. Gold Spring Laboratory Press, New York.
204. **Sampson, T. R., S. D. Saroj, A. C. Llewellyn, Y. L. Tzeng, and D. S. Weiss.** 2013. A CRISPR/Cas system mediates bacterial innate immune evasion and virulence. Nature **497:**254-257.
205. **Sanger, F., S. Nicklen, and A. R. Coulson.** 1977. DNA sequencing with chain-terminating inhibitors. Proc Natl Acad Sci U S A. **74:**5463-5467.
206. **Sartingen, S., E. Rozdzinski, A. Muscholl-Silberhorn, and R. Marre.** 2000. Aggregation substance increases adherence and internalization, but not translocation, of Enterococcus faecalis through different intestinal epithelial cells in vitro. Infection and Immunity **68:**6044-6047.
207. **Sava, I. G., E. Heikens, and J. Huebner.** 2010. Pathogenesis and immunity in enterococcal infections. Clin.Microbiol.Infect. **16:**533-540.

208. **Sava, I. G., F. Zhang, I. Toma, C. Theilacker, B. Li, T. F. Baumert, O. Holst, R. J. Linhardt, and J. Huebner.** 2009. Novel interactions of glycosaminoglycans and bacterial glycolipids mediate binding of enterococci to human cells. J.Biol.Chem. **284:**18194-18201.
209. **Sayers, E. W., T. Barrett, D. A. Benson, E. Bolton, S. H. Bryant, K. Canese, V. Chetvernin, D. M. Church, M. Dicuccio, S. Federhen, M. Feolo, I. M. Fingerman, L. Y. Geer, W. Helmberg, Y. Kapustin, S. Krasnov, D. Landsman, D. J. Lipman, Z. Lu, T. L. Madden, T. Madej, D. R. Maglott, A. Marchler-Bauer, V. Miller, I. Karsch-Mizrachi, J. Ostell, A. Panchenko, L. Phan, K. D. Pruitt, G. D. Schuler, E. Sequeira, S. T. Sherry, M. Shumway, K. Sirotkin, D. Slotta, A. Souvorov, G. Starchenko, T. A. Tatusova, L. Wagner, Y. Wang, W. J. Wilbur, E. Yaschenko, and J. Ye.** 2012. Database resources of the National Center for Biotechnology Information. Nucleic Acids Res. **40:**D13-25.
210. **Schleifer, K. H., and R. Kilppe- Bälz.** 1984. Transfer of *Streptococcus faecalis* and *Streptococcus faecium* to the Genus *Enterococcus* norn. rev. as *Enterococcus faecalis* comb. nov. and *Enterococcus faecium* comb. nov. International Journal of Systemic Bacteriology**:**31 - 34.
211. **Schlievert, P. M., P. J. Gahr, A. P. Assimacopoulos, M. M. Dinges, J. A. Stoehr, J. W. Harmala, H. Hirt, and G. M. Dunny.** 1998. Aggregation and binding substances enhance pathogenicity in rabbit models of Enterococcus faecalis endocarditis. Infection and Immunity **66:**218-223.
212. **Schwartz, D. C., and C. R. Cantor.** 1984. Separation of yeast chromosome-sized DNAs by pulsed field gradient gel electrophoresis. Cell. **37:**67-75.
213. **Schwarz, F. V., V. Perreten, and M. Teuber.** 2001. Sequence of the 50-kb conjugative multiresistance plasmid pRE25 from Enterococcus faecalis RE25. Plasmid **46:**170-187.
214. **Semedo, T., M. A. Santos, M. F. Lopes, J. J. Figueiredo Marques, M. T. Barreto Crespo, and R. Tenreiro.** 2003. Virulence factors in food, clinical and reference Enterococci: A common trait in the genus? Syst Appl Microbiol. **26:**13-22.
215. **Shankar, N., A. S. Baghdayan, and M. S. Gilmore.** 2002. Modulation of virulence within a pathogenicity island in vancomycin-resistant Enterococcus faecalis. Nature **417:**746-750.
216. **Shankar, N., A. S. Baghdayan, R. Willems, A. M. Hammerum, and L. B. Jensen.** 2006. Presence of pathogenicity island genes in Enterococcus faecalis isolates from pigs in Denmark. J Clin Microbiol **44:**4200-4203.
217. **Shankar, N., P. Coburn, C. Pillar, W. Haas, and M. Gilmore.** 2004. Enterococcal cytolysin: activities and association with other virulence traits in a pathogenicity island. Int.J.Med.Microbiol. **293:**609-618.
218. **Shankar, N., C. V. Lockatell, A. S. Baghdayan, C. Drachenberg, M. S. Gilmore, and D. E. Johnson.** 2001. Role of Enterococcus faecalis surface protein Esp in the pathogenesis of ascending urinary tract infection. Infect Immun **69:**4366-4372.
219. **Shankar, V., A. S. Baghdayan, M. M. Huycke, G. Lindahl, and M. S. Gilmore.** 1999. Infection-derived Enterococcus faecalis strains are enriched in esp, a gene encoding a novel surface protein. Infection and Immunity **67:**193-200.
220. **Sifri, C. D., E. Mylonakis, K. V. Singh, X. Qin, D. A. Garsin, B. E. Murray, F. M. Ausubel, and S. B. Calderwood.** 2002. Virulence Effect of Enterococcus

faecalis Protease Genes and the Quorum-Sensing Locus fsr in Caenorhabditis elegans and Mice. Infection and Immunity **70:**5647-5650.

221. **Sillanpää, J., C. Chang, K. V. Singh, M. C. Montealegre, S. R. Nallapareddy, B. R. Harvey, H. Ton-That, and B. E. Murray.** 2013. Contribution of Individual Ebp Pilus Subunits of *Enterococcus faecalis* OG1RF to Pilus Biogenesis, Biofilm Formation and Urinary Tract Infection. PloS one **8:**e68813.
222. **Singh, K. V., R. J. Lewis, and B. E. Murray.** 2009. Importance of the epa locus of Enterococcus faecalis OG1RF in a mouse model of ascending urinary tract infection. J Infect Dis **200:**417-420.
223. **Singh, K. V., S. R. Nallapareddy, and B. E. Murray.** 2007. Importance of the ebp (endocarditis- and biofilm-associated pilus) locus in the pathogenesis of Enterococcus faecalis ascending urinary tract infection. J.Infect.Dis. **195:**1671-1677.
224. **Singh, K. V., S. R. Nallapareddy, E. C. Nannini, and B. E. Murray.** 2005. Fsr-independent production of protease(s) may explain the lack of attenuation of an Enterococcus faecalis fsr mutant versus a gelE-sprE mutant in induction of endocarditis. Infection and Immunity **73:**4888-4894.
225. **Singh, K. V., S. R. Nallapareddy, J. Sillanpaa, and B. E. Murray.** 2010. Importance of the collagen adhesin ace in pathogenesis and protection against Enterococcus faecalis experimental endocarditis. PLoS.Pathog. **6:**e1000716.
226. **Sokatch, J. T., and I. C. Gunsalus.** 1957. Aldonic acid metabolism. I. Pathway of carbon in an inducible gluconate fermentation by *Streptococcus faecalis*. J Bacteriol. **73:**452-460.
227. **Solheim, M., A. Aakra, L. G. Snipen, D. A. Brede, and I. F. Nes.** 2009. Comparative genomics of Enterococcus faecalis from healthy Norwegian infants. BMC Genomics **10:**194.
228. **Solheim, M., A. Aakra, H. C. Vebø, L. Snipen, and I. F. Nes.** 2007. Transcriptional responses of Enterococcus faecalis V583 to bovine bile and sodium dodecyl sulfate. Appl Environ Microbiol **73:**5767-5774.
229. **Solheim, M., M. C. Brekke, L. G. Snipen, R. J. Willems, I. F. Nes, and D. A. Brede.** 2011. Comparative genomic analysis reveals significant enrichment of mobile genetic elements and genes encoding surface structure-proteins in hospital-associated clonal complex 2 Enterococcus faecalis. BMC Microbiol **11:**3.
230. **Sorek, R., V. Kunin, and P. Hugenholtz.** 2008. CRISPR - a widespread system that provides acquired resistance against phages in bacteria and archaea. Nature reviews. Microbiology **6:**181-186.
231. **Southern, E. M.** 1975. Detection of specific sequences among DNA fragments separated by gel electrophoresis. J Mol Biol. **98:**503-517.
232. **Southern, E. M.** 1979. Measurement of DNA length by gel electrophoresis. Anal Biochem. **100:**319-323.
233. **Stamatakis, A.** 2006. RAxML-VI-HPC: maximum likelihood-based phylogenetic analyses with thousands of taxa and mixed models. . Bioinformatics. **22:**2688-2690.
234. **Starikova, I., M. Al-Haroni, G. Werner, A. P. Roberts, V. Sørum, K. M. Nielsen, and P. J. Johnsen.** 2013. Fitness costs of various mobile genetic elements in *Enterococcus faecium* and *Enterococcus faecalis*. J Antimicrob Chemother. **[Epub ahead of print]**.

235. **Stevens, R. H., M. R. Ektefaie, and D. E. Fouts.** 2011. The annotated complete DNA sequence of *Enterococcus faecalis* bacteriophage φEf11 and its comparison with all available phage and predicted prophage genomes. FEMS Microbiol Lett. **317:**9-26.
236. **Stewart, P. S., and M. J. Franklin.** 2008. Physiological heterogeneity in biofilms. Nature reviews. Microbiology **6:**199-210.
237. **Strommenger, B., C. Kettlitz, G. Werner, and W. Witte.** 2003. Multiplex PCR assay for simultaneous detection of nine clinically relevant antibiotic resistance genes in *Staphylococcus aureus*. J Clin Microbiol. **41:**4089-4094.
238. **Sussmuth, S. D., A. Muscholl-Silberhorn, R. Wirth, M. Susa, R. Marre, and E. Rozdzinski.** 2000. Aggregation substance promotes adherence, phagocytosis, and intracellular survival of Enterococcus faecalis within human macrophages and suppresses respiratory burst. Infection and Immunity **68:**4900-4906.
239. **Swoboda, J. G., J. Campbell, T. C. Meredith, and S. Walker.** 2010. Wall teichoic acid function, biosynthesis, and inhibition. Chembiochem. **11:**35-45.
240. **Szemes, T., B. Vlkova, G. Minarik, L. Tothova, H. Drahovska, J. Turna, and P. Celec.** 2010. On the origin of reactive oxygen species and antioxidative mechanisms in Enterococcus faecalis. Redox report : communications in free radical research **15:**202-206.
241. **Tendolkar, P. M., A. S. Baghdayan, M. S. Gilmore, and N. Shankar.** 2004. Enterococcal surface protein, Esp, enhances biofilm formation by Enterococcus faecalis. Infection and Immunity **72:**6032-6039.
242. **Tendolkar, P. M., A. S. Baghdayan, and N. Shankar.** 2005. The N-terminal domain of enterococcal surface protein, Esp, is sufficient for Esp-mediated biofilm enhancement in Enterococcus faecalis. The Journal of Bacteriology **187:**6213-6222.
243. **Tendolkar, P. M., A. S. Baghdayan, and N. Shankar.** 2006. Putative surface proteins encoded within a novel transferable locus confer a high-biofilm phenotype to Enterococcus faecalis. The Journal of Bacteriology **188:**2063-2072.
244. **Teng, F., K. D. Jacques-Palaz, G. M. Weinstock, and B. E. Murray.** 2002. Evidence that the enterococcal polysaccharide antigen gene (*epa*) cluster is widespread in *Enterococcus faecalis* and influences resistance to phagocytic killing of *E. faecalis*. Infection and Immunity **70:**2010-2015.
245. **Teng, F., K. V. Singh, A. Bourgogne, J. Zeng, and B. E. Murray.** 2009. Further characterization of the epa gene cluster and Epa polysaccharides of Enterococcus faecalis. Infect Immun **77:**3759-3767.
246. **Teuber, M., F. Schwarz, and V. Perreten.** 2003. Molecular structure and evolution of the conjugative multiresistance plasmid pRE25 of Enterococcus faecalis isolated from a raw-fermented sausage. International Journal of Food Microbiology **88:**325-329.
247. **Theilacker, C., Z. Kaczynski, A. Kropec, F. Fabretti, T. Sange, O. Holst, and J. Huebner.** 2006. Opsonic antibodies to Enterococcus faecalis strain 12030 are directed against lipoteichoic acid. Infect Immun **74:**5703-5712.
248. **Theilacker, C., P. Sanchez-Carballo, I. Toma, F. Fabretti, I. Sava, A. Kropec, O. Holst, and J. Huebner.** 2009. Glycolipids are involved in biofilm accumulation and prolonged bacteraemia in Enterococcus faecalis. Mol.Microbiol. **71:**1055-1069.

249. **Theilacker, C., I. Sava, P. Sanchez-Carballo, Y. Bao, A. Kropec, E. Grohmann, O. Holst, and J. Huebner.** 2011. Deletion of the glycosyltransferase bgsB of Enterococcus faecalis leads to a complete loss of glycolipids from the cell membrane and to impaired biofilm formation. BMC Microbiol **11:**67.
250. **Thomas, C. M.** 2000. Paradigms of plasmid organization. Mol Microbiol. **37:**485-491.
251. **Thomas, V. C., Y. Hiromasa, N. Harms, L. Thurlow, J. Tomich, and L. E. Hancock.** 2009. A fratricidal mechanism is responsible for eDNA release and contributes to biofilm development of Enterococcus faecalis. Mol Microbiol **72:**1022-1036.
252. **Thomas, V. C., L. R. Thurlow, D. Boyle, and L. E. Hancock.** 2008. Regulation of autolysis-dependent extracellular DNA release by Enterococcus faecalis extracellular proteases influences biofilm development. Journal of bacteriology **190:**5690-5698.
253. **Thurlow, L. R., V. C. Thomas, S. D. Fleming, and L. E. Hancock.** 2009. *Enterococcus faecalis* capsular polysaccharide serotypes C and D and their contributions to host innate immune evasion. Infect Immun. **77:**5551-5557.
254. **Thurlow, L. R., V. C. Thomas, and L. E. Hancock.** 2009. Capsular polysaccharide production in Enterococcus faecalis and contribution of CpsF to capsule serospecificity. Journal of bacteriology **191:**6203-6210.
255. **Thurlow, L. R., V. C. Thomas, S. Narayanan, S. Olson, S. D. Fleming, and L. E. Hancock.** 2010. Gelatinase contributes to the pathogenesis of endocarditis caused by Enterococcus faecalis. Infect Immun **78:**4936-4943.
256. **Toledo-Arana, A., J. Valle, C. Solano, M. J. Arrizubieta, C. Cucarella, M. Lamata, B. Amorena, J. Leiva, J. R. Penades, and I. Lasa.** 2001. The enterococcal surface protein, Esp, is involved in Enterococcus faecalis biofilm formation. Applied and Environmental Microbiology **67:**4538-4545.
257. **Top, J., L. M. Schouls, M. J. M. Bonten, and R. J. L. Willems.** 2004. Multiple-locus variable-number tandem repeat analysis, a novel typing scheme to study the genetic relatedness and epidemiology of Enterococcus faecium isolates. Journal of Clinical Microbiology **42:**4503-4511.
258. **Ubeda, C., V. Bucci, S. Caballero, A. Djukovic, N. C. Toussaint, M. Equinda, L. Lipuma, L. Ling, A. Gobourne, D. No, Y. Taur, R. R. Jenq, M. R. van den Brink, J. B. Xavier, and E. G. Pamer.** 2013. Intestinal microbiota containing Barnesiella species cures vancomycin-resistant *Enterococcus faecium* colonization. Infect Immun. **81:**965-973.
259. **Ubeda, C., Y. Taur, R. R. Jenq, M. J. Equinda, T. Son, M. Samstein, A. Viale, N. D. Socci, M. R. van den Brink, M. Kamboj, and E. G. Pamer.** 2010. Vancomycin-resistant *Enterococcus* domination of intestinal microbiota is enabled by antibiotic treatment in mice and precedes bloodstream invasion in humans. The Journal of clinical investigation **120:**4332-4341.
260. **Uttley, A. H., C. H. Collins, J. Naidoo, and R. C. George.** 1988. Vancomycin-resistant enterococci. Lancet **1:**57-58.
261. **Vallet-Gely, I., B. Lemaitre, and F. Boccard.** 2008. Bacterial strategies to overcome insect defences. Nat Rev Micro **6:**302-313.
262. **van Schaik, W., and R. J. Willems.** 2010. Genome-based insights into the evolution of enterococci. Clin Microbiol.Infect **16:**527-532.
263. **Vanek, N. N., S. I. Simon, K. Jacques-Palaz, M. M. Mariscalco, G. M. Dunny, and R. M. Rakita.** 1999. Enterococcus faecalis aggregation

substance promotes opsonin-independent binding to human neutrophils via a complement receptor type 3-mediated mechanism. FEMS Immunol.Med.Microbiol. **26:**49-60.

264. **Vankerckhoven, V., T. Van Autgaerden, C. Vael, C. Lammens, S. Chapelle, R. Rossi, D. Jabes, and H. Goossens.** 2004. Development of a multiplex PCR for the detection of asa1, gelE, cylA, esp, and hyl genes in enterococci and survey for virulence determinants among European hospital isolates of Enterococcus faecium. J Clin Microbiol **42:**4473-4479.
265. **Vebø, H. C.** 2010. An explorative study of *Enterococcus faecalis* transcriptional responses to infection-relevant growth environments. . Ph. D. . Norwegian University of Life Sciences, Ås.
266. **Vebø, H. C., L. Snipen, I. F. Nes, and D. A. Brede.** 2009. The transcriptome of the nosocomial pathogen *Enterococcus faecalis* V583 reveals adaptive responses to growth in blood. PloS one **4:**e7660.
267. **Vebø, H. C., M. Solheim, L. Snipen, I. F. Nes, and D. A. Brede.** 2010. Comparative genomic analysis of pathogenic and probiotic Enterococcus faecalis isolates, and their transcriptional responses to growth in human urine. PloS one **5:**e12489.
268. **Vesić, D., and C. J. Kristich.** 2013. A Rex family transcriptional repressor influences H2O2 accumulation by *Enterococcus faecalis*. J Bacteriol. **195:**1815-1824.
269. **Wagner, P. L., and M. K. Waldor.** 2002. Bacteriophage control of bacterial virulence. Infect Immun. **70:**3985-3993.
270. **Wardal, E., I. Gawryszewska, W. Hryniewicz, and E. Sadowy.** 2013. Abundance and diversity of plasmid-associated genes among clinical isolates of *Enterococcus faecalis*. Plasmid. **:**pii: S0147-0619X(0113)00079-00076.
271. **Waters, C. M., C. L. Wells, and G. M. Dunny.** 2003. The aggregation domain of aggregation substance, not the RGD motifs, is critical for efficient internalization by HT-29 enterocytes. Infection and Immunity **71:**5682-5689.
272. **Weaver, K. E., S. M. Kwong, N. Firth, and M. V. Francia.** 2009. The RepA_N replicons of Gram-positive bacteria: a family of broadly distributed but narrow host range plasmids. Plasmid **61:**94-109.
273. **Weaver, K. E., L. B. Rice, and G. Churchward.** 2002. Plasmids and Transposons, p. 219-264. *In* M. S. Gilmore (ed.), The enterococci: Pathogenesis, Molecular Biology and Antibiotic Resistance, vol. 1. ASM press, Washington, DC.
274. **Weinberger, A. D., and M. S. Gilmore.** 2012. CRISPR-Cas: to take up DNA or not-that is the question. Cell Host Microbe. **12:**125-126.
275. **Weinberger, A. D., C. L. Sun, M. M. Pluciński, V. J. Denef, B. C. Thomas, P. Horvath, R. Barrangou, M. S. Gilmore, W. M. Getz, and J. F. Banfield.** 2012. Persisting viral sequences shape microbial CRISPR-based immunity. PLoS Comput Biol. **8:**e1002475.
276. **Weinberger, A. D., Y. I. Wolf, A. E. Lobkovsky, M. S. Gilmore, and E. V. Koonin.** 2012. Viral diversity threshold for adaptive immunity in prokaryotes. MBio. **3:**e00456-00412.
277. **Wells, C. L., E. A. Moore, J. A. Hoag, H. Hirt, G. M. Dunny, and S. L. Erlandsen.** 2000. Inducible expression of Enterococcus faecalis aggregation substance surface protein facilitates bacterial internalization by cultured enterocytes. Infection and Immunity **68:**7190-7194.

278. **Werner, G., T. M. Coque, C. M. Franz, E. Grohmann, K. Hegstad, L. Jensen, W. van Schaik, and K. Weaver.** 2013. Antibiotic resistant enterococci-Tales of a drug resistance gene trafficker. Int J Med Microbiol. **pii: S1438-4221:**00042-00048.
279. **Werner, G., C. Fleige, B. Ewert, J. A. Laverde-Gomez, I. Klare, and W. Witte.** 2010. High-level ciprofloxacin resistance among hospital-adapted *Enterococcus faecium* (CC17). Int.J.Antimicrob.Agents **35:**119-125.
280. **Werner, G., C. Fleige, A. T. Feßler, M. Timke, M. Kostrzewa, M. Zischka, T. Peters, H. Kaspar, and S. Schwarz.** 2012. Improved identification including MALDI-TOF mass spectrometry analysis of group D streptococci from bovine mastitis and subsequent molecular characterization of corresponding *Enterococcus faecalis* and *Enterococcus faecium* isolates. Vet.Microbiol. **In Press**.
281. **Werner, G., A. R. Freitas, T. M. Coque, J. E. Sollid, C. Lester, A. M. Hammerum, L. Garcia-Migura, L. B. Jensen, M. V. Francia, W. Witte, R. J. Willems, and A. Sundsfjord.** 2011. Host range of enterococcal vanA plasmids among Gram-positive intestinal bacteria. The Journal of antimicrobial chemotherapy **66:**273-282.
282. **Werner, G., B. Hildebrandt, I. Klare, and W. Witte.** 2000. Linkage of determinants for streptogramin A, macrolide-lincosamide-streptogramin B, and chloramphenicol resistance on a conjugative plasmid in *Enterococcus faecium* and dissemination of this cluster among streptogramin-resistant enterococci. Int.J.Med.Microbiol. **290:**543-548.
283. **Werner, G., I. Klare, and W. Witte.** 1999. Large conjugative *vanA* plasmids in vancomycin-resistant *Enterococcus faecium*. . Journal of Clinical Microbiology **37:**2383-2384.
284. **Werner, G., B. Strommenger, and W. Witte.** 2008. Acquired vancomycin resistance in clinically relevant pathogens. Future Microbiology **3:**547 - 562.
285. **Werner, G., R. J. Willems, B. Hildebrandt, I. Klare, and W. Witte.** 2003. Influence of transferable genetic determinants on the outcome of typing methods commonly used for *Enterococcus faecium*. . Journal of Clinical Microbiology **41:**1499-1506.
286. **Willems, R. J., W. P. Hanage, D. E. Bessen, and E. J. Feil.** 2011. Population biology of Gram-positive pathogens: high-risk clones for dissemination of antibiotic resistance. FEMS Microbiol.Rev.
287. **Willems, R. J., J. Top, W. van Schaik, H. Leavis, M. Bonten, J. Sirén, W. P. Hanage, and J. Corander.** 2012. Restricted gene flow among hospital subpopulations of *Enterococcus faecium*. mBio. **3:**e00151-00112.
288. **Winstel, V., C. Liang, P. Sanchez-Carballo, M. Steglich, M. Munar, B. M. Bröker, J. R. Penadés, U. Nübel, O. Holst, T. Dandekar, A. Peschel, and G. Xia.** 2013. Wall teichoic acid structure governs horizontal gene transfer between major bacterial pathogens. Nat Commun. **4:**2345.
289. **Winzer, K., and P. Williams.** 2001. Quorum sensing and the regulation of virulence gene expression in pathogenic bacteria. Int J Med Microbiol. **291:**131-143.
290. **Woodford, N., D. Morrison, B. Cookson, and R. C. George.** 1993. Comparison of high-level gentamicin-resistant Enterococcus faecium isolates from different continents. Antimicrobial Agents and Chemotherapy **37:**681-684.

291. **Wooley, R. E., P. S. Gibbs, T. P. Brown, and J. J. Maurer.** 2000. Chicken embryo lethality assay for determining the virulence of avian *Escherichia coli* isolates. Avian Dis. **44:**318-324.
292. **Xu, Y., B. E. Murray, and G. M. Weinstock.** 1998. A cluster of genes involved in polysaccharide biosynthesis from *Enterococcus faecalis* OG1RF. . Infection and Immunity **66:**4313-4323.
293. **Xu, Y., K. V. Singh, X. Qin, B. E. Murray, and G. M. Weinstock.** 2000. Analysis of a gene cluster of Enterococcus faecalis involved in polysaccharide biosynthesis. Infection and Immunity **68:**815-823.
294. **Yebra, M. J., M. Zúñiga, S. Beaufils, G. Pérez-Martínez, J. Deutscher, and V. Monedero.** 2007. Identification of a gene cluster enabling *Lactobacillus casei* BL23 to utilize myo-inositol. Appl Environ Microbiol. **73:**3850-3858.
295. **Zeng, J., F. Teng, G. M. Weinstock, and B. E. Murray.** 2004. Translocation of Enterococcus faecalis strains across a monolayer of polarized human enterocyte-like T84 cells. Journal of Clinical Microbiology **42:**1149-1154.
296. **Zhang, J., R. Chiodini, A. Badr, and G. Zhang.** 2011. The impact of next-generation sequencing on genomics. Journal of genetics and genomics = Yi chuan xue bao **38:**95-109.
297. **Zhang, X., J. E. Vrijenhoek, M. J. Bonten, R. J. Willems, and W. van Schaik.** 2011. A genetic element present on megaplasmids allows Enterococcus faecium to use raffinose as carbon source. Environ Microbiol **13:**518-528.
298. **Zhang, X., J. E. P. Vrijenhoek, M. J. M. Bonten, R. J. Willems, and W. van Schaik.** 2009. A large conjugative plasmid confers the ability to utilize à-galactoside sugars as carbon source in E. faecium ESCMID Conference on Enterococci: from Animals to Man, Conference Proceedings **-:**34-34.
299. **Zhou, Y., Y. Liang, K. H. Lynch, J. J. Dennis, and D. S. Wishart.** 2011. PHAST: a fast phage search tool. Nucleic Acids Res. **39 (Web Server issue)**.
300. **Zischka, M., C. Kuenne, J. Blom, P. W. Dabrowski, B. Linke, T. Hain, A. Nitsche, A. Goesmann, J. Larsen, L. B. Jensen, W. Witte, and G. Werner.** 2012. Complete genome sequence of the porcine isolate *Enterococcus faecalis* D32. J Bacteriol. **194:**5490-5491.

11 Acknowledgements

At the end of my thesis, I would like to thank all those people who supported me and made this thesis possible.

Above all, it is important to me to thank my family, especially my parents, Matthias, my grandparents and my little sweet child Karl, for their everlasting personal support and great patience at all times.

This thesis would not have been possible without the constant help, support and patience of my principal supervisor and project initiator PD Dr. Guido Werner (Robert Koch Institute (RKI), D). I am extremely grateful for the systemic guidance and great effort during the progress of this study, so that I could advance myself professionally and personally.

I also would like to express my sincere gratitude to my mentor and supervisor Prof. Dr. Dieter Jahn (TU Braunschweig, D), and to Dr. Florian Bittner (TU Braunschweig, D), that he has kindly agreed to be the chairman of the audit committee.

I am thankful to Prof. Dr. Wolfgang Witte (RKI, D) for giving me the opportunity to work within the fascinating scientific field of enterococci and for his support during the course of this project.

I also would like to acknowledge the financial and technical support of the RKI and the Federal Ministry of Education and Research (“UroGenOmics” consortium; 0315833C).

Especially, I am grateful to all my colleagues at the RKI, especially to Carola Fleige and Uta Geringer for their technical assistance and helpful instructions, to PD Dr. Andreas Nitsche and the entire sequencing laboratory of the RKI for performing

the 454 sequencing, and to P. Wojtek Dabrowski for his help with diverse software issues.

Furthermore, I would like to thank our cooperation partners for their support and fruitful collaboration, especially I express my gratitude to Prof. Dr. Johannes Hübner, Dominique Wobser and Dr. Türkan Sakinc (University of Freiburg, D), to Dr. Torsten Hain and Dr. Carsten T. Künne (University of Giessen, D), to Dr. Alexander Goesmann, Jochen Blom and Dr. Burkhard Linke (Center for Biotechnology (CeBiTec)/University of Bielefeld, D), to Prof. Dr. Rolf Daniel and Dr. Sonja Voget (University of Göttingen, D), to Prof. Dr. Dietmar Schomburg and Dr. Kerstin Schmidt-Hohagen (TU Braunschweig, D), to Prof. Dr. Hafez M. Hafez and Dr. Rüdiger Hauck (Free University of Berlin, D), and also to Eurofins MWG-Operon for services rendered.

Special thanks to Ingolf Nes and Margrete Solheim (Oslo/Ås, N), Ewa Sadowy (Warsaw, PL), Patricia Ruiz-Garbajosa and Teresa M. Coque (Madrid, ESP), Rob J. Willems (Utrecht, NL), Jesper Larsen and Lars B. Jensen (Copenhagen, DK), Henning Böhme (Wernigerode, D), Dianelys Quinones (Havanna, CU), Nobomitsu Kobayashi (Sapporo, JP), and all of the other clinical laboratories in Germany for the kind gift of strains.

Finally, I would like to take this opportunity to express my profound gratitude to my friends Nadine and Lisa for their support and motivation at all times.